INTERNATIONAL REVIEW OF CYTOLOGY A SURVEY OF CELL BIOLOGY

Volume 233

Kwang W. Jeon

International Review of
Cytology

A Survey of
Cell Biology

VOLUME 233

International Review of Cytology
A Survey of Cell Biology

Edited by

Kwang W. Jeon
Department of Biochemistry
University of Tennessee
Knoxville, Tennessee

VOLUME 233

ELSEVIER
ACADEMIC
PRESS

AMSTERDAM • BOSTON • HEIDELBERG • LONDON
NEW YORK • OXFORD • PARIS • SAN DIEGO
SAN FRANCISCO • SINGAPORE • SYDNEY • TOKYO
Academic Press is an imprint of Elsevier

Front cover photograph: (A), Structure of parenchymal cells in the apical part of a 3-day-old etiolated wheat seeding. (For more details see Chapter 4, figure 3A)

This book is printed on acid-free paper. ♾

Elsevier Academic Press.
525 B Street, Suite 1900, San Diego, California 92101-4495, USA
84 Theobald's Road, London WC1X 8RR, UK
http://www.academicpress.com

International Standard Book Number: 0-12-364637-5

PRINTED IN THE UNITED STATES OF AMERICA
04 05 06 07 08 9 8 7 6 5 4 3 2 1

CONTENTS

The Bacterial Flagellar Motor: Structure and Function of a Complex Molecular Machine

Seiji Kojima and David F. Blair

Apoptosis in Plants: Specific Features of Plant Apoptotic Cells and Effect of Various Factors and Agents

B. F. Vanyushin, L. E. Bakeeva, V. A. Zamyatnina, and N. I. Aleksandrushkina

Cell Biology of Leydig Cells in the Testis

Syed G. Haider

The Exocyst Complex in Polarized Exocytosis

Shu-Chan Hsu, Daniel TerBush, Mathew Abraham, and Wei Guo

This Page Intentionally Left Blank

CONTRIBUTORS

Numbers in parentheses indicate the pages on which the authors' contributions begin.

Mathew Abraham (243), *Department of Biology, University of Pennsylvania, Philadelphia, Pennsylvania 19104*

N. I. Aleksandrushkina (135), *Belozersky Institute of Physico Chemical Biology, Lomonosov Moscow State University, Moscow 119992, Russia*

L. E. Bakeeva (135), *Belozersky Institute of Physico Chemical Biology, Lomonosov Moscow State University, Moscow 119992, Russia*

M. Benjamin (1), *School of Biosciences, Cardiff University, Cardiff CF10 3US, United Kingdom*

David F. Blair (93), *Department of Biology, University of Utah, Salt Lake City, Utah 84112*

Wei Guo (243), *Department of Biology, University of Pennsylvania, Philadelphia, Pennsylvania 19104*

Syed G. Haider (181), *Institute of Anatomy II, Heinrich Heine University, D-40225 Düsseldorf, Germany*

Shu-Chan Hsu (243), *Department of Cell Biology and Neuroscience, Rutgers University, Piscataway, New Jersey 08854*

Seiji Kojima (93), *Department of Biology, University of Utah, Salt Lake City, Utah 84112*

Lynne M. Quarmby (47), *Department of Biological Sciences, Simon Fraser University, Burnaby, British Columbia, Canada V5A 1S6*

J. R. Ralphs (1), *School of Biosciences, Cardiff University, Cardiff CF10 3US, United Kingdom*

Daniel TerBush (243), *Department of Biochemistry and Molecular Biology, Uniformed Services, University of the Health Sciences, Bethesda, Maryland 20814*

B. F. Vanyushin (135), *Belozersky Institute of Physico Chemical Biology, Lomonosov Moscow State University, Moscow 119992, Russia*

V. A. Zamyatnina (135), *Belozersky Institute of Physico Chemical Biology, Lomonosov Moscow State University, Moscow 119992, Russia*

Biology of Fibrocartilage Cells

M. Benjamin and J. R. Ralphs
School of Biosciences, Cardiff University, Cardiff CF10 3US, United Kingdom

Fibrocartilage is an avascular tissue that is best documented in menisci, intervertebral discs, tendons, ligaments, and the temporomandibular joint. Several of these sites are of particular interest to those in the emerging field of tissue engineering. Fibrocartilage cells frequently resemble chondrocytes in having prominent rough endoplasmic reticulum, many glycogen granules, and lipid droplets, and intermediate filaments together with and actin stress fibers that help to determine cell organization in the intervertebral disc. Fibrocartilage cells can synthesize a variety of matrix molecules including collagens, proteoglycans, and noncollagenous proteins. All the fibrillar collagens (types I, II, III, V, and XI) have been reported, together with FACIT (types IX and XII) and network-forming collagens (types VI and X). The proteoglycans include large, aggregating types (aggrecan and versican) and small, leucine-rich types (decorin, biglycan, lumican, and fibromodulin). Less attention has been paid to noncollagenous proteins, although tenascin-C expression may be modulated by mechanical strain. As in hyaline cartilage, matrix metalloproteinases are important in matrix turnover and fibrocartilage cells are capable of apoptosis.

KEY WORDS: Fibrocartilage, Menisci, Tendons, Ligaments, Intervertebral disc, Temporomandibular joint, Collagens, Proteoglycans.

I. Introduction

Few researchers would claim to be studying fibrocartilage for its own sake, though many are interested in a great diversity of tissues or organs that contain fibrocartilage. These include menisci, intervertebral (IV) discs, tendons, ligaments, and the temporomandibular joint (TMJ) among many

others. It is this that has provided the stimulus for the current review. We have sought to bring together, from a wide diversity of research areas, key aspects of the cell biology of fibrocartilage and the nature of the extracellular matrix (ECM) that characterizes the tissue.

Our hope is that workers with a primary interest in fibrocartilage from one location will benefit from a knowledge of fibrocartilage in another. We have paid particular attention to highlighting the wide variety of ECM molecules that fibrocartilage cells secrete, for this is an area of much current interest. It is the nature of the ECM, of course, that determines the physical properties of the tissue and its ability to resist compression and shear—often in addition to having considerable tensile strength. Many of the ECM molecules that characterize fibrocartilages of all types are also secreted by the cells of other cartilage types. Hence, we hope that our review will be of interest to those whose primary attention is focused on articular hyaline cartilage.

The differentiation of fibrocartilage cells is an important issue, particularly in relation to tissue engineering and the influence of mechanical load on fibrocartilage development. Hence, we have given developmental studies due consideration, but tried to avoid unnecessary overlap with our earlier review on the developmental biology of tendons and ligaments (Benjamin and Ralphs, 2000).

II. Properties of Fibrocartilage and Fibrocartilage Cells

A. Identity of Fibrocartilage

Fibrocartilage has been reported in mammals, birds, reptiles, amphibia, and fish (Benjamin and Evans, 1990; Carvalho and Felisbino, 1999). In its clearest form, it can easily be recognized both by routine histology and immunohistochemistry. Histologically, a ''typical'' fibrocartilage is an avascular and aneural tissue that has large, rounded or oval cells embedded in an ECM in which collagen and/or elastic fibers are readily visible, as in ordinary dense fibrous connective tissue. However, in addition, there is a small quantity of amorphous, pericellular, and territorial matrix that stains metachromatically with toluidine blue. It is the ability to distinguish fibers in routine histology preparations that is central to distinguishing fibrocartilage from hyaline cartilage. In hyaline cartilage, fibers are not normally visible in routine sections, for fiber staining is masked by the rest of the matrix (Stockwell, 1979). Immunohistochemically, fibrocartilage is typically characterized by the presence of type II collagen and aggrecan, as in hyaline cartilage (Benjamin and Ralphs, 1998). The absence of either molecule from the body as a whole can have severe effects on skeletogenesis (Aszodi *et al*., 1998; Watanabe *et al*., 1994).

The practical difficulty in trying to define fibrocartilage precisely is that there are no clear boundaries enabling histological and immunohistochemical features to form the basis of an empirical definition. Thus type II collagen and aggrecan, for example, can be expressed in many noncartilaginous tissues, for example, muscle (Boyan *et al*., 1992) or tissues in the developing ear (Ishibe *et al*., 1989). Nor can fibrocartilage be defined with greater ease on the basis of its biochemical composition. Eyre *et al*. (2002) have pointed out that knee joint menisci (which are one of the best known fibrocartilages) contain only a small quantity of type II collagen, in what is largely a type I collagen-rich matrix, but that human IV discs contain roughly equal quantities of both. Thus, it must be accepted that fibrocartilage cannot always be distinguished unambiguously from either dense fibrous connective tissue on the one hand or hyaline (and occasionally elastic) cartilage on the other. There is a continuous spectrum of tissues between these two extremes and fibrocartilage always merges imperceptibly with one or the other. Thus, the typical, hyaline articular cartilage covering the head of the humerus, for example, is often fibrocartilaginous near the attachment of the rotator cuff tendons and fibrocartilage in menisci, IV discs, tendons, and ligaments blends with fibrous tissue. Thus, fibrocartilage should be regarded as a ''transitional tissue'' and the reader cannot assume that a tissue present at one location, or developmental stage, is the same as another.

The idea that fibrocartilage is a transitional tissue is in line with its developmental origin, for it can differentiate from both dense fibrous connective tissue and hyaline cartilage (Benjamin and Ralphs, 2000; Kampen and Tillmann, 1998). This makes it difficult to know what to call its cells. We choose simply to refer to them as fibrocartilage cells (Benjamin and Ralphs, 1995, 1996, 1997a,b, 1998, 2000, 2001), whereas others call them fibrochondrocytes (Agarwal *et al*., 2001; Araujo *et al*., 2002; Carvalho *et al*., 2000; Isoda and Saito, 1998; Jacoby *et al*., 1993; Jasser *et al*., 1994). However, the terms fibroblasts or cartilage cells (chondrocytes) may sometimes be applicable, although not interchangeable, according to the developmental origin of the tissue. Such difficulties in defining cell phenotypes are not, of course, restricted to fibrocartilage, but are often a general problem in skeletal biology (Beresford, 1981).

B. Localization of Fibrocartilage

The numerous sites at which fibrocartilage has been documented are summarized in Table I. Particularly with the more common locations, only selected references are given, and no attempt is made to direct the reader to the first occasion on which a particular tissue was reported. The fibrocartilages that have attracted the greatest attention are those in the anulus

TABLE I
Distribution of Fibrocartilage

Site	Ref(s).
Anulus fibrosus	Hayes *et al*. (2001)
Menisci and other intraarticular discs	Berkovitz and Pacy (2000); Nagy and Daniel (1992)
Articular fibrocartilages on mammalian membrane bones (including temporomandibular joint)	Chaves *et al*. (2002); Hu *et al*. (2003); Luder (1998)
Avian articular cartilages	Beresford (1981)
Wrap-around regions of tendons and ligaments	Abrahamsson *et al*. (1989); Benjamin and Ralphs (1998); Carvalho *et al*. (2000); Covizi *et al*. (2001); Vogel and Koob (1989)
Tendon and ligament entheses	Benjamin and McGonagle (2001); Benjamin *et al*. (1986); Hems and Tillmann (2000); Kumai *et al*. (2002); Suzuki *et al*. (2002)
Periostea	Benjamin *et al*. (1993b, 1995); Stilwell and Gray (1954)
Plantar (volar plate) of fingers and toes	Deland *et al*. (1995); Lewis *et al*. (1998)
Pubic symphysis	Ortega *et al*. (2003); Samuel *et al*. (1996)
Symphysis menti	Trevisan and Scapino (1976)
Acetabular and glenoid labra	Aboul-Mahasen *et al*. (2002); Podromos *et al*. (1990)
Penile bone	Izumi *et al*. (2000)
Marsupial patella (“patelloid”)	Holladay *et al*. (1990); Reese *et al*. (2001)
Tympanic membrane	Kuijpers *et al*. (1999)
Suprapatella	Benjamin *et al*. (1991); Bland and Ashhurst (1997)
Fracture repair callus	Claes *et al*. (2002); Loboa *et al*. (2001)
Heart skeleton	Balogh *et al*. (1971); Egerbacher *et al*. (2000)
Fibrocartilaginous emboli in the spinal cord	Bockenek and Bach (1990); Junker *et al*. (2000)
Fibrocartilaginous pseudotumour in the femur	Gedikoglu *et al*. (2001)
Equine digital cushions	Bowker *et al*. (1998)
Articular fibrocartilage in the sacroiliac joint	Kampen and Tillmann (1998)
Foramen lacerum	Tauber *et al*. (1999)
Osteophytes	Gelse *et al*. (2003); Koki *et al*. (2002)
Articular cartilage repair tissue	Horas *et al*. (2003)
Posterior longitudinal ligament in patients with Forestier’s disease (DISH)	Patel *et al*. (2002)

fibrosus of the IV disc, knee joint menisci, TMJ, tendons, and ligaments (Figs. 1 and 2). It is important to note that all of these contain fibrocartilage, but also have regions of dense fibrous connective tissue. Furthermore, the balance of fibrous and fibrocartilaginous tissues can change with age, notably in the articular disc of the TMJ. This is more fibrocartilaginous in older people (Berkovitz and Pacy, 2000).

In tendons and ligaments, fibrocartilage is found in regions compressed against bony or fibrous pulleys and at certain entheses, that is, at their skeletal attachments (Fig. 1). The former sites have been called "wrap-around" regions by Vogel and Koob (1989). Wrap-around regions are particularly characteristic of tendons in the limbs that change the direction of muscle pull by bending around pulleys. Among the most thoroughly investigated is the compressed region of the bovine deep digital flexor tendon that presses against the proximal sesamoid bones at the metatarsophalangeal

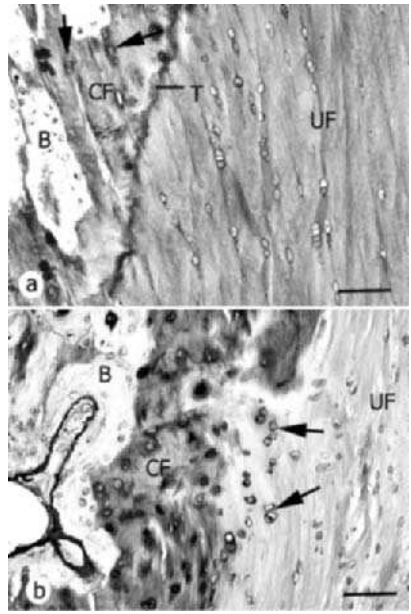

FIG. 1 Fibrocartilages associated with the enthesis organ of the human Achilles tendon. (a) The enthesis fibrocartilage at the attachment of tendon to the calcaneus. Rows of fibrocartilage cells are conspicuous in the zone of uncalcified fibrocartilage (UF), but cells are also present (arrows) in the zone of calcified fibrocartilage (CF), which lies deep to the tidemark (T) and adjacent to the bone (B). (b) Periosteal fibrocartilage on the calcaneus immediately next to the osteotendinous junction. This fibrocartilage also has zones of calcified (CF) and uncalcified (UF) tissue, although a tidemark is not evident. Note that the cells in the deeper part of the uncalcified fibrocartilage are hypertrophied and surrounded by a strongly staining territorial matrix (arrows). Bars: 100 μm. Toluidine blue.

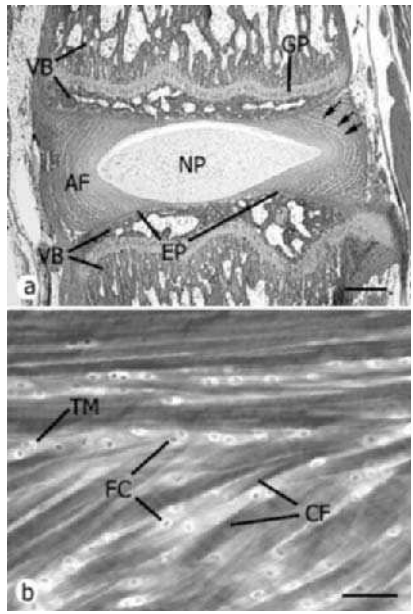

FIG. 2 Among the best documented fibrocartilages are those of (a) the intervertebral disc and (b) the knee joint menisci. (a) A low-power view of the whole intervertebral disc in a mouse tail, showing the location of the anulus fibrosus (AF) in relation to the vertebral bodies (VB) between which it spans, and the nucleus pulposus (NP) it surrounds. The anulus contains numerous collagenous lamellae (arrows) and is an avascular tissue that relies heavily on diffusion via the adjacent vertebral end plates (EP). GP, growth plate. Bar: 0.5 mm. Hematoxylin and eosin. (b) In the human knee joint menisci, the fibrocartilage cells (FC) are surrounded by a pale-staining territorial matrix (TM) and can be clearly distinguished from their associated bundles of collagen fibers (CF). Bar: 50 μm. Hematoxylin and eosin.

joint. This bovine tendon has been extensively used as a model for wrap-around tendons by Vogel and colleagues (Evanko and Vogel, 1990, 1993; Koob and Vogel, 1987; Koob *et al*., 1992; Robbins and Vogel, 1994; Robbins *et al*., 1997; Vogel, 1995, 1996; Vogel and Koob, 1989; Vogel *et al*., 1984, 1994). However, numerous, wrap-around fibrocartilaginous tendons and ligaments also occur in humans (Benjamin *et al*., 1995). At many locations, there is a complementary fibrocartilage on the opposing surface of the bony or fibrous pulley (Fig. 1b; Benjamin *et al*., 1995; Stilwell and Gray, 1954). Enthesis fibrocartilage is particularly characteristic of tendons and ligaments that attach to the epiphyses or apophyses of long bones, and to the short bones of the carpus and tarsus (Benjamin and Ralphs, 1995, 1998, 2000; Benjamin *et al*., 1986; Suzuki *et al*., 2002). By contrast, tendons that attach to long bone shafts have fibrous entheses (Benjamin *et al*., 1986; Suzuki *et al*.,

2002). Matyas *et al.* (1995) have shown a good correlation between the distribution of fibrocartilage cells at the femoral enthesis of the rabbit medial collateral ligament and the site of principal compressive stresses, as predicted by finite element analysis. This is in line with the classic view of Altmann (1964), that fibrocartilage is present at sites in response to compression and/or shear.

The term "enthesis organ" has been coined by Benjamin and McGonagle (2001) to emphasize that there is more to stress dissipation at an enthesis than simply that which occurs at the bony interface itself. The term is most applicable to fibrocartilaginous entheses, for here there can be fibrocartilaginous specializations both in the tendon itself and the bone surface, immediately adjacent to the insertion site. The former has been called "sesamoid fibrocartilage" by analogy with sesamoid bones (which also lie within tendons), and the latter "periosteal fibrocartilage," because it is formed from periosteum (Fig. 1b; Rufai *et al.*, 1995a). The archetypal enthesis organ is that associated with the Achilles tendon (Benjamin and McGonagle, 2001; Rufai *et al.*, 1995a). Where there is a prominent superior tuberosity on the calcaneus, this is covered by periosteal fibrocartilage, and this presses against sesamoid fibrocartilage in the deep part of the tendon when the foot is dorsiflexed (Rufai *et al.*, 1995a). These two fibrocartilages are separated by the retrocalcaneal bursa, which facilitates free movement between tendon and bone according to the foot position. Consequently, the enthesis organ can be compared to a synovial joint, and has been aptly described as "half-joint, half-bursa" (Canoso, 1998). It serves to dissipate stress concentration away from the enthesis and thus to reduce the risk of wear and tear. An enthesis organ containing several phenotypically distinct fibrocartilages has also been found in the tendon of the tibialis posterior at its navicular insertion site (Moriggl *et al.*, 2003).

Fibrocartilage has come to attract renewed interest from rheumatologists, for it is widely recognized that the tissue is of fundamental importance in understanding the etiology of the seronegative spondyloarthropathies (Benjamin and McGonagle, 2001). This is a range of diseases that include ankylosing spondylitis, psoriatic arthritis, Reiter's syndrome, reactive arthritis, undifferentiated spondyloarthropathy, and inflammatory bowel disease–associated arthritis. It is proposed either that there is an autoimmune reaction against some antigen present in fibrocartilage (Maksymowych, 2000) or that the presence of fibrocartilage at targeted sites signifies an underlying biomechanical basis for the disease (Benjamin and McGonagle, 2001; McGonagle *et al.*, 2002). Intriguingly, the presence of fibrocartilage rather than hyaline cartilage is associated with sclerosis of the underlying bone in patients with osteitis condensans (Berthelot *et al.*, 1995). It seems that joints covered with hyaline cartilage are largely spared comparable changes in this disease.

C. Avascularity of Fibrocartilage

Fibrocartilage is generally regarded as an avascular tissue (Benjamin and Evans, 1990; Koch and Tillmann, 1995; Petersen *et al*., 2002). The lack of blood vessels is related to its compression tolerance, for vessel lumena would be closed by pressure. Avascularity must also be promoted by the presence of antiangiogenic factors and, indeed, chondromodulin 1, a potent anti-angiogenic factor in hyaline cartilage (Hiraki *et al*., 1997), has been reported in the anulus fibrosus (Takao *et al*., 2000). Furthermore, vascular endothelial cell growth factor (VEGF) is downregulated in the fibrocartilaginous, wrap-around region of the tibialis posterior tendon (Petersen *et al*., 2002) and tissue inhibitors of matrix metalloproteinases (TIMPs; Kapila and Xie, 1998) and thrombospondin (Miller and McDevitt, 1991) have been found in meniscal fibrocartilage. TIMPs are ancient eukaryotic proteins that include four distinct isoforms, and TIMPs 1 and 2 are known to have anti-angiogenic properties in other tissues (Brew *et al*., 2000; Gomez *et al*., 1997). The thrombospondins are currently attracting considerable attention because of their potential as antiangiogenic, therapeutic agents for treating tumors (Vailhe and Feige, 2003).

The IV disc is regarded as the largest avascular tissue in humans (Eyre *et al*., 2002; Ishihara and Urban, 1999; Urban *et al*., 2001) and, as with other fibrocartilages, its lack of blood vessels is a limiting factor determining the number of viable cells (Horner and Urban, 2001). As with any avascular tissue, IV disc cells depend on diffusion from adjacent tissues for their survival and their metabolism is typically anaerobic. As a result of lactic acid accumulation during glycolysis, the pH around the cells is low (Urban, 2001). Razaq *et al*. (2000) have suggested that this is of central importance in ECM turnover—perhaps mediated by changes in intracellular pH. A key nutrient pathway for the IV disc is via its cartilage end plate (Fig. 2a). If this becomes calcified, as in patients with scoliosis, the nutrient supply to the disc cells is compromised and degeneration is likely to ensue (Bibby *et al*., 2001).

D. Fibrocartilage Innervation

Nerve fibers immunoreactive for calcitonin gene-related peptide (CGRP) have been reported in several tissues in the rat that are generally regarded as "fibrocartilaginous." These include the IV disc, knee joint menisci, and the articular disc of the temporomandibular joint (TMJ; Schwab and Funk, 1998). The presence of neural elements has also been documented in the triangular fibrocartilage complex of the human wrist (Ohmori and Azuma, 1998). However, where nerve fibers are present in any of these fibrocartilages, they are usually most typical of the more fibrous regions of the tissue

(Gray, 1999; Kaapa *et al*., 1994; Kojima *et al*., 1990; Mine *et al*., 2000; Palmgren *et al*., 1999). The general paucity of nerve fibers in fibrocartilage itself may be associated with the presence of aggrecan, for Johnson *et al*. (2002) have shown that this inhibits the outgrowth of neuronal processes *in vitro*. Nevertheless, nerve fibers have been documented in the enthesis fibrocartilage of rabbit knee joint menisci (Gao *et al*., 1994).

E. Structure of Fibrocartilage Cells

1. General Cell Structure

Fibrocartilage cells often lie in lacunae (Fig. 3) that are presumed to be shrinkage artifacts, as in hyaline articular cartilage. Such a detachment of cells from the ECM probably relates to the inadequate preservation of their pericellular matrix by routine processing. On occasion, several cells can occupy the same lacuna and this is likely to reflect cell division with little ensuing ECM synthesis.

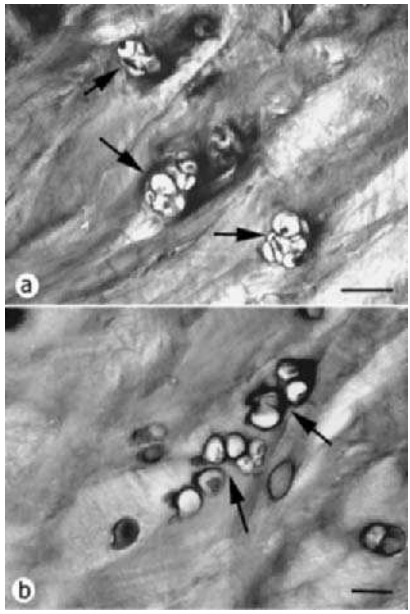

FIG. 3 Clusters of fibrocartilage cells (arrows) from the human Achilles (a) and biceps brachii (b) tendons. Such clusters are common in tendons and ligaments and are reminiscent of the groups of cells that are found in articular cartilage in the early stages of osteoarthritis. Note that the cells are shrunken within lacunae and that the fibrocartilage cells in (b) are surrounded by a strongly staining territorial ECM. Bars: (a) 50 μm; (b) 20 μm. Toluidine blue.

Like chondrocytes, enthesis fibrocartilage cells are generally round or oval, isolated within their ECM, and have little or no direct contact with each other. This is evidenced by the lack of gap junctional communication between enthesis fibrocartilage cells in the rat Achilles tendon (Ralphs *et al.*, 1998). In contrast, adjacent fibroblasts in the tensional part of the tendon form an elaborate three-dimensional network of cells that do communicate with each other by gap junctions, both between and within the longitudinal rows of cells (McNeilly *et al.*, 1996). As gap junctional communication is a well-known feature of osteocytes (Donahue, 2000), the isolation of fibrocartilage cells creates a barrier to direct communication between bone and tendon cells (Ralphs *et al.*, 1998). Martin *et al.* (2003) have speculated that the rounded form of tendon fibrocartilage cells shows that they are less strongly attached to the pericellular ECM than the spindle-shaped tendon fibroblasts. They suggest that this may be an adaptation to minimize cell deformation during tendon compression.

Ultrastructurally, tendon and periosteal fibrocartilage cells have many features typical of chondrocytes in hyaline cartilage—dilated rough endoplasmic reticulum, glycogen granules, lipid droplets, and numerous intermediate filaments (Rufai *et al.*, 1996). In the cells of the rat suprapatella (a fibrocartilage on the deep surface of the quadriceps tendon in many mammals), glycogen and lipid accumulate with age, and whorls of intermediate filaments become particularly prominent (Benjamin *et al.*, 1991). According to Le Graverand *et al.* (2001a), meniscal fibrocartilage cells can occasionally be ciliated and have centrosomes.

In pathological tissue, fibrocartilage cells can be arranged in cell clusters (Fig. 3) similar to those characteristic of early osteoarthritic, hyaline articular cartilage (Hough, 2001). These clusters have been described in several tendon and ligament entheses (Kumai and Benjamin, 2002; Moriggl *et al.*, 2003; Rufai *et al.*, 1995), IV discs (Johnson *et al.*, 2001), and menisci (Le Graverand *et al.*, 2001b). Those at the calcaneal enthesis of the plantar fascia in humans are particularly intriguing, for they occur at a fibrocartilaginous enthesis that is directly weight bearing and thus comparable to an articular cartilage (Kumai and Benjamin, 2002). This analogy is further strengthened by the association of clusters with other degenerative changes typical of osteoarthritic cartilage—that is, fissuring of the matrix and peripheral osteophytes at the margin of the enthesis fibrocartilage. However, it should be noted that chondrocyte clustering can also be seen in normal articular cartilage—even in the ankle joint, where osteoarthritis is rarely reported (Schumacher *et al.*, 2002).

Le Graverand *et al.* (2001b) have proposed a mechanism for cluster formation within the rabbit meniscus from knees in which the anterior cruciate ligament (ACL) has been transected. Disruption of a cellular network of meniscal cells by apoptosis isolates groups of cells within the ECM.

These assume a more chondrogenic phenotype, divide, and form the characteristic clones. The increase in cluster size with time probably reflects continued cell division, and it is not surprising that cluster cells in the IV disc immunolabel for proliferating cell nuclear antigen (Johnson *et al*., 2001). Intriguingly, such cells communicate with each other via gap junctions that contain connexin 43 (Le Graverand *et al*., 2001b). This is in contrast to enthesis fibrocartilage cells in the rat Achilles tendon, which are isolated within the ECM (Ralphs *et al*., 1998). As there is no comparable model for triggering degenerative disease at entheses, it is not possible to say whether fibrocartilage cell clusters in tendons and ligaments also increase in size with time. It seems unlikely that their formation involves any modulation of cells from a fibroblastic to a fibrocartilaginous phenotype, for the clusters develop within a region that is already fibrocartilaginous (Rufai *et al*., 1995a).

The strong expression of cluster cells in menisci for type X collagen suggests that the surrounding ECM is calcified (Le Graverand *et al*., 2001b), as in osteoarthritic articular cartilage (Boos *et al*., 1999). The onset of calcification may be associated with the local degradation of aggrecan, for there is a strong link in articular cartilage between the presence of matrix-degrading enzymes and chondrocytic clusters (Chubinskaya *et al*., 1998). Yet, related evidence is conflicting. Most reports, whether based on *in vivo* (Shapses *et al*., 1994) or *in vitro* (Eanes *et al*., 1992; Sun and Kandel, 1999) studies, have shown that aggrecan gene expression is downregulated in association with calcification. However, Mwale *et al*. (2002) have shown that aggrecan is retained *in vivo* around chondrocytes from the bovine fetal physis, immediately before calcification. They argue that aggrecan may even promote calcification, rather than inhibit it.

2. Cytoskeleton and Cell–Matrix Interactions

The fibrocartilage cell phenotype, and the ability of such cells to migrate, differentiate, and promote the growth of the tissue as a whole, must depend on adhesive interactions between the cells and the ECM that surrounds them—that is, the pericellular matrix. In the chondrocytes of articular cartilage, a key cell surface receptor for matrix interactions is CD44. This binds to hyaluronan (HA) in the ECM, which in turn binds to aggrecan, ensuring that the proteoglycan (PG) is locally concentrated around the cells (Nofal and Knudson, 2002). Once a pericellular matrix is established, this could have a nucleating influence as a template for the subsequent development of territorial matrix (Schenk *et al*., 1986). This is often particularly characteristic of fibrocartilage (Fig. 1b). In addition, as the pericellular matrix is likely to have a mechanical role in modifying the principal stresses and strains relating to chondrocytes (Guilak and Mow, 2000), it probably has a similar effect on fibrocartilage cells as well. Nofal and Knudson (2002) have suggested that

the pericellular ECM could act as a reservoir for the absorption and release of macromolecules. This function could be compromised if the cells cannot interact normally with their matrix.

As the cytoskeleton is believed to play a key role in ECM interactions (Benjamin *et al*., 1994; Nofal and Knudson, 2002), the large numbers of intermediate filaments in fibrocartilage cells may be particularly significant (Izumi *et al*., 2000; Merrilees and Flint, 1980; Ralphs *et al*., 1991, 1992; Rufai *et al*., 1992; Tischer *et al*., 2002). Typically, these filaments immunolabel for vimentin, but they may also contain cytokeratins and glial fibrillary acidic protein (Kasper and Stosiek, 1990). Intermediate filaments are believed to be of mechanical significance and could confer compression tolerance on the cells themselves and/or relay information about changes in the ECM via their association with integrins in the cell membrane (Benjamin *et al*., 1994). Their numbers are increased in fibrocartilage cells in experimental osteoarthritis that is induced by perforating the articular disc of the rabbit TMJ (Lang *et al*., 1993).

In some tissues at least, fibrocartilage cells can also contain α-smooth muscle actin, a nonpolymerized form of actin (Ahluwalia *et al*., 2001; Kambic *et al*., 2000; Leonardi *et al*., 2002; Mueller *et al*., 1999). Cai *et al*. (2001) have suggested that this may be associated with the putative differentiation of fibrocartilage cells from mesenchymal stem cells in the bone marrow, for these stem cells also express this protein. On the other hand, actin stress fibers are a prominent feature of cells in the outer part of the developing anulus fibrosus (Hayes *et al*., 1999). Here, they direct cell elongation and control the deposition of oriented ECM via junctional complexes that involve vinculin and $\alpha_5\beta_1$-integrins. This in turn promotes the formation of oriented fibronectin at the cell surface and regularly aligned collagen fibrils between the cells. Immediately after birth, actin stress fibers disappear, as fibrocartilage cells differentiate within the developing anulus. Thus, stress fibers are not a feature of normal adult IV discs, but are responsible for the organization of its fibrocartilage cells during early development. According to Leonardi *et al*. (2002), actin synthesis is upregulated in the cells of TMJ discs that show evidence of degenerative change, and Kambic *et al*. (2000) have reported increased levels of actin during the repair of knee joint menisci. The actin cytoskeleton is known to be of key importance in maintaining a chondrocytic phenotype (Daniels and Solursh, 1991).

III. Synthesis of Extracellular Matrix

Fibrocartilage cells can synthesize a wide variety of ECM molecules, not only during the development of the tissue, but also in its fully differentiated state. This is in line with the view that fibrocartilage is a dynamic tissue that

responds to changes in cytokine and mechanical factors (Robbins *et al.*, 1997). The ECM molecules synthesized by fibrocartilage cells include numerous collagens and PGs, together with various noncollagenous proteins and glycoproteins. Collectively, these not only influence the physical properties of the ECM, but also provide a reservoir for storing various growth factors. This is one of the ways by which the ECM can influence the growth and differentiation of the cells within it (Iozzo, 1999) and thus maintain the fibrocartilage phenotype.

A. Collagens

Collagens are a major component of the ECM of all connective tissues and more than 20 types (the product of 33 genes) are currently recognized (Myllyharju and Kivirikko, 2001). They are characterized by the presence of at least one domain with a triple helix—known as a COL domain. The helix consists of three polypeptide α chains that wind around each other.

Collagens are broadly classed as fibrillar or nonfibrillar (Ayad *et al.*, 1998). As their name suggests, the former comprise molecules that aggregate together to form fibrils, whereas the latter is a diverse collection of collagens that do not aggregate in the ECM in this way. The fibrillar collagens include types I, II, III, V, and XI and are associated with 10 distinct polypeptide chains (Ottani *et al.*, 2002). Several subtypes of nonfibrillar collagens are recognized, including the FACIT (fibril-associated collagens with interrupted triple helices) collagens that sit on the surface of collagen fibrils (van der Rest *et al.*, 1991). They include types IX, XII, XIV, XVI, and XIX collagens. In fibrillar collagens, the fibrils form highly ordered, quarter-staggered polymers in the ECM and the overlapping form contributes substantially to their high tensile strength. Fibrillar collagens are synthesized as procollagen precursor molecules and assembled into fibrils in the ECM after the proteolytic digestion of terminal propeptides.

The fibrillar collagens are of particular importance in fibrocartilage and all have been reported in one tissue or another. In its most typical form, fibrocartilage is characterized by its dual content of types I and II collagen. However, the relative proportions of these collagens can vary. Thus, knee joint menisci contain more type I collagen than type II (McDevitt and Webber, 1990), whereas the anulus fibrosus contains roughly equal quantities of both (Eyre *et al.*, 2002) and osteophytic fibrocartilage is reputed to lack type I collagen (Aigner *et al.*, 1995). Some fibrocartilages contain type IIA collagen, which is normally more characteristic of noncartilaginous tissues (Zhu *et al.*, 2001). Both types I and II collagens can form heterofibrils: type I is associated with type V and/or type III, and type II collagen with type XI (Kielty *et al.*, 1993). Whether the same fibrocartilage cell can synthesize

both types I and II collagen probably varies according to the tissue. The *in situ* hybridization study of Perez-Castro and Vogel (1999) suggests that some fibrocartilage cells in the wrap-around region of the bovine deep flexor tendon can synthesize both. They found that mRNAs for types I and II collagen were present in 75 and 50% of cells, respectively. This must mean that at least 25% of the cells are synthesizing both. It is also possible that a single cell can synthesize both collagens, but at different stages of tissue differentiation. This could be occurring in the fibrocartilaginous rat suprapatella, which expresses only type II collagen in old age (Benjamin *et al.*, 1991). The same fibrocartilage cell could also produce both collagens in the anulus fibrosus of the IV disc. As type I collagen is expressed there before type II, this would account for the pericellular location of type II collagen in adult rat discs. It is also unclear whether both types I and II collagen can be found in the same fibril. This again probably varies from site to site, but in rabbit knee joint menisci (Bland and Ashhurst, 1996), and the rat anulus fibrosus (Hayes *et al.*, 2001), immunohistochemical studies suggest that there is little overlap in distribution.

Nonfibrillar collagen types have been well documented at several sites, for example, IV discs (Eyre *et al.*, 2002), ligament and tendon fibrocartilage (Koch and Tillmann, 1995; Milz *et al.*, 1998, 1999, 2001, 2002a; Sagarriga Visconti *et al.*, 1996), and menisci (Landesberg *et al.*, 1996). These include FACIT (types IX and XII) and network-forming collagens (types VI and X). Type VI collagen is a thin, beaded, filamentous collagen that can also form hexagonal networks (Wiberg *et al.*, 2002). It is present in most tissues and has been reported in many tendon fibrocartilages, where it typically has a pericellular distribution, as in articular cartilage (Felisbino and Carvalho, 1999; Milz *et al.*, 1998, 1999, 2000, 2001, 2002a). Its expression is upregulated in osteoarthritis (Pullig *et al.*, 1999) and wound healing (Oono *et al.*, 1993), suggesting that it has a role in maintaining tissue integrity and in connective tissue remodeling. According to Araujo *et al.*, (2002), the presence of chondroitin and dermatan sulfate is essential for its assembly, because the treatment of meniscal fibrocartilage cells with chondroitinase ABC disrupts its formation and creates pericellular spaces. The pericellular location of type VI collagen suggests that it may be important in enabling fibrocartilage cells to interact with PGs.

Although type IX collagen probably accounts for only a small proportion of the total collagens in any fibrocartilage, the phenotypic consequences of mutations suggest that it is important in the IV disc, although its exact role is less clear (Eyre *et al.*, 2002). It is a FACIT collagen that is also considered a PG because of its glycosaminoglycan (GAG) component (Roughley and Lee, 1994). It lies on the surface of type II/XI heterofibrils and is presumably important for stabilizing the fibrils, binding them together or connecting them to PGs (Buckwalter and Mankin, 1997). Type III collagen is often

implicated in tissue repair, for it may be capable of cross-linking types I and II collagens and stabilizing delicate repair tissue (Liu *et al*., 1995). Type XII collagen may also be important, for there is a marked increase in its expression in healing fibrocartilaginous entheses (Thomopoulos *et al*., 2002). These authors suggest that it strengthens the lateral interactions between type I collagen fibrils, or between these fibrils and the amorphous ECM.

Type X collagen is a short-chain, network-forming collagen, typical of the hypertrophic chondrocytes of epiphysial growth plates (Chan and Jacenko, 1998) and articular fibrocartilage (Rabie and Hagg, 2002). Its appearance precedes the onset of endochondral ossification and thus it may play a role in events associated with that process—that is, mineralization, vascular invasion, matrix stabilization, or the creation of a red bone marrow environment (Jacenko *et al*., 2001). It has also been identified in the zone of calcified fibrocartilage at entheses (Fujioka *et al*., 1998; Fukuta *et al*., 1998; Niyibizi *et al*., 1996) and in association with normal and pathological menisci (Bluteau *et al*., 1999; Le Graverand *et al*., 2001b). Its presence at insertion sites is particularly intriguing, for it has been suggested that enthesis fibrocartilage acts as a miniature growth plate during development (Gao *et al*., 1996; Knese and Biermann, 1958). Its expression in rabbit menisci is increased in the osteoarthritis (OA)-induced joints of ACL-transected knees (Bluteau *et al*., 2001). It is conspicuous around the cartilage cell clusters that develop in OA and it is probably significant that the ECM around such clusters is commonly calcified (Le Graverand *et al*., 2001b). Nevertheless, despite the common association between type X collagen and matrix calcification, this molecule is not universally present in calcified fibrocartilage or, indeed, calcified hyaline cartilage. It is reputably absent from the peripheral fibrocartilaginous regions of costal cartilage (which typically begin to calcify during the second decade of life) associated with the human first rib (Claassen *et al*., 1996) and from the deep calcified layer of articular cartilage in normal synovial joints (Boos *et al*., 1999). Whether any such failures to detect type X collagen immunohistochemically reflect technical difficulties (e.g., epitope masking) is unclear, although prolonged pretreatment of sections with hyaluronidase has been associated with the demonstration of type X collagen in uncalcified articular cartilage (Lammi *et al*., 2002).

In certain fibrocartilages, the orientation of collagen fibers is highly regulated and determined early in development, before the appearance of any fibrocartilage cells. In adults, the fibrillar pattern can account for particular types of fibrocartilage injury—for example, delamination in the anulus fibrosus of the IV disc that is thought to be associated with repetitive interlaminar shear (Goel *et al*., 1995). The lamellae of the anulus contain collagen fibers that are arranged parallel to each other within each individual layer, but lie at right angles in adjacent lamellae. Hence, there is a conspicuous, criss-cross

pattern of type I collagen-rich fibers in the anulus that is governed by the preceding orientation of fibroblasts that subsequently differentiate into fibrocartilage cells (Hayes *et al*., 1999). It is not until after lamellae have been established that the fibroblastic cells of the outer anulus differentiate into fibrocartilage cells. This is probably why type II collagen labeling in IV discs is restricted to the vicinity of the cells themselves (Hayes *et al*., 2001). Although this may be an example of the same cell synthesizing both types I and II collagen (see above), it seems likely that these collagen types are not secreted simultaneously, but sequentially at different stages in the differentiation of the fibrocartilage cell. This is probably also what happens at tendon entheses and menisci. In fibrocartilaginous tendon or ligament entheses, there are often parallel bundles of collagen fibers directed toward the hard tissue interface and the rows of fibrocartilage cells between them develop by the metaplasia of fibroblasts (Gao *et al*., 1996). The menisci of the knee joint are also characterized by highly ordered arrangements of collagen fibers (Petersen and Tillmann, 1998). Nevertheless, there are other fibrocartilages where there is a less orderly arrangement of collagen fibers. This has been described as a ''grid-fibrous'' arrangements of fibers in the fibrocartilage covering the mandibular condyle in humans (Luder 1997, 1998) and as a ''basketweave'' arrangement in the wrap-around fibrocartilage of tendons (Benjamin and Ralphs, 2000).

B. Proteoglycans

PGs are composed of GAG side chains organized around a central core protein. A distinction is made between large, aggregating and small, leucine-rich PGs (Iozzo and Murdoch, 1996). The former comprise aggrecan, versican, neurocan, and brevican (Iozzo, 1998; Wight, 2002) and are collectively referred to as ''lecticans'' or ''hyalectans'' for they have globular domains that bind HA and a C-type lectin motif that binds to other proteins in the ECM (Iozzo and Murdoch, 1996; Ruoslahti, 1996). The small, leucine-rich proteoglycans (SLRPs—pronounced ''slurps'') are an ever-expanding family of molecules characterized by a central protein domain of leucine-rich repeats, on either side of which are two cysteine-rich regions (Iozzo and Murdoch, 1996). They include decorin, biglycan, lumican, fibromodulin, keratocan, osteoadherin, epiphycan, mimican, asporin, opticin, and PRELP (proline/arginine-rich, end leucine-rich repeat protein) (Henry *et al*., 2001; Iozzo, 1998, 1999; Reardon *et al*., 2000). The archetypal SLRP is decorin, but the status of PRELP and asporin as PGs is uncertain (Iozzo, 1998; Reardon *et al*., 2000). Many, but not all, of the SLRPs have been reported in fibrocartilage cells and as with the large aggregating PGs, they are likely to be multifunctional molecules capable of inducing numerous pleiotropic

responses, yet also showing evidence of functional redundancy (Reardon *et al.*, 2000).

The GAG chains of PGs are long, unbranched polysaccharides that consist of repeating disaccharide units, each of which has an amino sugar. They have an abundance of negatively charged sulfate or carboxyl groups and thus attract a balancing population of cations into the tissue. This increases osmolarity (i.e., creates a Donnan effect), which in turn promotes the retention of water (Buckwalter and Mankin, 1997). Hyaluronan, chondroitin, keratan, dermatan, and heparan sulfates are some of the GAGs that have been reported in the many tendon fibrocartilages investigated by ourselves and our collaborators (Benjamin *et al.*, 1993a; Boszczyk *et al.*, 2001; Gao *et al.*, 1996; Lewis *et al.*, 1998; Milz *et al.*, 1998, 1999, 2000, 2001; Moriggl *et al.*, 2001; Ralphs *et al.*, 1991; Rufai *et al.*, 1992; Tischer *et al.*, 2002; Waggett *et al.*, 1998). They have often been demonstrated before the PGs with which they are associated.

1. Large Aggregating Proteoglycans

Both aggrecan and versican have been detected in several fibrocartilages (see Benjamin and Ralphs, 1998, and Benjamin and McGonagle, 2001, for a review). They often have a reciprocal distribution in relation to fibrillar collagens. Thus, in the developing rat IV disc, versican is associated with regions that immunolabel strongly for type I collagen, and aggrecan with type II collagen-rich regions (Hayes *et al.*, 2001). A similar association has been noticed in the human Achilles tendon enthesis (Waggett *et al.*, 1998).

Aggrecan is particularly important as a "water-trapping" molecule in both hyaline and fibrocartilage and is confined in the ECM when the tissue is compressed, by a cohesive meshwork of collagen fibrils (Buckwalter and Mankin, 1997). This functional association between the ECM molecules probably accounts for the compression-tolerating and stress-dissipating role of enthesis fibrocartilage (see Benjamin and McGonagle, 2001, for a review). However, like other PGs, aggrecan is likely to have a number of other important functions in fibrocartilage. Its gel-like properties could enable it to immobilize ECM proteins or restrict their actions, it could block their activity by steric hindrance, protect them from matrix-degrading enzymes, or act as a reservoir for their delayed release. Aggrecan is synthesized intracellularly as PG monomers, rich in keratan and chondroitin sulfate side chains that are attached to a protein core. The monomers are then assembled within the ECM into large aggregates by the link proteins that connect the G1 one domains of aggrecan to HA in a noncovalent manner (Hascall and Sajdera, 1970). In articular cartilage at least, more than 300 aggrecan monomers can be associated with a single supramolecular complex (Buckwalter and Rosenberg, 1983). However, these modular units do not

immediately aggregate with HA, and their speed of incorporation into the characteristic supramolecular complexes varies with age (Bayliss *et al.*, 2000; Oegema, 1980). Some of the large, but nonaggregating PGs in both articular cartilage and fibrocartilage probably represent degradation products of aggrecan (Buckwalter *et al.*, 1994; Heinegård and Sommarin, 1987).

Versican is most typically secreted by fibroblasts and is thus the characteristic large, aggregating PG found in the purely tensional, dense fibrous connective tissue regions of tendons and ligaments (Campbell *et al.*, 1996). However, it is also present in fibrocartilages, including those of the IV disc (Melrose *et al.*, 2001) and knee joint menisci (Le Graverand *et al.*, 1999), and is additionally expressed by smooth muscle cells (Yao *et al.*, 1994). It is thought to have a number of diverse functions. Like aggrecan, it can bind to HA to form highly hydrated, supramolecular aggregates (Roughley and Lee, 1994) and thus may contribute to swelling pressure. Versican can stimulate cell proliferation, promote (via its G1 domain) and inhibit (via its G3 domain) cell adhesion, and influence cell shape by enhancing pericellular matrix synthesis (Wight, 2002). Thus, the presence of versican at key developmental stages in the IV disc could allow the cells to proliferate and condense into anlagen, and then by its disappearance it could promote chondrogenic differentiation in the anulus (Hayes *et al.*, 2001). Both versican and aggrecan have a C-type, lectin-like moiety in the G3 domain that has been shown to bind other ECM molecules—for example, fibulins 1 and 2 (Aspberg *et al.*, 1999; Olin *et al.*, 2001).

2. Small, Leucine-Rich Proteoglycans

The SLRPs have fewer GAG chains and a shorter protein core, and occupy less volume in the ECM than the large, aggregating supramolecular complexes of PGs (Buckwalter and Mankin, 1997). Unlike the latter, they are not thought to influence the physical properties of connective tissues directly, but to play a dual indirect role via their effect on collagen fibrillogenesis and their cytokine-binding properties (Iozzo, 1997). At least three SLRPs (decorin, fibromodulin, and lumican) can delay the formation of fibrils in *in vitro* assays (Iozzo, 1998). In each case, it is the core protein rather than the GAG side chains that seems critical for fibril interactions. It binds fibrillar collagens at the site of the gaps between the staggered fibrils (Iozzo, 1997). In contrast, the extending GAG side chains are thought to maintain interfibrillar space and thus contribute to controlling tissue hydration (Iozzo, 1997; Scott, 1995).

Decorin is generally upregulated, and biglycan downregulated, by transforming growth factor β (TGF-β) (Iozzo, 1998). Consequently, these SLRPs may modulate the bioavailability and stability of cytokines in the ECM (Redini, 2001). They can also influence the activity of cytokine receptors

(Santra *et al.*, 2002) and are thought to be implicated in matrix turnover (Iozzo, 1998). Different isoforms exist and it is reasonable to assume that these differ in their cytokine-binding activity (Tufvesson *et al.*, 2002). Many of the SLRPs colocalize and interact with fibrillar collagens and can inhibit the lateral growth of fibrils that form spontaneously during *in vitro* assays (Chakravarti *et al.*, 1998). It seems that the core protein of decorin, rather than its GAG side chains, mediates the role of decorin in fibrillogenesis (Iozzo, 1999). Mice homozygous for null mutations produced by the targeted gene disruption of decorin (Danielson *et al.*, 1997), lumican (Chakravarti *et al.*, 1998), and fibromodulin (Svensson *et al.*, 1999) all show clear structural alterations in their collagen fibrils. In both lumican and decorin knockout mice, the skin is loose and fragile (Chakravarti *et al.*, 1998; Iozzo, 1999), and in lumican knockout mice, at least, it is reminiscent of that in patients with Ehlers-Danlos syndrome (Chakravarti *et al.*, 1998).

Decorin is synthesized by fibrocartilage cells in both tendons and IV discs (Melrose *et al.*, 2001; Perez-Castro and Vogel, 1999), although it disappears as fibrocartilage develops with age in the center of the rabbit meniscus (Kavanagh and Ashhurst, 2001) and is more typical of the fibrous than fibrocartilaginous parts of the TMJ disc (Mizoguchi *et al.*, 1998). Like fibromodulin, it binds to type II collagen (Hedbom and Heinegård, 1989, 1993) and numerous functions have been suggested for it. In addition to a role in modulating fibrillogenesis in connective tissues by organizing and stabilizing the type II collagen network (Keene *et al.*, 2000; Neame *et al.*, 2000; Vogel and Trotter, 1987; Vogel *et al.*, 1984), it may also be involved in controlling angiogenesis (Davies *et al.*, 2001; Kinsella *et al.*, 2000), inhibiting soft tissue calcification (Scott and Haigh, 1985), and regulating tumor growth, by acting as an antagonist to epidermal growth factor receptor (Santra *et al.*, 2002).

Biglycan has been reported in numerous tendon fibrocartilages, including the wrap-around fibrocartilage of the bovine deep flexor tendon (Evanko and Vogel, 1990), the compressed malleolar region of the human tibialis posterior tendon (Vogel *et al.*, 1993), and the insertions of the human Achilles (Waggett *et al.*, 1998) and supraspinatus (Thomopoulos *et al.*, 2002) tendons. It has also been reported in the articular disc of the TMJ (Mizoguchi *et al.*, 1998; Scott *et al.*, 1995) and in developing ovine IV discs (Melrose *et al.*, 2001). In contrast to decorin (which has a single dermatan sulfate side chain), biglycan has two such chains (Roughley and Lee, 1994). It also has a striking ability to organize type VI collagen into hexagonal networks (Wiberg *et al.*, 2002)—a collagen that is typical of many fibrocartilages (see above). The functions of biglycan are even less well understood than those of decorin, although biglycan "knockouts" develop an osteoporotic phenotype (Iozzo, 1999). Whether this is directly related to altered collagen fibrillogenesis in the bone is unclear. The prominence of biglycan in fetal tissues

(Melrose *et al*., 2001) suggests a role in controlling the fibrillogenesis of collagen or elastic fibers during development. It is thus worth noting that Reinboth *et al*. (2002) have shown that biglycan forms a ternary complex with tropoelastin and microfibril-associated glycoprotein 1 (MAGP-1) and suggested that it controls the elastinogenic phase of elastic fiber formation. It may also be significant that its expression is upregulated in surgically repaired fibrocartilaginous entheses, at a time when decorin expression is downregulated (Thomopoulos *et al*., 2002).

Lumican has been found in both the anulus fibrosus and nucleus pulposus of human lumbar IV discs (Sztrolovics *et al*., 1999). In early development, it is particularly characteristic of the nucleus, although there is an age-related increase in the anulus fibrosus of juveniles. Hence by adulthood, there are comparable quantities in both major regions of the disc. Fibromodulin is widespread and in the lumbar IV discs it becomes more prominent with increasing degeneration (Sztrolovics *et al*., 1999). In the anulus fibrosus, there is an age-related change toward a form of fibromodulin that lacks keratan sulfate in its glycoprotein.

A particularly intriguing PG that has attracted attention is superficial zone protein. This has now been renamed proteoglycan 4 (PRG4) and it is thought to be the same molecule as lubrican (Jay *et al*., 2001). It was originally isolated from the culture medium of explants derived from the superficial zone of bovine articular cartilage (Schumacher *et al*., 1994), but it is also conspicuous at the surface of fibrocartilaginous wrap-around tendons, where its expression increases with age (Rees *et al*., 2002). In contrast to other PGs in cartilage, PRG4 is not tightly bound within the ECM, for it is released into synovial fluid. It may have a role in lubrication and be important for preventing cell attachment to articular surfaces—whether in wrap-around tendons or in the articular cartilages of synovial joints. This hypothesis is supported by the finding that increased tendon adhesion occurs in the intrasynovial regions of human tendons in patients with camptodactyly–arthropathy–coxa vara–pericarditis (CACP) syndrome (Ochi *et al*., 1983). Mutations in the CACP gene have been identified as the cause of CACP (Marcelino *et al*., 1999). The same gene encodes a protein homologous to PRG4 (Flannery *et al*., 1999; Jay *et al*., 2000).

C. Noncollagenous Proteins and Glycoproteins

Less attention has been paid to the noncollagenous proteins/glycoproteins of hyaline or fibrocartilage. Annexin V (also called annexin A5 or anchorin II) is a cell surface protein, which binds cell surfaces to collagen in the ECM in several connective tissues, including articular cartilage (Pfaffle *et al*., 1990). Although it has not yet been reported in fibrocartilage, its importance in

regulating apoptosis and matrix vesicle-initiated calcification of hyaline cartilage (von der Mark and Mollenhauer, 1997) makes it likely that it is present here as well. It is also significant that annexin V is upregulated in osteoarthritic hyaline cartilage (Mollenhauer *et al.*, 1999), for the fibrocartilages asociated with tendon entheses can show parallel degenerative changes (see Benjamin and McGonagle, 2001, for a review).

1. Tenascin-C

Tenascin-C is a large, multifunctional ECM glycoprotein with a hexameric structure. Its expression in a variety of tissues is often transient and restricted during embryonic development, but it can be reexpressed in adults during both normal and pathological tissue remodeling (Jones and Jones, 2000). Intriguingly, its production by enthesis fibrocartilage cells at the osteotendinous junction of the rat quadriceps tendon can be modulated by changes in mechanical load (Jarvinen *et al.*, 1999). This suggests that it may be a mediator of adaptive responses. In normal rats, tenascin is abundantly expressed at the hard–soft tissue interface, but when the knee joints of animals are cast-immobilized for 3 weeks, immunohistochemical labeling for tenascin-C disappears. However, with intensive programs of remobilization, tenascin expression can be restored to normal levels. Martin *et al.* (2003) have suggested that the antiadhesive properties of tenascin-C enable fibrocartilage cells to resist compression by promoting a loose attachment of cells to the ECM. They argue that this is why the molecule is more characteristic of compressed than tensional segments of bovine flexor tendons. The modulation of tenascin-C expression by altered mechanical strain has also been reported in several other cell types—neonatal rat heart muscle cells, chick embryo fibroblasts, vascular smooth muscle cells, and rat bone (see Jones and Jones, 2000, for a review). Intriguingly, no detectable gross anatomical or histological abnormalities have been reported in tenascin-C knockout mice (Saga *et al.*, 1992). This perhaps suggests that the functions of tenascin-C can also be performed by related tenascin molecules.

2. Elastin

Although relatively little attention has been directed to elastic fibers in fibrocartilage, our own observations (Milz and Benjamin, unpublished observations) and those of others suggest that these fibers can be prominent in tendon and IV disc fibrocartilage. At first sight, this conflicts with the comments of Kielty *et al.* (2002) that elastic fibers are not characteristic of tendon. However, their remarks probably apply more to the tensional regions of tendons than their compressive, wrap-around regions, for elastic fibers have now been demonstrated in frog (de Carvalho and Campos Vidal

Bde, 1995) and mammalian tendon fibrocartilages (Covizi, 2001; Ritty *et al*., 2002). They are also present in mammalian IV discs (Yu, 2002). At both sites, they probably help to restore tissue shape after deformation of the tendon under load (De Carvalho and Campos Vidal Bde, 1995).

Elastic fibers consist of a scaffold of fibrillin-containing microfibrils around which the amorphous elastin component can be organized (Kielty *et al*., 2002). The elastin molecule itself is synthesized as the soluble precursor molecule tropoelastin, which is deposited on the surface of the microfibrils (Kielty *et al*., 2002). In IV discs, both the elastin and fibrillin constituents of elastic fibers have been demonstrated (Yu, 2002) and in mammalian, deep digital flexor tendons, microfibril-associated glycoproteins 1 and 2 (MAGPs 1–2) have been detected (Ritty *et al*., 2002).

3. Laminin

Laminin is a matrix glycoprotein associated with the control of cell adhesion and behavior. It is a major constituent of basement membranes, but has also been reported in pericellular association with fibrocartilage cells (Kolts *et al*., 1994). In developing rat IV discs, laminin is present in the nucleus pulposus at embryonic day 16 (E16), and is weakly detected in the inner anulus (Hayes *et al*., 2001). By E20, it is present throughout the disc in association with type IV collagen, and forms a series of basement membrane-like structures between the cell sheets of the outer anulus. This may relate to the ability of each cell to deposit and organize its own individual collagenous lamella (Hayes *et al*., 2001). As the laminin-binding proteins on endothelial cell surfaces may be important in detecting changes in shear forces associated with altered blood flow rates (Gloe and Pohl, 2002), this protein could play a similar role in fibrocartilage, for this tissue must also be capable of withstanding shear.

D. Calcified Fibrocartilage

Although calcification can occur pathologically in knee joint menisci and other articular discs (Berger and Buckwalter, 1990), it is also a normal feature of all fibrocartilages that are attached to bone, including enthesis fibrocartilage and the articular fibrocartilage of synovial joints (Benjamin and Ralphs, 1998; Benjamin *et al*., 2002). The calcified fibrocartilage is typically separated from the unmineralized tissue by a calcification front known as the tidemark (Fig. 1a), as in articular hyaline cartilage (Broom and Poole, 1982). In epiphyseal tendons and ligaments that attach to bone adjacent to articular cartilage, the two tidemarks are directly continuous with each other (Benjamin *et al*., 1986). In a normal enthesis, the calcified fibrocartilage is avascular, the tidemark straight, and the bone–fibrocartilage junction highly

irregular. The latter interface is the true tissue boundary and its irregularity increases resistance to shear between tendon/ligament and bone and the surface area for diffusion between the two tissues. The computer modeling studies of Milz *et al.* (2002b), on the enthesis of the human Achilles tendon, suggest that three-dimensional overlap of the two tissues is a key factor in anchoring the tendon to the bone and thus in transferring tensile load from the former to the latter. In contrast, the tidemark simply represents a mechanical boundary between hard and soft tissues. It is where the soft tissues fall away from the bone during the maceration of a skeletal preparation (Benjamin *et al.*, 1986). Collagen fibers are continuous across the tidemark, but they do not extend across the cartilage–bone junction to any significant extent, wherever this is the site of an erosion front during development (Milz *et al.*, 2002b; Teshima *et al.*, 1999). The separation of the two boundaries is likely to be critical in promoting the stress-dissipating role of the calcified fibrocartilage zone.

Much of what we know about tidemarks and the underlying calcified zone comes from studies on hyaline cartilage rather than fibrocartilage. However, the observations of Oettmeier *et al.* (1989) on tidemark changes in osteoarthritic hyaline cartilage (tidemark duplication, interruption or absence and the spreading of calcification into what is normally uncalcified tissue) also apply to adjacent enthesis fibrocartilage in osteoarthritic shoulder joints (Harwood and Benjamin, unpublished observations). In articular hyaline cartilage, tidemark duplication has also been interpreted as a sign of ageing or calcified cartilage thickening after loading (see Havelka and Horn, 1995, for a review). However, multiple tidemarks can sometimes be present in normal articular cartilages from young adults (Havelka and Horn, 1995). Tetracycline labeling suggests that the tidemark is a region of rapid mineral turnover and there is enzyme–histochemical evidence to suggest that the cells remain viable even though they are embedded in a calcified ECM (Havelka and Horn, 1995). The overall thickness of the zone varies greatly from site to site. It is a dynamic characteristic that reflects the balance between encroaching calcification of the neighboring soft tissue by an advancing tidemark, and ossification at the tissue boundary as calcified fibrocartilage is eroded and replaced by bone. Thus, it seems likely that the zone of calcified fibrocartilage is remodeled in much the same way as the underlying subchondral bone (Norrdin *et al.*, 1999). Whether this is accelerated in periarthritis as in osteoarthritis is unclear. On occasion, authors have reported that the zone of calcified enthesis fibrocartilage increases in thickness with age (Gao *et al.*, 1994; Shea *et al.*, 2002). According to Shea *et al.* (2002), the areal contribution of calcified fibrocartilage to the cortical shell on the greater trochanter increases with age and thus the decreasing vascularity of the cortical shell may predispose this region to damage. This may have a particular bearing on hip fractures in the elderly.

E. ECM Turnover

The ECM of connective tissues can be degraded by a family of zinc-dependent enzymes called the matrix metalloproteinases (MMPs), or "matrixins," that includes collagenases (MMP-1), gelatinases (MMP-2, MMP-9), and stromelysins (MMP-3; Murphy and Reynolds, 1993). It can also be degraded by aggrecanases 1 and 2 (Caterson *et al.*, 2000). These are members of the ADAMTS (a disintegrin and metalloproteinase with thrombospondin motif) family of proteins. Both MMPs and ADAMTS are involved in the turnover of type II collagen and aggrecan. Both families of enzymes are thought to be important in tissue homeostasis, for they are expressed in the articular cartilage and menisci of normal rabbit knee joints as well as degenerate tissue (Bluteau *et al.*, 2001). The activity of MMPs is regulated by a group of inhibitor enzymes known as TIMPs (tissue inhibitor of metalloproteinases) that bind covalently to the matrix-degrading enzymes (Brew *et al.*, 2000; Woessner and Nagase, 2000). Matrix degradation occurs both during normal development and in pathological conditions such as osteo- and rheumatoid arthritis. MMPs are probably induced in response to increased levels of proinflammatory cytokines and the proteolytic fragments of ECM macromolecules such as collagens and fibronectin (Hu *et al.*, 2000). These degradative enzymes are expressed by fibrocartilage cells in the intraarticular disc of the TMJ (Breckon *et al.*, 1996) and by those in the articular cartilage covering the mandibular condyle (Tanaka *et al.*, 2000). At the latter site, there is a good correlation between the severity of osteoarthritis and the number of MMP-positive fibrocartilage cells. However, although gene expression for MMPs in rabbit knee joint menisci in experimentally induced OA is enhanced, aggrecanase gene expression remains stable (Bluteau *et al.*, 2001). This raises the possibility that aggrecanase activity is predominantly regulated at the posttranscriptional level.

Within the developing TMJ disc, fibrocartilage cells synthesize high levels of stromolysin and gelatinase A-B (Breckon *et al.*, 1996). This may suggest that remodeling of the ECM is necessary to accommodate an increasing number of cells in a tissue that is growing rapidly (Breckon *et al.*, 1996). On the other hand, it is important to interpret any evidence of MMP induction with caution, for as Hu *et al.* (2000) have pointed out, it does not necessarily mean that there is increased ECM degradation. MMPs are secreted in an inactive form (their activation hinges on the cleavage of a propeptide; Curran and Murray, 1999) and can be inhibited by TIMPs. Their activation also depends on the activation of other regulatory mechanisms, for example, the plasminogen–plasmin system and other active MMPs (Hu *et al.*, 2000).

Relaxin significantly decreases the collagen content of the fibrocartilage in the rat pubic symphysis, without changing the ratio of type I collagen to type II collagen (Samuel *et al.*, 1996). These authors showed that the effect is

antagonized by progesterone and suggested that relaxin plays a role in the ECM modification of the pubic symphysis that occurs during pregnancy. There are clear parallels with the ECM destruction of articular cartilage by matrix metalloproteases in patients with osteoarthritis (Steinetz and Lust, 1994). Intriguingly therefore, compounds with a chondroprotective effect on articular cartilage inhibit the symphyseal relaxation that is induced by relaxin (Steinetz and Lust, 1994). Furthermore, Kapila and Xie (1998) have sought to determine whether relaxin has any bearing on the greater prevalence of disease in the TMJ (which is lined by fibrocartilage) in women than men. Early passage fibrocartilage cells isolated from the articular surfaces of the joint showed a dose-dependent response to relaxin. MMP1 (collagenase 1) and MMP3 (stromelysin 1) expression was upregulated, but there was no effect on their inhibitors (TIMP 1 and 2). Interestingly, if the cells were primed with β-estradiol (which was used because TMJ disease is most typical of women in child-bearing years), the maximal modulation by MMP1 and MMP3 occurred at far lower concentrations of relaxin.

IV. Development of Fibrocartilage and the Influence of Mechanical Strain

A. Formation of Fibrocartilage

At all major sites where fibrocartilage is present, it forms relatively late in development and differentiates either from immature hyaline cartilage or dense fibrous connective tissue (Benjamin and Ralphs, 2000; Ralphs *et al.*, 1992). If new fibrocartilage forms in adults, its development is often regarded as a form of metaplasia. This may be controlled by parathyroid hormone-related peptide (PTHrP), Indian hedgehog (Ihh), bone morphogenetic protein 6 (BMP-6), and the receptors PTHR and Ptc. These have all been demonstrated in areas of hypertrophic chondrocytes that are related to osteophyte formation in the cervical spines of a mouse model of spondylosis (Nakase *et al.*, 2002). Cell division of fibrocartilage precursor cells may also contribute, for there is evidence to suggest that there is prominent labeling for proliferating cell nuclear antigen at the developing entheses of rat cruciate ligaments (Nawata *et al.*, 2002). Appropriate mechanical stimulation is critical to fibrocartilage formation. Its cells first appear in the TMJ disc of the rabbit, during the second week after birth, and a fully developed disc is established in conjunction with adult occlusion (Nagy and Daniel, 1992). When occlusal forces are increased experimentally by raising the bite on one side of the jaw, there is increased expression of aggrecan in the condylar cartilage,

suggesting that fibrocartilage modulation is increased with increasing levels of compressive forces in the bite (Mao *et al.*, 1998).

Experimental studies *in vivo* on tendons that have been surgically translocated to remove the normal compressive and shear loads to which they are subject (where they wrap around bony pulleys), suggests that the maintenance of a fibrocartilage phenotype depends on intermittent compression and/or shear (see Vogel, 1995, for a review). This is supported by experiments *in vitro* showing that uniaxial compression of explants, from a fibrocartilaginous region of the deep bovine flexor tendon, upregulates aggrecan synthesis (Koob *et al.*, 1992). Aggrecan (and biglycan) mRNA levels are also increased in explants of fetal bovine tendons cultured under compressive load before any fibrocartilage has developed (Robbins *et al.*, 1997). Robbins *et al.* (1997) suggest that the fetal tendons respond to compressive load by increasing the synthesis of TGF-β. This stimulates PG synthesis and establishes the fibrocartilage phenotype. A load-dependent effect of hydrostatic pressure on aggrecan synthesis by cultured chondrocytes has also been demonstrated by Ikenoue *et al.* (2003). By contrast, we know little of the effects of cyclic compression *in vitro* on collagen turnover in tendons, although unconfined compression exerted on articular cartilage increases the quantity of denatured collagen (Thibault *et al.*, 2002).

Wren *et al.* (2000) argue that the differentiation of tendon fibrocartilage is associated with changes in the local permeability of the tendon. They have proposed that the low permeability of fibrocartilaginous regions maintains fluid pressures, and protects solid components in the ECM from forces that could disrupt matrix organization. Of course, both forces act on the bone as well as the tendon—and thus the periosteum becomes fibrocartilaginous as well (Benjamin *et al.*, 1995). Remove or modify such forces and the tissue phenotype changes accordingly. Thus, whereas the intertubercular sulcus, which houses the tendon of the long head of biceps, normally has a thick, fibrocartilaginous periosteum, this tissue regresses if the tendon is torn (Benjamin *et al.*, 1993b). Under such circumstances, the bone surface would no longer be subject to the same mechanical stimulation. Equally, the articular fibrocartilages of the human TMJ are markedly thinner in edentate individuals—that is, where occlusal forces are substantially reduced (Taddei *et al.*, 1991). Malaviya *et al.* (2000), like several others before them, have also shown that the fibrocartilage that develops in wrap-around tendons in response to compression and shear, can be replaced by fibrous tissue if the tendons are surgically translocated away from their bony pulleys.

Fibrocartilage on the surface of the mandibular condyle (Öberg and Carlson, 1979) and that forming the inner part of the anulus fibrosus of the IV disc (Rufai *et al.*, 1995b) develops from hyaline cartilage. However, in the disc, there are suggestions that the cartilage cells form a developmental pathway distinct from that in developing hyaline cartilage, for despite their

chondrocytic phenotype in early discs, they synthesize type IIA procollagen (Zhu *et al.*, 2001). Type IIB procollagen is more typical of chondrocytes (Sandell *et al.*, 1994).

Immobilization of chick embryos early in development inhibits the normal appearance of the fibrocartilaginous, plantar tarsal sesamoid of the tibiotarsal joint, and the development of the menisci in the tibiofemoral joint (Mikic *et al.*, 2000). However, the underlying mechanism is fundamentally different at these two sites. Whereas menisci start to develop in pharmacologically immobilized embryos at much the same time as in controls but subsequently involute, the sesamoids never appear at all and the tibiotarsal joint is ankylosed. Thus, although mechanical stimulation plays a role in the development of both fibrocartilages, movement is integral to the formation of sesamoids from the very earliest stages, whereas the initial formation of menisci is intrinsically regulated. In this respect, the development of avian tibiotarsal menisci resembles that of their autopodial tendons (Benjamin and Ralphs, 2000).

Dynamic compression of porcine meniscal explants significantly increases the expression of nitric oxide (NO), a molecule believed to play a role in mechanical signal transduction (Fink *et al.*, 2001). Exposing fibrocartilage cells extracted from the rabbit TMJ and cultured in the presence of recombinant human interleukin 1β to intermittent tensile stress also upregulates NO production and NO synthase activity (Agarwal *et al.*, 2001). Furthermore, it induces cyclooxygenase 2 (COX-2) activity in these cells, and this in turn is associated with the production of prostaglandin E_2. Fibrocartilage cells isolated from the articular surfaces of the chick tibia and subjected to mechanical strain *in vitro* release larger quantities of HA into the culture medium than do control cells (Dowthwaite *et al.*, 1999). They also express higher levels of CD44 (hyaluronan-binding protein) and show evidence of differential expression of HA synthase activity.

Forceful bending of mouse tails places one side of the coccygeal IV discs under increased tension and the other under increased compression (Court *et al.*, 2001). This results in selective cell death and downregulation of aggregan synthesis, suggesting that these events are triggered by ECM compression. Such findings are in line with previous work on human discs from scoliotic patients, in whom aggrecan concentration is lower on the concave side of the disc (Crean *et al.*, 1997). However, in this study, there was a more general diminution of type II collagen gene expression on both sides of the disc. Crean *et al.* (1997) interpret this to mean that type II collagen synthesis was reduced by immobilization under static load, rather than by the nature of the loading itself (compressive or tensile). The *in vitro* studies of Court *et al.* (2001) suggest that there is a threshold of tissue strain that initiates cell death in the anulus fibrosus.

An increase in the expression of S-100 (an acidic, calcium-binding protein) has been reported to accompany the metaplasia of fibroblasts to fibrocartilage

cells (Leonardi *et al*., 2000; Magro *et al*., 1995; Narama *et al*., 1996). Such chondroid metaplasia occurs in the articular disc of the TMJ in response to mechanical injury (Leonardi *et al*., 2002) and is also a feature of a rare connective tissue tumor called an elastofibroma (Magro *et al*., 1995). S-100 is expressed in growing tumors, as they rub against adjacent bone. It is also present in injured cranial cruciate ligaments of the dog before fibrocartilaginous metaplasia (Magro *et al*., 1995; Narama *et al*., 1996). Thus, S-100 protein may be one of the factors implicated in enabling cells to acquire a chondrogenic potential.

B. Cell Turnover

Apoptosis is well documented in hyaline articular cartilage, where it has been linked with matrix degradation, calcification, and osteophyte formation (Hashimoto *et al*., 2002). Chondrocyte apoptotic bodies and matrix vesicles contain enzymes that are necessary for calcification of the ECM (Hashimoto *et al*., 1998). Apoptosis also occurs in fibrocartilage, for it has been reported in the medial meniscus of osteoarthritic, rabbit knee joints (Le Graverand *et al*., 2001b) and in IV discs (Gruber and Hanley, 1998). The mechanisms controlling the programmed cell death of fibrocartilage cells have not been thoroughly investigated, although far greater attention has been paid to it in hyaline cartilage. Here, the transcription factor Sox9 can suppress apoptosis (Akiyama *et al*., 2002) and VEGF-mediated capillary invasion and nitric oxide can promote it (Hashimoto *et al*., 2002). Stress-activated protein kinases are known to be upstream regulators in other tissues and their expression is increased in cultured tendon cells subjected to cyclic strain (Arnoczky *et al*., 2002).

Whether there is any quantitative relationship between repetitive loading and apoptosis in any type of cartilage is unclear. However, such a correlation is likely because of the association between repetitive loading of hyaline cartilage and osteoarthritis, and between repetitive loading of wrap-around tendons and overuse injuries. In articular cartilage, apoptosis is a feature of the deep calcified zone (Adams and Horton, 1998)—and as discussed above, there is a comparable region in fibrocartilaginous entheses (Benjamin and Ralphs, 1995, 1997a, 1998).

V. Fibrocartilage Cells and Tissue Engineering

The rapidly developing field of tissue engineering offers exciting possibilities for tissue repair and regeneration. The basic general principle is that cells are artificially manipulated to promote the repair of tissues and organs. Both

in vivo cell-mediated tissue regeneration and *in vitro* systems are being developed and there are three main requirements for both—a suitable cell system, an artificial ECM (called a ''scaffold''), and the right cocktail of growth factors (Tabata, 2001). There is also an increasing recognition that appropriate mechanical stimulation is necessary for creating good tissue constructs (Shieh and Athanasiou, 2003) and that isolating cartilage cells together with their native ECM (i.e., as chondrons) for *in vitro* tissue engineering can enhance matrix synthesis (Larson *et al.*, 2002). Gao *et al.* (2001) have described the production of a tissue-engineered graft of bone and fibrocartilage in which they report collagen–fiber continuity across the interface between the tissues. They engineered the cell types of both tissues from mesenchymal-derived stem cells from rat bone marrow. After clonal expansion *in vitro*, they promoted fibrocartilage formation by TGF-β treatment of cells grown within a sponge manufactured from a hyaluronan derivative, and promoted bone cell formation with an osteogenic supplement.

Tissue engineering of menisci is currently attracting considerable interest, because of the important role that menisci are now known to play in transmitting load across joints. Those in the knee transmit much of the load acting on the joint (Aagaard and Verdonk, 1999; Rath and Richmond, 2000). They can adapt their shape to the changing geometry of articular surfaces, thus preventing small contact areas and reducing local peak forces (Beek *et al.*, 2001). They are also thought to promote lubrication, contribute to joint stability, and act as shock absorbers (Rath and Richmond, 2000). Orthopedic surgeons no longer conduct routine meniscectomies, for they are believed to accelerate the onset of osteoarthritis. Hence, the repair of the inner, avascular part of damaged menisci has become a highly topical issue. However, it is curious that fibrocartilage is regarded as an inferior repair material when it appears during the healing of articular cartilage (Bouwmeester *et al.*, 1999). Gastel *et al.* (2001) have used a collagen-based scaffold derived from the intestinal submucosa to encourage the regeneration of surgically damaged menisci. They reported an excellent quality of tissue integration with evidence of fibrocartilage cells having migrated into the graft. Isoda and Saito (1998) have successfully used a fibrin gel as a scaffold in meniscal defects, to encourage cell division and matrix synthesis of rabbit fibrocartilage cells. The cell culture studies of Kasemkijwattana *et al.* (2000) suggest that several growth factors that are characteristic of wound hematomas [epidermal growth factor (EGF), basic fibroblast growth factor (bFGF), platelet-derived growth factor AB (PDGF-AB), and TGF-α] can stimulate the proliferation of meniscal fibrocartilage cells and/or collagen synthesis. Thus, these cytokines (in isolation or combination) may have considerable potential for meniscal repair when used in conjunction with appropriate scaffolds. The strategic addition of growth factors is also important for maximizing the integration of tissue grafts used for replacing

damaged ACL (Anderson *et al*., 2001). The soft–hard tissue integration of grafts and the re-formation of enthesis fibrocartilage in rabbit knees were improved by adding exogenous bone growth factor. Alternatively, gene therapy or myoblast-mediated gene transfer may be viable options for delivering growth factors to a lesion site (Kasemkijwattana *et al*., 2000).

VI. Concluding Remarks

Since the first comprehensive, general review on fibrocartilage (Benjamin and Evans, 1990), there have been considerable advances in our knowledge and understanding of this tissue in virtually all the major sites at which it is found. Yet fibrocartilage still cannot be defined with any greater precision or clarity—and is unlikely ever to be. We must thus accept that it is, by "definition," a transitional tissue with diverse characteristics, and guard against the assumption inherent in some studies, that fibrocartilage at one site is necessarily the same as that at another.

The current interest in tissue engineering, and in the repair and regeneration of articular cartilage, ensures that an understanding of fibrocartilage cells will continue to be important. It will undoubtedly give further impetus to work exploring the relationship between mechanical load and fibrocartilage cell differentiation. The whole evolving field of "mechanobiology" is an exciting one. Frost's (1987) visionary concept of bone as a "mechanostat," maintaining strain levels within certain defined boundaries so that there are distinct modeling and remodeling thresholds, could be profitably applied to the numerous fibrocartilages dealt with in this review.

Undoubtedly, the direction of fibrocartilage research will continue to be partly shaped by developments in our understanding of articular hyaline cartilage. We thus await with interest a greater understanding of how the controls, now known to operate on mesenchymal cells that differentiate to form hyaline cartilage, are also involved in the metaplasia of fibrocartilage from fibroblasts.

References

Aagaard, H., and Verdonk, R. (1999). Function of the normal meniscus and consequences of meniscal resection. *Scand. J. Med. Sci. Sports* **9,** 134–140.

Aboul-Mahasen, L. M., and Sadek, S. A. (2002). Developmental morphological and histological studies on structures of the human fetal shoulder joint. *Cells Tissues Organs* **170,** 1–20.

Abrahamsson, S. O., Lundborg, G., and Lohmander, L. S. (1989). Segmental variation in microstructure, matrix synthesis and cell proliferation in rabbit flexor tendon. *Scand. J. Plast. Reconstr. Hand Surg.* **23,** 191–198.

Adams, C. S., and Horton, W. E. (1998). Chondrocyte apoptosis increases with age in the articular cartilage of adult animals. *Anat. Rec.* **250,** 418–425.

Agarwal, S., Long, P., Gassner, R., Piesco, N. P., and Buckley, M. J. (2001). Cyclic tensile strain suppresses catabolic effects of interleukin-1β in fibrochondrocytes from the temporomandibular joint. *Arthritis Rheum.* **44,** 608–617.

Ahluwalia, S., Fehm, M., Meaney Murray, M., Martin, S. D., and Spector, M. (2001). Distribution of smooth muscle actin-containing cells in the human meniscus. *J. Orthop. Res.* **19,** 659–664.

Aigner, T., Dietz, U., Stoss, H., and von der Mark, K. (1995). Differential expression of collagen types I, II, III, and X in human osteophytes. *Lab. Invest.* **73,** 236–243.

Akiyama, H., Chaboissier, M. C., Martin, J. F., Schedl, A., and de Crombrugghe, B. (2002). The transcription factor Sox9 has essential roles in successive steps of the chondrocyte differentiation pathway and is required for expression of Sox5 and Sox6. *Genes Dev.* **16,** 2813–2828.

Altmann, K. (1964). Zur kausalen Histiogenese des Knorpels: W. Roux's Theorie und experimentelle Wirklichkeit. *Z. Anat. Entwicklungs* **37,** 1–167.

Anderson, K., Seneviratne, A. M., Izawa, K., Atkinson, B. L., Potter, H. G., and Rodeo, S. A. (2001). Augmentation of tendon healing in an intraarticular bone tunnel with use of a bone growth factor. *Am. J. Sports Med.* **29,** 689–698.

Araujo, V. G., Figueiredo, C. A., Joazeiro, P. P., Mora, O. A., and Toledo, O. M. (2002). In vitro rapid organization of rabbit meniscus fibrochondrocytes into chondro-like tissue structures. *J. Submicrosc. Cytol. Pathol.* **34,** 335–343.

Arnoczky, S. P., Tian, T., Lavagnino, M., Gardner, K., Schuler, P., and Morse, P. (2002). Activation of stress-activated protein kinases (SAPK) in tendon cells following cyclic strain: The effects of strain frequency, strain magnitude, and cytosolic calcium. *J. Orthop. Res.* **20,** 947–952.

Aspberg, A., Adam, S., Kostka, G., Timpl, R., and Heinegård, D. (1999). Fibulin-1 is a ligand for the C-type lectin domains of aggrecan and versican. *J. Biol. Chem.* **274,** 20444–20449.

Aszodi, A., Chan, D., Hunziker, E., Bateman, J. F., and Fassler, R. (1998). Collagen II is essential for the removal of the notochord and the formation of intervertebral discs. *J. Cell Biol.* **143,** 1399–1412.

Ayad, S., Boot-Handford, R. P., Humphries, M. J., Kadler, K. E., and Shuttleworth, C. A. (1998). "The Extracellular Matrix Facts Book," 2nd Ed. Academic Press, London.

Balogh, K., Ferris, J. A., and Aherne, W. A. (1971). Fibrocartilage in the heart. *Lancet* **17,** 802–803.

Bayliss, M. T., Howat, S., Davidson, C., and Dudhia, J. (2000). The organization of aggrecan in human articular cartilage: Evidence for age-related changes in the rate of aggregation of newly synthesized molecules. *J. Biol. Chem.* **275,** 6321–6327.

Beek, M., Koolstra, J. H., van Ruijven, L. J., and van Eijden, T. M. (2001). Three-dimensional finite element analysis of the cartilaginous structures in the human temporomandibular joint. *J. Dent. Res.* **80,** 1913–1918.

Benjamin, M., and Evans, E. J. (1990). Fibrocartilage. *J. Anat.* **171,** 1–15.

Benjamin, M., and McGonagle, D. (2001). The anatomical basis for disease localisation in seronegative spondyloarthropathy at entheses and related sites. *J. Anat.* **199,** 503–526.

Benjamin, M., and Ralphs, J. R. (1995). Functional and developmental anatomy of tendons and ligaments. *In* "Respetitive Motion Disorders of the Upper Extremity" (S. L. Gordon, S. J. Blair, and L. J. Fine, Eds.), pp. 185–203. American Academy of Orthopaedic Surgeons, Rosemont, IL.

Benjamin, M., and Ralphs, J. R. (1996). Tendons in health and disease. *Man. Ther.* **1,** 186–191.

Benjamin, M., and Ralphs, J. R. (1997a). Tendons and ligaments: An overview. *Histol. Histopathol.* **12,** 1135–1144.

Benjamin, M., and Ralphs, J. R. (1997b). Cells, tissues and structures of the musculoskeletal system. *Curr. Opin. Orthop.* **8,** 29–33.

Benjamin, M., and Ralphs, J. R. (1998). Fibrocartilage in tendons and ligaments: An adaptation to compressive load. *J. Anat.* **193,** 481–494.

Benjamin, M., and Ralphs, J. R. (2000). The cell and developmental biology of tendons and ligaments. *Int. Rev. Cytol.* **196,** 85–130.

Benjamin, M., and Ralphs, J. R. (2001). Entheses: The bony attachments of tendons and ligaments. *Ital. J. Anat. Embryol.* **106**(suppl. 1), 151–157.

Benjamin, M., Evans, E. J., and Copp, L. (1986). The histology of tendon attachments to bone in man. *J. Anat.* **149,** 89–100.

Benjamin, M., Tyers, R. N., and Ralphs, J. R. (1991). Age-related changes in tendon fibrocartilage. *J. Anat.* **179,** 127–136.

Benjamin, M., Ralphs, J. R., Shibu, M., and Irwin, M. (1993a). Capsular tissues of the proximal interphalangeal joint: Normal composition and effects of Dupuytren's disease and rheumatoid arthritis. *J. Hand Surg. Br.* **18,** 371–376.

Benjamin, M., Ralphs, J. R., Newell, R. L. M., and Evans, E. J. (1993b). Loss of the fibrocartilaginous lining of the intertubercular sulcus associated with rupture of the tendon of the long head of biceps brachii. *J. Anat.* **182,** 281–285.

Benjamin, M., Archer, C. W., and Ralphs, J. R. (1994). Cytoskeleton of cartilage cells. *Microsc. Res. Tech.* **28,** 372–377.

Benjamin, M., Qin, S., and Ralphs, J. R. (1995). Fibrocartilage associated with human tendons and their pulleys. *J. Anat.* **187,** 625–633.

Benjamin, M., Kumai, T., Milz, S., Boszczyk, B. M., Boszczyk, A. A., and Ralphs, J. R. (2002). The skeletal attachment of tendons: Tendon "entheses." *Comp. Biochem. Physiol. A Mol. Integr. Physiol.* **133,** 931–945.

Beresford, W. A. (1981). "Chondroid Bone, Secondary Cartilage, and Metaplasia." Urban and Schwarzenberg, Baltimore, MD.

Berger, R. A., and Buckwalter, J. A. (1990). Calcium pyrophosphate dihydrate crystal deposition patterns in the triangular fibrocartilage complex. *Orthopedics* **13,** 75–80.

Berkovitz, B. K., and Pacy, J. (2000). Age changes in the cells of the intra-articular disc of the temporomandibular joints of rats and marmosets. *Arch. Oral Biol.* **45,** 987–995.

Berthelot, J. M., Mabille, A., Nomballais, M. F., Maugars, Y., Robert, R., and Prost, A. (1995). Osteitis condensans of the clavicle: does fibrocartilage play a role? A report of two cases with spontaneous clinical and roentgenographic resolution *Rev. Rhum. Engl. Ed.* **62,** 501–516.

Bibby, S. R. S., Jones, D. A., Lee, R. B., Yu, J., and Urban, J. P. G. (2001). The pathophysiology of the intervertebral disc. *Joint Bone Spine* **68,** 537–542.

Bland, Y. S., and Ashhurst, D. E. (1996). Changes in the content of the fibrillar collagens and the expression of their mRNAs in the menisci of the rabbit knee joint during development and ageing. *Histochem. J.* **28,** 265–274.

Bland, Y. S., and Ashhurst, D. E. (1997). Fetal and postnatal development of the patella, patellar tendon and suprapatella in the rabbit: Changes in the distribution of the fibrillar collagens. *J. Anat.* **190,** 327–342.

Bluteau, G., Labourdette, M.-C., Ronzière, T., Conrozier, P., Mathieu, D., Herbage, F., and Mallein-Gerin, F. (1999). Type X collagen in rabbit and human meniscus. *Osteoarthritis Cartilage* **7,** 498–501.

Bluteau, G., Conrozier, T., Mathieu, P., Vignon, N. E., Herbage, D., and Mallein-Gerin, F. (2001). Matrix metalloproteinase-1, -3, -13 and aggrecanase-1 and -2 are differentially expressed in experimental osteoarthritis. *Biochim. Biophys. Acta* **1526,** 147–158.

Bockenek, W. L., and Bach, J. R. (1990). Fibrocartilaginous emboli to the spinal cord: A review of the literature. *J. Am. Paraplegia Soc.* **13,** 18–23.

Boos, N., Nerlich, A. G., Wiest, I., von der Mark, K., Ganz, R., and Aebi, M. (1999). Immunohistochemical analysis of type-X-collagen expression in osteoarthritis of the hip joint. *J. Orthop. Res.* **17,** 495–502.

Boszczyk, B. M., Boszczyk, A. A., Putz, R., Büttner, A., Benjamin, M., and Milz, S. (2001). An immunohistochemical study of the dorsal capsule of the lumbar and thoracic facet joints. *Spine* **26,** E338–E343.

Bouwmeester, P., Kuijer, R., Terwindt-Rouwenhorst, E., van der Linden, T., and Bulstra, S. (1999). Histological and biochemical evaluation of perichondrial transplants in human articular cartilage defects. *J. Orthop. Res.* **17,** 843–849.

Bowker, R. M., Van Wulfen, K. K., Bowker, R. M., van Wulfen, K. K., Springer, S. E., and Linder, K. E. (1998). Functional anatomy of the cartilage of the distal phalanx and digital cushion in the equine foot and a hemodynamic flow hypothesis of energy dissipation. *Am. J. Vet. Res.* **59,** 961–968.

Boyan, B. D., Schwartz, Z., Swain, L. D., Khare, A. G., Heckman, J. D., Ramirez, V., Peters, P., and Carnes, D. L., Jr. (1992). Initial effects of partially purified bone morphogenetic protein on the expression of glycosaminoglycan, collagen, and alkaline phosphatase in nonunion cell cultures. *Clin. Orthop.* **278,** 286–304.

Breckon, J. J. W., Hembry, R. M., Reynolds, J. J., and Meikle, M. C. (1996). Identification of matrix metalloproteinases and their inhibitor in the articular disc of the craniomandibular joint of the rabbit. *Arch. Oral Biol.* **41,** 315–322.

Brew, K., Dinakarpandian, D., and Nagase, H. (2000). Tissue inhibitors of metalloproteinases: Evolution, structure and function. *Biochim. Biophys. Acta* **1477,** 267–283.

Broom, N. D., and Poole, C. A. (1982). A functional–morphological study of the tidemark region of articular cartilage maintained in a non-viable physiological condition. *J. Anat.* **135,** 65–82.

Buckwalter, J. A., and Mankin, H. J. (1997). Articular cartilage. I. Tissue design and chondrocyte–matrix interactions. Instructional Course Lectures, American Academy of Orthopaedic Surgeons. *J. Bone Joint Surg.* **79,** 600–611.

Buckwalter, J. A., and Rosenberg, L. (1983). Structural changes during development in bovine fetal epiphyseal cartilage. *Collagen Relat. Res.* **3,** 489–504.

Buckwalter, J. A., Roughley, P. J., and Rosenberg, L. C. (1994). Age-related changes in cartilage proteoglycans: Quantitative electron microscopic studies. *Microsc. Res. Tech.* **28,** 398–408.

Cai, D., Marty-Roix, R., Hsu, H. P., and Spector, M. (2001). Lapine and canine bone marrow stromal cells contain smooth muscle actin and contract a collagen–glycosaminoglycan matrix. *Tissue Eng.* **7,** 829–841.

Campbell, M. A., Tester, A. M., Handley, C. J., Checkley, G. J., Chow, G. L., Cant, A. E., and Winter, A. D. (1996). Characterization of a large chondroitin sulfate proteoglycan present in bovine collateral ligament. *Arch. Biochem. Biophys.* **329,** 181–190.

Canoso, J. J. (1998). The première enthesis. *J. Rheumatol.* **25,** 1254–1256.

Carvalho, H. F., and Felisbino, S. L. (1999). The development of the pressure-bearing tendon of the bullfrog *Rana catesbeiana*. *Anat. Embryol.* **200,** 55–64.

Carvalho, H. F., Felisbino, S. L., Covizi, D. Z., Della Colleta, H. H., and Gomes, L. (2000). Structure and proteoglycan composition of specialized regions of the elastic tendon of the chicken wing. *Cell Tissue Res.* **300,** 435–446.

Caterson, B., Flannery, C., Hughes, C. E., and Little, C. B. (2000). Mechanisms involved in cartilage proteoglycan catabolism. *Matrix Biol.* **19,** 333–344.

Chakravarti, S., Magnuson, T., Lass, J. H., Jepsen, K. J., LaMantia, C., and Carroll, H. (1998). Lumican regulates collagen fibril assembly: Skin fragility and corneal opacity in the absence of lumican. *J. Cell Biol.* **141,** 1277–1286.

Chan, D., and Jacenko, O. (1998). Phenotypic and biochemical consequences of collagen X mutations in mice and humans. *Matrix Biol.* **17,** 169–184.

Chaves, K., Munerato, M. C., Ligocki, A., Lauxen, I., and de Quadros, O. F. (2002). Microscopic analysis of the temporomandibular joint in rabbits (*Oryctolagus cuniculus* L.) using an occlusal interference. *Cranio.* **20,** 116–124.

Chubinskaya, S., Cs-Szabo, G., and Kuettner, K. E. (1998). ADAM-10 message is expressed in human articular cartilage. *J. Histochem. Cytochem.* **46,** 723–729.

Claassen, H., Kampen, W. U., and Kirsch, T. (1996). Localization of collagens and alkaline phosphatase activity during mineralization and ossification of human first rib cartilage. *Histochem. Cell Biol.* **105,** 213–219.

Claes, L., Eckert-Hubner, K., and Augat, P. (2002). The effect of mechanical stability on local vascularization and tissue differentiation in callus healing. *J. Orthop. Res.* **20,** 1099–1105.

Court, C., Colliou, O. K., Chin, J. R., Liebenberg, E., Bradford, D. S., and Lotz, J. C. (2001). The effect of static in vivo bending on the murine intervertebral disc. *Spine J.* **1,** 239–245.

Covizi, D. Z., Felisbino, S. L., Gomes, L., Pimentel, E. R., and Carvalho, H. F. (2001). Regional adaptations in three rat tendons. *Tissue Cell* **33,** 483–490.

Crean, J. K. G., Roberts, S., Jaffray, D. C., Eisenstein, S. M., and Duance, V. C. (1997). Matrix metalloproteinases in the human intervertebral disc: Role in disc degeneration and scoliosis. *Spine* **22,** 2877–2884.

Curran, S., and Murray, G. I. (1999). Matrix metalloproteinases in tumour invasion and metastasis. *J. Pathol.* **189,** 300–308.

Daniels, K., and Solursh, M. (1991). Modulation of chondrogenesis by the cytoskeleton and extracellular matrix. *J. Cell Sci.* **100,** 249–254.

Danielson, K. G., Baribault, H., Holmes, D. F., Graham, H., Kadler, K. E., and Iozzo, R. V. (1997). Targeted disruption of decorin leads to abnormal collagen fibril morphology and skin fragility. *J. Cell Biol.* **136,** 729–743.

Davies Cde, L., Melder, R. J., Munn, L. L., Mouta-Carriera, C., Jain, R. K., and Boucher, Y. (2001). Decorin inhibits endothelial migration and tube-like structure formation: Role of thrombospondin-1. *Microvasc. Res.* **62,** 26–42.

De Carvalho, H. F., and Campos Vidal Bde, C. (1995). The elastic system of a pressure-bearing tendon of the bullfrog *Rana catesbeiana*. *Anat. Anz.* **177,** 397–404.

Deland, J. T., Lee, K. T., Sobel, M., and DiCarlo, E. F. (1995). Anatomy of the plantar plate and its attachments in the lesser metatarsal phalangeal joint. *Foot Ankle Int.* **16,** 480–486.

Donahue, H. J. (2000). Gap junctions and biophysical regulation of bone cell differentiation. *Bone* **26,** 417–422.

Dowthwaite, G. P., Ward, A. C., Flannely, J., Suswillo, R. F., Flannery, C. R., Archer, C. W., and Pitsillides, A. A. (1999). The effect of mechanical strain on hyaluronan metabolism in embryonic fibrocartilage cells. *Matrix Biol.* **18,** 523–532.

Eanes, E. D., Hailer, A. W., Midura, R. J., and Hascall, V. C. (1992). Proteoglycan inhibition of calcium phosphate precipitation in liposomal suspensions. *Glycobiology* **2,** 571–578.

Egerbacher, M., Weber, H., and Hauer, S. (2000). Bones in the heart skeleton of the otter (*Lutra lutra*). *J. Anat.* **196,** 485–491.

Evanko, S. P., and Vogel, K. G. (1990). Ultrastructure and proteoglycan composition in the developing fibrocartilaginous region of bovine tendon. *Matrix* **10,** 420–436.

Evanko, S. P., and Vogel, K. G. (1993). Proteoglycan synthesis in fetal tendon is differentially regulated by cyclic compression in vitro. *Arch. Biochem. Biophys.* **307,** 153–164.

Eyre, D. R., Matsui, Y., and Wu, J.-J. (2002). Collagen polymorphisms of the intervertebral disc. *Biochem. Soc. Trans.* **30,** 844–848.

Felisbino, S. L., and Carvalho, H. F. (1999). Identification and distribution of type VI collagen in tendon fibrocartilages. *J. Submicrosc. Cytol. Pathol.* **31,** 187–195.

Fink, C., Fermor, B., Weinberg, J. B., Pisetsky, D. S., Misukonis, M. A., and Guilak, F. (2001). The effect of dynamic mechanical compression on nitric oxide production in the meniscus. *Osteoarthritis Cartilage* **9,** 481–487.

Flannery, C. R., Hughes, C. E., Schumacher, B. L., Tudor, D., Aydelotte, M. B., Kuettner, K. E., and Caterson, B. (1999). Articular cartilage superficial zone proteoglycan (SZP) is homologous to megakaryocyte stimulating factor precursor and is a multifunctional proteoglycan with potential growth-promoting, cytoprotective and lubricating properties in cartilage metabolism. *Biochem. Biophys. Res. Commun.* **254,** 535–541.

Frost, H. M. (1987). Bone "mass" and the "mechanostat": A proposal *Anat. Rec.* **219,** 1–9.

Fujioka, H., Thakur, R., Wang, G. J., Mizuno, K., Balian, G., and Hurwitz, S. R. (1998). Comparison of surgically attached and non-attached repair of the rat Achilles tendon–bone interface: Cellular organization and type X collagen expression. *Connect. Tissue Res.* **37,** 205–218.

Fukuta, S., Oyama, M., Kavalkovich, K., Fu, F. H., and Niyibizi, C. (1998). Identification of types II, IX and X collagens at the insertion site of the bovine Achilles tendon. *Matrix Biol.* **17,** 65–73.

Gao, J., Oqvist, G., and Messner, K. (1994). The attachments of the rabbit medial meniscus: A morphological investigation using image analysis and immunohistochemistry. *J. Anat.* **185,** 663–667.

Gao, J., Messner, K., Ralphs, J. R., and Benjamin, M. (1996). An immunohistochemical study of enthesis development in the medial collateral ligament of the rat knee joint. *Anat. Embryol.* **194,** 399–406.

Gao, J., Dennis, J. E., Solchaga, L. A., Awadallah, A. S., Goldberg, V. M., and Caplan, A. I. (2001). Tissue-engineered fabrication of an osteochondral composite graft using rat bone marrow-derived mesenchymal stem cells. *Tissue Eng.* **7,** 363–371.

Gastel, J. A., Muirhead, W. R., Lifrak, J. T., Fadale, P. D., Hulstyn, M. J., and Labrador, D. P. (2001). Meniscal tissue regeneration using a collagenous biomaterial derived from porcine small intestine submucosa. *Arthroscopy* **17,** 151–159.

Gedikoglu, G., Aksoy, M. C., and Ruacan, S. (2001). Fibrocartilaginous mesenchymoma of the distal femur: Case report and literature review. *Pathol. Int.* **51,** 638–642.

Gelse, K., Soder, S., Eger, W., Diemtar, T., and Aigner, T. (2003). Osteophyte development-molecular characterization of differentiation stages. *Osteoarthritis Cartilage* **11,** 141–148.

Gloe, T., and Pohl, U. (2002). Laminin binding conveys mechanosensing in endothelial cells. *News Physiol. Sci.* **17,** 166–169.

Goel, V. K., Monroe, B. T., Gilbertson, L. G., and Brinkman, P. (1995). Interlaminar shear stresses and laminae separation in the disc: Finite element analysis of the L3–L4 motion segment subjected to axial compressive loads. *Spine* **20,** 2197–2203.

Gomez, D. E., Alonso, D. F., Yoshiji, H., and Thorgeirsson, U. P. (1997). Tissue inhibitors of metalloproteinases: Structure, regulation and biological functions. *Eur. J. Cell Biol.* **74,** 111–122.

Gray, J. C. (1999). Neural and vascular anatomy of the menisci of the human knee. *J. Orthop. Sports Phys. Ther.* **29,** 23–30.

Gruber, H. E., and Hanley, E. N., Jr. (1998). Analysis of aging and degeneration of the human intervertebral disc: Comparison of surgical specimens with normal controls. *Spine* **23,** 751–757.

Guilak, F., and Mow, V. C. (2000). The mechanical environment of the chondrocyte: A biphasic finite element model of cell–matrix interactions in articular cartilage. *J. Biomech.* **33,** 1663–1673.

Hascall, V. C., and Sajdera, S. W. (1970). Physical properties and polydispersity of proteoglycan from bovine nasal cartilage. *J. Biol. Chem.* **245,** 4920–4930.

Hashimoto, S., Ochs, R. L., Rosen, F., Quach, J., McCabe, G., Solan, J., Seegmiller, J. E., Terkeltaub, R., and Lotz, M. (1998). Chondrocyte-derived apoptotic bodies and calcification of articular cartilage. *Proc. Nat. Acad. Sci. USA* **95,** 3094–3099.

Hashimoto, S., Creighton-Achermann, L., Takahashi, L., Amiel, D., Coutts, R. D., and Lotz, M. (2002). Development and regulation of osteophyte formation during experimental osteoarthritis. *Osteoarthritis Cartilage* **10,** 180–187.

Havelka, S., and Horn, V. (1995). Observations on the tidemark and calcified layer of articular cartilage. *In* "Biology of the Synovial Joint" (C. W. Archer, B. Caterson, M. Benjamin, and J. R. Ralphs, Eds.), pp. 331–346. Harwood Academic Publishers, Amsterdam.

Hayes, A. J., Benjamin, M., and Ralphs, J. R. (1999). Role of actin stress fibres in the development of the intervertebral disc: Cytoskeletal control of extracellular matrix assembly. *Dev. Dyn.* **215,** 179–189.

Hayes, A. J., Benjamin, M., and Ralphs, J. R. (2001). Extracellular matrix in development of the intervertebral disc. *Matrix Biol.* **20,** 107–121.

Hedbom, E., and Heinegård, D. (1989). Interaction of a 59-kDa connective tissue matrix protein with collagen I and collagen II. *J. Biol. Chem.* **264,** 6898–6905.

Hedbom, E., and Heinegård, D. (1993). Binding of fibromodulin and decorin to separate sites on fibrillar collagens. *J. Biol. Chem.* **268,** 27307–27312.

Heinegård, D., and Sommarin, Y. (1987). Proteoglycans: An overview. *Methods Enzymol.* **144,** 305–319.

Hems, T., and Tillmann, B. (2000). Tendon entheses of the human masticatory muscles. *Anat. Embryol.* **202,** 201–208.

Henry, S. P., Takanosu, M., Boyd, T. C., Mayne, P. M., Eberspaechert, H., de Crombrugge, B., Höök, M., and Mayne, R. (2001). Expression pattern and gene characterization of asporin: A newly discovered member of the leucine-rich repeat protein family. *J. Biol. Chem.* **276,** 12212–12221.

Hiraki, Y., Inoue, H., Iyama, K., Kamizono, A., Ochiai, M., Shukunami, C., Iijima, S., Suzuki, F., and Kondo, J. (1997). Identification of chondromodulin I as a novel endothelial cell growth inhibitor: Purification and its localization in the avascular zone of epiphyseal cartilage. *J. Biol. Chem.* **272,** 32419–32426.

Holladay, S. D., Smith, B. J., Smallwood, J. E., and Hudson, L. C. (1990). Absence of an osseous patella and other observations in Macropodidae stifle. *Anat. Rec.* **226,** 112–114.

Horas, U., Pelinkovic, D., Herr, G., Aigner, T., and Schnettler, R. (2003). Autologous chondrocyte implantation and osteochondral cylinder transplantation in cartilage repair of the knee joint: A prospective, comparative trial. *J. Bone Joint Surg. Am.* **85,** 185–192.

Horner, H. A., and Urban, J. P. (2001). Effect of nutrient supply on the viability of cells from the nucleus pulposus of the intervertebral disc. *Spine* **36,** 2543–2549.

Hough, A. J. (2001). Pathology of osteoarthritis. *In* "Osteoarthritis" (R. W. Moskowitz, D. S. Howell, R. D. Altman, J. A. Buckwalter, and V. M. Goldberg, Eds.), 3rd Ed., pp. 69–99. Saunders, Philadelphia, PA.

Hu, B., Kapila, Y. L., Buddhikot, M., Shiga, M., and Kapila, S. (2000). Coordinate induction of collagenase-1, stromelysin-1 and urokinase plasminogen activator (uPA) by the 120-kDa cell-binding fibronectin fragment in fibrocartilaginous cells: uPA contributes to activation of procollagenase-1. *Matrix Biol.* **19,** 657–669.

Hu, K., Qiguo, R., Fang, J., and Mao, J. J. (2003). Effects of condylar fibrocartilage on the biomechanical loading of the human temporomandibular joint in a three-dimensional, nonlinear finite element model. *Med. Eng. Phys.* **25,** 107–113.

Ikenoue, T., Trindade, M. C., Lee, M. S., Lin, E. Y., Schurman, D. J., Goodman, S. B., and Smith, R. L. (2003). Mechanoregulation of human articular chondrocyte aggrecan and type II collagen expression by intermittent hydrostatic pressure in vitro. *J. Orthop. Res.* **21,** 110–116.

Iozzo, R. V. (1997). The family of the small leucine-rich proteoglycans: Key regulators of matrix assembly and cellular growth. *Crit. Rev. Biochem. Mol. Biol.* **32,** 141–174.

Iozzo, R. V. (1998). Matrix proteoglycans: From molecular design to cellular function. *Annu. Rev. Biochem.* **67,** 609–652.

Iozzo, R. V. (1999). The biology of the small, leucine-rich proteoglycans: Functional network of interactive proteins. *J. Biol. Chem.* **274,** 18843–18846.

Iozzo, R. V., and Murdoch, A. D. (1996). Proteoglycans of the extracellular environment: Clues from the gene and protein side offer novel perspectives in molecular diversity and function. *FASEB J.* **10,** 598–614.

Ishibe, T., Cremer, M. A., and Yoo, T. J. (1989). Type II collagen distribution in the ear of the guinea pig fetus. *Ann. Otol. Rhinol. Laryngol.* **98,** 648–654.

Ishihara, H., and Urban, J. P. (1999). Effects of low oxygen concentrations and metabolic inhibitors on proteoglycan and protein synthesis rates in the intervertebral disc. *J. Orthop. Res.* **17,** 829–835.

Isoda, K., and Saito, S. (1998). In vitro and in vivo fibrochondrocyte growth behavior in fibrin gel: An immunohistochemical study in the rabbit. *Am. J. Knee Surg.* **11,** 209–216.

Izumi, K., Yamaoka, I., and Murakami, R. (2000). Ultrastructure of the developing fibrocartilage of the os penis of rat. *J. Morphol.* **243,** 187–191.

Jacenko, O., Chan, D., Franklin, A., Ito, S., Underhill, C. B., Bateman, J. F., and Campbell, M. R. (2001). A dominant interference collagen X mutation disrupts hypertrophic chondrocyte pericellular matrix and glycosaminoglycan and proteoglycan distribution in transgenic mice. *Am. J. Pathol.* **159,** 2257–2269.

Jacoby, A. S., Melrose, J., Robinson, B. G., Hyland, V. J., and Ghosh, P. (1993). Secretory leucocyte proteinase inhibitor is produced by human articular cartilage chondrocytes and intervertebral disc fibrochondrocytes. *Eur. J. Biochem.* **218,** 951–957.

Jarvinen, T. A., Jozsa, L., Kannus, P., Jarvinen, T. L. N., Kvist, M., Hurme, T., Isola, J., Kalimo, H., and Jarvinen, M. (1999). Mechanical loading regulates tenascin-C expression in the osteotendinous junction. *J. Cell Sci.* **112,** 3157–3166.

Jasser, M. Z., Mitchell, P. G., and Cheung, H. S. (1994). Induction of stromelysin-1 and collagenase synthesis in fibrochondrocytes by tumor necrosis factor-α. *Matrix Biol.* **14,** 241–249.

Jay, G. D., Britt, D. E., and Cha, C.-J. (2000). Lubrican is a product of megakaryocyte stimulating factor gene expression by human synovial fibroblasts. *J. Rheumatol.* **27,** 594–600.

Jay, G. D., Tantravahi, U., Britt, D. E., Barrach, H. J., and Cha, C.-J. (2001). Homology of lubrican and superficial zone protein (SZP): Products of megakaryocyte stimulating factor (MSF) gene expression by human synovial fibroblasts and articular chondrocytes localized to chromosome 1 q25. *J. Orthop. Res.* **19,** 677–687.

Johnson, W. E., Eisenstein, S. M., and Roberts, S. (2001). Cell cluster formation in degenerate lumbar intervertebral discs is associated with increased disc cell proliferation. *Connect. Tissue Res.* **42,** 197–207.

Johnson, W. E., Caterson, B., Eisenstein, S. M., Hynds, D. L., Snow, D. M., and Roberts, S. (2002). Human intervertebral disc aggrecan inhibits nerve growth in vitro. *Arthrritis Rheum.* **46,** 2658–2664.

Jones, P. L., and Jones, F. S. (2000). Tenascin-C in development and disease: Gene regulation and cell function. *Matrix Biol.* **19,** 581–596.

Junker, K., van den Ingh, T. S., Bossard, M. M., and van Nes, J. J. (2000). Fibrocartilaginous embolism of the spinal cord (FCE) in juvenile Irish wolfhounds. *Vet. Q.* **22,** 154–156.

Kaapa, E., Gronblad, M., Holm, S., Liesi, P., Murtomaki, S., and Vanharanta, H. (1994). Neural elements in the normal and experimentally injured porcine intervertebral disk. *Eur. Spine J.* **3,** 137–142.

Kambic, H. E., Futani, H., and McDevitt, C. A. (2000). Cell, matrix changes and α-smooth muscle actin expression in repair of the canine meniscus. *Wound Repair Regen.* **8,** 554–561.

Kampen, W. U., and Tillmann, B. (1998). Age-related changes in the articular cartilage of human sacroiliac joint. *Anat. Embryol.* **198,** 505–513.

Kapila, S., and Xie, Y. (1998). Targeted induction of collagenase and stromelysin by relaxin in unprimed and β-estradiol-primed diarthrodial joint fibrocartilaginous cells but not in synoviocytes. *Lab. Invest.* **78,** 925–938.

Kasemkijwattana, C., Menetrey, J., Goto, H., Niyibizi, C., Fu, F. H., and Huard, J. (2000). The use of growth factors, gene therapy and tissue engineering to improve meniscal healing. *Mater. Sci. Eng.* **C13,** 19–28.

Kasper, M., and Stosiek, P. (1990). Detection of GFAP in vertebral fibrocartilage in human fetal and newborn tissue. *Acta Histochem.* **88,** 25–27.

Kavanagh, E., and Ashhurst, D. E. (2001). Distribution of biglycan and decorin in collateral and cruciate ligaments and menisci of the rabbit knee joint. *J. Histochem. Cytochem.* **49,** 877–885.

Keene, D. R., San Antonio, J. D., Mayne, R., McQuiilan, D. J., Sarria, G., Santoro, S. A., and Iozzo, R. V. (2000). Decorin binds near the C-terminus of type I collagen. *J. Biol. Chem.* **275,** 21801–21804.

Kielty, C. M., Hopkinson, I., and Grant, M. E. (1993). Collagen: The collagen family—structure, assembly, and organization in the extracellular matrix. *In* "Connective Tissue and Its Heritable Disorders: Molecular, Genetic, and Medical Aspects" (P. Royce and B. Steinmann, Eds.), 2nd Ed., pp. 103–147. Wiley-Liss, New York.

Kielty, C. M., Sherratt, M. J., and Shuttleworth, C. A. (2002). Elastic fibres. *J. Cell Sci.* **115,** 2817–2828.

Kinsella, M. G., Fischer, J. W., Mason, D. P., and Wight, T. N. (2000). Retrovirally mediated expression of decorin by macrovascular endothelial cells: Effects on cellular migration and fibronectin fibrillogenesis in vitro. *J. Biol. Chem.* **275,** 13924–13932.

Knese, K.-H., and Biermann, H. (1958). Die Knochenbildung an Sehnen- und Bandsätzen im Bereich ursprüunglich chondraler Apophysen. *Z. Zellforsch.* **49,** 142–187.

Koch, S., and Tillmann, B. (1995). The distal tendon of the biceps brachii: Structure and clinical correlations. *Anat. Anz.* **177,** 467–474.

Kojima, Y., Maeda, T., Arai, R., and Shichikawa, K. (1990). Nerve supply to the posterior longitudinal ligament and the intervertebral disc of the rat vertebral column as studied by acetylcholinesterase histochemistry. I. Distribution in the lumbar region. *J. Anat.* **169,** 237–246.

Koki, A., Khan, N. K., Woerner, B. M., Dannenberg, A. J., Olson, L., Seibert, K., Edwards, D., Hardy, M., Isakson, P., and Masferrer, J. L. (2002). Cyclooxygenase-2 in human pathological disease. *Adv. Exp. Med. Biol.* **507,** 177–184.

Kolts, I., Tillmann, B., and Lullmann-Rauch, R. (1994). The structure and vascularization of the biceps brachii long head tendon. *Anat. Anz.* **176,** 75–80.

Koob, T. J., and Vogel, K. G. (1987). Proteoglycan synthesis in organ cultures from regions of bovine tendon subjected to different mechanical forces. *Biochem. J.* **246,** 589–598.

Koob, T. J., Clark, P. E., Hernandez, D. J., Thurmond, F. A., and Vogel, K. G. (1992). Compression loading in vitro regulates proteoglycan synthesis by tendon fibrocartilage. *Arch. Biochem. Biophys.* **298,** 303–312.

Kuijpers, W., Peters, T. A., and Tonnaer, E. L. G. M. (1999). Nature of the tympanic membrane insertion into the tympanic bone of the rat. *Hearing Res.* **128,** 80–88.

Kumai, T., and Benjamin, M. (2002). Heel spur formation and the subcalcaneal enthesis of the plantar fascia. *J. Rheumatol.* **29,** 1957–1964.

Kumai, T., Takakura, Y., Rufai, A., Milz, S., and Benjamin, M. (2002). An anatomical basis for the injury patterns of the anterior talofibular ligament of the ankle joint. *J. Anat.* **200,** 457–466.

Lammi, P. E., Lammi, M. J., Hyttinen, M. M., Panula, H., Kiviranta, I., and Helminen, H. J. (2002). Site-specific immunostaining for type X collagen in noncalcified articular cartilage of canine stifle knee joint. *Bone* **31,** 690–696.

Landesberg, R., Takeuchi, E., and Puzas, J. E. (1996). Cellular, biochemical and molecular characterization of the bovine temporomandibular joint disc. *Arch. Oral Biol.* **41,** 761–767.

Lang, T. C., Zimny, M. L., and Vijayagopal, P. (1993). Experimental temporomandibular joint disc perforation in the rabbit: A gross morphologic, biochemical, and ultrastructural analysis. *J. Oral Maxillofac. Surg.* **51,** 1115–1128.

Larson, C. M., Kelley, S. S., Blackwood, D., Banes, A. J., and Lee, G. M. (2002). Retention of the native chondrocyte pericellular matrix results in significantly improved matrix production. *Matrix Biol.* **21,** 349–359.

Le Graverand, M.-P. H., Ou, Y., Schield-Yee, T., Barclay, L., Hart, D., Natsume, T., and Rattner, J. B. (2001a). The cells of the rabbit meniscus: Their arrangement, interrelationship, morphological variations and cytoarchitecture. *J. Anat.* **198,** 525–535.

Le Graverand, M.-P. H., Sciore, P., Eggerer, J., Rattner, J. P., Vignon, E., Barclay, L., Hart, D. A., and Rattner, J. B. (2001b). Formation and phenotype of cell clusters in osteoarthritic meniscus. *Arthritis Rheum.* **44,** 1808–1818.

Leonardi, R., Villari, L., Bernasconi, G., Piacentini, C., Baciliero, U., and Travali, S. (2000). Cellular S-100 protein immunostaining in human dysfunctional temporomandibular joint discs. *Arch. Oral Biol.* **45,** 411–418.

Leonardi, R., Villari, L., Piacentini, C., Bernasconi, G., Travali, S., and Caltabiano, C. (2002). Immunolocalization of vimentin and α-smooth muscle actin in dysfunctional human temporomandibular joint disc samples. *J. Oral Rehabil.* **29,** 282–286.

Lewis, A. R., Ralphs, J. R., Kneafsey, B., and Benjamin, M. (1998). Distribution of collagens and glycosaminoglycans in the joint capsule of the proximal interphalangeal joint of the human finger. *Anat. Rec.* **250,** 281–291.

Liu, S. H., Yang, R. S., A1-Shaikh, R., and Lane, J. M. (1995). Collagen in tendon, ligament, and bone healing: A current review. *Clin. Orthop.* **318,** 265–278.

Loboa, E. G., Beaupre, G. S., and Carter, D. R. (2001). Mechanobiology of initial pseudarthrosis formation with oblique fractures. *J. Orthop. Res.* **19,** 1067–1072.

Luder, H. U. (1997). Frequency and distribution of articular tissue features in adult human mandibular condyles: A semiquantitative light microscopic study. *Anat. Rec.* **248,** 18–28.

Luder, H. U. (1998). Age changes in the articular tissue of human mandibular condyles from adolescence to old age: A semiquantitative light microscopic study. *Anat. Rec.* **251,** 439–447.

Magro, G., Giannone, G., Carrubba, G., Belfiore, G., and Grasso, S. (1995). S-100 protein expression in a case of elastofibroma dorsi. *Pathologica* **87,** 528–530.

Maksymowych, W. P. (2000). Ankylosing spondylitis: At the interface of bone and cartilage. *J. Rheumatol.* **27,** 2295–2301.

Malaviya, P., Butler, D. L., Boivin, G. P., Smith, F. N., Barry, F. P., Murphy, J. M., and Vogel, K. G. (2000). An in vivo model for load-modulated remodeling in the rabbit flexor tendon. *J. Orthop. Res.* **18,** 116–125.

Mao, J. J., Rahemtulla, F., and Scott, P. G. (1998). Proteoglycan expression in the rat temporomandibular joint in response to unilateral bite raise. *J. Dent. Res.* **77,** 1520–1528.

Marcelino, J., Carptenm, J. D., Suwairi, W. M., Gutierrez, O. M., Schwartz, S., Robbins, C., Sood, R., Makalowska, I., Baxevanis, A., Johnstone, B., Laxer, R. M., Zemel, L., Kim, C. A., Herd, J. K., Ihle, J., Williams, C., Johnson, M., Raman, V., Alonso, L. G., Brunoni, D., Gerstein, A., Papadopoulos, N., Bahabri, S. A., Trent, J. M., and Warman, M. L. (1999). CACP, encoding a secreted proteoglycan, is mutated in camptodactyly–arthropathy–coxa vara–pericarditis syndrome. *Nat. Genet.* **23,** 319–322.

Martin, J. A., Mehr, D., Pardubsky, P. D., and Buckwalter, J. A. (2003). The role of tenascin-C in adaptation of tendons to compressive loading. *Biorheology* **40,** 321–329.

Matyas, J. R., Anton, M. G., Shrive, N. G., and Frank, C. B. (1995). Stress governs tissue phenotype at the femoral insertion of the rabbit MCL. *J. Biomech.* **28,** 147–157.

McDevitt, C. A., and Webber, R. J. (1990). The ultrastructure and biochemistry of meniscal cartilage. *Clin. Orthop.* **252,** 8–18.

McGonagle, D., Marzo-Ortega, H., O'Connor, P., Gibbon, W., Pease, C., Reece, R., and Emery, P. (2002). The role of biomechanical factors and HLA-B27 in magnetic resonance imaging-determined bone changes in plantar fascia enthesopathy. *Arthritis Rheum.* **46,** 489–493.

McNeilly, C. M., Banes, A. J., Benjamin, M., and Ralphs, J. R. (1996). Tendon cells in vivo form a three dimensional network of cell processes linked by gap junctions. *J. Anat.* **190,** 593–600.

Melrose, J., Ghosh, P., and Taylor, T. K. (2001). A comparative analysis of the differential spatial and temporal distributions of the large (aggrecan, versican) and small (decorin, biglycan, fibromodulin) proteoglycans of the intervertebral disc. *J. Anat.* **198,** 3–15.

Merrilees, M. J., and Flint, M. H. (1980). Ultrastructural study of tension and pressure zones in a rabbit flexor tendon. *Am. J. Anat.* **157,** 87–106.

Mikic, B., Johnson, T. L., Chhabra, A. B., Schalet, B. J., Wong, M., and Hunziker, E. B. (2000). Differential effects of embryonic immobilization on the development of fibrocartilaginous skeletal elements. *J. Rehab. Res. Dev.* **37,** 127–133.

Miller, R. R., and McDevitt, C. A. (1991). Thrombospondin in ligament, meniscus and intervertebral disc. *Biochim. Biophys. Acta* **1115,** 85–88.

Milz, S., McNeilly, C., Putz, R., Ralphs, J. R., and Benjamin, M. (1998). Fibrocartilages in the extensor tendons of the interphalangeal joints of human toes. *Anat. Rec.* **252,** 264–270.

Milz, S., Putz, R., Ralphs, J. R., and Benjamin, M. (1999). Fibrocartilage in the extensor tendons of the human metacarpophalangeal joints. *Anat. Rec.* **256,** 139–145.

Milz, S., Valassis, G., Büttner, A., Maier, M., Putz, R., Ralphs, J. R., and Benjamin, M. (2000). Fibrocartilage in the transverse ligament of the human acetabulum. *J. Anat.* **198,** 223–228.

Milz, S., Schlüter, T., Putz, R., Moriggl, B., Ralphs, J. R., and Benjamin, M. (2001). Fibrocartilage in the transverse ligament of the human atlas. *Spine* **26,** 1765–1771.

Milz, S., Regner, F., Putz, R., and Benjamin, M. (2002a). Immunohistochemical studies on the tendon of the superior oblique muscle of the human eye and its associated pulley. *Invest. Ophthalmol. Vis. Sci.* **4,** 1330–1334.

Milz, S., Rufai, A., Buettner, A., Putz, R., Ralphs, J. R., and Benjamin, M. (2002b). Three-dimensional reconstructions of the Achilles tendon insertion in man. *J. Anat.* **200,** 145–152.

Mine, T., Kimura, M., Sakka, A., and Kawai, S. (2000). Innervation of nociceptors in the menisci of the knee joint: An immunohistochemical study. *Arch. Orthop. Trauma Surg.* **120,** 201–204.

Mizoguchi, I., Scott, P. G., Dodd, C. M., Rahemtulla, F., Sasano, Y., Kuwabara, M., Satoh, S., Saitoh, S., Hatakeyama, Y., Kagayama, M., and Mitani, H. (1998). An immunohistochemical study of the localization of biglycan, decorin and large chondroitin-sulphate proteoglycan in adult rat temporomandibular joint disc. *Arch. Oral Biol.* **43,** 889–898.

Mollenhauer, J., Mok, M. T., King, K. B., Gupta, M., Chubinskaya, S., Koepp, H., and Cole, A. A. (1999). Expression of anchorin CII (cartilage annexin V) in human young, normal adult, and osteoarthritic cartilage. *J. Histochem. Cytochem.* **47,** 209–220.

Moriggl, B., Jax, P., Milz, S., Büttner, A., and Benjamin, M. (2001). Fibrocartilage at the entheses of the suprascapular (superior transverse scapular) ligament of man: A ligament spanning two regions of a single bone. *J. Anat.* **199,** 539–545.

Moriggl, B., Kumai, T., Milz, S., and Benjamin, M. (2003). The structure and histopathology of the "enthesis organ" at the navicular insertion of the tendon of tibialis posterior *J. Rheumatol.* **30,** 508–517.

Mueller, S. M., Schneider, T. O., Shortkroff, S., Breinan, H. A., and Spector, M. (1999). α-Smooth muscle actin and contractile behavior of bovine meniscus cells in type I and type II collagen–GAG matrices. *J. Biomed. Biomates. Res.* **45,** 157–166.

Murphy, G., and Reynolds, J. J. (1993). Extracellular matrix degradation. *In* "Connective Tissues and Its Heritable Disorders: Molecular, Genetic, and Medical Aspects" (P. Royce and B. Steinmann, Eds.), 2nd Ed., pp. 287–316. Wiley-Liss, New York.

Mwale, F., Tchetina, E., Wu, C. W., and Poole, A. R. (2002). The assembly and remodeling of the extracellular matrix in the growth plate in relationship to mineral deposition and cellular

hypertrophy: An in situ study of collagens II and IX and proteoglycan. *J. Bone Miner. Res.* **17,** 275–283.

Myllyharju, J., and Kivirikko, K. I. (2001). Collagens and collagen-related diseases. *Ann. Med.* **33,** 7–21.

Nagy, N. B., and Daniel, J. C. (1992). Development of the rabbit craniomandibular joint in association with tooth eruption. *Arch. Oral Biol.* **37,** 271–280.

Nakase, T., Ariga, K., Meng, W., Iwasaki, M., Tomita, T., Myoui, A., Yonenobu, K., and Yoshikawa, H. (2002). Distribution of genes for parathyroid hormone (PTH)-related peptide, Indian hedgehog, PTH receptor and patched in the process of experimental spondylosis in mice. *J. Neurosurg.* **97**(suppl. 1), 82–87.

Narama, I., Masuoka-Nishiyama, M., Matsuura, T., Ozaki, K., Nagatani, M., and Morishima, T. (1996). Morphogenesis of degenerative changes predisposing dogs to rupture of the cranial cruciate ligament. *J. Vet. Med. Sci.* **58,** 1091–1097.

Nawata, K., Minamizaki, T., Yamashita, Y., and Teshima, R. (2002). Development of the attachment zones in the rat anterior cruciate ligament: Changes in the distributions of proliferating cells and fibrillar collagens during postnatal growth. *J. Orthop. Res.* **20,** 1339–1344.

Neame, P. J., Kay, C. J., McQuyillan, D. J., Beales, M. P., and Hassell, J. R. (2000). Independent modulation of collagen fibrillogenesis by decorin and lumican. *Cell. Mol. Life Sci.* **57,** 859–863.

Niyibizi, C., Sagarrigo Visconti, C., Gibson, G., and Kavalkovich, K. (1996). Identification and immunolocalization of type X collagen at the ligament–bone interface. *Biochem. Biophys. Res. Commun.* **222,** 584–589.

Nofal, G. A., and Knudson, C. B. (2002). Latrunculin and cytochalasin decrease chondrocyte matrix retention. *J. Histochem. Cytochem.* **50,** 1313–1323.

Norrdin, R. W., Kawcak, C. E., Capwell, B. A., and McIlwaith, C. W. (1999). Calcified cartilage morphometry and its relation to subchondral bone remodelling in equine arthrosis. *Bone* **24,** 109–114.

Öberg, T., and Carlsson, G. E. (1979). Macroscopic and microscopic anatomy of the temporomanibular joint. *In* "Temporomandibular Joint Function and Dysfunction" (G. A. Zarb and G. E. Carlsson, Eds.), pp. 101–118. Munksgaard, Copenhagen.

Ochi, T., Iwase, R., Okabe, N., Fink, C. W., and Ono, K. (1983). The pathology of the involved tendons in patients with familial arthropathy and congenital camptodactyly. *Arthritis Rheum.* **26,** 896–900.

Oegema, T. R., Jr. (1980). Delayed formation of proteoglycan aggregate structures in human articular cartilage disease states. *Nature* **288,** 583–585.

Oettmeier, R., Abendroth, K., and Oettmeier, S. (1989). Analyses of the tidemark on human femoral heads. II. Tidemark changes in osteoarthrosis—a histological and histomorphometric study in non-decalcified preparations. *Acta Morphol. Hung.* **37,** 169–180.

Ohmori, M., and Azuma, H. (1998). Morphology and distribution of nerve endings in the human triangular fibrocartilage complex. *J. Hand Surg. Br.* **23,** 522–525.

Olin, A. I., Morgelin, M., Sasak, T., Timpl, R., Heinegård, D., and Aspberg, A. (2001). The proteoglycans aggrecan and versican form networks with fibulin-2 through their lectin domain binding. *J. Biol. Chem.* **276,** 1253–1261.

Oono, T., Specks, U., Eckes, B., Majewski, S., Hunzelmann, N., Timpl, R., and Krieg, T. (1993). Expression of type VI collagen mRNA during wound healing. *J. Invest. Dermatol.* **100,** 329–334.

Ortega, H. H., Munoz-De-Toro, M. M., Luque, E. H., and Montes, G. S. (2003). Morphological characteristics of the interpubic joint (symphysis pubica) of rats, guinea pigs and mice in different physiological situations: A comparative study. *Cells Tissues Organs* **173,** 105–114.

Ottani, V., Martini, D., Franchi, M., Ruggeri, A., and Raspanti, M. (2002). Hierarchical structures in fibrillar collagens. *Micron* **33,** 587–596.

Palmgren, T., Gronblad, M., Virri, J., Kaapa, E., and Karaharju, E. (1999). An immunohistochemical study of nerve structures in the anulus fibrosus of human normal lumbar intervertebral discs. *Spine* **24,** 2075–2079.

Patel, N. P., Wright, N. M., Choi, W. W., McBride, D. Q., and Johnson, J. P. (2002). Forestier disease associated with a retroodontoid mass causing cervicomedullary compression. *J. Neurosurg.* **96**(suppl. 2), 190–196.

Perez-Castro, A. V., and Vogel, K. G. (1999). In situ expression of collagen and proteoglycan genes during development of fibrocartilage in bovine deep flexor tendon. *J. Orthop. Res.* **17,** 139–148.

Petersen, W., and Tillmann, B. (1998). Collagenous fibril texture of the human knee joint menisci. *Anat. Embryol.* **197,** 317–324.

Petersen, W., Pufe, T., Kurz, B., Mentlein, R., and Tillmann, B. (2002). Angiogenesis in fetal tendon development: Spatial and temporal expression of the angiogenic peptide vascular endothelial cell growth factor. *Anat. Embryol.* **205,** 263–270.

Pfaffle, M., Borcher, M., Deutzmann, R., von der Mark, K., Fernandez, M. P., Selmin, O., Yamada, Y., Martin, G., Ruggiero, F., and Garrone, R. (1990). Anchorin CII, a collagen-binding chondrocyte surface protein of the calpactin family. *Prog. Clin. Biol. Res.* **349,** 147–157.

Prodromos, C. C., Ferry, J. A., Schiller, A. L., and Zarins, B. (1990). Histological studies of the glenoid labrum from fetal life to old age. *J. Bone Joint Surg. Am.* **72,** 1344–1348.

Pullig, O., Weseloh, G., and Swoboda, B. (1999). Expression of type VI collagen in normal and osteoarthritic human cartilage. *Osteoarthritis Cartilage* **7,** 191–202.

Rabie, A. B., and Hagg, U. (2002). Factors regulating mandibular condylar growth. *Am. J. Orthod. Dentofacial Orthop.* **122,** 401–409.

Ralphs, J. R., Benjamin, M., and Thornett, A. (1991). Cell and matrix biology of the suprapatella in the rat: A structural and immunocytochemical study of fibrocartilage in a tendon subject to compression. *Anat. Rec.* **231,** 167–177.

Ralphs, J. R., Tyers, R. N., and Benjamin, M. (1992). Development of functionally distinct fibrocartilages at two sites in the quadriceps tendon of the rat: The suprapatella and the attachment to the patella. *Anat. Embryol.* **185,** 181–187.

Ralphs, J. R., Benjamin, M., Waggett, A. D., Russell, D. C., Messner, K., and Gao, J. (1998). Regional differences in cell shape and gap junction expression in rat Achilles tendon: Relation to fibrocartilage differentiation. *J. Anat.* **193,** 215–222.

Rath, E., and Richmond, J. C. (2000). The menisci: Basic science and advances in treatment. *Br. J. Sports Med.* **34,** 252–257.

Razaq, S., Urban, J. P., and Wilkins, R. J. (2000). Regulation of intracellular pH by bovine intervertebral disc cells. *Cell. Physiol. Biochem.* **10,** 109–115.

Reardon, A. J., Le Goff, M., Briggs, M. D., McLeod, D., Sheehan, J. K., Thornton, D. J., and Bishop, P. N. (2000). Identification in vitreous and molecular cloning of opticin, a novel member of the family of leucine-rich repeat proteins of the extracellular matrix. *J. Biol. Chem.* **275,** 2123–2129.

Redini, F. (2001). Structure et régulation de l'expression des protéoglycanes du cartilage articulaire. *Pathol. Biol.* (*Paris*) **49,** 364–375.

Rees, S. G., Davies, J. R., Tudor, D., Flannery, C. R., Hughes, C. E., Dent, C. M., and Caterson, B. (2002). Immunolocalisation and expression of proteoglycan 4 (cartilage superficial zone proteoglycan) in tendon. *Matrix Biol.* **21,** 593–602.

Reese, S., Pfuderer, U. R., Bragulla, H., Loeffler, K., and Budras, K. D. (2001). Topography, structure and function of the patella and the patelloid in marsupials. *Anat. Histol. Embryol.* **30,** 289–294.

Reinboth, B., Hanssen, E., Cleary, E. G., and Gibson, M. A. (2002). Molecular interactions of biglycan and decorin with elastic fiber components: Biglycan forms a ternary complex with tropoelastin and microfibril-associated glycoprotein 1. *J. Biol. Chem.* **277,** 3950–3957.

Ritty, T. M., Ditsios, K., and Starcher, B. C. (2002). Distribution of the elastic fiber and associated proteins in flexor tendon reflects function. *Anat. Rec.* **268,** 430–440.

Robbins, J. R., and Vogel, K. G. (1994). Regional expression of mRNA for proteoglycans and collagen in tendon. *Eur. J. Cell Biol.* **64,** 264–270.

Robbins, J. R., Evanko, S. P., and Vogel, K. G. (1997). Mechanical loading and TGF-β regulate proteoglycan synthesis in tendon. *Arch. Biochem. Biophys.* **342,** 203–211.

Roughley, P. J., and Lee, E. R. (1994). Cartilage proteoglycans: Structure and potential functions. *Microsc. Res. Tech.* **28,** 385–397.

Rufai, A., Benjamin, M., and Ralphs, J. R. (1992). Development and ageing of phenotypically distinct fibrocartilages associated with the rat Achilles tendon. *Anat. Embryol.* **186,** 611–618.

Rufai, A., Ralphs, J. R., and Benjamin, M. (1995a). Structure and histopathology of the insertional region of the human Achilles tendon. *J. Orthop. Res.* **13,** 585–593.

Rufai, A., Benjamin, M., and Ralphs, J. R. (1995b). The development of fibrocartilage in the rat intervertebral disc. *Anat. Embryol.* **192,** 53–62.

Rufai, A., Ralphs, J. R., and Benjamin, M. (1996). Ultrastructure of fibrocartilages at the insertion of the rat Achilles tendon. *J. Anat.* **189,** 185–191.

Ruoslahti, E. (1996). Brain extracellular matrix. *Glycobiology* **6,** 489–492.

Saga, Y., Yagi, T., Ikawa, Y., Sakakura, T., and Aizawa, S. (1992). Mice develop normally without tenascin. *Genes Dev.* **6,** 1821–1831.

Sagarriga Visconti, C., Kavalkovich, K., Wu, J., and Niyibizi, C. (1996). Biochemical analysis of collagens at the ligament–bone interface reveals presence of cartilage-specific collagens. *Arch. Biochem. Biophys.* **328,** 135–142.

Samuel, C. S., Butkus, A., Coghlan, J. P., and Bateman, J. F. (1996). The effect of relaxin on collagen metabolism in the nonpregnant rat pubic symphysis: The influence of estrogen and progesterone in regulating relaxin activity. *Endocrinology* **137,** 3884–3890.

Sandell, L. J., Nalin, A. M., and Reife, R. A. (1994). Alternative splice form of type II procollagen mRNA (IIA) is predominant in skeletal precursors and non-cartilaginous tissues during early mouse development. *Dev. Dyn.* **199,** 129–140.

Santra, M., Reed, C. C., and Iozzo, R. V. (2002). Decorin binds to a narrow region of the epidermal growth factor (EGF) receptor, partially overlapping but distinct from the EGF-binding epitope. *J. Biol. Chem.* **277,** 35671–35981.

Schenk, R. K., Eggli, P. S., and Hunziker, E. B. (1986). Articular cartilage morphology. *In* "Articular Cartilage Biochemistry" (K. E. Kuettner, R. Schleyerbach, and V. C. Hascall, Eds.), pp. 3–22. Raven Press, New York.

Schumacher, B. L., Block, J. A., Schmid, T. M., Aydelotte, M. B., and Kuettner, K. E. (1994). A novel proteoglycan synthesized and secreted by chondrocytes of the superficial zone of articular cartilage. *Arch. Biochem. Biophys.* **15,** 144–152.

Schumacher, B. L., Su, J.-L., Lindley, K. M., Kuettner, K. E., and Cole, A. A. (2002). Horizontally oriented clusters of multiple chondrons in the superficial zone of ankle, but not knee articular cartilage. *Anat. Rec.* **266,** 241–248.

Schwab, W., and Funk, R. H. (1998). Innervation pattern of different cartilaginous tissues in the rat. *Acta Anat.* (*Basel*) **163,** 184–190.

Scott, J. E. (1995). Extracellular matrix, supramolecular organisation and shape. *J. Anat.* **187,** 259–269.

Scott, P. G., and Haigh, M. (1985). Proteoglycan–type I collagen fibril interactions in bone and non-calcified connective tissues. *Biosci. Rep.* **5,** 71–81.

Scott, P. G., Nakano, T., and Dodd, C. M. (1995). Small proteoglycans from different regions of the fibrocartilaginous temporomandibular joint disc. *Biochim. Biophys. Acta* **1244,** 121–128.

Shapses, S. A., Sandell, L. J., and Ratcliffe, A. (1994). Differential rates of aggrecan synthesis and breakdown in different zones of the bovine growth plate. *Matrix Biol.* **14,** 77–86.

Shea, J. E., Hallows, R. K., Ricks, S., and Bloebaum, R. D. (2002). Microvascularization of the hypermineralized calcified fibrocartilage and cortical bone in the sheep proximal femur. *Anat. Rec.* **268,** 365–370.

Shieh, A. C., and Athanasiou, K. A. (2003). Principles of cell mechanics for cartilage tissue engineering. *Ann. Biomed. Eng.* **31,** 1–11.

Steinetz, B. G., and Lust, G. (1994). Inhibition of relaxin-induced pubic symphyseal ''relaxation'' in guinea pigs by glycosaminoglycan polysulfates and pentosan polysulfate *Agents Actions* **42,** 74–80.

Stilwell, D. L., and Gray, D. J. (1954). The structure of bony surfaces in contact with tendons. *Anat. Rec.* **118,** 358–359.

Stockwell, R. A. (1979). ''Biology of Cartilage Cells.'' Cambridge University Press, Cambridge.

Sun, Y., and Kandel, R. (1999). Deep zone articular chondrocytes in vitro express genes that show specific changes with mineralization. *J. Bone Miner. Res.* **14,** 1916–1925.

Suzuki, D., Murakami, G., and Minoura, N. (2002). Histology of the bone–tendon interfaces of limb muscles in lizards. *Ann. Anat.* **184,** 363–377.

Svensson, L., Aszodi, A., Reinholt, F. P., Fassler, R., Heinegård, D., and Oldberg, A. (1999). Fibromodulin-null mice have abnormal collagen fibrils, tissue organization, and altered lumican deposition in tendon. *J. Biol. Chem.* **274,** 9636–9647.

Sztrolovics, R., Alini, M., Mort, J. S., and Roughley, P. J. (1999). Age-related changes in fibromodulin and lumican in human intervertebral discs. *Spine* **24,** 1765–1771.

Tabata, Y. (2001). Recent progress in tissue engineering. *Drug Discov. Today* **6,** 483–487.

Taddei, C., Frank, R. M., and Cahen, P. M. (1991). Effects of complete denture wearing on temporomandibular joints: A histomorphometric study. *J. Prosthet. Dent.* **65,** 692–698.

Takao, T., Iwaki, T., Kondo, J., and Hiraki, Y. (2000). Immunohistochemistry of chondromodulin-I in the human intervertebral discs with special reference to the degenerative changes. *Histochem. J.* **32,** 545–550.

Tanaka, A., Kawashiri, S., Kumagai, S., Takatsuka, S., Narinobou, M., Nakagawa, K., and Tanaka, S. (2000). Expression of matrix metalloproteinase-2 in osteoarthritic fibrocartilage from human mandibular condyle. *J. Oral Pathol. Med.* **29,** 314–320.

Tauber, M., van Loveren, H. R., Jallo, G., Romano, A., and Keller, J. T. (1999). The enigmatic foramen lacerum. *Neurosurgery* **44,** 386–391.

Teshima, R., Nawata, K., Hagino, H., Morio, Y., Inoue, M., and Irizawa, Y. (1999). Effects of weight bearing on the tidemark and osteochondral junction of articular cartilage: Histomorphometric analyses of 7 normal femoral heads. *Acta Orthop. Scand.* **70,** 381–386.

Thibault, M., Poole, A. R., and Buschmann, M. D. (2002). Cyclic compression of cartilage/bone explants in vitro leads to physical weakening, mechanical breakdown of collagen and release of matrix fragments. *J. Orthop. Res.* **20,** 1265–1273.

Thomopoulos, S., Hattersley, G., Rosen, V., Mertens, M., Galatz, L., Williams, G. R., and Soslowsky, L. J. (2002). The localized expression of extracellular matrix components in healing tendon insertion sites: An in situ hybridization study. *J. Orthop. Res.* **20,** 454–463.

Tischer, T., Milz, S., Maier, M., Schiecker, M., and Benjamin, M. (2002). An immunohistochemical study of the rabbit suprapatella: A sesamoid fibrocartilage in the quadriceps tendon containing aggrecan. *J. Histochem. Cytochem.* **50,** 955–960.

Trevisan, R. A., and Scapino, R. P. (1976). Secondary cartilages in growth and development of the symphysis menti in the hamster. *Acta Anat.* **94,** 40–58.

Tufvesson, E., Malmstrom, J., Marko-Varga, G., and Westergren-Thorsson, G. (2002). Biglycan isoforms with differences in polysaccharide substitution and core protein in human lung fibroblasts. *Eur. J. Biochem.* **269,** 3688–3696.

Urban, J. C. (2001). The role of the physicochemical environment in determining disc cell behaviour. *Biochem. Soc. Trans.* **6,** 858–864.

Urban, M. R., Fairbank, J. C., Etherington, P. J, Loh, FRCA, L., Winlove, C. P., and Urban, J. P. (2001). Electrochemical measurement of transport into scoliotic intervertebral discs in vivo using nitrous oxide as a tracer. *Spine* **26,** 984–990.

Vailhe, B., and Feige, J. J. (2003). Thrombospondins as anti-angiogenic therapeutic agents. *Curr. Pharm. Des.* **9,** 583–588.

van der Rest, M., Aubert-Foucher, E., Dublet, B., Eichenberger, D., Font, B., and Goldschmidt, D. (1991). Structure and function of the fibril-associated collagens. *Biochem. Soc. Trans.* **19,** 820–824.

Vogel, K. G. (1995). Fibrocartilage in tendon: A response to compressive load. *In* "Repetitive Motion Disorders of the Upper Extremity" (S. L. Gordon, S. J. Blair, and L. J. Fine, Eds.), pp. 205–215. American Academy of Orthopaedic Surgeons, Rosemont, IL.

Vogel, K. G. (1996). The effect of compressive loading on proteoglycan turnover in cultured fetal tendon. *Connect. Tissue Res.* **34,** 227–237.

Vogel, K. G., and Koob, T. J. (1989). Structural specialization in tendons under compression. *Int. Rev. Cytol.* **115,** 267–293.

Vogel, K. G., and Trotter, J. A. (1987). The effect of proteoglycans on the morphology of collagen fibrils formed in vitro. *Collagen Relat. Res.* **7,** 105–114.

Vogel, K. G., Paulsson, M., and Heinegård, D. (1984). Specific inhibition of type I and type II collagen fibrillogenesis by the small proteoglycan of tendon. *Biochem. J.* **223,** 587–597.

Vogel, K. G., Sandy, J. D., Pogany, G., and Robbins, J. R. (1994). Aggrecan in bovine tendon. *Matrix Biol.* **14,** 171–179.

Vogel, K. G., Ordog, A., Pogany, G., and Olah, J. (1993). Proteoglycans in the compressed region of human tibialis posterior tendon and in ligaments. *J. Orthop. Res.* **11,** 68–77.

Von der Mark, K., and Mollenhauer, J. (1997). Annexin V interactions with collagen. *Cell. Mol. Life Sci.* **53,** 539–545.

Waggett, A., Kwan, A., Woodnutt, D., Ralphs, J., and Benjamin, M. (1998). Characterisation of collagens and proteoglycans at the insertion of the human Achilles tendon. *Matrix Biol.* **16,** 457–470.

Watanabe, H., Kimata, K., Line, S., Strong, D., Gao, L. Y., Kozak, C. A., and Yamada, Y. (1994). Mouse cartilage matrix deficiency (cmd) caused by a 7 bp deletion in the aggrecan gene. *Nat. Genet.* **7,** 154–157.

Wiberg, C., Heinegård, D., Wenglén, C., Timpl, R., and Mörgelin, M. (2002). Biglycan organizes collagen VI into hexagonal-like networks resembling tissue structures. *J. Biol. Chem.* **277,** 49120–49126.

Wight, T. N. (2002). Versican: A versatile extracellular matrix proteoglycan in cell biology. *Curr. Opin. Cell Biol.* **14,** 617–623.

Woessner, J. F., and Nagase, H. (2000). Matrix metalloproteinases and TIMPs. Oxford University Press, Oxford.

Wren, T. A., Beaupre, G. S., and Carter, D. R. (2000). Mechanobiology of tendon adaptation to compressive loading through fibrocartilaginous metaplasia. *J. Rehabil. Res. Dev.* **37,** 135–143.

Yao, L. Y., Moody, C., Schonherr, E., Wight, T. N., and Sandell, L. J. (1994). Identification of the proteoglycan versican in aorta and smooth muscle cells by DNA sequence analysis, in situ hybridization and immunohistochemistry. *Matrix Biol.* **14,** 213–225.

Yu, J. (2002). Elastic tissue of the intervertebral disc. *Biochem. Soc. Trans.* **30,** 848–852.

Zhu, Y., McAlinden, A., and Sandell, L. J. (2001). Type IIA procollagen in development of the human intervertebral disc: Regulated expression of the NH_2-propeptide by enzymic processing reveals a unique developmental pathway. *Dev. Dyn.* **220,** 350–362.

This Page Intentionally Left Blank

Cellular Deflagellation

Lynne M. Quarmby
Department of Biological Sciences, Simon Fraser University, Burnaby,
British Columbia, Canada V5A 1S6

Deciliation, also known as deflagellation, flagellar autotomy, flagellar excision, or flagellar shedding, refers to the process whereby eukaryotic cells shed their cilia or flagella, often in response to stress. Used for many decades as a tool for scientists interested in the structure, function, and genesis of cilia, deciliation itself is a process worthy of scientific investigation. Deciliation has numerous direct medical implications, but more profoundly, intriguing relationships between deciliation, ciliogenesis, and the cell cycle indicate that understanding the mechanism of deciliation will contribute to a deeper understanding of broad aspects of cell biology. This review provides a critical examination of diverse data bearing on this problem. It also highlights current deficiencies in our understanding of the mechanism of deciliation.

KEY WORDS: Deciliation, Microtubule severing, Katanin, Centrin, Calcium, *Chlamydomonas*, Cilia, Flagella, Intraflagellar transport, Cell cycle.

I. Introduction

Eukaryotic cilia and flagella are organelles of motility and sensory perception. From the complex and powerful flagella of human sperm to the flaccid yet exquisitely sensitive cilia of olfactory epithelia; from the large cilia of ctenophores to the tiny primary cilia of vertebrate cells; from the classic structure of a *Chlamydomonas* flagellum to the highly modified cilia of the outer segments of light sensing rod cells, cilia and flagella are built around a common fundamental structure. The appendages of particular cells are, by tradition, referred to as either cilia or flagella, but when referring to the eukaryotic organelle there is no unique feature that dictates the use of one term or the other. This review uses the terms interchangeably.

Cilia are anchored in the cytoplasm by their attachment to basal bodies (Figs. 1 and 2). Basal bodies are differentiated centrioles. The essential structure is a short cylinder made of nine triplet microtubules (A, B, and C tubules) and many accessory proteins, most of them as yet undefined. The nine outer doublet microtubules of the axoneme extend from the A and B tubules of the nine basal body triplets. The doublets extend through what is commonly called the flagellar transition zone. The structural details of the transition zone vary, but all cilia have a transition zone that includes a sophisticated structure internal to the nine outer doublets, and various attachments to the membrane outside of the ring of doublets. In certain cells, such as vertebrate photoreceptor cells which have a modified cilium that we know as the outer segment, the axoneme does not exist beyond the transition zone. In more traditionally ciliated cells, distal to the transition zone the nine outer doublets extend into the cilium proper, which is usually

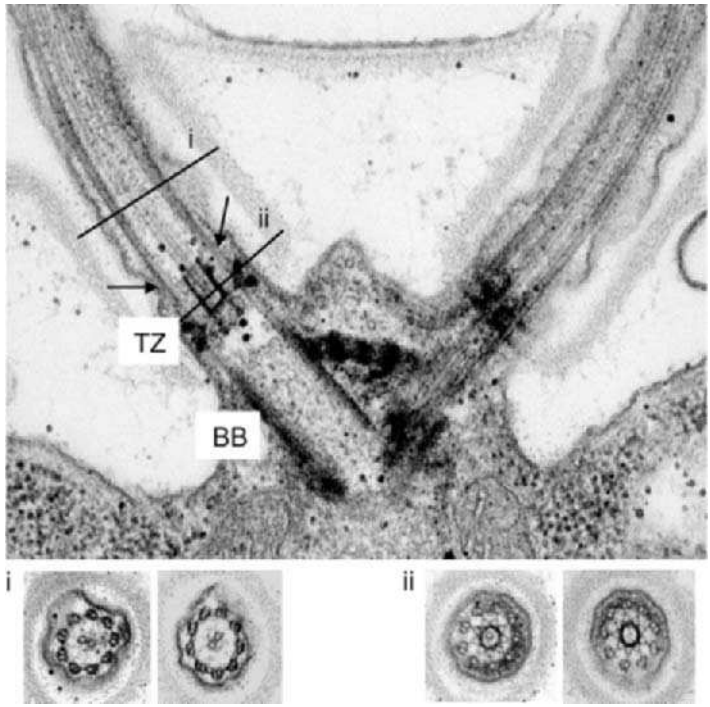

FIG. 1 Electron micrographs of *Chlamydomonas reinhardtii. Top*: A longitudinal TEM of the apical region, showing basal bodies and flagella. TZ, flagellar transition zone; BB, basal body. The arrows indicate the site of outer doublet microtubule severing during deflagellation. *Bottom*: Cross-sections through (i) the flagella and (ii) the transition zone. Note the stellate fibers connecting outer doublet microtubules to the central cylinder of the transition zone. Images by Peter Beech (Deakin University, Australia).

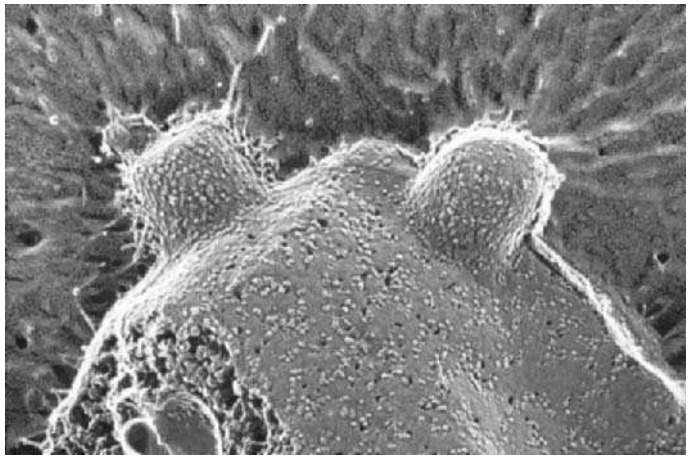

FIG. 2 Freeze-fracture scanning electron micrograph of deflagellated *Chlamydomonas reinhardtii*. Image by Ursula Goodenough (Washington University, St. Louis, MO).

elaborated by the addition of the central pair of singlet microtubules and many accessory structures. It is at the distal end of the transition zone, at the base of the flagellum, that deflagellation occurs.

Deflagellation is the shedding of flagella that occurs in response to a wide range of stimuli. It involves the precise severing of the nine outer doublet microtubules at the distal end of the transition zone, and the fission of the membrane between the cell body and the flagella. This review provides a brief history of human awareness of this cellular behavior, some ideas about why cells do it, a detailed review of progress in elucidating the mechanism, and the relationship of deciliation to other basal body/centriole-related activities such as the cell cycle and the formation of new flagella.

II. Historical Background

A. Deciliation as a Laboratory Tool

Whatever deflagellation might be doing for cells, for several decades it has served scientists as an extraordinary tool for elucidating flagellar structure, the mechanism of assembly and maintenance of this structure, the mechanism of ciliary motility, and the segregation of sensory functions into cilia. Much of what we know about cilia can be attributed to the fact that cells deciliate and that insightful pioneering scientists noted this fact and exploited it.

Deflagellation of cells as diverse as algae and sea urchin embryos occurs at a specific site, at the distal end of the flagellar transition zone (Blum, 1971; Chakrabarti *et al*., 1998; Lewin and Lee, 1985). Severing of the outer doublet microtubules is followed by fission of the flagellar membrane, thereby creating two separate compartments: the flagellaless cell, and the isolated flagellum, encased in its membrane. Deflagellated cells will synchronously regenerate new flagella, allowing studies of the synthesis, transport, and posttranslational modification and assembly of flagellar proteins. Flagella and flagellar fractions are easily prepared, facilitating biochemical characterization of their components. Demembranated axonemes can be reactivated with ATP and have been useful for *in vitro* studies of the mechanism and control of flagellar motility. The study of many different cells has contributed to our understanding of cilia, but the premier model organism for work in this area is *Chlamydomonas reinhardtii*. This unicellular biflagellate provides the opportunity to correlate genetic and biochemical data with cell biological observations such as flagellar waveform, beat frequency, and intraflagellar transport (see below). Genetic studies in *Chlamydomonas* have identified $\sim$100 loci that influence flagellar assembly and function, including regulation of flagellar length and number. Because the flagellar apparatus of all eukaryotes is highly conserved, many of the cloned genes have been matched with homologs in animal genomes.

A thorough review of the voluminous scientific literature on cilia and ciliogenesis is beyond the scope of this review, but a thumbnail sketch of aspects relevant to the topic of deciliation is provided. The reader is referred to some of the many excellent reviews available on the topic of flagellar structure and function (Dutcher, 2001; Kamiya, 2002; Mitchell, 2000; Rosenbaum and Witman, 2002; Silflow and Lefebvre, 2001). In spite of our extensive knowledge of eukaryotic cilia, many fascinating problems remain, such as the mechanism by which the central pair apparatus regulates ciliary waveform (Wargo and Smith, 2003), and the mechanisms by which eukaryotic cilia are built and maintained (Rosenbaum and Witman, 2002). The latter problem is of particular interest here because new data indicate a connection between the mechanisms of deciliation and the mechanisms of ciliary assembly and maintenance.

It was recognized early that regeneration of flagella after deflagellation provides a unique opportunity to study the genesis of an organelle (Rosenbaum and Child, 1967). In both *Chlamydomonas* (Lefebvre *et al*., 1978; Weeks *et al*., 1977) and sea urchin embryos (Gong and Brandhorst, 1987) deciliation results in an enhancement of tubulin gene transcription that is not a consequence of a depleted pool of unpolymerized tubulin. The accumulation of tubulin transcripts is a consequence of both activation of transcription and stabilization of the message (Lefebvre and Rosenbaum, 1986). These events occur in response to a signal that is either generated by

deflagellation or is a branch of the signaling pathway that triggers deflagellation. Other flagellar genes are also upregulated in response to deflagellation; it appears that the regulation of mRNA abundance is complex and results from several regulatory events. Although DNA response elements have been identified, a program of flagellar gene induction has not yet been described (Kang and Mitchell, 1998, and references therein). The signal that activates the transcription and stabilization machinery is calcium, but some experiments indicate that this calcium signal is distinct from the calcium signal that activates the machinery of deflagellation (Cheshire and Keller, 1991; and see Section IV). It is clear that a program of gene regulation is activated by deflagellation, leading ultimately to the synthesis of building material for the replacement flagella. But how are these building blocks assembled into new flagella?

First, it is important to recognize that flagella are dynamic structures. Assembly occurs at the distal tip of the flagellum (Johnson and Rosenbaum, 1992) and depends on the transport of material along the axoneme to the tip. Key insights into this process derive from the discovery, in *Chlamydomonas*, of intraflagellar transport, or IFT (Kozminski *et al*., 1993).

Intraflagellar transport is the microtubule-based movement of particles (known as IFT rafts) from the base to the tip of the flagellum (anterograde) and back again (retrograde). The particles, sandwiched between the outer doublet microtubules and the flagellar membrane, are thought to carry building blocks for both the axoneme and the flagellar membrane in the anterograde direction (Rosenbaum and Witman, 2002). Particles moving in the retrograde direction are thought to be the core of the IFT raft, returning to the base of the flagella to pick up new cargo and perhaps return defective components to the cytoplasm. The anterograde motor is kinesin-II (Kozminski *et al*., 1995; Piperno *et al*., 1996; Walther *et al*., 1994) and the retrograde motor is cytoplasmic dynein 1b (Pazour *et al*., 1998, 1999; Porter *et al*., 1999). The transport cycle occurs in four phases and there are mutant strains of *Chlamydomonas* with defects in each of the phases (Iomini *et al*., 2001). There are mutations affecting IFT in many different organisms, suggesting that IFT is required for the assembly and maintenance of all eukaryotic motile and nonmotile cilia and flagella, including sensory and primary cilia (Pazour and Rosenbaum, 2002). Isolation of *Chlamydomonas* flagella via deflagellation provides large quantities of flagella and allows the purification of IFT rafts (Cole *et al*., 1998). Peptide sequences from the purified polypeptides are leading to identification of most of the raft proteins and their homologs in other species (Pazour and Rosenbaum, 2002; Rosenbaum and Witman, 2002). Defects in IFT are associated with several human pathologies, including polycystic kidney disease, retinal degeneration, situs inversus, and are likely to be associated with Senior–Loken syndrome and Bardet–Biedl syndrome

(El Zien *et al.*, 2003; Marszalek and Goldstein, 2000; Pazour and Rosenbaum, 2002; Sloboda, 2002).

Flagellar assembly occurs primarily at the distal tip of the flagellum, and is dependent on IFT. The plus ends of axonemal microtubules are found at the distal tip and it is the plus ends of microtubules that provide highly localized signals important for effecting cell polarity (Small and Kaverina, 2003). Many different microtubule-associated proteins (MAPs) bind selectively to the plus ends, and this heterogeneous population of proteins is thought to play important roles in eliciting cascades of highly localized interactions that affect microtubule dynamics and function (Galjart and Perez, 2003). Thus, it is not surprising that disassembly of flagella is observed at the distal tip. However, flagella are dynamic structures and assembly and disassembly continue, in balance, in full-grown flagella (Marshall and Rosenbaum, 2001; Stephens, 1997). Because disassembly is independent of IFT, and independent of flagellar length (Marshall, 2002; Marshall and Rosenbaum, 2001), it may occur along the length and/or at the base of the flagellum (Stephens, 2000; see also Section VI).

Although we have long known that cilia are sensory organelles of vision and olfaction, new data are indicating a sensing role for primary cilia, which are found on most vertebrate cells (Pazour and Witman, 2003). In addition to its role in the assembly and maintenance of sensory cilia, IFT may also function to target and regulate signaling proteins of the cilia (Pan and Snell, 2002). Deciliation was key to the first localization of membrane proteins specific to cilia. By comparing electrical recordings before and after deciliation, and during ciliary regeneration in *Paramecium caudatum*, Dunlap (1977) and Ogura and Takahasi (1976) discovered that Ca^{2+} channels are localized to the ciliary membranes.

Experiments suggest that proteins essential to IFT may play roles in deflagellation, and vice versa (Parker and Quarmby, 2003). One possibility is that this reflects a role for IFT in regulating the signaling proteins of deflagellation. An alternative, and perhaps more interesting, explanation is that there are common elements in the mechanism for flagellar disassembly by resorption and deflagellation. This topic is discussed in Section VI.

B. Deciliation as a Diagnostic Tool

In addition to providing a useful tool for science, deciliation has technical application as an indicator. One example is in the diagnosis of shellfish disease. Deciliation of the velar epithelium of the larval stages of shellfish is used as an early indicator of bacterial infection in oysters and clams (Bower, 2001; Montes *et al.*, 2001). Deciliation of respiratory and oviduct epithelia and deflagellation of sperm also provide useful indicators in the diagnosis of

human ailments. This is discussed in the following section on the deciliation of cells in their natural environments.

C. Deciliation and the Natural History of Cells

The value of deflagellation to scientists is clear (see above), but what is in it for the cell? Why do cells deflagellate? Do they deflagellate in response to stimuli normally encountered in their environment? Is deciliation an adaptive physiological behavior, a pathological response, or a phenomenon that occurs only in the laboratories of scientists interested in flagella?

Taking the last question first, deflagellation definitely occurs without stressful inducements by researchers. According to Blum (1971), as early as 1895 Wilson reported that sperm of the sea urchin, *Toxopneustes*, deflagellates during fertilization. Deflagellation of sperm is a common, but not universal, observation. A few shed their flagella before entering the egg, but for most the separation of basal body from axoneme occurs after entry into the egg. It is likely that this separation occurs by a severing mechanism similar to what happens during deflagellation of cells that are not within oocytes.

The first report documenting a physiological function for deflagellation appeared more than 40 years ago. As cited by Blum (1971), Vivier and Andre (1961) observed deciliation of the ventral surfaces of *Paramecium* during mating. Presumably the loss of cilia facilitates close apposition of the membranes before fusion. To my knowledge, the signaling process in this pathway remains unknown.

Lewin *et al.* (1982) suggest that because deflagellation is a means by which a cell can quickly reduce the area of permeable surface, it may have a positive survival value for species liable to be subjected to unfavorable physicochemical conditions. This hypothesis led Lewin and Burrascano (1983) to name the first deflagellation-defective mutant of *Chlamydomonas*, *fa*, for flagellar autotomy, after the process of autotomy whereby amphibians shed and replace a damaged limb (this mutant is now known as *fa1*-1). In unpublished experiments, my laboratory has tested this hypothesis by subjecting *Chlamydomonas* cells to a variety of deflagellation-inducing stresses, and comparing the survivorship of wild-type cells with the survivorship of *fa1*-1 (and other deflagellation mutants described below). In no instance have we detected reduced survivorship in deflagellation-defective mutants. Although it is possible that we have failed to test specific environmental conditions that would reveal a selective advantage, it is unlikely that surviving noxious environments have provided the selective force for the evolution of deciliation.

An alternative idea is that the natural breakpoint in cilia (Blum, 1971) is a consequence of the way that they are built—that is, a consequence of their evolutionary history rather than a selected trait. This does not preclude the

possibility that different ciliated cells have evolved specialized pathways that incorporate this property of cilia into adaptive behaviors, including but not limited to surviving noxious environments. For example,

- Anecdotal reports indicate that deciliation might provide protists with a means of escape from predation (Pickett-Heaps and Pickett-Heaps, 1995).
- Sperm deflagellate in response to environmental toxins, including fluoride (Chinoy and Narayana, 1994); sperm also deflagellate on fertilization (Paweletz *et al*., 1987).
- Respiratory epithelial cells deciliate in response to smoke (Moss, personal communication, 2003).
- Upper respiratory infections can cause deciliation of upper respiratory tract mucosa (Willoughby *et al*., 1992).
- Ciliation and deciliation of the oviduct epithelium constitute a continuous, hormonally controlled process throughout the menstrual cycle (Reeder and Shirley, 1999; Verhage *et al*., 1979).
- Deciliation of the oviduct can also be triggered by infection (Stalheim and Gallagher, 1977).

Deciliation is a highly conserved behavior. In addition to the cell types mentioned above, many other cells have been observed to deciliate, including olfactory epithelia (Friedrich and Korsching, 1997), sea urchin embryos (Auclair and Siegel, 1966), mollusc gills (Stephens, 1975), and brain ependymal cilia (Mohammed *et al*., 1999). Given that the structure of the axoneme is highly conserved, and that deflagellation is widely observed, it is likely that the mechanism of excision is also conserved, involving orthologous proteins and processes. But what of the signaling pathways that culminate in excision? As detailed above, the life histories of cells that deciliate vary dramatically. The stimulus for the ciliated epithelium of the oviduct to shed its cilia is different from the mating-inspired deciliation of *Paramecium*, or predator-encouraged deflagellation of *Chlamydomonas*, or tail loss on fertilization by sperm. Either different cell types have evolved entirely different ways to trigger deflagellation, or there is a common pathway that is tapped by different environmental stimuli.

III. Signal Transduction Pathways to Deflagellation

A. General

For years, calcium has been implicated as the intracellular messenger that triggers deflagellation in a wide variety of cells (Dunlap, 1977; Goldstein, 1974; Huber *et al*., 1986; Quarmby *et al*., 1992; Rosenbaum and Carlson,

1969; Sanders and Salisbury, 1989; Thompson *et al.*, 1974). But none of these experiments directly addressed whether Ca^{2+} activates the key event in deflagellation, severing of the outer doublet microtubules of the axoneme. The most direct observation documenting the role of calcium in triggering this process was made by Lohret *et al.* (1998). In these experiments, *Chlamydomonas* cells were stripped of their cell walls and their membranes were removed by detergent in the presence of EGTA. Under these conditions the flagellar axoneme remains attached to its basal body, and the two basal bodies remain connected. These structures, referred to as flagellar–basal body complexes (FBBCs), were purified by centrifugation in Percoll gradients. When 1 m*M* calcium is added to this preparation, the axonemes are released from their respective basal bodies at the same site as severing occurs during deflagellation of intact cells (Lohret *et al.*, 1998). This result is consistent with other reports that indicated that 1 m*M* calcium induces deflagellation in cells permeabilized with a nonionic detergent (Sanders and Salisbury, 1989, 1994).

The experiments by Lohret *et al.* (1998) and Sanders and Salisbury (1989 and 1994) indicate that calcium can activate the machinery of deflagellation. But is calcium the physiological trigger? Almost certainly, it is. Other cations either do not trigger severing or do so only at high concentrations (Evans *et al.*, 1997; Huber *et al.*, 1986; Sanders and Salisbury, 1994). Furthermore, many of the agents that stimulate deflagellation are known to elevate intracellular calcium (Braun and Hegemann, 1999); others are suspected of doing so.

Progress in understanding the machinery that is activated by calcium is reviewed in Section V. First, however, it is worth reviewing what is known about how the calcium signal is generated in response to various deflagellation-inducing agents. All the agents reviewed here are tools used by scientists in the laboratory to induce deflagellation. Virtually nothing is known about the signaling pathways that mediate physiologically relevant stimuli such as hormones (deciliation of the epithelial cells of the oviduct and ampulla), smoke (respiratory epithelia), fluoride (sperm), predators (*Chlamydomonas*), and cell–cell contact (*Paramecium*; sperm penetration into egg). If a calcium-sensitive junction between the cilium proper and the ciliary transition zone is an essential aspect of building a cilium, then different cells might evolve completely independent approaches to severing this connection process under cell-specific circumstances. On the other hand, if deciliation evolved as an asset in its own right, then we might anticipate that a common signaling pathway might be activated by all cells that deflagellate. This question remains unresolved; evidence for both perspectives can be found in the data reviewed below.

Efforts to develop methods for the efficient isolation of intact cilia led to the use of complex protocols, many involving the simultaneous use of more than one form of chemical and/or physical stress to induce deciliation (Goldstein, 1974). The following section discusses only the specific individual

agents that have been used to trigger deflagellation in experiments that might provide insight into the signaling pathways involved.

B. Deflagellating Agents

1. Chloral Hydrate

Chloral hydrate is a sedative–hypnotic that is sometimes used to relieve anxiety or to induce sleep. It has long been a drug of abuse (Anonymous, 1880); a solution of chloral hydrate and alcohol constituted the infamous Mickey Finn. The capacity of chloral hydrate to act as a mitotic inhibitor has been known almost as long (Hertwig and Hertwig, 1886, as cited by Kennedy and Brittingham, 1968). More recently, it has also been used to induce deciliation (Kennedy and Brittingham, 1968).

Chloral hydrate (trichloroacetaldehyde monohydrate) is a relatively lipophilic compound, and its mode of action is not known. Dunlap (1977) proposed that chloral hydrate might cause deciliation of *Paramecium* by raising intracellular calcium. Measurements of the effects of chloral hydrate on intracellular calcium or on calcium influx have not been made in cells that deciliate in response to chloral hydrate. However, in Ptk2 cells, chloral hydrate causes up to a 20-fold increase in cytosolic calcium within 15 s and elevated levels of calcium are sustained for several minutes (Lee *et al.*, 1987). In this system, chloral hydrate disrupts mitosis, probably mediated by the effects of calcium on the mitotic spindle (Lee *et al.*, 1987). These effects occur when chloral hydrate is applied to the outside of the cell, but not when it is injected (Lee *et al.*, 1987), suggesting that chloral hydrate is binding to the surface of the cell and activating a signal transduction pathway.

The cellular target of chloral hydrate is not known, but it can inhibit membrane ATPases *in vitro* (Bergesse *et al.*, 1983). Of these, the transporter that is most sensitive to inhibition by this drug is Ca/Mg-ATPase (Bergesse *et al.*, 1983). Ca-ATPase normally pumps calcium out of the cell, and thus its inhibition could lead to an increase in cytosolic calcium. Lee *et al.* (1987) report that EGTA inhibits chloral hydrate-induced increases in cytosolic calcium, thus supporting the idea that chloral hydrate exerts its effects by affecting movement of Ca^{2+} across the plasma membrane.

In the context of the studies on organic acids reviewed below, it is interesting to note that chloral hydrate has a carboxylic acid group. Other weak organic acids trigger deflagellation via release of protons in the cytoplasm (see below). However, the pK_a value for chloral hydrate is $\sim$10; therefore, it is unlikely that it is activating the same pathways described below.

Choral hydrate is lipophilic and may disrupt membrane structure. Consequently, it is likely to affect the function of diverse membrane proteins and

lipids. However, it is unlikely that choral hydrate is permeabilizing the membrane: 7.5% choral hydrate injected into a cell has no effect on intracellular calcium concentration, whereas 0.1% applied to the outside of the cell causes a 20-fold increase in the concentration of intracellular calcium (Lee *et al.*, 1987).

2. Dibucaine

Dibucaine is an amide local anesthetic. The mechanism of action of dibucaine is poorly understood, in part because it has a number of cellular targets (Butterworth and Striachartz, 1990) and more continue to be defined. It has been shown that dibucaine can induce apoptosis via activation of caspases and induction of a unique permeability transition that leads to the release of cytochrome *c* from mitochondria (Arita *et al.*, 2000; Kushnareva *et al.*, 2001).

Some of the effects of dibucaine are likely to be nonspecific, occurring only at high concentrations, whereas others, including anesthetic effects, occur at much lower concentrations. At relatively low concentrations, dibucaine allosterically inhibits activation of voltage-gated sodium channels (Catteral, 1992; Flowers *et al.*, 2002). At higher concentrations, dibucaine interacts with membrane lipids, particularly phospholipids, and is reported to displace Ca^{2+} from membranes (see Nicolson *et al.*, 1976, and references therein). Dibucaine treatment also causes an increase in the fluidity of the plasma membrane (Papahadjopoulos *et al.*, 1975; Poste *et al.*, 1975). The perturbation of membrane structure affects the activity of membrane proteins (Suwalsky *et al.*, 2001), and consequent destabilization of transmembrane proteins (Senisterra and Lepock, 2000). Because the site of action of dibucaine is hydrophobic, and the proteins affected are membrane proteins, it has been difficult to distinguish lipid from protein effects. Nevertheless, the available data suggest that dibucaine induces deciliation by activating (or inhibiting) a signaling pathway, rather than via generalized disruption of the plasma membrane.

Thompson *et al.* (1974) developed methodology for the use of dibucaine to induce efficient deciliation of *Tetrahymena*, using conditions that allow the cells to survive and regenerate their cilia. Although deciliation by dibucaine is used routinely by many researchers on a range of different cells (including *Chlamydomonas*; Witman *et al.*, 1978), the cellular pathway from treatment to deciliation has not been specifically studied. Given the limited data available, it is possible that dibucaine induces deflagellation by transiently disrupting the integrity of the membrane, allowing direct access of extracellular Ca^{2+} to the machinery of deflagellation. However, because dibucaine effectively induces deflagellation at sublethal concentrations, it is tempting to speculate that it does so via effects on specific proteins.

Dibucaine-induced deflagellation is not inhibited by La^{3+}, suggesting that it is not activating influx of Ca^{2+} through a protein (Quarmby, unpublished observation, 1996). The idea that dibucaine is not activating a calcium influx pathway is supported by evidence that dibucaine inhibits ion channels and transporters (Anteneodo *et al.*, 1994; Catteral, 1992). It follows that dibucaine might produce the calcium signal of deflagellation by inhibiting extrusion of calcium from the cytosol—either out of the cell or into membrane-bound stores—thereby producing an accumulation of Ca^{2+} in the cytosol. It is also possible that deciliation is triggered via the Ca^{2+} released from calcium-binding proteins and lipids when they are destabilized by dibucaine.

3. Temperature

Lewin *et al.* (1982) reported that temperatures above 40 °C induced *Chlamydomonas moewusii* to shed its flagella. Elevated temperature and dibucaine both induce the synthesis of heat shock proteins (Coss and Smith, 1991). Therefore, elevated temperature might induce deflagellation in the same way as dibucaine, whether that is by disruption of membrane integrity; or by disruption of membrane proteins, leading to inhibition of Ca^{2+} extrusion from the cytosol; or by release of Ca^{2+} from lipids and proteins.

Many of the strains of *Chlamydomonas* that are now known as temperature-sensitive flagellar assembly mutants, such as *fla10*-1, which carries a defect in a motor subunit of the anterograde kinesin (Kozminski *et al.*, 1995), were originally isolated in a screen for temperature-sensitive mutants defective in motility (Huang *et al.*, 1977). These "drop-down" or "*dd*" mutants, drop to the bottom of the test tube at the restrictive temperature, because of lack of motility. Many of these strains were later renamed *fla* to reflect the observation that their loss of motility was a consequence of a defect in flagellar assembly (Adams *et al.*, 1982). Although several of these strains have clear flagellar assembly defects, some of them, most notably *fla2*, have (at best) subtle assembly defects, but deflagellate much more readily than wild type on transfer to the restrictive temperature, 33 °C (Huang *et al.*, 1977; Parker and Quarmby, 2003). This suggests that elevated temperature might induce deflagellation in wild-type cells via the inactivation of specific proteins, presumably proteins that play roles in both deflagellation and flagellar assembly. The relationship between deflagellation and flagellar assembly is complex and is discussed in Section VI.

4. Alcohol

Many of the early protocols for isolating cilia involved the use of ethanol to stimulate deciliation: cells were incubated in ethanol and then transferred to a

solution of digitonin (Child and Mazia, 1956); or transferred from ethanol to high KC1 or cold glycerol (Child, 1959); or treated with ethanol, acetic acid, and calcium (Watson and Hopkins, 1962). There were many variations on the ethanol-based approach as workers strove to define conditions for the efficient isolation of intact cilia. In 1983, Lewin and Burrascano showed that the concentration of ethanol needed to induced deflagellation in *Chlamydomonas* was influenced by pH, temperature, and the chemical composition of the medium—all factors that we know now as deflagellation agents in their own right. Nevertheless, it is by now established that ethanol, without the aid of pH and/or temperature shock, triggers deflagellation (Huber *et al*., 1986; Lewin and Burrascano, 1983).

In *Dunaliella tertiolecta*, deflagellation occurs only at ethanol concentrations that kill the cells (Huber and Lewin, 1987). Extracellular calcium was not necessary for either effect, but given the established requirement for Ca^{2+} in deflagellation, it is likely that Ca^{2+} leaked from internal stores triggered deflagellation in the dying cells. In contrast, *Chlamydomonas* and *Tetraselmus* deflagellate at concentrations of ethanol well below lethal levels (Lewin and Burrascano, 1983; Lewin *et al*., 1982). In *Chlamydomonas reinhardtii*, extracellular Ca^{2+} is required for ethanol-induced deflagellation (Huber *et al*., 1986). In these experiments the cells were not deprived of Ca^{2+} before treatment with ethanol; therefore, the requirement for Ca^{2+} suggests that ethanol triggers Ca^{2+} influx rather than release from internal stores (which can become depleted during incubation of cells in Ca^{2+}-free buffer). The amount of Ca^{2+} required for ethanol-induced deflagellation (50% of cells deflagellate after 10 s in 1 m*M* Ca^{2+}) is comparable to the amount of Ca^{2+} required for pH shock-induced deflagellation and much more than required for deflagellation of detergent-permeabilized cells (Huber *et al*., 1986; Quarmby and Hartzell, 1994; Sanders and Salisbury, 1989). This raises the possibility that ethanol is stimulating the same signaling pathway that is activated in response to pH shock.

5. pH Shock

pH shock is a common protocol used by researchers interested in isolating flagella for biochemical work (Witman *et al*., 1972). In the standard protocol for the preparation of flagella, cells are briefly exposed to a solution of pH 4. If the cells are returned to neutral media within 1 or 2 min they survive and rapidly regrow their flagella. Consequently this treatment is also useful for studying the assembly of flagella and their components.

Weak organic acids will trigger living cells to deflagellate, but acid does not trigger the machinery of deflagellation directly (Quarmby and Hartzell, 1994; Quarmby, unpublished observations, 1997). What is the signalling pathway activated by pH shock and how does it induce deflagellation?

Deflagellation is not induced by a rapid drop in extracellular pH, for example, brief exposure to 10 m*M* glycine-HCl, pH 3.68 (Hartzell *et al*., 1993). Nor is deflagellation induced by pH shock with strong organic acids, such as aspartic, phosphoric, citric, and tartaric (pK_a values of 1.99, 2.15, 3.13, and 3.04, respectively). pH shock triggers deflagellation only when the acid employed is a weak acid such as carbonic, formic, or acetic (pK_a values of 6.35, 3.75, and 4.76, respectively). Hartzell *et al*. (1993) showed that deflagellation in response to pH shock depends on acidification of the cytosol by the acid. When protonated, most weak organic acids are highly membrane permeant and can mediate a flux of protons into the cell. Succinate is a weak dicarboxylic acid (pK_a values of 4.21 and 5.64) that is not very membrane permeant even when fully protonated; it does not induce deflagellation. In contrast, protonated benzoate has higher membrane permeability than acetate and it triggers deflagellation at lower concentrations. Taken together, these data indicate that pH shock triggers deflagellation via acidification of the cytosol. But what are the cytosolic effectors?

Intracellular pH is implicated in the regulation of a variety of cellular functions (Roos and Boron, 1981). Many reactions in cellular biochemistry produce or consume protons, and protons can affect the activities of enzymes, ion channels, and protein–protein interactions, as well as participate in electrical signals. Consequently, it is often difficult to pinpoint the relevant molecular effector of a response to pH change. Nevertheless, in the case of acid-induced deflagellation, some progress has been made.

a. Requirement for Calcium Influx Deflagellation induced by pH shock requires an influx of extracellular calcium (Quarmby and Hartzell, 1994). When the relatively membrane-permeant benzoic acid is used at 50 m*M*, deflagellation is induced in response to a relatively mild pH shock to pH 6.0 (Hartzell *et al*., 1993). Quarmby and Hartzell (1994) used buffers of defined calcium concentration, made by using 1,2-bis(*o*-aminophenoxy)ethane-*N*,*N*,*N*′,*N*′-tetraacetic acid (BAPTA), which is an effective Ca^{2+} buffer at pH 6 as well as at neutral pH (Tsien, 1980), to demonstrate that 1 m*M* extracellular calcium is required for effective induction of deflagellation in response to pH shock (50 m*M* benzoate, pH 6.0). Solutions made cation-free by pretreatment with Chelex give the same results: cells do not deflagellate in solutions supplemented with 1 m*M* calcium, but do deflagellate when 1 m*M* calcium is added (Quarmby and Hartzell, 1994).

Chlamydomonas cells are difficult to patch clamp (Quarmby and Hartzell, personal communication, 1993; Yoshimura, 1998), and so a ^{45}Ca influx assay was developed to study the acid-activated influx of calcium (Quarmby and Hartzell, 1994). On the basis of this assay, with its first time point at 3 s, there are two phases of calcium influx activated by pH shock: an initial rapid phase and a prolonged phase (Quarmby, 1996). Diverse channel

blockers, including Cd^{2+}, flufenamic acid, D-600, nifedipine, nicardipine, and SKF-96365, block the sustained phase of calcium influx, but they do not block the initial rapid phase; nor do they block deflagellation (Quarmby, 1996). Gd^{3+} and La^{3+} block all of the acid-induced influx of calcium at the same concentrations at which they block deflagellation (Quarmby, 1996), suggesting that the initial rapid phase of calcium influx plays a role in mediating pH shock-induced deflagellation.

The *adfl*-1 mutant of *Chlamydomonas reinhardtii*, which is defective in pH shock-induced deflagellation, is also defective in pH shock-induced calcium influx (Quarmby and Hartzell, 1994). The calcium-activated machinery of these cells is intact because they can be induced to deflagellate in response to other stimuli (Quarmby and Hartzell, 1994). Therefore, acid-stimulated calcium influx plays an essential role in signaling pH shock-induced deflagellation. Mutations in the *ADF1* gene disrupt this pathway (Finst *et al.*, 1998). Therefore, cloning the *ADF1* gene will provide important insight into how acidification activates calcium influx. My laboratory has mapped the *ADF1* gene (Bradley, Montpetit, Petresca, and Quarmby, unpublished observation, 2003); unfortunately, *ADF1* maps to a recalcitrant region of the genome that defines a gap in the first release of the *Chlamydomonas* nuclear genome sequence.

In summary, three lines of evidence provide strong support for the idea that calcium influx is an essential component of the pH shock-induced signaling pathway that culminates in deflagellation: (1) extracellular calcium is required for pH shock-induced deflagellation (Quarmby and Hartzell, 1994); (2) when the initial phase of calcium influx is blocked, so too is deflagellation (Quarmby, 1996); and (3) a mutant, *adf1*-1, that is defective in acid-activated calcium influx does not deflagellate in response to pH shock. Is this calcium influx activated directly by protons, and does it directly activate the machinery of deflagellation? Or are there other players in the signaling cascade?

It is well established that acid-activated calcium influx is essential for pH shock-induced deflagellation and it has been clearly established that calcium activates the machinery of flagellar shedding (see Section V). However, the calcium that enters the cell in response to acidification may not directly activate deflagellation. It has been established that pH shock-induced deflagellation requires on the order of 1 m*M* Ca^{2+} (Quarmby and Hartzell, 1994), whereas deflagellation of detergent-permeabilized cells or FBBCs requires ~1 μ*M* Ca^{2+} (Lohret *et al.*, 1999; Sanders and Salisbury, 1989). Evans *et al.* (1997) found that Sr^{2+} supports pH shock-induced deflagellation, but does not support deflagellation of detergent-permeabilized cells, even at concentrations as high as 10 m*M* (i.e., 10,000-fold higher than the concentration of Ca^{2+} that activates severing under the same conditions). These data suggest that the initial influx of Ca^{2+} (or Sr^{2+}) leads, directly or

indirectly, to a second calcium signal generated by release of an internal store of Ca^{2+}. The following discusses the possible subcellular localization of the calcium influx pathway, and then returns to the question of the role of intracellular stores of calcium.

b. Localization of the Calcium Influx Pathway Electron microscopy of freeze-etch replicas has revealed a "ciliary necklace" of particles decorating the transition membrane at the base of the cilium (Gilula and Satir, 1972). Gilula and Satir (1972) reported that the necklace is observed in the transition region where the ciliary membrane joins the plasma membrane and where extensions from the outer doublet microtubules connect to the membrane. They speculated that the necklace may be involved in the control of localized membrane permeability, serving to regulate ciliary beat in motile cilia and mechanoreception in ciliary receptors. However, the necklace was later observed on immotile sensory cilia, such as the connecting cilium of rod photoreceptors (Rohlich, 1975) and the olfactory kinocilia (Breipohl *et al.*, 1980), indicating that this structure might play a more fundamental role in ciliary biology. Descriptions of the necklace continue to appear in the literature (e.g., Thai *et al.*, 2002), but its identity and function remain unknown. Could the particles of the ciliary necklace be manifestations of the calcium influx pathway that triggers deflagellation in response to pH shock?

Calcium channels are found on ciliary membranes and are important for the regulation of motility (Beck and Uhl, 1994; Dunlap, 1977; Pazour *et al.*, 2002b; Ren *et al.*, 2001; Tamm, 1994). Is the acid-activated calcium influx pathway of deflagellation also found on ciliary membranes? The *Chlamydomonas* mutant, *bld*-2, is defective in the ϵ-tubulin gene and does not build basal bodies and flagella (Dutcher *et al.*, 2002; Goodenough and St. Clair, 1975), yet these cells express nearly normal levels of acid-stimulated calcium influx (Quarmby, 1996). It is possible that in this case, the channels are inserted into the plasma membrane instead of the flagellar membrane simply because there are no flagella. In a more direct approach, isolated flagella do no accumulate calcium in response to pH shock (Quarmby, 1996). Once again, however, there is an important caveat: perhaps the integrity of the flagellar membranes was not high; there was no good positive control for these experiments. The experiments that may shed the most light on the localization of this pathway are those addressing the inactivation/reactivation of the pH shock pathway.

As described above, pH shock activates two distinct phases of calcium influx: a slow, sustained phase preceded by the rapid initial influx of calcium that is necessary to induce deflagellation (Quarmby, 1996). The initial rapid phase disappears after deflagellation, but is restored by 30 min, at which time the flagella have grown to about one-quarter length (Quarmby, 1996). Consistent with this result, we find that when cells are subjected to a second pH

shock while regrowing their flagella after the first pH shock, only flagella longer than 3 μm are shed (Chandler and Quarmby, unpublished observation, 2002). When cells are treated with colchicine, they do not regrow their flagella after deflagellation (Quarmby, 1996; Rosenbaum *et al.*, 1969). Such cells do, however, recover the rapid initial influx of calcium in response to acid, albeit somewhat slower than untreated cells (Quarmby, 1996). These data indicate that flagellar assembly is not required for reassembly of the signaling pathway that was inactivated after pH shock.

The rapid phase of the calcium influx pathway is not inactivated by transient acidification or by the calcium signal that is generated in response to the initial pH shock: the *fa1*-1 deflagellation defective mutant of *Chlamydomonas* shows wild-type levels of acid-induced calcium influx. Fifteen minutes after a pH shock, wild-type cells exhibit none of the initial rapid phase of calcium influx in response to a second pH shock, whereas *fa1*-1 cells respond as robustly as they did to the first pulse (Quarmby, 1996). These data suggest that inactivation of the pathway might be associated with the physical changes that occur in the flagellar transition zone coincident with deflagellation (see Section V). Although the flagellar transition zone and its associated ciliary necklace remain associated with the cell body after deflagellation (Gilula and Satir, 1972; Lewin and Lee, 1985), this region undergoes structural changes (Sanders and Salisbury, 1989; and see below) that would be likely to affect the function of associated ion channels and other membrane proteins.

c. Does PLC Play a Role? Inositol phospholipid metabolism is activated during acid-induced deflagellation (Quarmby *et al.*, 1992). This is a common cellular pathway for increasing intracellular calcium concentration by release from internal stores (reviewed by Clapham, 1995). Activated phospholipase C (PLC) hydrolyzes phosphatidylinositol 4,5-bisphosphate [PtdIns(4,5)P_2] into inositol 1,4,5-trisphosphate [Ins(1,4,5)P_3] and diacylglycerol. The Ins(1,4,5)P_3 then binds to the inositol trisphosphate (IP_3) receptor, a ligand-gated calcium channel in the membrane of the endoplasmic reticulum (ER), thereby triggering release of calcium from the ER into the cytosol. In pH-shocked *Chlamydomonas* cells, Ins(1,4,5)P_3 accumulates to levels 10-fold higher than baseline (Quarmby *et al.*, 1992). This increase is accompanied by a corresponding decrease in PtdIns(4,5)P_2, indicating that the accumulation of Ins(1,4,5)P_3 is a consequence of the activation of PLC. A coincident accumulation of diacylglycerol (DAG) is not observed, but there is an accumulation of phosphatidic acid, suggesting that DAG kinase is also activated. Activation of PLC is clearly not a consequence of deflagellation: the deflagellation-defective mutant, *fa1*-1, activates PLC as robustly as wild-type cells in response to pH shock (Quarmby *et al.*, 1992). But does activation of PLC actually mediate deflagellation, or is it an independent response to acidification?

A number of observations support the idea that activation of PLC plays an essential role in transducing the signal of cytosolic acidification into the calcium signal that triggers the deflagellation machinery, but none of the evidence is compelling. The first piece of supporting evidence comes from use of the aminoglycoside antibiotic, neomycin, which binds PtdIns(4,5)P_2 preventing its hydrolysis by PLC. Neomycin inhibits both activation of PLC and deflagellation in response to pH shock (Quarmby *et al.*, 1992), but unpublished data from my laboratory (see below) indicates that neomycin blocks deflagellation by a mechanism independent of its block on PLC.

As described above, it is well established that pH shock induces a calcium influx essential for deflagellation (Quarmby and Hartzell, 1994). This calcium influx and the consequent deflagellation are both blocked by La^{3+} (Quarmby and Hartzell, 1994). Yueh and Crain (1993) reported that La^{3+} does not inhibit PLC activation in response to pH shock, suggesting that, if PLC activation is in the deflagellation pathway, it must be upstream of calcium influx. As described above, neomycin blocks both activation of PLC and deflagellation induced by pH shock (Quarmby *et al.*, 1992; Yueh and Crain, 1993). Therefore, if PLC is in the pathway, then neomycin is predicted to block pH shock-activated calcium influx. Surprisingly, neomycin does not inhibit acid-induced calcium influx (Quarmby, unpublished observation, 1996). The simplest explanation is that while neomycin is probably inhibiting PLC by binding to PtdIns(4,5)P_2, it must also be blocking the cellular response to calcium influx by affecting an additional target. In other words, neomycin must be blocking deflagellation by a PLC-independent mechanism.

The second line of evidence supporting the idea that PLC mediates the deflagellation signal is that activation of PLC precedes deflagellation (Yueh and Crain, 1993). In the original experiments, 5 s was the first time point for which measurements of Ins(1,4,5)P_3 could be made (Quarmby *et al.*, 1992). By this time, the entire population of cells had completed deflagellation. Obviously, if PLC transduces the signal to deflagellate, its activation must precede deflagellation. To address this issue, Yueh and Crain (1993) developed continuous-flow rapid-quench techniques to measure the early events of deflagellation. During the first 400 ms after acidification (acetic acid to pH 4.3–4.5) they observed a 1.6- to 2-fold increase in Ins(1,4,5)P_3 levels. Although there was some variability in when the peak occurred (between 200 and 400 ms), it always preceded deflagellation. Neomycin inhibited both Ins(1,4,5)P_3 accumulation and deflagellation in these rapid-flow experiments (Yueh and Crain, 1993). These authors noted that the early peak in Ins(1,4,5)P_3 was indeed a peak that approached baseline after $\sim$150 ms, and thus it was distinct from the much larger peak of Ins(1,4,5)P_3 observed 50 s after pH shock (Quarmby *et al.*, 1992; Yueh and Crain, 1993).

In summary, the evidence for the involvement of PLC in signaling deflagellation reduces to a simple correlation: deflagellation is preceded by a 1.6- to 2-fold accumulation of Ins(1,4,5)P_3 (Yueh and Crain, 1993). Several pharmacological tools have been developed to evaluate the role of Ins(1,4,5)P_3-sensitive calcium stores in various cellular responses. Unfortunately, in *Chlamydomonas*, these drugs have no effect on the deflagellation pathway at modest concentration, and dramatically affect motility and viability at higher concentrations (Quarmby, unpublished observation, 1996). Does this mean that *Chlamydomonas* does not have IP_3 receptors, or that the receptors are different enough from their mammalian counterparts that the drugs do not recognize them? Version 1 of the *Chlamydomonas* nuclear genome sequence has been released (http://genome.jgi-psf.org/chlre1/chlre1.-home.html). There is at least one PLC, but no identifiable IP_3 receptor (as of March 2003). The role of PLC activation in mediating pH shock-induced deflagellation remains an open question.

6. Mastoparan

Mastoparan is a wasp venom tetradecapeptide that is a potent activator of heterotrimeric G proteins (Higashijima *et al*., 1990). Mastoparan triggers deflagellation of *Chlamydomonas* and also activates PLC in *Chlamydomonas* (Munnik *et al*., 1998; Quarmby *et al*., 1992). The inactive mastoparan analog, Mas-17 (Higashijima *et al*., 1990), did not cause either deflagellation or activation of PLC (Quarmby *et al*., 1992). These data led to speculation that mastoparan triggers deflagellation via activation of a G protein-sensitive PLC and subsequent release of calcium from Ins(1,4,5)P_3-sensitive stores. However, as described above for pH shock-induced deflagellation and PLC activation, a causal relationship between PLC activation and deflagellation has not been established.

Mastoparan, like other amphipathic peptides, can render plasma membranes permeable. As described by Sanders and Salisbury (1989), cells permeabilized with nonionic detergent in calcium-containing buffer will deflagellate. An experiment using Evans blue to assess permeability of *C. reinhardtii* and *C. moewussi* over a range of concentrations of mastoparan indicates that, at least in *C. reinhardtii*, mastoparan concentrations that are sufficient to induce deflagellation (2–10 μM) also permeabilize the cell (Munnik *et al*., 1998). This suggests that previous studies of mastoparan-induced deflagellation of *C. reinhardtii* (Quarmby and Hartzell, 1994; Quarmby *et al*., 1992; Yueh and Crain, 1993) may have been a consequence of membrane permeabilization. In contrast, the same concentration range of mastoparan triggers deflagellation of *C. moewussi*, without increased permeability to Evans blue (Munnik *et al*., 1998). However, there is evidence

suggesting that mastoparan-triggered deflagellation in *C. reinhardtii* does not depend on membrane permeabilization.

When Sanders and Salisbury (1989) used Nonidet P-40 (NP-40) to permeabilize *C. reinhardtii* cells, deflagellation was induced only when >1 μM Ca^{2+} was present in the buffer. In contrast, mastoparan-induced deflagellation of *C. reinhardtii* occurs in buffers containing only nanomolar Ca^{2+}, suggesting that the source of calcium for mastoparan-induced deflagellation is internal stores (Quarmby and Hartzell, 1994). In support of this idea, we have also observed that although treatment with mastoparan does induce Ca^{2+} influx, this influx can be completely blocked by 20 μM La^{3+}, without inhibiting mastoparan-induced deflagellation (Quarmby and Hartzell, 1994). Furthermore, the *adf1* mutant strain of *C. reinhardtii*, which is defective in acid-activated Ca^{2+} influx and does not deflagellate in response to pH shock, does deflagellate in response to treatment with mastoparan (Quarmby and Hartzell, 1994). Taken together, these data indicate that mastoparan does not trigger deflagellation via activation of calcium influx. Given the correlation with activation of PLC, it is tempting to speculate that mastoparan triggers deflagellation by release of Ca^{2+} from stores that are sensitive to $Ins(1,4,5)P_3$.

7. Alcian Blue

In *Paramecium* and *Tetrahymena*, alcian blue activates novel receptor-operated Ca^{2+} conductance, thereby affecting chemorepulsion and secretion (Francis and Hennessey, 1995; Hennessey *et al*., 1995; Tamm, 1994). In contrast, alcian blue induces *Chlamydomonas* to deflagellate (Evans and Keller, 1997b). These authors suggest that, like secretion and chemorepulsion, alcian blue-induced deflagellation may also be mediated via a receptor-operated calcium influx.

Alcian blue-induced deflagellation has a number of unique properties that may illuminate our understanding of the signaling pathway(s) that culminate in deflagellation. Evans and Keller (1997b) observed that, in populations of *Chlamydomonas* cells stimulated with threshold concentrations of alcian blue (0.00005%, w/v) the majority of cells shed only their *cis* flagellum (*cis* and *trans* flagella are defined on the basis of their relative proximity to the eyespot). And when deflagellation in cells treated with saturating concentrations of alcian blue (0.0005%, w/v) was attenuated by Cd^{2+}, up to 50% of the population of cells retained their *trans* flagellum (Evans and Keller, 1997b). A similar phenomenon is observed when conditional flagellar assembly mutants deflagellate in response to a temperature shift (Parker and Quarmby, unpublished observation, 2003; see also Section VI).

Alcian blue–induced deflagellation is completely blocked by neomycin (10 μM), ruthenium red (10 μM), La^{3+} (20 μM), and partially by Cd^{2+} (50 μM; Evans and Keller, 1997b). It is dependent on extracellular Ca^{2+}, but *adf1* mutants, which do not deflagellate in response to pH shock, do

deflagellate when treated with alcian blue (Evans and Keller, 1997b). Therefore, if alcian blue is acting through a receptor-operated calcium channel, as it does in *Paramecium*, the pathway to activate calcium influx is distinct from the pathway activated in response to pH shock. Minimally, the proton sensor, or a component in the pathway between proton sensing and the activation of calcium influx pathway (be it a channel, a transporter, or an exchanger), must be different.

Cells regrow their flagella in the continued presence of threshold concentrations of alcian blue, but they do not redeflagellate in response to either pH shock, or higher concentrations of alcian blue. Evans and Keller (1997b) interpret this phenomenon as receptor desensitization. This is similar to the inactivation of calcium influx that makes cells refractory to redeflagellation in response to pH shock (Quarmby, 1996). In the case of pH shock, both the calcium influx pathway and the ability to deflagellate in response to pH shock recover within 15 min, when flagella are approximately one-quarter full length (Quarmby, 1996).

Although *adf1* cells deflagellate in response to treatment with alcian blue, unlike wild-type cells, they fail to regrow their flagella, in spite of a modest induction of expression of flagellar genes (Evans and Keller, 1997b). This is similar to what is observed when wild-type cells deflagellate in response to pH shock in the presence of Sr^{2+} and no Ca^{2+} (Evans *et al.*, 1997). This suggests that Ca^{2+} influx through the *ADF1* pathway plays a role in triggering the program of events required to build new flagella.

8. Mechanical Shear

A commonly employed protocol for inducing deflagellation is to expose cells to the shear forces of a VirTis homogenizer (VirTis, Gardiner, NY) (Rosenbaum and Child, 1967). As long as there is calcium in the buffer, and the cells in question are not *fa* mutants, this treatment appears to activate normal calcium-induced axonemal severing and flagellar shedding. Cells induced to deflagellate by mechanical shear survive the treatment and rapidly grow new flagella. When *Chlamydomonas fa* mutants are subjected to this protocol, they do not survive (Cheshire *et al.*, 1994), possibly because the flagella are broken at random places and cannot reseal efficiently if the outer doublet microtubules are broken at unequal lengths. The pathway activated by mechanical shear has not been carefully investigated. Given that shear-induced deflagellation is not inhibited by La^{3+}, neomycin, or ruthenium red (Evans and Keller, 1997a), it is unlikely that shear is serving to gate a stretch-activated calcium-permeant ion channel. It is most likely that the high shear forces required to induce deflagellation are transiently perturbing the plasma membrane, allowing an influx of calcium.

9. A Dedicated Signaling Pathway for Deflagellation?

Is there a "deflagellation signaling pathway" per se? Although it remains an open question whether there is a common signal transduction path that initiates deflagellation, the actual mechanism of deciliation is likely to be universal.

IV. Molecular Mechanism of Deciliation

Two primary events must occur to produce the deciliation response: membrane fission and axoneme severing. Few experiments have focused on the processes mediating membrane fission in this system. In many cilia there are electron-dense fibers that connect the outer doublet microtubules to the membrane in the region of the flagellar transition zone. These may facilitate membrane fission by constricting the flagellar membrane when the axoneme in this region constricts during deciliation (see below). A careful electron microscopy (EM) study of deciliating *Tetrahymena* revealed that by the time cilia are shed from the cell, there is complete, or close to complete, closure of the membrane over the stub (Satir *et al*., 1976).

The outer segments of rod photoreceptors are modified cilia; the outer segment itself lacks an axoneme, but the narrow neck region that connects the outer segment to the inner segment (or cell body) is homologous to the ciliary transition zone. The distal region of the outer segments is shed on a diurnal cycle, facilitating renewal of the discs (Nguyen-Legros and Hicks, 2000). Disc renewal requires transport of materials through the connecting cilium, by a process common to all eukaryotic cilia and flagella—intraflagellar transport, or IFT (Pazour *et al*., 2002a). The shedding of discs involves a process analogous to the membrane fission that occurs in cilia during deciliation. Light-induced disc shedding, like deciliation, depends on an influx of extracellular calcium (Besharse *et al*., 1986).

Parallels to the membrane fission event may be found in other forms of autotomy, for example, autotomy of the ejected viscera of a disturbed holothurian (sea cucumber; Garcia-Arraras and Greenberg, 2001), or the shedding of nerve terminals during remodeling of neurons (Sotnikov, 2002). But it is also possible that the combination of breakage of the outer doublets, constriction of the axoneme, and mild external shear forces is all that is necessary for the membrane to seal. This would be analogous to cytokinesis mutants that can successfully divide if the two daughter cells crawl apart until the bridge between them is eventually broken.

Considerably more experimental attention has been paid to the mechanism of axonemal severing during deciliation. The following sections review this

work. As described above, the intracellular signal that ultimately activates the machinery of deflagellation is calcium. This section therefore begins with a discussion of the role of the calcium-binding protein, centrin.

A. Role of Centrin

Sanders and Salisbury (1989, 1994) proposed a model for deflagellation wherein the microtubules are broken by shear force exerted by calcium-induced contraction of fibers in the flagellar transition zone. The principal player in this model is the calcium-binding protein, centrin (also known as caltractin).

The centrins are a small subfamily of the 20-kDa EF-hand calmodulin-like protein family. They are ubiquitously associated with basal bodies/centrioles, centrosomes, mitotic spindle poles, and yeast spindle pole bodies (Salisbury, 1995; Spang *et al*., 1993). Centrin(s) appears to play an important role in centriole duplication, but what that role is, and whether it is the same in different organisms, remains to be determined (Salisbury *et al*., 2002). The common situation for centriole duplication is the assembly of a daughter centriole adjacent to the mother centriole. This suggests that a templating structure is established by the mother centriole. Similarly, in yeast, new spindle pole bodies (highly derived centrosomes) are assembled adjacent to mother spindle pole bodies. Although the yeast spindle pole body is clearly distinct from the centriole, there are important similarities, both functionally and structurally, and the early steps of replication may be conserved (Adams and Kilmartin, 2000). In yeast, the centrin gene *CDC31* is essential for spindle pole body duplication and cell cycle progression (Baum *et al*., 1986, 1988). CDC31 localizes to the spindle pole body half-bridge, where it is thought to play a role in nucleating the assembly of the daughter spindle pole body (Adams and Kilmartin, 2000; Spang *et al*., 1993). Similarly, in the green alga, *Spermatozopsis similis*, centrin localizes to fibers connecting the new probasal body to the existing basal body (Lechtreck and Grunow, 1999). The *vfl*-2 strain of *Chlamydomonas* carries a partial loss of function mutation in the centrin gene. These cells show a defect in the templated pathway for basal body (centriole) duplication, but *de novo* centriole assembly is unaffected (Marshall *et al*., 2001). Centrin is also essential for the *de novo* assembly of basal bodies that occurs in spermatids of the water fern, *Marsilea* (Klink and Wolniak, 2001). Humans and mice have three centrin genes: centrin 1 is expressed in differentiated ciliated epithelial cells and sperm (Hart *et al*., 1999; Laoukili *et al*., 2000), centrin 2 is a centriolar protein required for centriole duplication (Salisbury *et al*., 2002), and centrin 3 is a pericentriolar protein important for centrosome replication (Middendorp *et al*., 2000). Taken together, these data from yeast, algae, and mammals

indicate that centrin is essential for the initial phase of centriole/basal body/spindle pole body formation, whether templated or *de novo*.

Centrin is present in several basal body-associated structures. In *Chlamydomonas*, centrin is found in the stellate fibers internal to the distal flagellar transition zone, the striated fibers that connect the two basal bodies, and the nucleus–basal body connector, a series of fibers that connect the basal body to the nucleus (Salisbury *et al*., 1988; Sanders and Salisbury, 1989; Taillon *et al*., 1992). The stellate fibers of the distal transition zone and the fibers of the nucleus–basal body connector contract in response to an increase in calcium, in the latter case drawing the nucleus into close proximity to the basal bodies (Salisbury *et al*., 1987; Wright *et al*., 1985). Similarly, in *Spermatozopsis*, centrin is abundant in a set of distal fibers that connect the basal bodies; calcium-induced contraction of these fibers reorients the basal bodies with respect to one another (McFadden *et al*., 1987). A centrin-like protein, spasmin, is associated with the contracile fibers in the spasmoneme of the vorticellid ciliates (Maciejewski *et al*., 1999).

The centrin-containing stellate fibers of the distal transition zone contract in response to calcium (Sanders and Salisbury, 1989, 1994). Because these fibers attach to the A tubule of the outer doublet microtubules in this region, one consequence of the contraction is that torsional stress is applied to the outer doublet microtubules. It is well established that ciliary beat frequency and waveform are regulated by calcium (Smith, 2002, and references therein). The twist and pull applied to the outer doublets by calcium-induced contraction of these centrin-containing fibers may serve to modulate motility or to mediate deflagellation.

Using polyclonal antibodies that recognize both centrin 1 and centrin 2, Laoukili *et al*. (2000) found centrin in the proximal region of the cilia of ciliated epithelial cells. Furthermore, these antibodies, and not an antibody raised against centrin 3, inhibited ciliary beat frequency (Laoukili *et al*., 2000). It is interesting that these experiments were done in the absence of calcium. I suspect that this is because calcium would have induced deciliation. In similar experiments with detergent-extracted cell models of *Chlamydomonas*, three different monoclonal anti-centrin antibodies inhibited calcium-induced deflagellation (Sanders and Salisbury, 1994).

At the time of deflagellation, the stellate structure contracts around the central cylinder in the distal region of the flagellar transition zone (Sanders and Salisbury, 1989). This contraction displaces the outer doublet microtubules inward (a 12% reduction in the overall diameter of the transition zone; a 42% reduction in the distance between the A tubule and the inner cylinder of the transition zone). There is also a change in pitch or doublet angle relative to the radius of the transition zone, from 9.6° to 22.1°. Sanders and Salisbury (1989 and 1994) propose that the combination of torsional and

transverse shear resulting from calcium-induced contraction of the stellate fibers is the most significant factor inducing deflagellation.

Although the role of calcium in signaling deflagellation is complex (see above), it has been clearly demonstrated that severing of the outer doublet microtubules is triggered by a free calcium concentration of $\sim 1\ \mu M$ (Lohret *et al.*, 1998). Observations that pH shock induces calcium influx (Quarmby, 1996; Quarmby and Hartzell, 1994), that pH shock induces contraction of the stellate fibers of the transition zone (Sanders and Salisbury, 1989), and that calcium induces contraction of centrin-containing fibers (Salisbury, 1983) are all consistent with the model that calcium-activated breakage of the microtubules is mediated by contraction of the stellate fibers. That centrin plays a key role in the contraction of fibers and consequent breakage of the microtubules is provided by the observation that monoclonal antibodies against centrin block both contraction of the stellate fibers and deflagellation. Centrin probably plays a role in deflagellation, but whether it is the key role suggested by the torsional shear model is controversial.

The controversy about the role of centrin in deflagellation arises from studies of the *vfl*-2 strain of *Chlamydomonas*. This strain carries a missense mutation in the centrin gene that converts the glutamic acid to a lysine at position 101, the first amino acid of the E-helix of the third EF-hand (Taillon *et al.*, 1992). This mutant strain has structural defects in all the centrin-containing fibers: the nucleus–basal body connector, the striated distal fibers, and the stellate fibers of the flagellar transition zone (Jarvik and Suhan, 1991; Wright *et al.*, 1989). The *vfl*-2 centrin is capable of binding to the basal bodies, but it does not polymerize into filamentous structures (Taillon *et al.*, 1992). There are striking defects in the flagellar transition zone: the highly organized transition cylinders and stellate fibers of the wild type are replaced by poorly organized electron-dense material (Jarvik and Suhan, 1991). Jarvik and Suhan (1991) and Wright *et al.* (1989) report that *vfl*-2 cells deflagellate normally. In contrast, Sanders and Salisbury (1994) report that *vfl*-2 cells deflagellate only if external shear forces, such as pipetting or vortexing, are applied in conjunction with dibucaine, acid, or detergent with calcium. In the absence of external shear forces, Sanders and Salisbury (1994) report that *vfl*-2 cells do not deflagellate under conditions that will induce wild-type cells to shed their flagella. When my laboratory examined the ability of *vfl*-2 to deflagellate, no deflagellation defect was observed (Lohret *et al.*, 1998). This is in contrast to the *fa1* and *fa2* deflagellation defective strains (see below), which can be subject to a great deal of external shear in the context of deflagellation-inducing agents without shedding their flagella (Finst *et al.*, 1998). Taken together, experiments from the three laboratories indicate that the *vfl*-2 mutation has a subtle effect on the ability of the cells to deflagellate. It may be that, as offered by Sanders and Salisbury (1994), *vfl*-2 cells require

an external shear force in order to deflagellate, a force that is not required by cells with normal centrin. I have observed paralyzed mutants of *Chlamydomonas* on a slide to which dibucaine has been added—in the absence of the shear force provided by beating flagella, the flagella are shed. On the other hand, cells with normal flagella can be vortexed or put through a Dounce homogenizer (Wheaton Science Products, Millville, NJ) and, unless a deflagellation-inducing chemical is present, these shear forces do not cause deflagellation. (Extreme shear, such as provided by a VirTishear homogenizer, will cause deflagellation; see above.) In short, modest external shear alone does not normally induce deflagellation, yet *vfl*-2 cells require mild shear in order to deflagellate. As described above, deflagellation involves a narrowing of the distal transition cylinder just below the point of axonemal severing (Lewin and Lee, 1985; Sanders and Salisbury, 1989). In *vfl*-2 cells, this narrowing does not occur (Jarvik and Suhan, 1991). Available data indicate that this constriction is caused by calcium-induced contraction of the centrin-based stellate fibers. But given that the outer doublet microtubules of *vfl*-2 cells are severed in the absence of contraction, contraction cannot be the cause of severing. Contraction may, however, facilitate separation of the flagella from the cell body in the absence of external shear forces.

In further support of this idea, the inward contraction and change in pitch of the outer doublet microtubules are not observed in the deflagellation-defective strain, *fa1*-1 (Sanders and Salisbury, 1989). At the time, this observation was taken as support for the model that contraction of the centrin-containing stellate fibers causes breakage of the microtubules: no contraction, no deflagellation. However, an alternative interpretation seems more likely: no deflagellation, no contraction. Perhaps it is the structural integrity of the outer doublet microtubules that retains the stellate fibers in their beautiful extended configuration. In support of this idea, in response to pH shock *fa1* cells exhibit the normal influx of calcium, they contain wild-type centrin and normal stellate fibers, yet in the absence of outer doublet severing, the fibers do not contract (Sanders and Salisbury, 1989). Given that the increase in intracellular calcium would activate contraction of centrin fibers in these cells, there are two explanations for the failure of the stellate fibers to contract: either they cannot contract if the outer doublets are not severed or the Fa1 protein itself is important for contraction of the stellate fibers. Finally, it should be noted that although different types of cells deflagellate, few have transition zones with a stellate array of contractile fibers.

If it is not centrin, what is the calcium-binding protein of deflagellation? The preceding text has argued that contraction of the stellate fibers is not the cause of axonemal microtubule severing. However, the *vfl*-2 mutant expresses a stable protein that, although it fails to form fibers, does localize to the flagellar transition zone (Taillon *et al*., 1992). It is clear that the *vfl*-2 centrin is capable of carrying out some essential function(s) because a deletion of the gene is

lethal (Dutcher, personal communication, 2000). Thus, even in *vfl*-2 cells, there is localization of partially functional centrin to the site of severing—given that no other candidate Ca^{2+}-binding protein has been implicated in deflagellation, the possibility remains that centrin is the calcium sensor of deflagellation.

B. Role of Katanin

In addition to their central role in the structure and function of eukaryotic cilia, microtubules are essential for cell division and cell polarity because they provide a network of tracks along which cellular components, including chromosomes, are transported. The organization and activity of the microtubule array of a cell are regulated primarily by controlling rates of growth and shrinkage at the ends of the protein polymers (dynamic instability). It has become apparent that microtubules can also be broken—a process called microtubule severing.

When McNally and Vale (1993) isolated a protein with microtubule-severing activity, they named it katanin, after the Japanese word for samurai sword, katana. The name is apt for a protein that can accomplish the dramatic feat of breaking a microtubule. Microtubules are 25-nm-diameter fibers, composed of αβ-tubulin dimers arranged in 13 protofilaments, which align to form a hollow tube; each tubulin dimer makes contact with the dimer above, the dimer below, and the dimers on each side (Nogales *et al*., 1999). Thus, breaking a microtubule involves disrupting tubulin–tubulin interactions around the circumference of the tubule. One model is that katanin disrupts a region on the wall of the microtubule and that the disruption is propagated around the circumference (Quarmby, 2000).

In animal cells katanin exists primarily as a heterodimer (McNally and Vale, 1993). The p60 subunit is an ATPase in the AAA family, and possesses microtubule-severing activity (McNally and Vale, 1993). The p80 subunit is a novel WD40 domain protein that is important in localizing p60 to centrosomes and to spindle poles (Hartman *et al*., 1998; McNally *et al*., 2000). The combined biochemical and biophysical data led to a model in which monomeric subunits of p60 exchange bound ADP for ATP, oligomerize, and assemble as a hexameric ring on the wall of a microtubule (Hartman and Vale, 1999; Hartman *et al*., 1998; McNally, 2000). Hydrolysis of ATP leads to a conformational change that exerts a force on the microtubule, leading to disruption of tubulin–tubulin interactions, and disassembly of the katanin hexamer (Hartman and Vale, 1999; McNally, 2000).

The microtubule-severing activity of katanin increases during mitosis (McNally and Vale, 1993; Vale, 1991). Katanin localizes to mitotic spindle poles (McNally *et al*., 2000) and is important for the redistribution of γ-tubulin at mitosis (Buster *et al*., 2002). In a study of *Xenopus* extracts, McNally and colleagues found four components that contribute to the

inhibition of katanin during interphase (McNally *et al*., 2002). All four inhibitory components appear to be either microtubule-associated proteins (MAPs) or proteins that influence the activity of MAPS. One of these components is XMAP230; inhibition of microtubule severing by XMAP230 is reversible by cyclin/cdk1, suggesting one mechanism for activation of severing during mitosis. McNally *et al*. (2002) also characterized the stimulatory effects of the polo-like kinase, Plx1. Plx1 colocalizes with katanin at spindle poles and increases katanin activity *in vitro*. Activation of katanin by Plx1 is mediated by phosphorylation of tubulin (McNally *et al*., 2002). Clearly, the regulation of microtubule severing is complex.

Katanin is involved in diverse cellular functions. In addition to a role in mitosis, it plays an essential role in meiosis in *Caenorhabditis elegans* (Srayko *et al*., 2000); it is also essential for the formation of neuronal axons (Ahmad *et al*., 1999). The *Chlamydomonas* katanin p80 subunit is essential for the formation of the central pair microtubules of the flagella (Smith, personal communication, 2003) whereas p60 may play a role in microtubule severing during deflagellation (Lohret *et al*., 1998, 1999). In this context it is interesting to note that the central pair is nucleated near the site of outer doublet severing during deflagellation.

Three lines of evidence support the idea that katanin plays a role in severing the outer doublet microtubules during deflagellation: (1) exogenous katanin can sever isolated axonemes; (2) katanin p60 antibodies block calcium-induced axonemal severing; and (3) *Chlamydomonas* katanin p60 is found in the distal transition zone, the site of axonemal severing during deflagellation (Lohret *et al*., 1998, 1999). Given that katanin is the only established microtubule-severing protein (see Quarmby, 2000), and these three points of evidence, it is likely that katanin mediates axonemal severing. However, genetic evidence is lacking. Developments in the use of RNA interference (RNAi) approaches in *Chlamydomonas* may address this deficiency (Fuhrmann *et al*., 2001). Katanin is a single-copy gene in *Chlamydomonas* and if it does play an essential role in mitosis, null mutations would be lethal (Lohret *et al*., 1999). RNAi approaches will allow production of hypomorph strains, which may reveal defects in other processes, such as deflagellation. Alternatively, a screen of temperature-sensitive lethal mutants could reveal a strain with a deflagellation defect that precedes cell cycle arrest.

C. Role of the Fa Proteins

My laboratory screened more than 26,000 mutagenized haploid clones of *Chlamydomonas* for defects in deflagellation, and isolated many new strains of deflagellation-defective mutants (Finst *et al*., 1998). Several of these are defective in Ca^{2+}-triggered axonemal microtubule severing and are classified

as *fa* mutants. Other new mutants, the *adf* mutants, are wild type for axonemal microtubule severing, but are defective in a Ca^{2+} influx pathway (see above; Quarmby, 1996; Quarmby and Hartzell, 1994).

Crosses between strains established that, on the basis of linkage, there were at least three different genes yielding mutants with defects in deflagellation. We constructed stable diploid strains and demonstrated that each of these groups defines a single gene (Finst *et al*., 1998). Thus, we have identified three genes, *ADF1, FA1*, and *FA2*, whose products are essential for deflagellation. A mutation in one of these genes, *FA1*, was first described in 1983, but the gene was not cloned until more recently (Finst *et al*., 2000; Lewin and Burrascano, 1983). *Fa2* mutants have a phenotype that is indistinguishable from the *fa1* mutants; the *FA2* gene has been cloned (Mahjoub *et al*., 2002).

The *C. reinhardtii* deflagellation-defective mutant, *fa1*-1, does not shed its flagella in response to any known stimulus (Lewin and Burrascano, 1983). Moreover, the addition of Ca^{2+} to detergent-permeabilized *fa1*-1 cells does not trigger the axonemal severing and deflagellation observed in wild-type cells (Lohret *et al*., 1998; Quarmby and Hartzell, 1994). By electron microscopy, the outer doublet microtubules of *fa1*-1 cells do not sever in response to pH shock (Sanders and Salisbury, 1989). In purified preparations of FBBCs, the only structural connection between the axoneme and the basal body is the transition zone region of the axoneme. We have found that wild-type complexes sever their axonemes in response to Ca^{2+}, whereas complexes isolated from *fa* mutants do not. This suggests that either the *fa* mutants are defective in axonemal severing activity, or their axonemes have lost the ability to be severed. It is unlikely that the *fa* defect is at the level of microtubule susceptibility to severing because *fa* axonemes can be severed *in vitro* by addition of the microtubule-severing ATPase, katanin, purified from sea urchin oocytes (Lohret *et al*., 1998). Taken together, these observations support the idea that the *fa* phenotype is a consequence of a defect in axonemal microtubule severing.

In *Chlamydomonas*, after the fusion of gametes, quadriflagellate dikaryons persist for approximately 2 h. For some recessive mutations, such as *adf1* mutants, components from the wild-type gamete can compensate for a deficiency in the mutant, and the defective phenotype of the mutant partner is rescued. That is, in *adf/ADF* dikaryons all four flagella are excised in response to stimulation (Quarmby and Hartzell, 1994). In contrast, even though all known *fa1* and *fa2* alleles are recessive to wild type in stable diploid strains, *fa/FA* dikaryons fail to excise the two flagella derived from the *fa* gamete (Finst *et al*., 1998). There are a number of possible explanations for the lack of rescue in the *fa* dikaryons. The simplest include (1) restricted access of proteins to the transition zone; (2) requirement for sequential assembly of proteins in a complex; (3) slow, or cell cycle-coupled, turnover of the Fa proteins; and (4) low abundance of the Fa proteins. Each of these

explanations is consistent with the existence of a stable complex of Fa proteins at the flagellar transition zone. Furthermore, Ca^{2+}-induced axonemal severing occurs in isolated wild-type FBBCs, indicating that the entire machinery for axonemal microtubule severing is a component of the detergent-resistant flagellar–basal body complex. On the basis of these data, it is likely that Fa1p and Fa2p play roles in a protein complex that (1) is anchored near the base of the flagellum and (2) culminates in the severing of axonemal microtubules when activated by Ca^{2+}.

FA1 encodes a 171-kDa protein with predicted coiled-coil and Ca/calmodulin binding domains (Finst *et al.*, 2000). To date, the public databases contain no proteins with highly significant sequence identity to Fa1p. Several mammalian proteins share approximately 35% overall sequence similarity to Fa1p, but this does not include any specific domains of particularly high similarity. The similar proteins include trichohyalin, involucrin, loricrin, and elastin—all proteins with structural or scaffolding roles. Thus, the similarity is consistent with the idea that Fa1p might play a structural role, perhaps serving to organize a microtubule-severing complex in the flagellar transition zone. The multicellular green alga, *Volvox*, has a gene for a protein that is nearly identical to Fa1p (Wagner and Quarmby, unpublished observation, 2001). One interpretation is that Fa1p is a Volvocales-specific protein, but the more likely explanation is 2-fold: (1) Fa1p has low sequence complexity, thus making the recognition of orthologs difficult and (2) the related issue that Fa1p might be performing scaffolding, rather than catalytic, functions, thereby being less constrained in the evolution of its amino acid sequence.

Fa1p is the first identified component of the flagellar transition zone (Finst *et al.*, 2000). We have discovered that *fa1* mutant strains have two additional phenotypes. The array of cytoplasmic microtubules is aberrant—there are fewer microtubules, most of which are shorter than normal, although some are excessively long (Mahjoub, Montpetit, and Quarmby, unpublished observations, 2002). *fa1* mutant cells are also slow to hatch from the mother cell wall, probably because of a delay in the assembly of flagella as the cells exit the cell cycle (Mahjoub, Montpetit, and Quarmby, unpublished observations, 2002).

FA2 encodes a 68-kDa protein, which has high (~40%) sequence identity with members of the Nek family (NIMA-related expressed protein kinases; Mahjoub *et al.*, 2002). The founding member of the Nek family is NIMA, a serine/threonine kinase that plays an essential role in regulating the G_2–M transition in *Aspergillus nidulans* (never in mitosis; Lu and Means, 1994). Neks have been implicated in G_2–M progression, chromatin condensation, and regulation of the centrosome cycle. Motivated by the basal body associated function of Fa2p, and the sequence homology with the Nek family, my laboratory undertook a detailed study of cell cycle progression in *fa2* mutant cells. We discovered that *fa2* cells are delayed in G_2–M progression, and flagellar assembly on exit from mitosis (Mahjoub *et al.*, 2002). We have

cloned cDNAs for nine additional Nek proteins in *Chlamydomonas* and speculate that one or more of these is partially compensating for Fa2p function during cell division in *fa2* null mutants (Bradley *et al*., 2004; Bradley and Quarmby, unpublished observations, 2004). The fact that *FA2*, a gene essential for axonemal microtubule severing during deflagellation, encodes an NIMA kinase is the first indication that this family of kinases might play a role in the regulation of katanin.

V. Deflagellation, Resorption, and the Cell Cycle

A. Deflagellation and Flagellar Disassembly

There are two ways for a cell to lose its flagella: they can be shed by the mechanism reviewed above, or they can be disassembled and resorbed by the cell. Most cells are probably capable of both processes. This section addresses the following question: Are these wholly independent pathways, or do they share common mechanisms and proteins?

Studies of *Chlamydomonas* flagella have identified a system of intraflagellar transport (IFT), powered by flagelloplasmic dyneins and kinesins, which carries proteins to the assembling flagellum and returns proteins to the cytoplasm during flagellar resorption (see overview in Section II). On the basis of studies with flagellar assembly (*fla*) mutants, it has been proposed that flagellar length is a consequence of the equilibrium balance between rates of assembly and disassembly, where assembly rates are length dependent (Marshall and Rosenbaum, 2001). Although it has not yet been studied directly, it is possible that the resorption of flagella that precedes cell division reflects an inhibition of anterograde IFT, an increase in the rate of retrograde IFT, or both. Perhaps the simplest way to address whether deflagellation and disassembly are overlapping processes is to ask whether IFT mutants have deflagellation defects and whether deflagellation mutants have flagellar disassembly defects.

The *Chlamydomonas* flagellar assembly mutant, *fla2*, has wild-type rates of anterograde IFT at the permissive temperature (20 °C), but at the same temperature the rate of retrograde IFT is reduced (Iomini *et al*., 2001). Do *fla2* cells have a deflagellation defect? Indeed they do! When *fla2* cells are shifted to the restrictive temperature (33 °C), the predominant result is that they shed their flagella (Huang *et al*., 1977; Parker and Quarmby, 2003). This result motivated a survey of the *fla* mutants for deflagellation defects. Although we have not found any that are deflagellation defective, several, but not all, *fla* mutants deflagellate on a shift to 33 °C, a temperature that does not induce deflagellation of wild-type cells (Parker and Quarmby, 2003). The tendency for *fla* mutants to deflagellate at the restrictive temperature, at a

time when most of these strains are undergoing flagellar resorption as a consequence of defects in IFT, complicates the interpretation of the role of IFT in flagellar length control.

Facile deflagellation of *fla* mutants suggests that IFT and deflagellation are related processes. That several different *fla* mutants deflagellate in response to a temperature shift indicates that the correspondence of the two phenotypes is not associated with a single gene product. Furthermore, the sites of both axonemal severing and IFT raft assembly are closely associated with the basal body (Deane *et al.*, 2001; Lewin and Lee, 1985). It appears that in the absence of continuous active turnover of the axoneme, the deflagellation pathway is activated. Does this mean that deflagellation is suppressed by active turnover of the axoneme? One idea is that tightly controlled removal of tubulin subunits from the base of the axoneme is part of normal axonemal turnover. Perhaps when IFT is inhibited, severing is no longer constrained, the axonemes are completely severed, and the flagella are shed.

Further support for the idea that IFT and deflagellation are related processes comes from studies of the *fa* mutants. The primary defect in *Chlamydomonas* cells with mutations in either the *FA1* or *FA2* gene is the inability to sever flagellar axonemes in response to calcium (reviewed above). Careful observation, however, has revealed that both *fa1* and *fa2* mutants have secondary phenotypes, including slow assembly of their flagella after exit from the cell cycle (Mahjoub *et al.*, 2002; Mahjoub, Montpetit, and Quarmby, unpublished observations, 2002).

Cells build new flagella not only in response to deflagellation, but also *de novo*, when they exit the cell cycle. Undoubtedly the same machinery for flagellar assembly will be employed in both instances, but there may be differences in the regulation. For example, when *fa1* cells regrow their flagella after being induced to resorb them by chemical treatment, the flagella grow out at the same rate as wild-type flagella (Mahjoub, Montpetit, and Quarmby, unpublished observations, 2002). However, when *fa1* cells exit mitosis, assembly of full-length flagella can take up to 18 h to complete, compared with 1–2 h for wild type (Mahjoub *et al.*, 2004). The flagella are about 2 μm long when the rate of assembly slows; the assembly of similarly short flagella is seen when deflagellated cells are treated with protein synthesis inhibitors during the regrowth phase (Rosenbaum *et al.*, 1969). This suggests that the program for induction of the synthesis and/or assembly of new flagellar building blocks is activated inefficiently after mitosis in this mutant. This is particularly interesting, given that the primary defect in these cells is that they are unable to deflagellate.

One final observation that connects flagellar assembly and deflagellation relates to the central pair microtubules. Central pair microtubules are a key component in the calcium signaling pathway that regulates flagellar dynein activity (see, e.g., Smith, 2002). As described above, central pair microtubules are nucleated near the site where the outer doublets are severed during

deflagellation and two subunits of katanin are implicated in these two processes (p80 in assembly of the central pair and p60 in the severing of the outer doublets). Several *Chlamydomonas* paralyzed flagella mutants lack the central pair microtubules, but one of these, *pf18*, has the intriguing additional phenotype of aberrant flagellar resorption during the light phase (Tuxhorn *et al*., 1998).

In conclusion, data indicate that either the fundamental mechanism or regulatory components of deflagellation and flagellar disassembly are shared. Understanding this relationship will provide important insights into both processes.

B. Deciliation and the Cell Cycle

As described above, the axoneme of cilia is a direct extension of the basal body, which is essentially a centriole. In many eukaryotic cells, the centriole is the focus of the centrosome and serves as the microtubule-organizing center of the cell. In cells that have centrosomes (i.e., most eukaryotes other than plants and fungi), these organelles play an important role in the coordination of the mitotic spindle and regulation of the cell cycle (Doxsey, 2001).

Although some ciliated cells may be terminally differentiated, most will reenter the cell cycle, and the basal body will once again function as the focus of spindle poles. In some species of green flagellates, for example, the flagella remain attached to their basal bodies, and the mitotic spindle forms between sister basal bodies (Kirk, 1998). More commonly, however, the cilia are either shed or resorbed for division. Thus, the related processes of deciliation and ciliary resorption are directly coupled to the cell cycle.

In *Chlamydomonas*, the flagella are disassembled and resorbed during preprophase (Kirk, 1998). At about the same time, basal body replication is completed. The two full-length basal bodies with their associated daughters, remain associated with the plasma membrane, and the mitotic spindle forms between them (Kirk, 1998). Basal bodies play an important role in coordinating karyokinesis and cytokinesis: *Chlamydomonas* mutants that lack basal bodies can divide, but there are serious problems associated with mispositioning of the spindle or the cleavage furrow or both (Ehler *et al*., 1995). Thus, as is the case in animal cells, centrioles are not required to serve as the microtubule-organizing center of the spindle, but they do play important roles in the coordination of the cell cycle (Rieder *et al*., 2001). Little is known about the proteins and mechanisms involved.

Chlamydomonas fa2 mutants, which are defective in calcium-activated axonemal severing, show delays at the G_2–M transition (Mahjoub *et al*., 2002). It is not yet known whether these two roles of Fa2p are a consequence

of its action on a common process, such as regulation of microtubule severing, or are due to effects on independent pathways. Severing of the axonemal microtubules is a basal body-associated microtubule-severing event that is clearly defective in *fa2* mutants (Finst *et al*., 1998). Microtubule severing has been implicated in mitosis, but its role remains unclear (reviewed by Quarmby, 2000). There are two events that occur at the G_2–M transition in *Chlamydomonas*, either of which might involve microtubule severing: (1) disassembly and resorption of the axoneme, and (2) disassembly of the interphase array of cytoplasmic microtubules in anticipation of spindle formation. Preliminary data from my laboratory indicate that flagellar resorption is slower in *fa2* and *fa1* mutants than it is in wild-type cells (Parker and Quarmby, 2003). However, it remains possible that Fa2p might play a G_2–M role independent of the activation of microtubule severing.

My laboratory is also characterizing another *Chlamydomonas* mutant, *dd-l-108*, isolated by Huang *et al*. (1977), which further illustrates the connection between deflagellation and the cell cycle (Chandler, Ringrose, Parker, and Quarmby, unpublished observation, 2003). *dd-l-108* cells deflagellate within hours of a shift to the restrictive temperature, and subsequently are unable to divide. The cells grow large and contain a single nucleus. One hypothesis is that temperature-induced deflagellation prevents *dd-l-108* cells from progressing through the cell cycle. A precedent for this idea is that deciliation interferes with cell cycle progression in *Tetrahymena* (Seyfert *et al*., 1985). Perhaps when axonemal microtubule severing is stimulated, so too is the severing of a subset of basal body-associated cytoplasmic microtubules. If this were to happen at a time other than when normally scheduled to occur (i.e., the G_2–M transition) it could cause a delay in the cell cycle. More experiments will be required to test this idea.

Further indication of a relationship between deflagellation and the cell cycle comes from studies of the primary cilia of vertebrate cells. The function(s) of these nearly ubiquitous tiny cilia are not known, but they have been hypothesized to play a role in controlling the cell cycle (Tucker and Pardee, 1979). Like the flagella of *Chlamydomonas*, primary cilia are disassembled and resorbed as the vertebrate cell enters mitosis (Rieder *et al*., 1979). Because primary cilia are found on cells in G_0, it has been proposed that the cilium may be important for maintaining the cell in a differentiated state (Tucker *et al*., 1979). There is growing evidence that primary cilia play sensory roles, perhaps including a signaling role essential for continued residence in G_0 (Pazour and Witman, 2003; Wheatley *et al*., 1996). In this case, stress-induced deciliation (of primary cilia) could be responsible for the dedifferentiation of cells in culture. To my knowledge, this idea has not been tested.

VI. Conclusions and Prospects for Future Research

Deciliation has been used by scientists for decades to make preparations of flagella and to study flagellar regeneration. Only recently has the mechanism of deflagellation become a focus for investigation. Although it is not yet clear whether deflagellation evolved as an adaptive behavior, many cells deflagellate in response to stressful stimuli.

Stress-induced deciliation is relevant to human health: sterility can be the result when testicular sperm deflagellate in response to ingested toxins; infection results when respiratory epithelia deciliate in response to excessive tobacco smoke; and the human oviduct responds to hormonal signals with a cycle of ciliation/deciliation. Studies on deciliation are also important for understanding the effects of local anesthetics—for example, lidocaine treatment during tracheobronchial fibroscopy and sampling of nasal mucosa cause deciliation of respiratory epithelia (Verra *et al.*, 1990). Furthermore, work on deflagellation will continue to contribute to our basic understanding of cilia and flagella. The relationship between deflagellation and IFT is particularly important because disruption of proteins involved in IFT in mice leads to blindness, polycystic kidney disease, and situs invertus, a randomization of left–right asymmetry of internal organs. Deflagellation also provides a valuable experimental system to study microtubule severing. Given that katanin is likely essential for cell division, and that two deflagellation mutants, *fa2* and *dd-l-108*, have cell cycle defects, work in this area will be of significance to cell cycle-related diseases, such as cancer. As ever, fundamental studies of cellular processes have broad implications.

What do we know about the mechanism of deflagellation? It is well established that the intracellular second messenger that triggers deflagellation is Ca^{2+}. However, the proteins involved in generating this calcium signal have not yet been identified. There is evidence that $Ins(1,4,5)P_3$ signaling may play a role, but this has not been firmly established. There is some evidence that the calcium-binding protein, centrin, might be the calcium sensor of deflagellation, but this too remains uncertain. Two proteins are clearly essential for severing of the axonemal microtubules in response to the calcium signal: an NIMA-related kinase, Fa2p, and a novel coiled-coil protein, Fa1p, have been identified by genetic approaches in *Chlamydomonas*. The microtubule-severing ATPase, katanin, has been implicated as the protein responsible for breaking the axonemal microtubules, but like centrin, the role for katanin has not yet been firmly established (i.e., genetic proof is lacking). Centrin and katanin are both single-copy genes in *Chlamydomonas*. Both of these genes have been implicated in the cell cycle; therefore, null mutations of either are likely lethal. This provides an additional challenge to demonstrating a role for these proteins in deflagellation.

The field of deflagellation research can be compared with a mountaineering expedition: we have carefully selected our gear and made a successful trek to base camp, but we have yet to reach the peak. I anticipate some spectacular views once deciliation is understood, but hard work and careful planning are needed to get there. Some of the most interesting consequences of understanding deciliation will be the decoding of the relationships between deciliation, the cell cycle, and intraflagellar transport. The following routes should provide interesting scenery along the way.

- Calcium imaging during deciliation to visualize the temporal and spatial characteristics of this signal; understanding the specificity of the signal and identifying how this particular calcium signal triggers deciliation: Cloning of *ADF1* and *FLA2* will contribute to understanding the calcium pathway. What is the calcium sensor? What are its properties? How is it different from the calcium sensor controlling flagellar beat frequency and waveform, mating, and intraflagellar transport? One prediction is that the calcium sensor of deflagellation needs to bind multiple calcium ions before it becomes activated. This would make it blind to the rapid transient calcium signals that must be regulating flagellar beat.
- Elucidating the mechanism of deciliation: What is the complete repertoire of proteins involved? How do the proteins work together to transduce a calcium signal into deciliation? What is involved in membrane fission, and what is the detailed mechanism of axonemal severing?
- Determining the evolutionary history of deciliation: Did it evolve as an adaptive behavior or is it a side product of a more fundamental process, such as IFT, that was later coopted by some cells to serve physiologically relevant functions?

There is a great deal of research that needs to be done before we understand deciliation. It is my sincerest hope that this review will trigger a deflagellation research response in some readers. See you on the mountain!

Acknowledgments

I owe a debt of gratitude to the generous spirit of the *Chlamydomonas* research community, many members of which have contributed ideas, reagents, and enthusiastic encouragement. I also thank current members of my laboratory, in particular Brian Bradley, Moe Mahjoub, Jeremy Parker, and Dr. Lena Suzuki, for lively discussions and comments on the manuscript. Experiments in my laboratory were supported by the Canadian Institutes of Health Research (CIHR Grant MOP-37861) and by the Natural Sciences and Engineering Research Council of Canada (NSERC Grant RGPIN 227132).

References

Adams, G. M. W., Huang, B., and Luck, D. J. L. (1982). Temperature-sensitive, assembly-defective falgella mutants of *Chlamydomonas reinhardtii*. *Genetics* **100,** 579–586.

Adams, I., and Kilmartin, J. V. (2000). Spindle pole body duplication: A model for centrosome duplication? *Trends Cell Biol.* **10,** 329–335.

Ahmad, F. J., Yu, W., McNally, F. J., and Baas, P. W. (1999). An essential role for katanin in severing microtubules in the neuron. *J. Cell Biol.* **145,** 301–315.

Anonymous (1880). Abuse of chloral hydrate. *Q. J. Inebriety* **4,** 53–54.

Anteneodo, C., Rodahl, A. M., Miering, E., Heynen, M. L., Senisterra, G. A., and Lepock, J. R. (1994). Interaction of dibucaine with the transmembrane domain of the Ca^{2+}-ATPase of sarcoplasmic reticulum. *Biochemistry* **33,** 12283–12290.

Arita, K., Utsumi, T., Kato, A., Kanno, T., Kobuchi, H., Inoue, B., Akiyama, J., and Utsumi, K. (2000). Mechanism of dibucaine-induced apoptosis in promyelocytic leukemia cells (HL-60). *Biochem. Pharmacol.* **60,** 905–915.

Auclair, W., and Siegel, B. W. (1966). Cilia regeneration in the sea urchin embryo: Evidence for a pool of ciliary proteins. *Science* **154,** 913–915.

Baum, P., Furlong, C., and Byers, B. (1986). Yeast gene required for spindle pole body duplication: Homology of its product with Ca^{2+}-binding proteins. *Proc. Natl. Acad. Sci. USA* **83,** 5512–5516.

Baum, P., Yip, C., Goetsch, L., and Byers, B. (1988). A yeast gene essential for regulation of spindle pole duplication. *Mol. Cell. Biol.* **8,** 5386–5397.

Beck, C., and Uhl, R. (1994). On the localization of voltage-sensitive calcium channels in the flagella of *Chlamydomonas reinhardtii*. *J. Cell Biol.* **125,** 1119–1125.

Bergesse, J. R., Domenech, C. E., and Balengno, H. F. (1983). Chloral hydrate inhibition of in vitro ATPase in membrane of rat erythrocytes and in microsomes of dog kidney external medulla. *Biochem. Pharm.* **32,** 3221–3225.

Besharse, J. C., Spratt, G., and Forestner, D. M. (1986). Light-evoked and kainic-acid-induced disc shedding by rod photoreceptors: Differential sensitivity to extracellular calcium. *J. Comp. Neurol.* **251,** 185–197.

Blum, J. J. (1971). Existence of a breaking point in cilia and flagella. *J. Theor. Biol.* **33,** 257–263.

Bower, S. M. (2001). Synopsis of infectious diseases and parasites of commercially exploited shellfish: Oyster velar virus disease (OVVD). URL: http://www-sci.pac.dfo-mpo.gc.ca/shelldis/pages/ovvdoy_e.htm.

Bradley, B. A., Wagner, J. J. D., and Quarmby, L. M. (2004). Identification and sequence analysis of six new members of the NIMA-related kinase family in *Chlamydomonas*. *J. Eukaryot. Microbiol.* **51,** 66–72.

Braun, F. J., and Hegemann, P. (1999). Direct measurement of cytosolic calcium and pH in living *Chlamydomonas reinhardtii* cells. *Eur. J. Cell Biol.* **78,** 199–208.

Breipohl, W., Mendoza, A. S., and Miragall, F. (1980). Freeze-etching studies on the ciliary necklace in the rat and chicken. *J. Anat.* **130,** 801–807.

Buster, D., McNally, K., and McNally, F. J. (2002). Katanin inhibition prevents the redistribution of γ-tubulin at mitosis. *J. Cell Sci.* **115,** 1083–1092.

Butterworth, J. F., and Striachartz, G. R. (1990). Molecular mechanisms of local anesthesia: A review. *Anesthesiol.* **72,** 711–734.

Catterall, W. A. (1992). Cellular and molecular biology of voltage-gated sodium channels. *Physiol. Rev.* **72,** S15–S48.

Chakrabarti, A., Schatten, H., Mitchell, K. D., Crosser, M., and Tayler, M. (1998). Chloral hydrate alters the organization of the ciliary basal apparatus and cell organelles in sea urchin embryos. *Cell Tissue Res.* **293,** 453–462.

Cheshire, J. L., and Keller, L. R. (1991). Uncoupling of *Chlamydomonas* flagellar gene expression and outgrowth from flagellar excision by manipulation of Ca^{2+}. *J. Cell Biol.* **115,** 1651–1659.

Cheshire, J. L., Evans, J. H., and Keller, L. R. (1994). Ca^{2+} signalling in the *Chlamydomonas* flagellar regeneration system: Cellular and molecular responses. *J. Cell Sci.* **107,** 2491–2498.

Child, F. M. (1959). The characterization of the cilia of *Tetrahymena pyriformis*. *Exp. Cell Res.* **18,** 258–267.

Child, F. M., and Mazia, D. (1956). A method for the isolation of the parts of ciliates. *Experientia* **12,** 161.

Chinoy, N. J., and Narayana, M. V. (1994). In vitro fluoride toxicity in human spermatozoa. *Reprod. Toxicol.* **8,** 155–159.

Clapham, D. E. (1995). Calcium signalling. *Cell* **80,** 259–268.

Cole, D. G., Diener, D. R., Himelblau, A. L., Beech, P. L., Fuster, J. C., and Rosenbaum, J. L. (1998). *Chlamydomonas* kinesin-II-dependent intraflagellar transport (IFT): particles contain proteins required for ciliary assembly in *Caenorhabditis elegans* sensory neurons. *J. Cell Biol.* **141,** 993–1008.

Coss, R. A., and Smith, N. N. (1991). Effect of external pH on heat sensitization by local anesthetic. *Int. J. Radiat. Oncol. Biol. Phys.* **20,** 59–64.

Deane, J. A., Cole, D. G., Seeley, E. S., Diener, D. R., and Rosenbaum, J. L. (2001). Localization of intraflagellar protein IFT52 identifies basal body transitional fibers as the docking site for IFT particles. *Curr. Biol.* **11,** 1586–1590.

Doxsey, S. (2001). Re-evaluating centrosome function. *Nat. Rev. Mol. Cell Biol.* **2,** 688–698.

Dunlap, K. (1977). Localization of calcium channels in *Paramecium*. *J. Physiol.* **271,** 119–133.

Dutcher, S. K. (2001). Motile organelles: The importance of specific tubulin isoforms. *Curr. Biol.* **11,** R419–R422.

Dutcher, S. K., Morrissette, N. S., Preble, A. M., Rackley, C., and Stanga, J. (2002). ϵ-Tubulin is an essential component of the centriole. *Mol. Biol. Cell* **13,** 3859–3869.

Ehler, L. L., Holmes, J. A., and Dutcher, S. K. (1995). Loss of spatial control of the mitotic spindle apparatus in a *Chlamydomonas reinhardtii* mutant strain lacking basal bodies. *Genetics* **141,** 945–960.

El Zien, L., Omran, H., and Bouvagnet, P. (2003). Lateralization defects and ciliary dyskinesia: Lessons from algae. *Trends Genet.* **19,** 162–167.

Evans, J. H., and Keller, L. R. (1997a). Calcium influx signals normal flagellar RNA induction following acid shock of *Chlamydomonas reinhardtii*. *Plant Mol. Biol.* **33,** 467–481.

Evans, J. H., and Keller, L. R. (1997b). Receptor-mediated calcium influx in *Chlamydomonas reinhardtii*. *J. Eukaryot. Microbiol.* **44,** 237–245.

Evans, J. H., Smith, J. L., and Keller, L. R. (1997). Ion selectivity in the *Chlamydomonas reinhardtii* flagellar regeneration system. *Exp. Cell Res.* **230,** 94–102.

Finst, R. J., Kim, P. J., and Quarmby, L. M. (1998). Genetics of the deflagellation pathway in *Chlamydomonas*. *Genetics* **149,** 927–936.

Finst, R. J., Kim, P. J., Griffis, E. R., and Quarmby, L. M. (2000). Falp is a 171 kDa protein essential for axonemal microtubule severing in *Chlamydomonas*. *J. Cell Sci.* **113,** 1963–1971.

Flowers, A., Creveling, A. K., Onwueme, C. R., and Daly, J. W. (2002). Reserpine: Interactions with batrachotoxin and brevetoxin sites on voltage-dependent sodium channels. *Cell. Mol. Neurol.* **22,** 1–12.

Francis, J. T., and Hennessey, T. M. (1995). Chemorepellents in *Paramecium* and *Tetrahymena*. *J. Eukaryot. Microbiol.* **42,** 78–83.

Friedrich, R. W., and Korsching, S. I. (1997). Combinatorial and chemotopic odorant coding in the zebrafish olfactory bulb visualized by optical imaging. *Neuron* **18,** 737–752.

Fuhrmann, M., Stahlberg, A., Govorunova, E., Rank, S., and Hegemann, P. (2001). The abundant retinal protein of the *Chlamydomonas* eye is not the photoreceptor for phototaxis and photophobic responses. *J. Cell Sci.* **114,** 3857–3863.

Galjart, N., and Perez, F. (2003). A plus-end raft to control microtubule dynamics and function. *Curr. Opin. Cell Biol.* **15,** 48–53.

Garcia-Arraras, J. E., and Greenberg, M. J. (2001). Visceral regeneration in holothurians. *Microsc. Res. Tech.* **55,** 438–451.

Gilula, N. B., and Satir, P. (1972). The ciliary necklace: A ciliary membrane specialization. *J. Cell Biol.* **53,** 494–509.

Goldstein, S. F. (1974). Isolated, reactivated and laser-irradiated cilia and flagella. *In* "Cilia and Flagella" (M. A. Sleigh, Ed.), pp. 111–130. Academic Press, New York.

Gong, Z., and Brandhorst, B. P. (1987). Stimulation of tubulin gene transcription by deciliation of sea urchin embryos. *Mol. Cell. Biol.* **7,** 4238–4246.

Goodenough, U. W., and St. Clair, H. S. (1975). BALD-2: A mutation affecting the formation of doublet and triplet sets of microtubules in *Chlamydomonas reinhardtii*. *J. Cell Biol.* **66,** 480–491.

Hart, P. E., Glantz, J. N., Orth, J. D., Poynter, G. M., and Salisbury, J. L. (1999). Testis-specific murine centrin, Cetn1: Genomic characterization and evidence for retroposition of a gene encoding a centrosome protein. *Genomics* **60,** 111–120.

Hartman, J. J., and Vale, R. D. (1999). Microtubule disassembly by ATP-dependent oligomerization of the AA enzyme katanin. *Science* **286,** 782–785.

Hartman, J. J., Mahr, J., McNally, K., Okawa, K., Akihiro, I., Thomas, S., Cheesman, S., Heuser, J., Vale, R. D., and McNally, F. J. (1998). Katanin, a microtubule-severing protein, is a novel AAA ATPase that targets to the cetnrosome using a WD40-containing subunit. *Cell* **93,** 277–287.

Hartzell, L. B., Hartzell, H. C., and Quarmby, L. M. (1993). Mechanisms of flagellar excision. I. The role of intracellular acidification. *Exp. Cell Res.* **208,** 148–153.

Hennessey, T. M., Kim, M. Y., and Satir, B. H. (1995). Lysozyme acts as a chemorepellant and secretagogue in *Paramecium* by activating a novel receptor operated Ca^{2+} conductance. *J. Membr. Biol.* **148,** 13–25.

Hertwig, O., and Hertwig, R. (1886). *Jena. Z. Naturw.* **13,** 121, 477; as cited in Kennedy, J. R., and Brittingham, E. (1968). Fine structure changes during chloral hydrate deciliation of *Paramecium Caudatun J. Ultrastruct. Res.* **22,** 530–545.

Higashijima, T., Burnier, J., and Ross, E. M. (1990). Regulation of G_i and G_o by mastoparan, related amphiphilic peptides, and hydrophobic amines. *J. Biol. Chem.* **265,** 14176–14186.

Huang, B., Rifkin, M. R., and Luck, D. J. L. (1977). Temperature-sensitive mutations affecting flagellar assembly and function in *Chlamydomonas reinhardtii*. *J. Cell Biol.* **72,** 67–85.

Huber, M. E., and Lewin, R. A. (1987). Ethanol-induced flagellar autotomy in *Dunaliella tertiolecta* Butcher (Chlorophyta Volvocales). *Phycologia* **26,** 138–141.

Huber, M. E., Wright, W. G., and Lewin, R. A. (1986). Divalent cations and flagellar autotomy in *Chlamydomonas reinhardtii* (Volvocales, Chlorophyta). *Phycologia* **25,** 408–411.

Iomini, C., Babaev-Khaimov, V., Sassaroli, M., and Piperno, G. (2001). Protein particles in *Chlamydomonas* flagella undergo a transport cycle consisting of four phases. *J. Cell Biol.* **153,** 13–24.

Jarvik, J. W., and Suhan, J. P. (1991). The role of the flagellar transition region: Inferences from the analysis of a *Chlamydomonas* mutant with defective transition region structures. *J. Cell Sci.* **99,** 731–740.

Johnson, K. A., and Rosenbaum, J. L. (1992). Polarity of flagellar assembly in *Chlamydomonas*. *J. Cell Biol.* **119,** 1605–1611.

Kamiya, R. (2002). Functional diversity of axonemal dyneins as studied in *Chlamydomonas* mutants. *Int. Rev. Cytol.* **219,** 115–155.

Kang, Y., and Mitchell, D. R. (1998). An intronic enhancer is required for deflagellation-induced transcriptional regulation of a *Chlamydomonas reinhardtii* dynein gene. *Mol. Biol. Cell* **9,** 3085–3094.

Kennedy, J. R., and Brittingham, E. (1968). Fine structure changes during chloral hydrate deciliation of *Paramecium caudatum*. *J. Ultrastruct. Res.* **22,** 530–545.

Kirk, D. L. (1998). *Volvox*: Molecular–Genetic Origins of Multicellularity and Cellular Differentiation,'' pp. 87–99. Cambridge University Press, New York.

Klink, V. P., and Wolniak, S. M. (2001). Centrin is necessary for the formation of the motile apparatus in spermatids of *Marsilea*. *Mol. Biol. Cell* **12,** 761–776.

Kozminski, K. G., Johnson, K. A., Forscher, P., and Rosenbaum, J. L. (1993). A motility in the eukaryotic flagellum unrelated to flagellar beating. *Proc. Natl. Acad. Sci. USA* **90,** 5519–5523.

Kozminski, K. G., Beech, P. L., and Rosenbaum, J. L. (1995). The *Chlamydomonas* kinesin-like protein FLA10 is involved in motility associated with the flagellar membrane. *J. Cell Biol.* **131,** 1517–1527.

Kushnareva, Y. E., Polster, B. M., Sokolove, P. M., Kinnally, K. W., and Fiskum, G. (2001). Mitochondrial precursor signal peptide induces a unique permeability transition and release of cytochrome *c* from liver and brain mitochondria. *Arch. Biochem. Biophys.* **386,** 251–260.

Laoukili, J., Perret, E., Middendorp, S., Houcine, O., Guennou, C., Marano, F., Bornens, M., and Tournier, F. (2000). Differential expression and cellular distribution of centrin isoforms during human ciliated cell differentiation in vitro. *J. Cell Sci.* **113,** 1355–1364.

Lechtreck, K. F., and Grunow, A. (1999). Evidence for a direct role of nascent basal bodies during spindle pole initiation in the green alga *Spermatozopsis similis*. *Protist* **150,** 163–181.

Lee, G. M., Diguiseppi, J., Gawdi, G. M., and Herman, B. (1987). Chloral hydrate disrupts mitosis by increasing intracellular free calcium. *J. Cell Sci.* **88,** 603–612.

Lefebvre, P. A., and Rosenbaum, J. L. (1986). Regulation of the synthesis and assembly of ciliary and flagellar proteins during regeneration. *Annu. Rev. Cell Biol.* **2,** 517–546.

Lefebvre, P. A., Nordstrom, S. A., Moulder, J. E., and Rosenbaum, J. L. (1978). Flagellar elongation and shortening in *Chlamydomonas*. IV. Effects of flagellar detachment, regeneration, and resorption on the induction of flagellar protein synthesis. *J. Cell Biol.* **78,** 8–27.

Lewin, R. A., and Burrascano, C. (1983). Another new kind of *Chlamydomonas* mutant, with impaired flagellar autotomy. *Experientia* **39,** 1397–1398.

Lewin, R. A., and Lee, K. W. (1985). Autotomy of algal flagella: Electron microscope studies of *Chlamydomonas* (Chlorophyceae) and *Tetraselmis* (Prasinophyceae). *Phycologia* **24,** 311–316.

Lewin, R. A., Lee, T.-H., and Fang, L.-S. (1982). Effects of various agents on flagellar activity, flagellar autotomy and cell viability in four species of *Chlamydomonas* (Chlorophyta: Volvocales). *In* ''Prokaryotic and Eukaryotic Flagella'' (W. B. Amos and J. G. Duckett, Eds.), pp. 421–437. *Soc. Exp. Biol. Symp. No. 35*. Cambridge University Press, London.

Lohret, T. A., McNally, F. J., and Quarmby, L. M. (1998). A role for katanin-mediated axonemal severing during *Chlamydomonas* deflagellation. *Mol. Biol. Cell* **9,** 421–437.

Lohret, T. A., Zhao, L., and Quarmby, L. M. (1999). Cloning of *Chlamydomonas* p60 katanin and localization to the site of outer doublet severing during deflagellation. *Cell Motil. Cytoskel.* **43,** 221–231.

Lu, K. P., and Means, A. R. (1994). Expression of the non-catalytic domain of the NIMA kinas causes a G_2 arrest in *Aspergillus nidulans*. *EMBO J.* **13,** 2103–2113.

Maciejewski, J. J., Vacchiano, E. J., McCutcheon, S. M., and Buhse, H. E., Jr. (1999). Cloning and expression of a cDNA encoding a *Vorticella convallaria* spasmin: An EF-hand calcium-binding protein. *J. Eukaryot. Microbiol.* **46,** 165–173.

Mahjoub, M. R., Montpetit, B., Zhao, L., Finst, R. J., Goh, B., Kim, A. C., and Quarmby, L. M. (2002). The *FA2* gene of *Chlamydomonas* encodes a NIMA family kinase with roles in cell cycle progression and microtubule severing during deflagellation. *J. Cell Sci.* **115,** 1759–1768.

Marshall, W. F. (2002). Size control in dynamic organelles. *Trends Cell Biol.* **12,** 414–419.

Marshall, W. F., and Rosenbaum, J. L. (2001). Intraflagellar transport balances continuous turnover of outer doublet microtubules: Implications for flagellar length control. *J. Cell Biol.* **155,** 405–414.

Marshall, W. F., Vucica, Y., and Rosenbaum, J. L. (2001). Kinetics and regulation of de novo centriole assembly: Implications for the mechanism of centriole duplication. *Curr. Biol.* **11,** 308–317.

Marszalek, J. R., and Goldstein, L. S. (2000). Understanding the functions of kinesin-II. *Biochim. Biophys. Acta* **1496,** 142–150.

McFadden, G. I., Schulze, D., Surek, B., Salisbury, J. L., and Malkonian, M. (1987). Basal body reorientation mediated by Ca^{2+}-modulated contractile protein. *J. Cell Biol.* **105,** 903–912.

McNally, F. J. (2000). Capturing a ring of samurai. *Nat. Cell Biol.* **2,** E4–E7.

McNally, F. J., and Vale, R. D. (1993). Identification of katanin, an ATPase that severs and disassembles stable microtubules. *Cell* **75,** 419–429.

McNally, K. P., Bazirgan, O. A., and McNally, F. J. (2000). Two domains of p80 katanin regulate microtubule severing and spindle pole targeting by p60 katanin. *J. Cell Sci.* **113,** 1623–1633.

McNally, K. P., Buster, D., and McNally, F. J. (2002). Katanin-mediated microtubule severing can be regulated by multiple mechanisms. *Cell Motil. Cytoskel.* **53,** 337–349.

Middendorp, S., Kuntziger, T., Abraham, Y., Holmes, S., Bordes, N., Paintrand, M., Paoletti, A., and Bornens, M. (2000). A role for centrin 3 in centrosome reproduction. *J. Cell Biol.* **148,** 405–416.

Mitchell, D. R. (2000). *Chlamydomonas* flagella. *J. Phycol.* **36,** 261–273.

Mohammed, B. J., Mitchell, T. J., Andrew, P. W., Hirst, R. A., and O'Callaghan, C. (1999). The effect of pneumococcal toxin, pneumolysin, on brain ependymal cilia. *Microb. Pathog.* **27,** 303–309.

Montes, J. F., Durfort, M., and Garcia-Valero, J. (2001). Parasitism by the protozoan *Perkinsus atlanticus* favours the development of opportunistic infections. *Dis. Aquat. Org.* **46,** 57–66.

Munnik, T., van Himbergen, J. A. J., ter Riet, B., Braun, F.-J., Irvine, R. F., van den Ende, H., and Musgrave, A. (1998). Detailed analysis of the turnover of polyphosphoinositides and phosphatidic acid upon activation of phospholipases C and D in *Chlamydomonas* cells treated with nonpermeabilizing concentrations of mastoparan. *Planta* **207,** 133–145.

Nguyen-Legros, J., and Hicks, D. (2000). Renewal of photoreceptor outer segments and their phagocytosis by the retinal pigment epithelium. *Int. Rev. Cytol.* **196,** 245–313.

Nicolson, G. L., Smith, J. R., and Poste, G. (1976). Effects of local anesthetics on cell morphology and membrane-associated cytoskeletal organization in BALB/3T3 cells. *J. Cell Biol.* **68,** 395–402.

Nogales, E., Whittaker, M., Milligan, R. A., and Downing, K. H. (1999). High-resolution model of the microtubule. *Cell* **96,** 79–88.

Ogura, A., and Takahashi, K. (1976). Artificial deciliation causes loss of calcium-dependent responses in *Paramecium*. *Nature* **264,** 170–172.

Pan, J., and Snell, W. J. (2002). Kinesin-II is required for flagellar sensory transduction during fertilization in *Chlamydomonas*. *Mol. Biol. Cell* **13,** 1417–1426.

Papahadjopoulos, D., Jacobson, K., Poste, G., and Shepherd, G. (1975). Effects of local anesthetics [sic] on membrane properties. I. Changes in the fluidity of phospholipid bilayers *Biochim. Biophys. Acta* **394,** 504–519.

Parker, J. D. K., and Quarmby, L. M. (2003). *Chlamydomonas fla10* and *fla2* mutants reveal a link between deflagellation and intraflagellar transport. *BMC Cell Biol.* **4,** 11.

Paweletz, N., Mazia, D., and Finze, E. M. (1987). Fine structural studies of the bipolarization of the mitotic apparatus in the fertilized sea urchin egg. I. The structure and behaviour of the centrosomes before fusion of the pronuclei. *Eur. J. Cell Biol.* **44,** 195–204.

Pazour, G. J., and Rosenbaum, J. L. (2002). Intraflagellar transport and cilia-dependent diseases. *Trends Cell Biol.* **12,** 551–555.

Pazour, G. J., and Witman, G. B. (2003). The vertebrate primary cilium is a sensory organelle. *Curr. Opin. Cell Biol.* **15,** 105–110.

Pazour, G. J., Wilkerson, C. G., and Witman, G. B. (1998). A dynein light chain is essential for retrograde particle movement in intraflagellar transport (IFT). *J. Cell Biol.* **141,** 979–992.

Pazour, G. J., Dickert, B. L., and Witman, G. B. (1999). The DHC1b (DCH2) isoform of cytoplasmic dynein is required for flagellar assembly. *J. Cell Biol.* **144,** 473–481.

Pazour, G. J., Baker, S. A., Deane, J. A., Cole, D. G., Dickert, B. L., Rosenbaum, J. L., Witman, G. B., and Besharse, J. C. (2002a). The intraflagellar transport protein, IFT88, is essential for vertebrate photoreceptor assembly and maintenance. *J. Cell Biol.* **157,** 103–113.

Pazour, G. J., San Agustin, J. T., Follit, J. A., Rosenbaum, J. L., and Witman, G. B. (2002b). Polycystin-2 localizes to kidney cilia and the ciliary level is elevated in orpk mice with polycystic kidney disease. *Curr. Biol.* **12,** R378–R380.

Pickett-Heaps, J., and Pickett-Heaps, J. (1995). "Cellular Evolution in the Green Algae: Volvocales, Tetrasporales and Chlorococcales." Video disc produced by Cytographics, Victoria, Australia.

Piperno, G., Mead, K., and Henderson, S. (1996). Inner dynein arms but not outer dynein arms require the activity of kinesin homologue protein KHP1(FLA10) to reach the distal part of flagella in *Chlamydomonas*. *J. Cell Biol.* **133,** 371–379.

Porter, M. E., Bower, R., Knott, J. A., Byrd, P., and Dentler, W. (1999). Cytoplasmic dynein heavy chain 1b is required for flagellar assembly in *Chlamydomonas*. *Mol. Biol. Cell* **10,** 693–712.

Poste, G., Papahadjopoulos, D., Jacobson, K., and Vail, W. J. (1975). Effects of local anesthetics on membrane properties. II. Enhancement of the susceptibility of mammalian cells to agglutination by plant lectins. *Biochim. Biophys. Acta* **394,** 520–539.

Quarmby, L. M. (1996). Ca^{2+} influx activated by low pH in *Chlamydomonas*. *J. Gen. Physiol.* **108,** 351–361.

Quarmby, L. M. (2000). Cellular samurai: Katanin and the severing of microtubules. *J. Cell Sci.* **113,** 2821–2827.

Quarmby, L. M., and Hartzell, H. C. (1994). Two distinct, calcium-mediated, signal transduction pathways can trigger deflagellation in *Chlamydomonas reinhardtii*. *J. Cell Biol.* **124,** 807–815.

Quarmby, L. M., Yueh, Y. G., Cheshire, J. L., Keller, L. R., Snell, W. J., and Crain, R. C. (1992). Inositol phospholipid metabolism may trigger flagellar excision in *Chlamydomonas reinhardtii*. *J. Cell Biol.* **116,** 737–744.

Reeder, R. L., and Shirley, B. (1999). Deciliation in the ampulla of the rat oviduct and effects of estrogen on the process. *J. Exp. Zool.* **283,** 71–80.

Ren, D., Navarro, B., Perez, G., Jackson, A. C., Hsu, S., Shi, Q., Tilly, J. L., and Clapham, D. E. (2001). A sperm ion channel required for sperm motility and male fertility. *Nature* **413,** 603–609.

Rieder, C. L., Jensen, C. G., and Jensen, L. C. (1979). The resorption of primary cilia during mitosis in a vertebrate (PtK1) cell line. *J. Ultrastruct. Res.* **68,** 173–185.

Rieder, C. L., Faruki, S., and Khodjakov, A. (2001). The centrosome in vertebrates: More than a microtubule-organizing center. *Trends Cell Biol.* **11,** 413–419.

Rohlich, P. (1975). The sensory cilium of retinal rods is analogous to the transitional zone of motile cilia. *Cell Tissue Res.* **161,** 421–430.

Roos, A., and Boron, W. F. (1981). Intracellular pH. *Physiol. Rev.* **61,** 296–434.

Rosenbaum, J. L., and Carlson, K. (1969). Cilia regeneration in protozoan flagellates. *J. Cell Biol.* **34,** 345–364.

Rosenbaum, J. L., and Child, F. M. (1967). Flagellar regeneration in protozoan flagellates. *J. Cell Biol.* **34,** 345–364.

Rosenbaum, J. L., and Witman, G. B. (2002). Intraflagellar transport. *Nat. Rev. Mol. Cell Biol.* **3,** 813–825.

Rosenbaum, J. L., Moulder, J. E., and Ringo, D. L. (1969). Flagellar elongation and shortening in *Chlamydomonas*: The use of cycloheximide and colchicines to study the synthesis and assembly of flagellar proteins. *J. Cell Biol.* **41,** 600–619.

Salisbury, J. L. (1983). Contractile flagellar roots: The role of calcium. *J. Submicrosc. Cytol.* **15,** 105–110.

Salisbury, J. L. (1995). Centrin, centrosomes, and mitotic spindle poles. *Curr. Opin. Cell Biol.* **7,** 39–45.

Salisbury, J. L., Sanders, M. A., and Harpst, L. (1987). Flagellar root contraction and nuclear movement during flagellar regeneration in *Chlamydomonas reinhardtii*. *J. Cell Biol.* **105,** 1799–1805.

Salisbury, J. L., Baron, A. T., and Sanders, M. A. (1988). The centrin-based cytoskeleton of *Chlamydomonas reinhardtii*: Distribution in interphase and mitotic cells. *J. Cell Biol.* **107,** 635–641.

Salisbury, J. L., Suino, K. M., Busby, R., and Springett, M. (2002). Centrin-2 is required for centriole duplication in mammalian cells. *Curr. Biol.* **12,** 1287–1292.

Sanders, M. A., and Salisbury, J. L. (1989). Centrin-mediated microtubule severing during flagellar excision in *Chlamydomonas reinhardtii*. *J. Cell Biol.* **108,** 1751–1760.

Sanders, M. A., and Salisbury, J. L. (1994). Centrin plays an essential role in microtubule severing during flagellar excision in *Chlamydomonas reinhardtii*. *J. Cell Biol.* **124,** 795–805.

Satir, B., Sale, W. S., and Satir, P. (1976). Membrane renewal after dibucaine deciliation of *Tetrahymena*. *Exp. Cell Res.* **97,** 83–91.

Senisterra, G. A., and Lepock, J. R. (2000). Thermal destabilization of transmembrane proteins by local anaesthetics. *Int. J. Hyperthermia* **16,** 1–17.

Seyfert, H.-M., Neufang, M., and Willecke, R. (1985). Deciliation interferes with cell-cycle progression in *Tetrahymena*. *Exp. Cell Res.* **158,** 159–169.

Silflow, C. D., and Lefebvre, P. A. (2001). Assembly and motility of eukaryotic cilia and flagella: Lessons from *Chlamydomonas reinhardtii*. *Plant Physiol.* **127,** 1500–1507.

Sloboda, R. D. (2002). A healthy understanding of intraflagellar transport. *Cell Motil. Cytoskel.* **52,** 1–8.

Small, J. V., and Kaverina, I. (2003). Microtubules meet substrate adhesions to arrange cell polarity. *Curr. Opin. Cell Biol.* **15,** 40–47.

Smith, E. F. (2002). Regulation of flagellar dynein by calcium and a role for an axonemal calmodulin and calmodulin-dependent kinase. *Mol. Biol. Cell* **13,** 3303–3313.

Sotnikov, O. S. (2002). Non-electrical functions of neurons. *Neurosci. Behav. Physiol.* **32,** 495–504.

Spang, A., Courtney, I., Fackler, U., Matzner, M., and Schiebel, E. (1993). The calcium-binding protein cell division cycle 31 of *Saccharomyces cerevisiae* is a component of the half bridge of the spindle pole body. *J. Cell Biol.* **123,** 405–416.

Srayko, M., Buster, D. W., Bazirgan, O. A., McNally, F. J., and Mains, P. E. (2000). MEI-1/MEI-2 katanin-like microtubule severing activity is required for *C. elegans* meiosis. *Genes Dev.* **14,** 1072–1084.

Stalheim, O. H., and Gallagher, J. E. (1977). Ureaplasmal epithelial lesions related to ammonia. *Infect. Immun.* **15,** 995–996.

Stephens, R. E. (1975). The basal apparatus: Mass isolation from the molluscan ciliated gill epithelium and a preliminary characterization of striated rootlets. *J. Cell Biol.* **64,** 408–420.

Stephens, R. E. (1997). Synthesis and turnover of embryonic sea urchin ciliary proteins during selective inhibition of tubulin synthesis and assembly. *Mol. Biol. Cell* **8,** 2187–2198.

Stephens, R. E. (2000). Preferential incorporation of tubulin into the junctional region of ciliary outer doublet microtubules: A model for treadmilling by lattice dislocation. *Cell Motil. Cytoskel.* **47,** 130–140.

Suwalsky, M., Schneider, C., Villena, F., Norris, B., Cardenas, H., Cuevas, F., and Sotomayor, C. P. (2001). Dibucaine-induced modification of sodium transport in toad skin and of model membrane structures. *Z. Naturforsch.* **56,** 614–622.

Taillon, B., Adler, S., Suhan, J., and Jarvik, J. (1992). Mutational analysis of centrin: An EF-hand protein associated with three distince contractile fibers in the basal body apparatus of *Chlamydomonas*. *J. Cell Biol.* **119,** 1613–1624.

Tamm, S. (1994). Ca^{2+} channels and signaling in cilia and flagella. *Trends Cell Biol.* **4,** 305–310.

Thai, C. H., Gambling, T. M., and Carson, J. L. (2002). Freeze fracture study of airway epithelium from patients with primary ciliary dyskinesia. *Thorax* **57,** 363–365.

Thompson, G. A., Baugh, C., and Walker, L. F. (1974). Nonlethal deciliation of *Tetrahymena* by a local anesthetic and its utility as a tool for studying cilia regeneration. *J. Cell Biol.* **61,** 253–257.

Tsien, R. Y. (1980). New calcium indicators and buffers with high selectivity against magniesium and protons: Design, synthesis and properties of prototype structure. *Biochemistry* **19,** 2396–2404.

Tucker, R. W., and Pardee, A. B. (1979). Centriole ciliation is related to quiescence and DNA synthesis is 3T3 cells. *Cell* **17,** 527–535.

Tucker, R. W., Scher, C. D., and Stiles, C. D. (1979). Centriole deciliation associated with the early response of 3T3 cells to growth factors but not to SV40. *Cell* **18,** 1065–1072.

Tuxhorn, J., Daise, T., and Dentler, W. L. (1998). Regulation of flagellar length in *Chlamydomonas*. *Cell Motil. Cytoskel.* **40,** 133–146.

Vale, R. D. (1991). Severing of stable microtubules by a mitotically activated protein in *Xenopus* egg extracts. *Cell* **64,** 827–839.

Verhage, H. G., Bareither, M. L., Jaffe, R. C., and Akbar, M. (1979). Cyclic changes in ciliation, secretion and cell height of the oviductal epithelium in women. *Am. J. Anat.* **156,** 505–521.

Verra, Escudier, F. E., Pinchon, M.-C., Fleury, J., Bignon, J., and Bernaudin, J-F. (1990). Effects of local anaesthetics (lidocaine) on the structure and function of ciliated respiratory epithelial cells. *Biol. Cell* **69,** 99–105.

Vivier, E., and Andre, J. (1961). *J. Protozool.* **8,** 416.; as cited in Blum, J. J. (1971). Existence of a breaking point in cilia and flagella *J. Theor. Biol.* **33,** 257–263.

Walther, Z., Vashishtha, M., and Hall, J. L. (1994). The *Chlamydomonas FLA10* gene encodes a novel kinesin-homologous protein. *J. Cell Biol.* **126,** 175–188.

Wargo, M. J., and Smith, E. F. (2003). Asymmetry of the central apparatus defines the location of active microtubule sliding in *Chlamydomonas* flagella. *Proc. Natl. Acad. Sci. USA* **100,** 137–142.

Watson, M. R., and Hopkins, J. M. (1962). Isolated cilia from *Tetrahymena pyriformis*. *Exp. Cell Res.* **28,** 280–295.

Weeks, D. P., Collis, P. S., and Gealt, M. A. (1977). Control of induction of tubulin synthesis in *Chlamydomonas reinhardi*. *Nature* **268,** 667–668.

Wheatley, D. N., Wang, A. M., and Strugnell, G. E. (1996). Expression of primary cilia in mammalian cells. *Cell Biol. Int.* **20,** 73–81.

Willoughby, R., Ecker, G., McKee, S., Riddolls, C., Vernaillen, C., Dubovi, E., Lein, D., Mahony, J. B., Chernesky, M., Nagy, E., *et al.* (1992). The effects of equine rhinovirus, influenza virus and herpesvirus infection on tracheal clearance rate in horses. *Can. J. Vet. Res.* **56,** 115–121.

Wilson, E. B (1895). An atlas of the tertilization and karyokinesis of the Ovum. New York, MacMillan.; as cited in Blum, J. J. (1971). Existence of a breaking point in cilia and flagella *J. Theor. Biol.* **33,** 257–263.

Witman, G. B., Carlson, K., Berliner, J., and Rosenbaum, J. (1972). *Chlamydomonas* flagella. I. Isolation and electrophoretic analysis of microtubules, matrix, membranes and mastigonemes. *J. Cell Biol.* **54,** 507–539.

Witman, G. B., Plummer, J., and Sander, G. (1978). *Chlamydomonas* flagella mutants lacking radial spokes and central tubules: Structure, composition and function of specific axonemal components. *J. Cell Biol.* **76,** 729–747.

Wright, R. L., Salisbury, J. L., and Jarvik, J. (1985). A nucleus-basal body connector in *Chlamydomonas reinhardtii* that may function in basal body localization or segregation. *J. Cell Biol.* **101,** 1903–1912.

Wright, R. L., Adler, S. A., Spanier, J. G., and Jarvik, J. W. (1989). The nucleus-basal body connector of *C. reinhardtii*: Evidence for a role in basal-body segregation and against essential roles in mitosis or in determining cell polarity. *Cell Motil. Cytoskel.* **14,** 516–526.

Yoshimura, K. (1998). Mechanosensitive channels in the cell body of *Chlamydomonas*. *J. Memb. Biol.* **166,** 149–155.

Yueh, Y. G., and Crain, R. C. (1993). Deflagellation of *Chlamydomonas reinhardtii* follows a rapid transitory accumulation of inositol 1,4,5-trisphosphate and requires Ca^{2+} entry. *J. Cell Biol.* **123,** 869–875.

This Page Intentionally Left Blank

The Bacterial Flagellar Motor: Structure and Function of a Complex Molecular Machine

Seiji Kojima and David F. Blair
Department of Biology, University of Utah, Salt Lake City, Utah 84112

The bacterial flagellar motor harnesses ion flow to drive rotary motion, at speeds reaching 100,000 rpm and with apparently tight coupling. The functional properties of the motor are quite well understood, but its molecular mechanism remains unknown. Studies of motor physiology, together with mutational and biochemical studies of the components, place significant constraints on the mechanism. Rotation is probably driven by conformational changes in membrane–protein complexes that form the stator. These conformational changes occur as protons move on and off a critical aspartate residue in the stator protein MotB, and the resulting forces are applied to the rotor protein FliG. The bacterial flagellum is a complex structure built from about two dozen proteins. Its construction requires an apparatus at the base that exports many flagellar components to their sites of installation by way of an axial channel through the structure. The sequence of events in assembly is understood in general terms, but not yet at the molecular level. A fuller understanding of motor rotation and flagellar assembly will require more data on the structures and organization of the constituent proteins.

KEY WORDS: Prokaryotic motility, Mechanoenzymes, Ion channels, Flagellar motor, Bacterial flagellar.

I. Introduction

Bacterial flagella are helical propellers turned by rotary motors in the cell membrane (Berg and Anderson, 1973). The fuel for rotation is the membrane gradient of ions, H^+ in most neutrophiles (Larsen *et al.*, 1974a; Manson *et al.*,

0074-7696/04 $35.00

1977; Shioi *et al*., 1980) and Na^+ in alkalophiles and marine *Vibrio* species (Hirota and Imae, 1983). Bacteria control their flagella so that swimming is directed toward environments that promote survival. In many species, including *Escherichia coli* and *Salmonella*, the motors can rotate either clockwise (CW) or counterclockwise (CCW), and cells direct their movement by regulating switching between the two directions (Larsen *et al*., 1974b; Silverman and Simon, 1974a). Some flagellated species exhibit other modes of swimming, such as unidirectional rotation punctuated by occasional stops (*Rhodobacter sphaeroides*) or regulated variations in motor speed (*Sinorhizobium meliloti*) (Armitage and Schmitt, 1997). In *E. coli* or *Salmonella*, CCW rotation allows several filaments on a cell to join in a bundle and drive the cell smoothly forward (a ''run''), whereas CW rotation disrupts the filament bundle and causes rapid somersaulting (a ''tumble''). When a cell swims in an isotropic environment, the flagellar motors reverse direction at random intervals, and the trajectory is a random walk consisting of runs of about 1 s alternating with short tumbles (Berg and Brown, 1972). In a spatial gradient of a chemical attractant such as serine or maltose, cells increase the duration of runs that happen to be carrying them up the gradient, while not altering (or only slightly shortening) runs down the gradient, thus biasing their movement toward regions of higher attractant concentration (Brown and Berg, 1974; Macnab and Koshland, 1972).

Much is known about the performance of the flagellar rotary motor and how it varies with load, membrane gradient, and other external variables. The sequence of events in flagellar assembly is largely understood, from extensive studies of assembly-defective mutants. Ultrastructural studies have provided an impressive picture of the overall shape of the flagellar motor, and genetic and biochemical studies have identified proteins that function in its assembly and rotation. Flagellar assembly and rotation remain scantly understood at the molecular level, however, mainly owing to a lack of structural information.

This review summarizes current knowledge of flagellar structure, function, and assembly, with emphasis on more recent insights into the rotation mechanism obtained from physiological and mutational studies. We briefly review the rotation mechanisms that have been proposed, and suggest the outlines of a mechanism that appears consistent with current knowledge of the motor. Most of the surveyed literature concerns the enteric species *Escherichia coli* and *Salmonella* or the marine species *Vibrio alginolyticus*, whose flagellar motors have been studied most extensively. Fuller discussions of motility and chemotaxis in other species can be found in other reviews (Armitage and Schmitt, 1997; England and Gober, 2001; Harshey and Toguchi, 1996; Wu and Newton, 1997).

II. Flagellar Assembly

A. Overview of Flagellar Structure

Most of the mass of the flagellum is in the long helical filament (Fig. 1A). The filament functions as a propeller to convert rotary motion into thrust and, accordingly, is quite rigid (Fujime *et al.*, 1972). It is a hollow tube formed from thousands of copies of a single protein called flagellin (or, in some species, a few closely related flagellins). The subunits are arranged on a lattice that

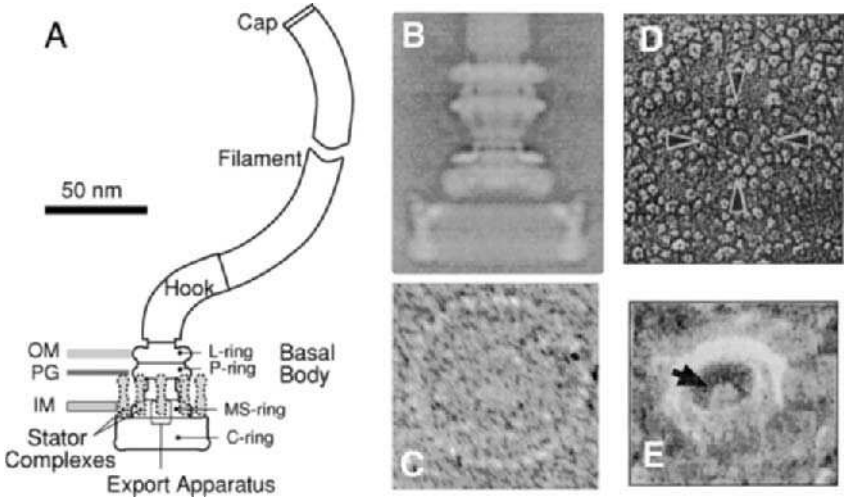

FIG. 1 (A) Diagram of the flagellum in a gram-negative bacterium. Gram-positive species lack the LP ring assembly. Only a part of the filament is shown, as it is quite long on this scale (~10 μm). OM, outer membrane; PG, peptidoglycan; IM, inner membrane. (B) Electron micrographic reconstruction of the flagellar basal body of *Salmonella* (side view). The image was obtained by averaging micrographs of single particles embedded in vitreous ice. The cytoplasm is down and the hook is up; only the bottommost portion of the hook is visible. (C) *En face* view of the C ring, viewed from the cytoplasmic side. Subunit structure is clearly visible. Rotational averaging and Fourier transforms demonstrate 34-fold rotational symmetry for this specimen (Thomas *et al.*, 1999). [(B) and (C) from DeRosier, with permission.] (D) Circular array of membrane-embedded particles, thought to be MotA–MotB protein complexes, that is, the stator. The larger particle in the center is the cell-proximal part of the basal body rod. The inner diameter of this particle ring is about 30 nm. The image is from *Salmonella*, but similar structures have been seen in several species. (From Khan, with permission.) (E) Central protrusion within the C ring that is probably the export apparatus essential for assembly of exterior structures of the flagellum. The view is from inside the cell. (From Aizawa, with permission.)

can be thought of as consisting of 11 protofilaments oriented approximately parallel to the filament axis (Mimori *et al.*, 1995; Trachtenberg and DeRosier, 1987). The overall helical shape of the filament arises from inequivalence among the protofilaments, with some being slightly longer than others because of differences in subunit packing (Calladine, 1978; Trachtenberg and DeRosier, 1991). The relative stability of the long-versus-short protofilament forms is sensitive to a variety of factors including pH, ionic strength, mechanical stress, and mutation, and filaments can take on several different helical forms depending on the circumstances (Kamiya and Asakura, 1977; Kanto *et al.*, 1991; Macnab and Ornston, 1977). A crystal structure was solved for most of the flagellin protein, revealing the molecular basis of subunit packing in the filament and the variations in packing that give rise to its helicity (Samatey *et al.*, 2001).

At its base the filament is joined to a slightly thicker structure termed the hook, which is thought to function as a flexible coupling. The hook is joined in turn to the basal body, a set of rings mounted coaxially on a rod (Depamphilis and Adler, 1971; Francis *et al.*, 1994; Khan *et al.*, 1992). Single-particle reconstructions of the basal body have achieved a resolution approaching 2 nm, revealing much detail in the shapes of the rings and rod (Francis *et al.*, 1994; Thomas *et al.*, 2001) (Fig. 1B). The rings are named for their locations relative to cell envelope structures. The LP ring assembly is at the level of the outer (lipopolysaccharide) membrane and peptidoglycan layer, and is thought to function as a bushing for the central rod. The MS ring is within and just above the cytoplasmic membrane (M, membrane; S, supramembrane). Mounted to the cytoplasmic face of the MS ring is a drum-shaped structure termed the C ring (Francis *et al.*, 1994; Khan *et al.*, 1992). Good *en face* views of the C ring show fine structure with either 33- or 34-fold rotational symmetry, depending on the specimen (Thomas *et al.*, 1999) (Fig. 1C).

The structure seen in the single-particle reconstructions is one that has survived purification, and it is known to lack some components necessary for rotation. The basal structure in Fig. 1B is probably just the rotating part, or rotor. The nonrotating part, or stator, is a circular array of protein complexes in the membrane around the rotor, which have been seen in freeze-fracture images (Coulton and Murray, 1978; Khan *et al.*, 1988) (Fig. 1D). The number of particles seen in each circular array ranges from 10 to 16, varying between species and also from motor to motor. The inner diameter of the array varies from 20 to 30 nm, depending on the method of sample preparation (Khan *et al.*, 1991) and the species (Khan *et al.*, 1988). As discussed further below, the individual protein complexes within the stator appear equivalent and can function independently to produce torque (Blair and Berg, 1988; Block and Berg, 1984).

B. Morphogenetic Pathway

A flagellum contains about two dozen proteins, most of which have been localized to particular features in the structure (Aizawa *et al.*, 1985; Homma *et al.*, 1987b) (Fig. 2). The sequence of events in flagellar assembly is understood in basic outline, from the study of partial structures produced in mutants blocked at successive steps (Fig. 2) (Iino, 1985; Jones and Macnab, 1990; Kubori *et al.*, 1992; Macnab, 2003; Suzuki and Komeda, 1981; Suzuki *et al.*, 1978). Generally speaking, assembly proceeds from inner structures to outer ones, but details of the process are complex; some steps have not been ordered precisely.

The MS ring and the innermost portion of the rod are all formed from the protein FliF, and overexpression of FliF is sufficient to cause accumulation of large numbers of these ring–rod structures in the membrane (Ueno *et al.*, 1992). The MS ring serves a central structural role, attaching to the C ring on its inner (cytoplasmic) face and to the rod in the periplasm. It also houses a multiprotein complex that functions to export most external proteins of the flagellum to their sites of installation, by way of a narrow axial channel through the structure (Aizawa, 2000; Macnab, 2003; Mimori *et al.*, 1995; Morgan *et al.*, 1993, 1995). This export apparatus (or a part of it) has been seen in bottom views of the flagellum, as a central protrusion inside the C ring (Katayama *et al.*, 1996; Zhao *et al.*, 1996) (Fig. 1E). It is evolutionarily and structurally related to the type III secretion apparatus utilized by many pathogens to pump effector proteins into their hosts (Bennett and Hughes, 2000; Kubori *et al.*, 1998; Macnab, 1999). The export apparatus is discussed further below; here we note that it must be functioning before the rod or any other features beyond the MS ring can be built.

Assembly of the MS ring is clearly an early step in flagellar assembly, but it is not certain whether it is completed separately from other steps. If the perimeter of the MS ring constitutes a barrier to movement of membrane proteins needed to form the export apparatus, then those export apparatus components must presumably assemble first and the MS ring assembles around them. If the MS ring does not block movement of the export apparatus proteins, then it could be completed first. The C ring probably assembles directly onto the MS ring: cells expressing FliF, FliG, FliM, and FliN can assemble MS/C rings that appear essentially normal, although showing some variability in size (Lux *et al.*, 2000; Young *et al.*, 2003). Deletion of any switch complex protein blocks flagellar assembly at an early stage, presumably by preventing completion of the export apparatus (Kubori *et al.*, 1992; Yamaguchi *et al.*, 1986a). Thus, assembly of the switch complex is either a prerequisite or corequisite for assembly of the export apparatus.

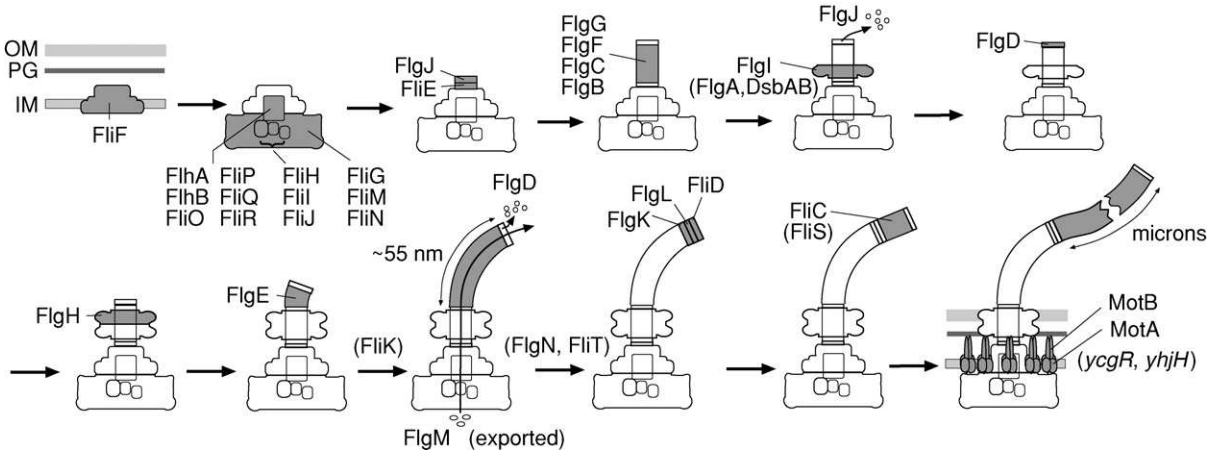

FIG. 2 Sequence of events in flagellar assembly. OM, outer membrane; PG, peptidoglycan; IM, inner membrane. At each step, the most recently added component(s) are shaded. The exact sequence of steps in switch complex and export apparatus assembly is uncertain (see text). MotA and MotB are shown being added last, but they might be installed and begin driving rotation at an earlier stage. Some steps require the action of helper proteins or genes in addition to the structural proteins; names of these are given in parentheses.

Once the export apparatus is functioning, the rod is constructed, using six proteins (Fig. 2). The bulk of the rod is formed from the proteins FlgB, FlgC, FlgF, and FlgG, probably arranged in that order proceeding outward (Homma *et al.*, 1990). At its inner end, the rod is joined to FliF by the protein FliE (Minamino *et al.*, 2000b). The protein FlgJ acts as a cap on the growing rod to facilitate the addition of subunits, and also has muramidase activity needed to penetrate the peptidoglycan layer (Hirano *et al.*, 2001; Nambu *et al.*, 1999). When the rod is complete, the P ring and then the L ring assemble onto it, using subunits of FlgI and FlgH, respectively. In contrast to other exterior components of the flagellum, FlgI and FlgH are exported by the conventional Sec pathway (Homma *et al.*, 1987a; Jones *et al.*, 1990). In addition to the structural subunit FlgI, assembly of the P ring requires the protein FlgA to act as FlgI chaperone in the periplasm (Nambu and Kutsukake, 2000) and the proteins DsbA and DsbB to catalyze formation of a needed disulfide bond (Dailey and Berg, 1993).

The hook assembles next, from more than 100 copies of the protein FlgE. Like rod assembly, hook assembly also requires a capping protein, in this case FlgD. Hook growth proceeds to a fairly well-determined length (55 ± 6 nm), and then the FlgD capping protein dissociates and is replaced by the protein FlgK. FlgK forms a short zone containing relatively few (on the order of 10) subunits, and is followed by FlgL and FliD, which also form short zones. FlgK, FlgL, and FliD are also called HAP1, HAP3, and HAP2 (HAP, hook-associated protein). Addition of FlgK and FlgL is facilitated by the chaperone FlgN, whereas FliD is chaperoned by FliT (Bennett and Hughes, 2001; Fraser *et al.*, 1999; Yokoseki *et al.*, 1995). FlgK and FlgL together will form a junction between the hook and the soon-to-be-added filament; FliD serves as a cap to facilitate polymerization of the filament subunits. The filament grows by the addition of FliC subunits between the FlgL and FliD zones. Filaments grow to indeterminate length, typically several microns, and can contain many thousands of subunits.

The membrane complexes that function as stator, mentioned above, are formed from the proteins MotA and MotB. The exact timing of MotA/MotB installation is not known. By suitable genetic manipulation, MotA and MotB can be made to incorporate last into otherwise assembled flagella (Blair and Berg, 1988; Block and Berg, 1984), but in the normal situation they might be installed earlier. Efficient installation of MotA and MotB into the motor appears not to be entirely spontaneous, but to involve the action of the *ycgR* and *yhjH* genes, whose precise roles are unknown (Ko and Park, 2000).

The flagellar export apparatus is a noteworthy machine in itself and is the subject of intense study. It includes six membrane proteins that are believed to form a complex housed in the MS ring (Fig. 3). These are FlhA, FlhB, FliO, FliP, FliQ, and FliR (Minamino and Macnab, 1999). Apart from the

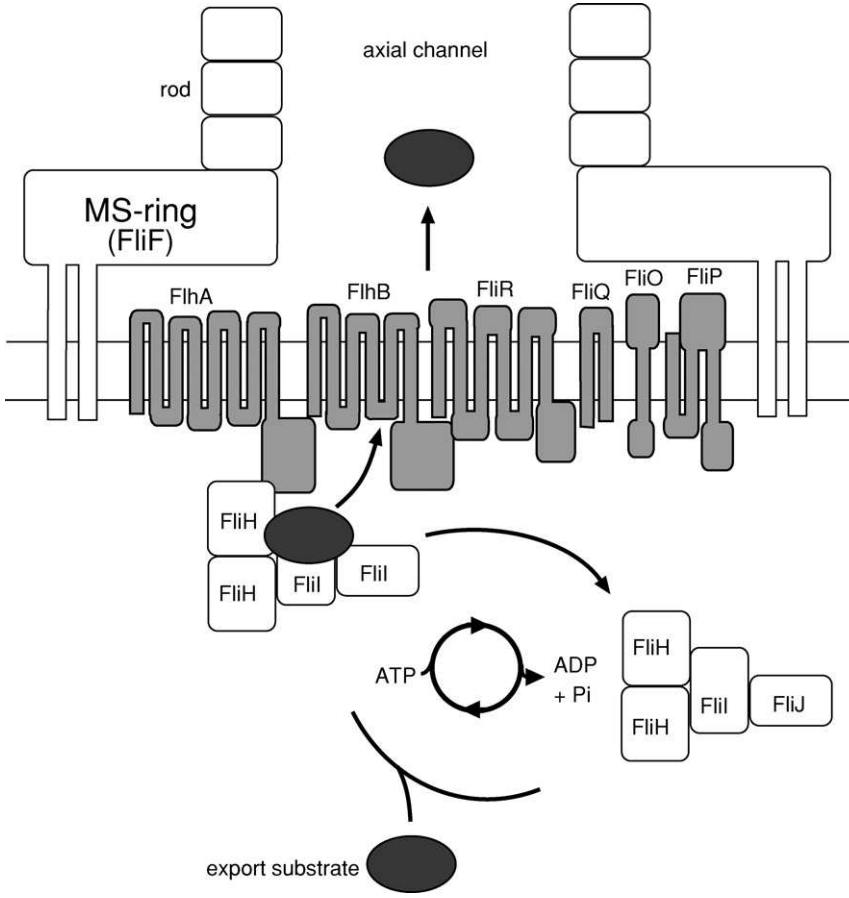

FIG. 3 Protein components of the flagellar export apparatus, and outlines of a highly simplified scheme for the events in export. The membrane components of the export apparatus are shown in gray, and their probable topologies as determined by sequence analysis are indicated. Stoichiometries are not known for these membrane components, but some are known to be present in more than one copy. The three soluble components shown are required for export of all substrates; export of certain flagellar components requires additional soluble proteins (FlgN, FliT, and FliS) that likely function as specific chaperones (cf. Fig. 2).

probable membrane topologies inferred from sequence analysis, little is known about the structures of these proteins. FlhA (75 kDa) and FlhB (42 kDa) are larger than the others and include sizable soluble domains in the cytoplasm. The other four consist largely of hydrophobic, presumably membrane-embedded segments. The stoichiometries and arrangements of the proteins in the complex are not known, but genetic studies provide some clues: certain *fliF* mutations can be suppressed by mutations in *flhA*,

suggesting interaction between the MS ring and the FlhA component of the export apparatus (Kihara *et al*., 2001). FliR and FlhB are joined into a single polypeptide in the species *Clostridium acetobutylicum* (Macnab, 2003; Nolling *et al*., 2001), implying that these proteins occur in equal number and are near each other in the complex.

Flagellar export also requires the soluble proteins FliH and FliI (Macnab, 2003; Minamino and Macnab, 1999). FliI is an ATPase that provides the energy for transport (Fan and Macnab, 1996). It shows significant sequence similarity to the β subunit of ATP synthase (Vogler *et al*., 1991), but the functional significance of this similarity, if any, is not clear. The ATPase activity is down regulated by binding to FliH, in a complex with stoichiometry $FliH_2FliI_1$ (Auvray *et al*., 2002; Gonzalez-Pedrajo *et al*., 2002; Minamino and Macnab, 2000a). Another soluble protein, FliJ, is needed for export of several, possibly all, substrates. FliJ interacts with FliH, FliI, and probably with substrate, most likely functioning as a general chaperone (Bennett and Hughes, 2000; Minamino *et al*., 2000a). A number of other cytosolic proteins are thought to function as chaperones for specific substrates, including the HAPs mentioned above (cf. Fig. 2). A reasonable proposal for the mechanism is that FliH–FliI–FliJ complexes bind to substrate proteins and deliver them to the membrane-bound part of the export apparatus, where they are released (or pushed) into the axial channel. One or more of these steps must be coupled to ATP hydrolysis by FliI, but the energy-coupling step has not yet been identified.

The protein substrates of the export apparatus fall into two classes according to whether they are needed relatively early in assembly, to form the rod and hook, or in the later steps of HAP addition and filament formation. At the appropriate stage in assembly, the export apparatus undergoes a switch in substrate specificity from the early to late components (Minamino and Macnab, 1999; Minamino *et al*., 1999a). FlhB is closely involved in this specificity switch, undergoing a specific bond cleavage that is necessary for it to occur (Minamino and Macnab, 2000b). The specificity switch is probably important to allow early components to be exported without competition from the much more abundant flagellin protein that will be used later for filament assembly (Macnab, 2003). It appears also to have a role in regulating hook length, which in *Salmonella* is held fairly close to 55 nm. The FlgE protein that forms the hook is the last-used substrate of the early class, and hook growth ceases when the export apparatus switches to late substrates. The flagellum contains many more hook subunits than rod subunits, and so the finding that the rod and hook subunits fall in a single export class (Hirano *et al*., 2003) raises a logistical problem. It seems that some mechanism should exist to ensure that hook subunits are not exported rapidly until rod assembly is complete, but clear evidence for such an ordering mechanism has not been found. Measurements of FlgE

levels in various mutant backgrounds suggested that posttranscriptional mechanisms might hold hook protein at a low level until rod assembly is complete (Bonifield *et al*., 2000). Another study gave evidence that FlgE might be expressed at normal levels during rod assembly, but exported into the periplasm where it is presumably degraded (Minamino and Macnab, 1999).

Hook length regulation involves the proteins FliK and FlhB (Hirano *et al*., 1994; Muramoto *et al*., 1998; Patterson-Delafield *et al*., 1973; Silverman and Simon, 1972; Suzuki *et al*., 1978). Null *fliK* mutants form aberrantly long hooks with no filament attached, and so FliK is believed to measure hook length in some way. The means of length measurement is not known, but a clue comes from the observation that FliK is an early-class substrate for flagellar export, and its export is more efficient when hooks are absent than when normal hooks are present (Minamino *et al*., 1999b). Thus, hook growth might be sensed as an increasing impedance to FliK export, providing feedback to the export apparatus in the form of increased FliK concentration at the flagellar base. Extragenic suppressors of *fliK* mutations are found in *flhB*, suggesting that FliK interacts with the export apparatus component FlhB to trigger the switch to late-class substrates and terminate export of hook subunits (Kutsukake *et al*., 1994; Williams *et al*., 1996). Alternatively, it has been proposed that the C ring functions as a measuring cup to deliver hook subunits to the export apparatus in a portion accurately sized to build a 55-nm hook (Makishima *et al*., 2001).

Much more structural data on the export apparatus will be needed to understand the molecular mechanisms of substrate recognition, specificity switching, and the coupling of ATP hydrolysis to transport. Structural studies on its components are thus a high priority. Many of the membrane components are hydrophobic and likely to provide challenging targets for structure determination.

C. Flagellar Gene Regulation

The flagellar genes are regulated temporally, roughly according to their order of use in flagellar synthesis. The regulatory mechanisms are complex, and we present here only an outline of the essential features of regulation, in *Salmonella*. More detailed discussion and a consideration of regulation in *Caulobacter* are provided in other reviews (Chilcott and Hughes, 2000; Macnab, 1992; Wu and Newton, 1997). To a first approximation, flagellar genes can be classified as early, middle, and late (Fig. 4). The early genes are *flhD* and *flhC*, so-called master controllers of flagellar synthesis. FlhD and FlhC form a tetrameric complex that directly activates transcription of many flagellar genes (Liu and Matsumura, 1994) and indirectly regulates all others

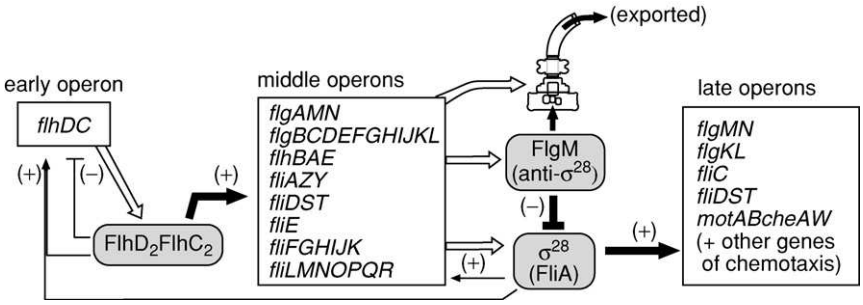

FIG. 4 Regulation of the flagellar genes. The flagellar operons fall into three groups, here termed early, middle, and late. Proteins that function in transcriptional regulation are shaded gray. Thick lines and (+) or (–) symbols indicate well-established regulatory mechanisms that stimulate or inhibit transcription, respectively. Thinner lines and (+) or (–) symbols indicate autogenous regulation of the *flhDC* operon, and of the middle operons, that is not yet as well understood but might also be important for matching flagellar gene expression to circumstances (Kutsukake, 1997a; Kutsukake and Iino, 1994). The *flhDC* operon at the top of this regulatory hierarchy is itself under complex control, by several inputs (see text). In addition to FlhD/FlhC, other major regulatory players are the flagellum-specific sigma factor σ^{28} that stimulates transcription of the late genes, and the anti-sigma factor FlgM that inhibits σ^{28} and is exported through the flagellum as a late-class substrate. Certain genes are transcribed from both middle and late promoters; these are indicated by boldface in the late operons box. Among the late genes are *cheA*, *cheW*, and other genes that do not encode flagellar components but function in the chemosensory pathway. Certain genes that appear in this scheme do not appear in the assembly scheme of Fig. 2: *flhE, fliL*, and *fliY* are of unknown function and can be deleted (in *Salmonella*) with no obvious effect on motility (Ikebe *et al*., 1999; Minamino *et al*., 1994; Schoenhals and Macnab, 1999); *fliZ* appears to enhance expression of middle-level operons, and mutations in it give a partial motility defect (Kutsukake *et al*., 1999). *Salmonella* contains some additional genes, not shown, which function in the phenomenon of flagellar phase variation (Chilcott and Hughes, 2000; Macnab, 1992).

(see below). Flagellar synthesis involves a large commitment of resources, and accordingly, the *flhDC* operon is under elaborate control. Expression of *flhDC* is linked to the cell cycle (Nishimura and Hirota, 1989; Pruss and Matsumura, 1996, 1997), and is regulated by inputs that include cAMP/CRP (Silverman and Simon, 1974b; Yokota and Gots, 1970), temperature (Adler and Templeton, 1967; Qualding and Stocker, 1962; Silverman and Simon, 1974b), the metabolite acetyl phosphate (Pruss and Wolfe, 1994), and salt or other solutes (Li *et al*., 1993; Shi *et al*., 1993). FlhDC level is also influenced by DNA structure, heat shock, transition to stationary phase, transition from liquid culture to plates, and (posttranscriptionally) by the ClpXP protease (Amsler *et al*., 1993; Bertin *et al*., 1994; Eberl *et al*., 1996; Shi *et al*., 1992; Shin and Park, 1995; Tomoyasu *et al*., 2002). The *flhDC* operon is regulated autogenously also, in one of two ways depending on downstream events: the FlhDC proteins stimulate transcription of their own operon when

another, downstream activator of flagellar genes (σ^{28}; see below) is also activated, but inhibit transcription of their operon when σ^{28} activity is low (Kutsukake, 1997a) (Fig. 4).

The $FlhD_2FlhC_2$ complex activates the transcription of more than 30 middle genes, which encode proteins needed to assemble the basal body/hook structure as well as regulatory proteins that control transcription of the late genes (Fig. 4). The late genes encode the flagellin and HAP proteins needed for filament assembly, and motility and chemotaxis genes needed for flagellar energization and control. The late genes are not transcribed strongly until the basal body/hook structures have been completed, and a defect in any basal body/hook protein will decrease their expression. This remarkable link between structure and gene expression involves a sigma factor that stimulates transcription of the late genes, σ^{28}, and a cognate antisigma factor, FlgM, that inhibits σ^{28} and can be exported through the flagellum as a late-class substrate. Cellular levels of FlgM remain high enough to inhibit σ^{28} until the basal body/hook is completed, at which time FlgM is exported from the cell and σ^{28} is freed to turn on transcription of *fliC* and the other late genes (Hughes *et al.*, 1993; Karlinsey *et al.*, 2000; Kutsukake, 1994; Liu and Matsumura, 1995) (Fig. 4).

Other stages in flagellar assembly might also serve as checkpoints for flagellar gene expression. Completion of the LP ring assembly appears also to be sensed, and to affect the level of FlgM protein by affecting the translation of its mRNA. This effect requires the gene *flk* (Karlinsey *et al.*, 1997, 1998), also called *rflH* (Kutsukake, 1997b). In its *rflH* guise, this gene was identified as an inhibitor of late-substrate export in certain genetic backgrounds, and was proposed to function as a second "gate" on flagellar export to block the premature export of late substrates (Kutsukake, 1997b). The protein product of the *flk* gene has not been localized, and its molecular mechanism remains unknown. Its sequence predicts a single membrane-crossing segment, and also includes a segment similar to the S1 domain of RNA-binding proteins (Karlinsey *et al.*, 1998). Flk might bind directly to *flgM* mRNA, and/or target ribosomes to the vicinity of the flagellum (Chilcott and Hughes, 2000). These intriguing possibilities await direct demonstration.

Certain flagellar genes—those encoding the HAP proteins, some export chaperones, and the FlgM regulatory protein—are transcribed from both middle and late promoters. Transcription of the HAP and chaperone genes from the middle promoters might speed the assembly of flagella during the initial transition from a nonflagellate to flagellate state, by ensuring that cellular pools of these proteins are already available at the time they are first needed. Transcription from late promoters presumably ensures that pools are maintained at a level sufficient to support ongoing flagellar synthesis, and, in the case of the filament-capping protein FliD, to allow repair of

filaments broken by mechanical stress. Similarly, transcription of *flgM* from a middle promoter is presumably most important for regulating the flagellate–nonflagellate transition, whereas transcription from the late promoter could provide a steady state FlgM level that prevents mature filaments from growing too long. FlgM should be exported more rapidly through short filaments than through long ones, and this length dependence might allow cells to boost flagellin production in response to filament breakage (Karlinsey *et al.*, 2000).

III. Flagellar Rotation

A. Proteins Involved in Rotation and Switching

Of the many proteins in the flagellum, just five–MotA, MotB, FliG, FliM, and FliN–appear to function in motor rotation per se, as judged by the fact that mutations in only these can prevent rotation without disrupting flagellar assembly (Macnab, 1992). As noted, MotA and MotB form the stator (Chun and Parkinson, 1988; Khan *et al.*, 1988). They are membrane proteins (Dean *et al.*, 1984; Stader *et al.*, 1986) and function together to conduct ions across the membrane (Blair and Berg, 1990; Stolz and Berg, 1991). FliG, FliM, and FliN form a rotomounted assembly termed the switch complex, which is essential not only for rotation but also for flagellar assembly and CW-CCW switching (Yamaguchi *et al.*, 1986a,b). The probable organization of these five motor proteins within the flagellum is illustrated in Fig. 5.

The circular arrays of membrane particles seen in freeze-fracture images (Fig. 1D) are almost certainly the MotA/MotB complexes, because they are not observed in mutants that lack the *motA* or *motB* gene (Khan *et al.*, 1988). The precise relationship between the MotA/MotB complexes and the rotor is not yet clear. The inner diameter of the particle rings is about 30 nm (Khan *et al.*, 1991). [Certain images show a significantly smaller diameter but this appears to be induced by deep etching (Khan *et al.*, 1991).] This is similar to the diameter of the MS-ring, and somewhat less than that of the C-ring (diameter $\sim$45 nm). Because the particles seen in freeze-fracture images were viewed from the periplasmic side of the membrane, their arrangement probably reflects the periplasmic domains of MotB molecules, which are fairly large and are thought to extend upward to contact the peptidoglycan (Chun and Parkinson, 1988; Demot and Vanderleyden, 1994). Interactions with the rotor occur through the cytoplasmic domain of MotA (Zhou *et al.*, 1998a). The rotor-stator interface could thus be at a greater radius, possibly near the outer edge of the C-ring, as pictured in Fig. 5.

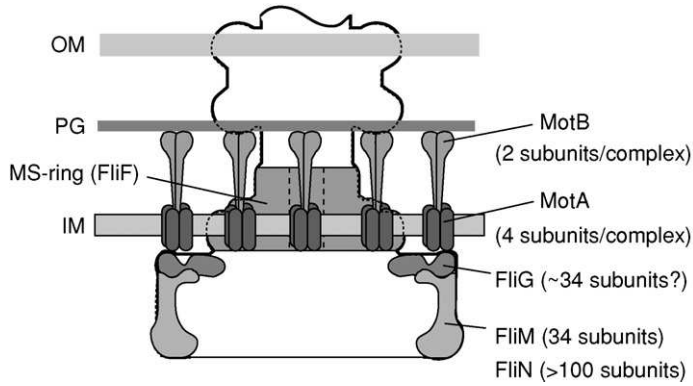

FIG. 5 Proteins that function in rotation. MotA and MotB form the stator complexes, anchored to the cell wall by a putative peptidoglycan-binding motif in the periplasmic domain of MotB. Each motor contains several (as many as eight) stator complexes, each with composition $MotA_4MotB_2$. FliF does not function directly in rotation, but forms the MS ring that is the mounting surface for the "switch complex" comprising FliG, FliM, and FliN. FliG is known to contact the MS ring directly, whereas FliM and FliN are somewhere farther down in the C ring. Exact protein locations are not known, and so details of the pictured arrangement are speculative.

FliM and FliN together form most of the C-ring (Francis *et al.*, 1994; Zhao *et al.*, 1996). FliM appears to function mainly in CW-CCW switching (Sockett *et al.*, 1992) and is the target for binding phospho-Che Y, the signaling molecule that is the output of the chemotaxis pathway (Welch *et al.*, 1993). Binding sites for phospho-CheY occur near the N terminus of FliM (Bren and Eisenbach, 1998; Mathews *et al.*, 1998; Toker and Macnab, 1997), and possibly also in the C-terminal domain (Mathews *et al.*, 1998). Mutational studies indicate that FliN has relatively small roles in switching and rotation (Irikura *et al.*, 1993; Lloyd *et al.*, 1996); it might have a mainly structural role, and/or could function in flagellar assembly (Vogler *et al.*, 1991). FliG is the rotor protein most involved in rotation (Irikura *et al.*, 1993; Lloyd *et al.*, 1996). The C-terminal domain of FliG, in particular, functions specifically in rotation (Lloyd *et al.*, 1996) and interacts with the stator protein MotA (Zhou *et al.*, 1998a). FliG binds to the protein FliF that forms the MS ring (Oosawa *et al.*, 1994). Difference electron micrographs of basal bodies with or without FliG show that at least part of the protein is near the bottom of the MS ring (Thomas *et al.*, 2001). The precise location of FliG is not known, however.

The switch complex contains many copies of each protein. By quantitative immunoblots and HPLC, each motor is estimated to contain 34 ($\pm$6) FliM molecules and 111 ($\pm$13) FliN molecules (Zhao *et al.*, 1996). Given the 34- or 33-fold symmetry seen in *en face* views of the C ring (Thomas *et al.*, 1999),

it is likely that the actual number of FliM molecules is close to 34, varying slightly from motor to motor. Equilibrium sedimentation experiments with purified switch complex proteins of *T. maritima* give evidence of a stable FliN tetramer and a stable FliM–FliN complex with 1:4 stoichiometry (Brown and Blair, unpublished). This suggests that each motor might contain 136 (4 times 34) copies of FliN. The number of FliG molecules is estimated to be about 44 per motor (Zhao *et al*., 1996), somewhat greater than the number estimated for FliM but probably still consistent with a 1:1 ratio of FliG to FliM, given the uncertainties. FliG binds to FliM (Marykwas and Berg, 1996; Tang *et al*., 1996; Toker and Macnab, 1997), and the simplest hypothesis is that they are present in equal numbers in the motor, about 34 copies each. However, some other data suggest that FliG might be present in fewer copies than FliM. When FliG is linked to FliF by a genetic fusion (recall that FliF forms the MS ring), the basal bodies appear essentially normal and the motors remain able to rotate (Francis *et al*., 1992; Thomas *et al*., 2001). The FliF:FliG ratio should then be 1:1, and by the foregoing reasoning the number of FliF subunits would also be 34. Two estimates of FliF stoichiometry were both in the neighborhood of 26 (Jones *et al*., 1990; Sosinsky *et al*., 1992). Uncertainties in those estimates might be great enough to allow a value of 34. But if the estimate of 26 FliF subunits is accurate, then there must be a mismatch in subunit number somewhere, most likely between FliG and FliM. In an extension of this idea, DeRosier and co-workers propose that multiple symmetries occur in the rotor, and that positions of subunit mismatch on the rotor might form special sites that interact with the stator and function to generate torque (Thomas *et al*., 1999).

The switch complex is so named because certain mutations in the FliG, FliM, and FliN proteins can greatly alter the CW–CCW bias of the motor (Yamaguchi *et al*., 1986b). Certain mutations in the stator proteins can also alter CW–CCW bias, but to a lesser extent (Garza *et al*., 1996). Switching is highly cooperative with respect to the cellular concentration of phospho-CheY, exhibiting a Hill coefficient of about 10 (Cluzel *et al*., 2000). This implies the involvement of many subunits and relatively strong coupling between them. A theory of allosteric transitions within a ring of subunits has been elaborated, and gives some insight into the magnitude of coupling necessary to account for the observed cooperativity (Duke *et al*., 2001).

Given the strong cooperativity (Cluzel *et al*., 2000) and the effects of mutations (Yamaguchi *et al*., 1986b), it seems fairly certain that switching occurs by conformational changes or other movements within the FliG–FliM–FliN complex. These movements in the switch complex most likely alter the rotor–stator interface to reverse the sign of the forces produced there. An alternative formal possibility is that forces at the rotor–stator interface remain the same but the rotor contains machinery that functions, like a reverse gear in a transmission, to reverse the sign of the resulting rotation.

This appears less likely. If switching alters the rotor–stator interface, then it must entail changes in the position or orientation of the C-terminal domain of FliG, the part of the rotor that interacts with the stator. As discussed below, X-ray structures of the C-terminal and middle domains of FliG provide some clues to the molecular basis of switching.

B. Flagellar Motor Physiology

Soon after the discovery that flagella rotate (Berg and Anderson, 1973), Silverman and Simon (1974a) described an experiment in which cells were attached to coverslips by single flagellar filaments and the rotation of individual motors was monitored by the resulting rotation of the cell body. Such "tethered" cells rotate relatively slowly (typically 10 Hz), owing to the large viscous load. Berg showed that the rotation is quite smooth and must therefore occur in relatively small steps (Berg, 1974). Tethered cell assays proved especially informative when joined to means for controlling the membrane proton gradient. Experiments with tethered, artifically energized cells produced the following key observations (Khan and Berg, 1983; Khan *et al.*, 1990; Manson *et al.*, 1980): (1) for a given protonmotive force (Δp), rotation speed varies inversely with the viscosity of the medium, implying constant torque; (2) torque is proportional to Δp, up to at least 150 mV; (3) for a given Δp, torque does not vary significantly with temperature between 5 and 40 $^{\circ}$C; and (4) for a given Δp, torque is the same in D_2O and H_2O.

The lack of any dependence on solvent isotope or temperature indicates that at the low speeds of tethered cells, the motor is not limited by rates of ion transfer, or any thermally promoted chemical or mechanical processes. In this low-speed regimen, speed appears to be determined by the overall energetics of the process rather than kinetic factors. The linear relationship between torque and protonmotive force is most simply explained by saying that slow-turning motors can convert chemical energy into mechanical energy with high efficiency, so that the work done in one revolution (2π times the torque) equals the total energy available from the proton gradient ($e\Delta p$ times the number of protons used per revolution).

The viscous load is smaller when motors turn flagellar filaments (Lowe *et al.*, 1987) or filament stubs attached to small spheres (Chen and Berg, 2000b), and load can also be reduced by application of an external torque (Berg and Turner, 1993; Berry and Berg, 1999; Washizu *et al.*, 1993). The rotation of such lightly loaded motors can be monitored by various light microscopic methods (Chen and Berg, 2000b; Lowe *et al.*, 1987; Magariyama *et al.*, 1994). Such measurements show that when the load is light the motors rotate at 300 Hz or faster, and the speed depends on both temperature and solvent isotope (Chen and Berg, 2000a,b; Lowe *et al.*, 1987). Thus,

when the external load is light the speed of the motor is determined by rates of internal processes, including (but not necessarily restricted to) rates of proton dissociation. Observations on Na^+-driven motors of *Vibrio* provide additional evidence that ion movements are rate limiting when the external load is light. The filaments of Na^+-driven motors have been clocked at 1700 Hz, five times faster than the highest speeds recorded for H^+-driven motors (Magariyama *et al*., 1994). Lithium can substitute for sodium in the *Vibrio* motor; the motor speed in Li^+ is about the same as in Na^+ when the viscous load is heavy but about 4-fold slower when the load is light (Liu *et al*., 1990).

Although the top speed of the *E. coli* motor is evidently limited by one or more proton dissociation processes, this speed does not vary appreciably with external pH in the range of pH 4.7–8.8, even when the load is light (Chen and Berg, 2000a). Such insensitivity to pH is notable, because the relative contributions of $\Delta\psi$ and ΔpH to Δp should vary greatly across this pH range (Slonczewski *et al*., 1981). The *E. coli* motor evidently has features that ensure that the pH gradient and electric–potential gradient are not only equivalent thermodynamically but are nearly equivalent kinetically. The situation may be different in the motors of *Bacillus subtilis* and *Streptococcus* (both gram-positive species), which show a greater dependence on pH (Khan *et al*., 1990; Shioi *et al*., 1980).

The torque-versus-speed characteristic of the motor is of particular interest for understanding the mechanism. Measurements employing electrorotation to control the load showed that the motor torque is approximately constant for speeds up to a particular ''knee'' value, thereafter decreasing approximately linearly to zero (Berg and Turner, 1993). The main features of this torque–speed relationship were subsequently confirmed in experiments that used small beads on flagellar stubs to control the load (Chen and Berg, 2000b) (Fig. 6A). An apparent barrier to backward rotation seen in the electrorotation experiments was later shown to be due to ellipticity in the rotating electric field used (Berry and Berg, 1997, 1999). This influenced only the measurements on cells forced to rotate backwards (i.e., in a direction opposite to the motor torque), and does not alter the shape of the torque–speed relationship measured at positive rotation speeds. As discussed by Berry and Berg (1999), a torque–speed relationship with this shape is indicative of a ''powerstroke'' mechanism in which chemical energy is used directly to drive rotation, and argues persuasively against a ''thermal ratchet'' mechanism in which chemical energy is used to rectify thermally driven movements of motor components (Fig. 6B).

The peripheral location of the MotA–MotB stator complexes suggests that these proteins could be incorporated last into otherwise complete motors. ''Resurrection'' experiments of Berg and co-workers show that this is in fact the case (Blair and Berg, 1988; Block and Berg, 1984). When *motA* or

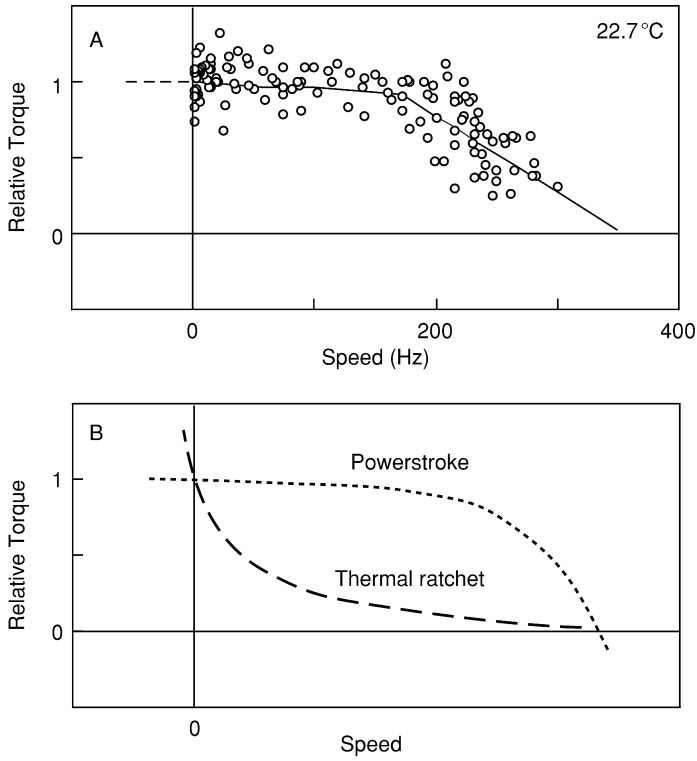

FIG. 6 (A) Torque–speed relation of the flagellar motor of *E. coli*, measured by monitoring the rotation of small beads attached to flagellar stubs (Chen and Berg, 2000b). (From Berg with permission.) Additional measurements using an optical trap (Berry and Berg, 1997) or electrorotation (Berry and Berg, 1999) show that the torque–speed relation continues essentially flat into the region of negative speed, as indicated by the dashed line. (B) Predicted torque–speed relations for a hypothetical motor that utilizes either a powerstroke mechanism in which chemical energy is used to actively drive motion of the rotor, or a thermal ratchet mechanism in which chemical energy is used to bias movements that are driven thermally. The thermal ratchet mechanism predicts a large drop in torque at even relatively low speeds, which is not observed. For a fuller discussion, see Berry and Berg (1999).

motB mutant cells were tethered and wild-type MotA or MotB proteins subsequently expressed from an inducible plasmid, the initially paralyzed cells began to rotate, slowly at first and then accelerating to normal speed in a series of equal steps. As many as eight steps were seen, showing that MotA and MotB are components in several, possibly eight, independent torque-generating units (Blair and Berg, 1988). Sodium-driven motors likewise contain several independent torque generators, as judged by stepwise decreases in torque observed in motors undergoing inhibition by a sodium

channel blocker. In that case, the number of torque generators was estimated to be between five and nine (Muramoto *et al.*, 1994).

More recently, resurrection experiments have been carried out on motors driving a light load (small polystyrene beads) (Ryu *et al.*, 2000). In contrast to tethered cells, which showed equal steps in speed, when the load was light the first torque generator installed in a motor drove rotation at almost its full final speed. This implies that the torque generators have a high duty ratio; that is, they constrain the movement of the rotor most of the time. If a stator complex were disengaged from the rotor for any appreciable time, then additional torque generators in the motor should increase its speed, even under light load.

As noted, a number of observations on tethered cells suggest that the motor has a fixed proton stoichiometry and is capable of converting chemical energy into work with high efficiency provided the speed is low. The measured motor torque can be used to estimate the proton stoichiometry under this assumption of tight coupling, and in any case places a lower bound on the stoichiometry on thermodynamic grounds. Measurements of motor torque vary somewhat, but one measurement that appears reliable is $\sim$290 pN·nm per torque generator, or $\sim$2300 pN·nm for a motor with a full complement of eight torque generators (Ryu *et al.*, 2000). Assuming 100% efficiency and a Δp of 160 mV (Slonczewski *et al.*, 1981), this would require a stoichiometry of about 70 H^+ per revolution for each torque generator, or $\sim$550 H^+ per revolution for the full motor.

The proton flux through the motor has been measured in experiments using *Streptococcus* cells energized with known, experimentally imposed gradients (Meister *et al.*, 1987). Three estimates of stoichiometry were obtained, ranging from 970 to 1450 H^+ per revolution and with an average value of 1140 H^+ per revolution. The measurements were fairly difficult ones and the uncertainties might be great enough to allow a true value of about 550. Proton flux has been measured in only one study and additional measurements would be valuable. Whatever the exact stoichiometry, the total flux of protons through the motor is quite great, about 200,000 H^+/s for a motor driving a light load at room temperature. The Na^+-driven motor of *Vibrio* must use about 1 million ions per second, given its greater speed.

Motor rotation presumably occurs by a sequence of discrete molecular events and should thus occur in steps. Steps in the rotation of tethered cells are difficult to see directly, because the flexible hook and filament act as an elastic damper to smooth the motion. By analyzing fluctuations in the rotation speed of tethered cells, Samuel and Berg showed that if intervals between steps follow a Poisson distribution, then the steps must number about 400 per revolution (Samuel and Berg, 1995). If other variable processes also contribute to the speed fluctuations, the number of steps could be larger; if the steps are clocked (i.e., some mechanism exists to decrease the variance

in step intervals), then the number could be smaller. A similar analysis was done with motors containing only one or a few torque generators, and showed that the individual torque generators step independently (Samuel and Berg, 1996).

C. Mutational Studies of Motor Proteins

Mutational studies have identified a number of important features in the proteins that function in rotation (Fig. 7). Most of the MotB protein is in the periplasm (Chun and Parkinson, 1988), and much of this periplasmic domain is dispensable for function (Muramoto and Macnab, 1998). Certain segments in the MotB periplasmic domain are essential for rotation, and

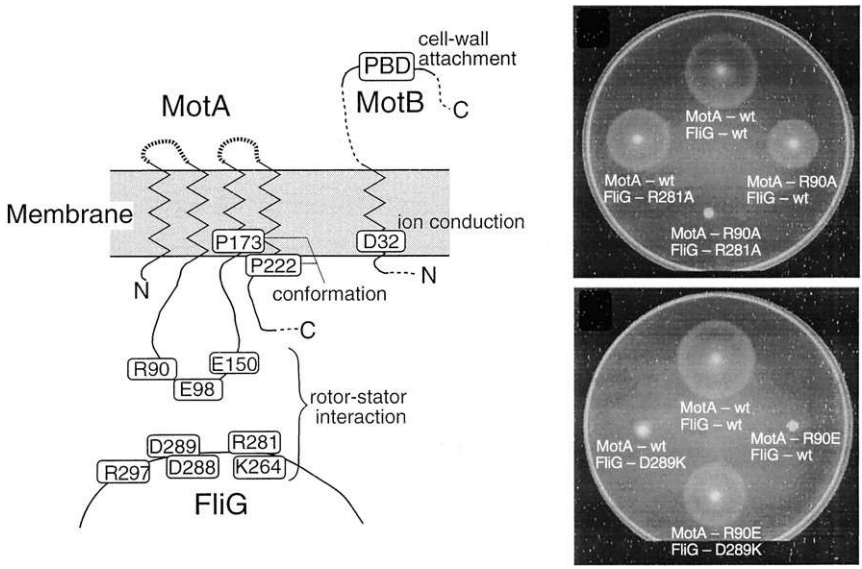

FIG. 7 *Left*: Functionally important elements of motor proteins, identified in mutational studies. Specific roles of residues are indicated where a probable assignment can be made. The periplasmic segments of MotA (thick dashed lines) do not have conserved critical residues but contain titratable residues that might function collectively to buffer the entrance of the channel. Thin dashed segments in MotA and MotB are the parts found dispensable for rotation in a study of 10-residue deletions (Muramoto and Macnab, 1998). PBD, peptidoglycan-binding domain. *Right*: Examples of synergism and suppression seen in FliG–MotA double mutants, demonstrating specific interactions between charged groups on the rotor and stator. Shown are soft agar plates, on which motile strains move out from the point of inoculation to form circular swarms while nonmotile (or nonchemotactic) strains form small, dense colonies. For additional examples and a summary of rotor–stator interactions most important for function, see Zhou *et al.* (1998a).

probably function to attach the stator to the peptidoglycan (Blair *et al.*, 1991; Chun and Parkinson, 1988; DeMot and Vanderleyden, 1994; Muramoto and Macnab, 1998). Some mutations in MotB appear to disrupt function by shifting the stator so that it is misaligned relative to the rotor, and certain of these can be suppressed by mutations in FliG or MotA (Garza *et al.*, 1996).

Many randomly generated mutations in MotA and MotB are found in the membrane segments, as might be expected for components in an ion-conducting complex (Blair and Berg, 1991; Blair *et al.*, 1991; Togashi *et al.*, 1997). A conserved aspartate residue near the inner end of the MotB membrane segment, Asp-32, is essential for rotation and likely functions directly in proton movement through the motor (Zhou *et al.*, 1998b). Tryptophan-scanning mutagenesis of the MotA membrane segments identified helix faces tolerant of bulky replacements, and showed that segments 1 and 2 are probably more exposed to lipid than segments 3 and 4 (Sharp *et al.*, 1995a). Mutational results were initially interpreted under the assumption that the complex contains a single copy of each protein. The complex is now known to contain multiple copies of MotA and MotB (Braun and Blair, 2001; Sato and Homma, 2000a,b), and some tryptophan-scanning results are reinterpreted below under this assumption of multiple subunits.

Much of MotA is in the cytoplasm, and this part of the protein is also important for rotation as judged by the occurrence of point mutations that disrupt function (Zhou and Blair, 1997). The cytoplasmic domain of MotA contains two conserved charge residues (Arg-90 and Glu-98) that are important for motor rotation in *E. coli*, and a third (Glu-150) that appears somewhat important (Zhou and Blair, 1997). These residues function collectively, with no single one critical, and charge is their essential property. Two proline residues near the inner ends of membrane segments 3 and 4 of MotA, Pro-173 and Pro-222, are also conserved and important for rotation (Braun *et al.*, 1999). These might regulate the conformation of the MotA–MotB complex, and/or control conformational changes.

Like the cytoplasmic domain of MotA, the C-terminal domain of FliG also contains conserved charged residues that are collectively important for rotation but not critical individually (Lloyd and Blair, 1997). Certain combinations of MotA mutations with FliG mutations show strong synergism or suppression, in a pattern that indicates that the charged groups of MotA interact with those of FliG (Zhou *et al.*, 1998a) (Fig. 7). Electrostatic interactions between the rotor and stator are thus essential for rotation of the *E. coli* motor. The role of these electrostatic interactions is not known. They might function to couple movements in the stator to rotation of the rotor, or to synchronize events in the stator and rotor. Because no single charged group at the MotA–FliG interface is critical for rotation, it seems unlikely that these interface residues form the pathway for protons energizing the motor (Zhou *et al.*, 1998a). The resiliency of this part of MotA (and

the unlikelihood that it functions directly in proton conduction) is further demonstrated by a mutational study of PomA, the ortholog of MotA found in the Na^+-driven motor of *Vibrio*. Two of the three charged residues implicated in rotation were mutated in this study. The residues previously found to be important in MotA were also the ones most sensitive to mutation in PomA, but for a given mutation the motility defects were less severe in PomA (Yorimitsu *et al.*, 2002). PomA might contain additional residues that contribute to rotor–stator interactions, or these interactions might be less important for function in the *Vibrio* motor.

As noted, FliG does not appear to contain essential binding sites for protons energizing the motor. Mutational studies of FliM and FliN likewise found no protonatable residues, acidic or basic, that are singly critical. Among protonatable residues, only Asp-32 in MotB appears critical. Replacement of Asp-32 with glutamate gave poorly functioning motors, and replacement with other residues stopped rotation altogether (Zhou *et al.*, 1998b). Proton conduction can be roughly assayed by a growth impairment that occurs as a result of proton leakage through overexpressed proteins (Blair and Berg, 1990); mutations in Asp-32 also blocked proton flow in this assay (Zhou *et al.*, 1998b).

If the proton pathway is formed by protonatable side chains of amino acid residues, the mutational results imply that the proton pathway is contained within the stator and includes residue Asp-32 of MotB. This residue is near the inner end of the MotB membrane segment, close to the cytoplasmic side of the membrane. The aspartate residue is conserved in the PomB protein of *Vibrio* (Asai *et al.*, 1997), and could therefore function as the ion-binding site in Na^+-type motors also. In *Vibrio*, elevated levels of cytoplasmic Na^+ inhibited rotation in the way expected for titration of an interior-facing Na^+-binding site, with an apparent dissociation constant of $\sim$50 m*M* (Yoshida *et al.*, 1990). As noted above, Na^+-type motors are specifically inhibited by sodium channel blockers such as phenamil. The phanamil-binding site also appears to be near the inner mouth of the channel: mutations that confer resistance to phenamil were found in PomA in residue 148, near the inner end of membrane segment 3, and in PomB near the critical Asp-24 residue (Jaques *et al.*, 1999; Kojima *et al.*, 1999).

Other ion-binding sites might exist in the motor, but at positions that are not conserved between species. Sequence alignments show that titratable groups are essentially absent from the membrane-embedded segments of MotA and MotB, but are fairly abundant in the short periplasmic segments of MotA and in the segment of MotB just exterior to the membrane. Titratable groups in these segments might buffer the entrance to the channel and facilitate the collection of protons at the rapid rates needed. Mutation of a glutamate residue near the entrance to the MotA channel gave a severe motility defect (Blair and Berg, 1990, 1991), and mutation of an aspartate

residue near the entrance to the PomA channel reduced the motor speed and altered its dependence on Na^+ concentration (Kojima *et al.*, 2000).

D. X-Ray Structure of a Rotor Protein

Efforts at X-ray structure determination were focused on the C-terminal domain of FliG, dubbed FliG-C, because this domain interacts with the stator and functions specifically in rotation. Full-length FliG and FliG-C from *E. coli* failed to crystallize, but FliG-C from the thermophilic bacterium *Thermotoga maritima* yielded crystals that diffracted to 2.4-Å resolution (Lloyd *et al.*, 1999). FliG-C is a compact domain formed mainly from α helices. The functionally important charged residues are found clustered together along a prominent ridge on the protein. On the basis of the mutational studies just described, it was proposed that this ridge is directed toward the stator to allow electrostatic interaction with the charged groups on MotA, and that switching might involve movements of this domain relative to the stator (Lloyd *et al.*, 1999).

The structural study was extended more recently to a larger FliG construct encompassing both the middle and C-terminal domains (FliG-MC), giving further insights into the organization of FliG molecules in the flagellum (Brown *et al.*, 2002). The FliG-MC protein consists of two compact, mainly helical domains connected by an α helix and a linker that includes two consecutive glycine residues (Fig. 8). FliG is known to bind to FliM, and mutations in FliG that affect this binding are found both in the middle domain and in the C-terminal domain on a face opposite the charged ridge (Marykwas and Berg, 1996). It was proposed that FliM binds to both the middle and C-terminal domains of FliG, and thereby dictates the relative orientation of these domains in the flagellum. CW–CCW switching might occur by movement of the C-terminal domain of FliG relative to the rest of FliG, under the control of FliM, with the Gly–Gly linker serving as a hinge. Manson and co-workers found that replacing one of the linker glycine residues with serine gave motors that could still rotate in either direction, but reversed less frequently than normal (Garza *et al.*, 1996).

E. Biochemical Studies of the Stator Complex

There are presently no high-resolution structural data on the MotA–MotB complexes. The membrane topologies of the Mot proteins are known (Chun and Parkinson, 1988; Zhou *et al.*, 1995) (Fig. 7). By a combination of gel-filtration chromatography and quantification of bands on Coommassie-stained gels, Sato and Homma (2000a) obtained evidence that the complex

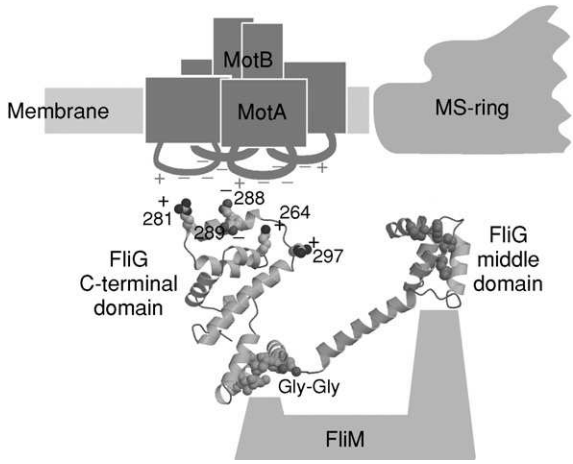

FIG. 8 Structure of FliG-MC (the middle and C-terminal domains of the rotor protein FliG) from *Thermotoga maritima*, and hypothesis for the position and orientation of FliG-MC in the flagellar motor. A single molecule is shown, but a motor actually contains many copies of FliG. The charge-bearing ridge on the C-terminal domain is hypothesized to interact with charged residues in the cytoplasmic domain of MotA. Residue numbers shown pertain to the *E. coli* protein. FliM binds to both the middle and C-terminal domains, possibly via a conserved surface-exposed sequence in the middle domain (residues EHPQ; pink) and a conserved hydrophobic patch on the C-terminal domain (green). A flexible linker between the domains might allow interdomain movements associated with CW–CCW switching. Determinants for binding to the MS ring are in an N-terminal domain of FliG, whose structure is not yet known. (Adapted from Brown *et al*., 2002.) (See also color insert.)

contains four copies of MotA and two copies of MotB. A targeted disulfide-cross-linking study gave evidence of two MotB molecules in the complex (Braun and Blair, 2001), and further cross-linking studies underway (Braun, Al-Mawsawi, and Blair, unpublished data) indicate that the complex contains at least four copies of MotA.

The PomA–PomB complex has been purified and shown to promote transmembrane Na^+ movement when reconstituted into proteoliposomes (Sato and Homma, 2000a). The Na^+ flux was less than it must be in the flagellar motor (on the order of 10 ions per second per channel), but nevertheless appears to reflect bona fide channel action, as it was inhibited in the expected ways by a sodium channel blocker or by Li^+. Full channel function might require the additional presence of MotX and MotY, outer membrane proteins that are essential for rotation of the Na^+ motor in *Vibrio* (McCarter, 1994a,b; Okabe *et al*., 2002).

Given the stoichiometry $MotA_4MotB_2$ (or $PomA_4PomB_2$), the complex should have a total of 18 membrane segments. Targeted cross-linking studies

underway are providing an initial picture of their organization (Fig. 9). A symmetric dimer of MotB segments is at the center of the complex (Braun and Blair, 2001). Segments 3 and 4 of four MotA molecules are arranged in an inner layer around the MotB segments, and segments 1 and 2 are probably on the outside, farther from MotB. This arrangement is consistent with tryptophan-scanning studies that showed that segments 3 and 4 are constrained by neighboring segments, whereas segments 1 and 2 are relatively unconstrained (Sharp *et al.*, 1995a). Segments 3 and 4 of MotA, and the MotB segments, appear most important for forming the proton channel(s). Few titratable groups are found in the residues that line the putative channel(s), which suggests that protons move from the periplasm to Asp-32 along a path formed mainly by water molecules.

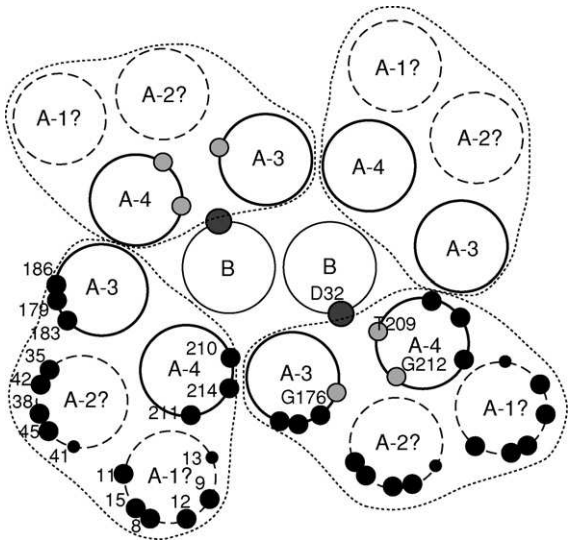

FIG. 9 Hypothesis for the arrangement of membrane segments in the $MotA_4MotB_2$ complex, as deduced from targeted disulfide cross-linking studies. The view is from the periplasmic side of the membrane. Dashed lines enclose the four segments within each MotA subunit. The arrangement pictured is for the inner (cytoplasmic) halves of the membrane segments, for which the most cross-linking data are available. The Asp-32 residues of the two MotB molecules (large gray circles) are widely separated and most likely function in two distinct proton channels, indicated by cross-hatching (Braun and Blair, 2001). Three other conserved residues that might face into the channel(s) are indicated (smaller gray circles). MotA segments 1 and 2 are somewhere around the outside of the complex, but their precise arrangement is not yet known. Black circles indicate positions in the MotA segments where tryptophan replacements were tolerated either fully (large balck circles) or partially (small black circles) (Sharp *et al.*, 1995a). In the MotB segment, Trp was not tolerated at positions in the inner half of the MotB segment (pertinent to the model pictured), but was tolerated at most positions in the outer half (not shown) (Sharp *et al.*, 1995b).

In the structural model that emerges from the cross-linking experiments, the two MotB segments are oriented so that their critical Asp-32 residues are widely separated from each other (Fig. 9). This suggests that they function in two distinct channels rather than a single central channel. A twin-barrel channel also fits with energy considerations outlined above. Each generator produces a torque that would require about 70 protons per revolution, whereas the motor contains in the neighborhood of 34 copies of FliG (possibly as few as 26, but probably not more than 50). The measured torque is thus close to what is expected if two protons pass through a torque generator each time it moves past an FliG subunit. A similar computation of the needed H^+ stoichiometry was made previously by Block and Berg, and they arrived at a similar estimate, 65 H^+ per torque generator per revolution (Block and Berg, 1984). Kinetic properties of the motor give additional evidence for a twin-barrel torque generator: the torque–speed relation is best accounted for by assuming that the motor utilizes the energy of two protons simultaneously (Berry and Berg, 1999). It is also worth noting that in simulations of an electrostatic model for the motor, Walz and Caplan (2000) could reproduce measured motor torque only by assuming 22 channels per motor, even more than assumed here.

The structure and mechanism of the stator complexes must be similar in proton-driven and sodium-driven motors, because the rotor of the proton type can be made to work with the stator of the sodium type, and vice versa (Asai *et al.*, 1999; Gosink and Hase, 2000). Chimeric proteins with membrane segments derived from a proton-type stator (of either *E. coli* or *R. sphaeroides*) can function with Na^+ ions, which implies that the main determinants of Na^+ specificity are not in the membrane segments (Asai *et al.*, 1999, 2000). The periplasmic domain of PomB, however, is required for Na^+-driven rotation in *Vibrio* cells. This domain might interact with the outer membrane proteins MotX and MotY, mentioned above. The roles of MotX and MotY are not known, but one possibility is that they conduct Na^+ ions across the outer membrane and deliver them to the PomA–PomB complex. The requirement for MotX and MotY appears specific to *Vibrio* cells, because when the *E. coli* motor is made to work with Na^+ ions (by use of a MotB–PomB chimera) MotX and MotY are not required for rotation (Asai *et al.*, 2003).

The presence of two MotB molecules per stator complex might reconcile an apparent discrepancy between the number of torque generators seen in torque restoration experiments (8) (Blair and Berg, 1988) and the number of particles seen in freeze-fracture images (10–12 in *E. coli* and as many as 16 in other species) (Coulton and Murray, 1978; Khan *et al.*, 1988). If the particles seen in freeze-fracture correspond mainly to the periplasmic domains of MotB molecules, then each torque generator could contribute two particles. In *E. coli* membranes the rings do not contain more than 12 particles, whereas

16 might be expected in a motor with a full complement of torque generators. Torque measurements on populations of wild-type cells indicated that motors do not typically contain a full complement of eight generators (Blair and Berg, 1988). Also, if any particles are displaced from the ring during sample preparation they would not be included in the count.

Given the absence of critical titratable groups on the rotor, proton movement must be coupled to rotor movement by some means other than direct binding. An obvious possibility is that proton association/dissociation at Asp-32 drives conformational changes in the stator that apply force to the rotor. To look for conformational changes in the stator, we examined the protease susceptibility of MotA in complex with either wild-type MotB or MotB with various replacements of Asp-32 (Kojima and Blair, 2001). Replacement of Asp-32 by asparagine, or by any other small uncharged amino acid, caused a conformational change in MotA that could be detected as a change in protease susceptibility. The sites of altered protease cleavage were in the cytoplasmic domain of MotA, in positions not far from the residues that interact with the rotor. These results support the proposal that protonation of Asp-32 causes a conformational change in the stator, in a part that interacts with the rotor.

IV. Models for the Rotation Mechanism

Many models have been proposed for the mechanism of the flagellar motor, and several have been elaborated in quantitative detail. None of the detailed models yet published fully accounts for present data on the motor. Most were developed before much molecular data were available, and some of the models were parameterized on the basis of physiological data that later proved inaccurate. Models have nevertheless provided some stimulus to thinking and experiments on the motor, and we review the more influential models here, outlining the major features that distinguish each. Models have been discussed in fuller detail by Berg and Turner (1993), Berry (2000), Berry and Armitage (1999), and Caplan and Kara-Ivanov (1993).

Some of the models invoke unusual physical phenomena such as Quincke rotation (Fuhr and Hagedorn, 1989) or ultrasonic oscillations (Atsumi, 2001), which, while interesting, appear to us unlikely to play a role in a biochemical system such as the flagellar motor. We discuss only models that utilize processes more familiar, or at least plausible, in the context of proteins and membranes. Five such models are diagrammed in Fig. 10. Each of the models involves a circular rotor interacting with one or more stator elements. The models differ in various details of geometry and in the mechanisms by which force is generated at the rotor–stator interface.

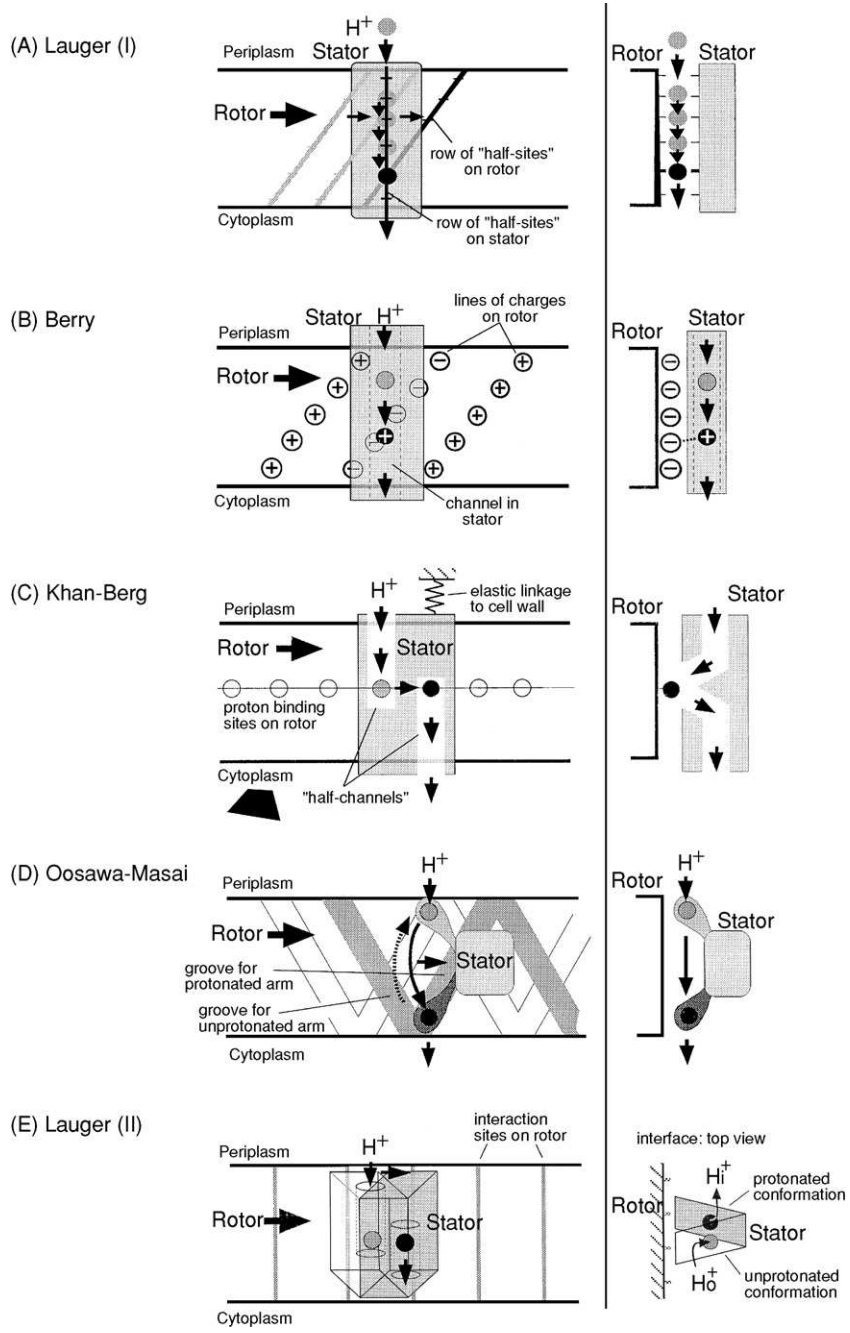
(A) Lauger (I)
H+
Periplasm
Stator
Rotor
row of "half-sites" on rotor
Cytoplasm
row of "half-sites" on stator
Rotor
Stator
(B) Berry
Stator
H+
lines of charges on rotor
Periplasm
Rotor
Cytoplasm
channel in stator
Rotor
Stator
(C) Khan-Berg
H+
elastic linkage to cell wall
Periplasm
Rotor
Stator
proton binding sites on rotor
Cytoplasm
"half-channels"
Rotor
Stator
(D) Oosawa-Masai
H+
Periplasm
Rotor
Stator
groove for protonated arm
groove for unprotonated arm
Cytoplasm
Rotor
H+
Stator
(E) Lauger (II)
interaction sites on rotor
Periplasm
H+
Rotor
Stator
Cytoplasm
interface: top view
Hi+
protonated conformation
Rotor
Stator
Ho+
unprotonated conformation

In an early proposal by Läuger (1977), the rotor and stator each contain rows of chemical groups (termed "half-sites") that are individually unable to bind protons, but that can bind a proton when a pair are brought together (model A in Fig. 10). The rows on the rotor and stator are apposed, and are tilted relative to each other so that they intersect at a single point, forming no more than one proton-binding site at a time. As the rotor turns, the point of intersection will move across the membrane, and if protons are constrained to move only between binding sites formed at the point of intersection, proton flow will be coupled to rotation. Switching of direction is achieved by a conformational change that reverses the tilt angle of the rows on the rotor, so that inward movement of the sites of intersection would correspond to rotation in the opposite direction. The mechanism allows some rotor movements unlinked to proton flow, and so is not tightly coupled. In the original version of the model the S ring was assumed to be the stator, but later versions were amended to allow the MotA–MotB complexes to function in this role (Kleutsch and Lauger, 1990; Lauger, 1988). Later versions also explicitly included an elastic linkage between the stator complexes and the cell wall, to allow the complexes to function independently.

Berry (1993) proposed a model in which protons move through a channel in the stator, and interact electrostatically with tilted rows of charged groups on the rotor to generate torque (Fig. 10, model B). The electrostatic interactions responsible for coupling occur over an appreciable distance, and the model predicts a significant leakage flux. The model postulates alternating rows of positive and negative charge on the rotor, and these form the basis for an innovative proposal for CW–CCW switching: direction change is assumed to involve a change in proton affinity (pK_a) of proton-binding groups in the stator, shifting them from a mostly deprotonated state to a mostly protonated state. When most sites in the channel are deprotonated, the proton current corresponds to a small number of protonated, inward-moving sites. When most sites are protonated, the proton current consists of a small number of "holes" that move outward and have relative charge of -1. Inward-moving protons would interact with the rows of negative charge to drive rotation in one direction, and outward-moving "holes" would interact with rows of positive charge to drive rotation the other way.

FIG. 10 Major classes of hypotheses for the rotation mechanism. All models envisage a circular rotor surrounded by multiple stator complexes. For all the models, the diagrams show just a single stator complex. *Left*: Views of the rotor edge, looking inward through the stator complex. *Right*: Tangential views of the rotor–stator interface, or (model E only) a top view of the interface. Black circles indicate the current position of a proton, and gray circles indicate a previous position(s). Protons flow from the periplasm to the cytoplasm (top to bottom in the diagrams) and, in the left-hand panels, the rotor moves from left to right. For more detailed explanations of the models, see text.

Refined versions of Berry's electrostatic model were elaborated by Elston and Oster (1997) and Walz and Caplan (2000). In the version of Elston and Oster, the stator is assumed to contain multiple, negatively charged proton-binding sites, and the charges on the rotor are assumed positive. The model predicts significant leakage flux and thus is not tightly coupled. Switching is by a mechanism analogous to Lauger's, involving a conformational change in the rotor that reverses the angle of the charged-group rows. An important feature of the analysis is the use of continuous mechanical variables and the applicable equations of motion (either Fokker-Planck or Langevin equations), rather than first-order transitions among discrete states, as is usually assumed. Although some features of the model do not match our current knowledge of the motor, this analytical approach might be fruitfully applied to more accurate modeling efforts once sufficient structural data are available.

Walz and Caplan (2000) undertook a detailed quantitative analysis of their model and showed that a single parameter set could account for the diverse physiological data then available. Unfortunately, some of the data used to describe the torque–speed relationship proved to be inaccurate (Berry and Berg, 1999). The electrostic interactions between rotor and stator were assumed sufficiently strong to give nearly tight coupling, in contrast to the other electrostatic models with similar geometry. As in the model of Elston and Oster, switching is assumed to occur by a conformational change in the rotor that reverses the angle of the charged-group arrays.

A model with quite different geometry was proposed by Khan and Berg (1983) and analyzed quantitatively by Meister *et al.* (1989) (Fig. 10, model C). The proton pathway consists mainly of two channels in the stator complex, each spanning about half the membrane thickness and offset in the middle so that the proton pathway is discontinuous. At the offset position, the half-channels contact a row of proton-binding sites on the rotor. A proton entering through the outer half-channel is deposited onto one of these sites on the rotor, and movement of the rotor carries it to the inner half-channel to allow its release into the cytosol. The motor is assumed to function as a "thermal ratchet": relative movement of the rotor and stator is driven thermally, but is constrained by rules relating to the proton occupancy of the sites on the rotor. Switching would occur by appropriate changes in these rules, possibly involving a conformational change in the rotor that brings a different set of binding sites into play. The stator complexes are assumed to attach to the cell wall by elastic linkages to allow independent function. If the constraints on rotor movement are sufficiently strict, then such a thermal ratchet mechanism can give tight coupling and would produce high torque at stall. The mechanism predicts a steep decrease in torque as the speed increases from zero, which is contrary to observation (Berry and Berg, 1999) (Fig. 6).

Oosawa and co-workers (Oosawa and Hayashi, 1986; Oosawa and Masai, 1982) proposed that rotation is driven by fairly large swinging movements in

a part of the stator that bridges to the rotor (Fig. 10, model D). The cross-bridge contains a proton-binding site that is exposed alternately to the periplasm and the cytosol. The rotor contains two sets of grooves, tilted in opposite directions, which interact preferentially with either the protonated or deprotonated state of the cross-bridge. The presence of a proton gradient will make the cross-bridges more protonated, on average, when moving inward than when moving outward. The cross-bridges will therefore tend to trace a zigzag path on the rotor, producing rotation. The model is of the loosely coupled type, as it predicts significant flux unliked to rotation.

In addition to the "proton turbine" model above, Lauger and co-workers proposed a model based on conformational transitions in the stator (Lauger, 1988) (Fig. 10, model E). The proton pathway is assumed to lie within the stator, and to include a proton-binding site that regulates conformational changes. Protonation of the site causes the stator to attach to the rotor and undergo a conformational change that pushes the rotor through some angle. The conformational change also exposes the site to the inside, allowing the proton to dissociate to the cytosol. After dissociation of the proton, the stator detaches from the rotor and returns to its starting position. Switching could occur by conformational changes in the rotor that alter its model of interaction with the stator (e.g., altering the timing of attachment/detachment), so that the movements in the stator drive movement in the opposite direction.

Models A and C involve essential proton-binding groups on the rotor, and so appear unlikely given the mutational results identifying Asp-32 as the only essential titratable residue. Model C is ruled out also by the torque–speed characteristic, which indicates a powerstroke rather than a thermal ratchet mechanism. Model B and its variants involve multiple proton-binding sites in the stator, and so are also ruled out by the finding of only a single critical proton-binding group. Biochemical studies provide evidence for conformational changes in the stator, but these appear to involve movements in the cytoplasmic domain, and appear unlikely to involve large transmembrane movements of the type envisioned in model D. Also, model D is loosely coupled whereas substantial evidence points to tight coupling. Model E has many features consistent with the available data. A minor shortcoming is that it includes states in which the rotor and stator do not interact, whereas experiments (Ryu *et al.*, 2000) and theoretical considerations (Berg, 2003) indicate that the rotor and stator must remain engaged most of the time.

V. Conclusion

The most pressing need at present is for more data on the structures and arrangement of flagellar proteins. Structures of the stator in both its unprotonated and protonated (or appropriately mutated) forms are needed

for understanding the mechanisms of ion movement and the protonation-linked conformational change. Structural information on the rotor in both its CW and CCW states will be essential for understanding torque production and direction switching. Structures of the export apparatus components, and a picture of their organization, is needed to understand flagellar assembly and the related process of virulence factor export in pathogens. Some of this structural data may be slow in coming, as several key components are membrane proteins, and most occur as components in large multiprotein complexes and might behave well only within that context.

Even in the absence of much structural knowledge, we can make a fairly specific proposal for the rotation mechanism. Given the physiological evidence for a powerstroke (Berg and Turner, 1993; Berry and Berg, 1999) and biochemical evidence for a conformational change in the stator (Kojima and Blair, 2001), we think it likely that rotation is driven by conformational changes in the stator, which occur as protons bind to and dissociate from Asp-32 of MotB. These conformational changes would apply force to the rotor, most likely on FliG, and would also gate access to the Asp-32 site so that protons entered the site from the periplasm and departed to the cytosol. The effect of the conformational change upon the rotor (the resultant direction of the push) would be determined by the types of interaction occurring at the rotor–stator interface, and switching could occur by changes at this interface. To account for the high duty ratio, the stator would have to remain engaged with the rotor in both (or all) of its conformations. For simple diagrams of such a mechanism see Braun *et al.* (1999), and Kojima and Blair (2001).

Acknowledgments

Work in our laboratory has been supported by grants from the National Science Foundation, the National Institutes of Health, the Japan Society for the Promotion of Science, and the University of Utah. Portions of this review are adapted from a previously published minireview entitled "Flagellar Movement Linked to Proton Translocation."

References

Adler, J., and Templeton, B. (1967). The effect of environmental conditions on the motility of *Escherichia coli*. *J. Gen. Microbiol.* **46,** 175–184.

Aizawa, S.-I. (2000). Flagella. *In* "Encyclopedia of Microbiology," 2nd Ed., pp. 380–389. Academic Press, San Diego, CA.

Aizawa, S.-I., Dean, G. E., Jones, C. J., Macnab, R. M., and Yamaguchi, S. (1985). Purification and characterization of flagellar hook-basal body complex of *Salmonella typhimurium*. *J. Bacteriol.* **161,** 836–849.

Amsler, C. D., Cho, M., and Matsumura, P. (1993). Multiple factors underlying the maximum motility of *Escherichia coli* as cultures enter post-exponential growth. *J. Bacteriol.* **175,** 6238–6244.

Armitage, J. P., and Schmitt, R. (1997). Bacterial chemotaxis: *Rhodobacter sphaeroides* and *Sinorhizobium meliloti*—variations on a theme? *Microbiology* **143,** 367–3682.

Asai, Y., Kojima, S., Kato, H., Nishioka, N., Kawagishi, I., and Homma, M. (1997). Putative channel components for a fast-rotating sodium-driven flagellar motor of a marine bacterium. *J. Bacteriol.* **179,** 5104–5110.

Asai, Y., Kawagishi, I., Sockett, R. E., and Homma, M. (1999). Hybrid motor with H^+ and Na^+-driven components can rotate *Vibrio* polar flagella by using Na^+ ions. *J. Bacteriol.* **181,** 6332–6338.

Asai, Y., Kawagishi, K., Sockett, R. E., and Homma, M. (2000). Coupling ion specificity of chimeras between H^+- and Na^+-driven motor proteins, MotB and PomB, in *Vibrio* polar flagella. *EMBO J.* **19,** 3639–3648.

Asai, Y., Yakushi, T., Kawagishi, I., and Homma, M. (2003). Ion-coupling determinants of Na^+-driven and H^+-driven flagellar motors. *J. Mol. Biol.* **327,** 453–463.

Atsumi, T. (2001). An ultrasonic motor model for bacterial flagellar motors. *J. Theor. Biol.* **213,** 31–51.

Auvray, F., Ozin, A. J., Claret, L., and Hughes, C. (2002). Intrinsic membrane targeting of the flagellar export ATPase FliI: Interaction with acidic phospholipids and FliH. *J. Mol. Biol.* **318,** 941–950.

Bennett, J. C. Q., and Hughes, C. (2000). From flagellum assembly to virulence: The extended family of type III export chaperones. *Trends Microbiol.* **8,** 202–204.

Bennett, J. C. Q., and Hughes, C. (2001). Substrate complexes and domain organization of the *Salmonella* flagellar export chaperones FlgN and FliT. *Mol. Microbiol.* **39,** 781–791.

Berg, H., and Brown, D. (1972). Chemotaxis in *Escherichia coli* analysed by three-dimensional tracking. *Nature* **239,** 500–504.

Berg, H. C. (1974). Dynamic properties of bacterial flagellar motors. *Nature* **249,** 77–79.

Berg, H. C. (2003). The rotary motor of bacterial flagella. *Annu. Rev. Biochem.* **72,** 19–54.

Berg, H. C., and Anderson, R. A. (1973). Bacteria swim by rotating their flagellar filaments. *Nature* **245,** 380–382.

Berg, H. C., and Turner, L. (1993). Torque generated by the flagellar motor of *Escherichia coli.*. *Biophys. J.* **65,** 2201–2216.

Berry, R. M. (1993). Torque and switching in the bacterial flagellar motor: An electrostatic model. *Biophys. J.* **64,** 961–973.

Berry, R. M. (2000). Theories of rotary motors. *Philos. Trans. R. Soc. Lond. B Biol. Sci.* **355,** 503–509.

Berry, R. M., and Armitage, J. P. (1999). The bacterial flagella motor. *Adv. Microb. Physiol.* **41,** 291–337.

Berry, R. M., and Berg, H. C. (1997). Absence of a barrier to backwards rotation of the bacterial flagellar motor demonstrated with optical tweezers. *Proc. Natl. Acad. Sci. USA* **94,** 14433–14437.

Berry, R. M., and Berg, H. C. (1999). Torque generated by the flagellar motor of *Escherichia coli* while driven backward. *Biophys. J.* **76,** 580–587.

Bertin, P., Terao, E., Lee, E. H., Lejeune, P., Colson, C., Danchin, A., and Collatz, E. (1994). The H-NS protein is involved in the biogenesis of flagella in *Escherichia coli*. *J. Bacteriol.* **176,** 5537–5540.

Blair, D. F., and Berg, H. C. (1988). Restoration of torque in defective flagellar motors. *Science* **242,** 1678–1681.

Blair, D. F., and Berg, H. C. (1990). The MotA protein of *E. coli* is a proton-conducting component of the flagellar motor. *Cell* **60,** 439–449.

Blair, D. F., and Berg, H. C. (1991). Mutations in the MotA protein of *Escherichia coli* reveal domains critical for proton conduction. *J. Mol. Biol.* **221,** 1433–1442.

Blair, D. F., Kim, D. Y., and Berg, H. C. (1991). Mutant MotB proteins in *Escherichia coli*. *J. Bacteriol.* **173,** 4049–4055.

Block, S. M., and Berg, H. C. (1984). Successive incorporation of force-generating units in the bacterial rotary motor. *Nature* **309,** 470–472.

Bonifield, H. R., Yamaguchi, S., and Hughes, K. T. (2000). The flagellar hook protein, FlgE, of *Salmonella enterica* serovar *Typhimurium* is posttranscriptionally regulated in response to the stage of flagellar assembly. *J. Bacteriol.* **182,** 4044–4050.

Braun, T. F., and Blair, D. F. (2001). Targeted disulfide cross-linking of the MotB protein of *Escherichia coli*: Evidence for two H^+ channels in the stator complex. *Biochemistry* **40,** 13051–13059.

Braun, T. F., Poulson, S., Gully, J. B., Empey, J. C., Van Way, S., Putnam, A., and Blair, D. F. (1999). Function of proline residues of MotA in torque generation by the flagellar motor of *Escherichia coli*. *J. Bacteriol.* **181,** 3542–3551.

Bren, A., and Eisenbach, M. (1998). The N terminus of the flagellar switch protein, FliM, is the binding domain for the chemotactic response regulator, CheY. *J. Mol. Biol.* **278,** 507–514.

Brown, D. A., and Berg, H. C. (1974). Temporal stimulation of chemotaxis in *Escherichia coli*. *Proc. Natl. Acad. Sci. USA* **71,** 1388–1392.

Brown, P. N., Hill, C. P., and Blair, D. F. (2002). Crystal structure of the middle and C-terminal domains of the flagellar rotor protein FliG. *EMBO J.* **21,** 3225–3234.

Calladine, C. R. (1978). Change of waveform in bacterial flagella: The role of mechanics at the molecular level. *J. Mol. Biol.* **118,** 457–479.

Caplan, S. R., and Kara-Ivanov, M. (1993). The bacterial flagellar motor. *Int. Rev. Cytol.* **147,** 97–164.

Chen, X., and Berg, H. C. (2000a). Solvent-isotope and pH effects on flagellar rotation in *Escherichia coli*. *Biophys. J.* **78,** 2280–2284.

Chen, X., and Berg, H. C. (2000b). Torque–speed relationship of the flagellar rotary motor of *Escherichia coli*. *Biophys. J.* **78,** 1036–1041.

Chilcott, G. S., and Hughes, K. T. (2000). Coupling of flagellar gene expression to flagellar assembly in *Salmonella enterica* serovar *Typhimurium* and *Escherichia coli*. *Microbiol. Mol. Biol. Rev.* **64,** 694–708.

Chun, S. Y., and Parkinson, J. S. (1988). Bacterial motility: Membrane topology of the *Escherichia coli* MotB protein. *Science* **239,** 276–278.

Cluzel, P., Surette, M., and Leibler, S. (2000). An ultrasensitive bacterial motor revealed by monitoring signaling proteins in single cells. *Science* **287,** 1652–1655.

Coulton, J. W., and Murray, R. G. E. (1978). Cell envelope associations of *Aquaspirillum serpens* flagella. *J. Bacteriol.* **136,** 1037–1049.

Dailey, F. E., and Berg, H. C. (1993). Mutants in disulfide bond formation that disrupt flagellar assembly in *Escherichia coli*. *Proc. Natl. Acad. Sci. USA* **90,** 1043–1047.

Dean, G. E., Macnab, R. M., Stader, J., Matsumura, P., and Burke, C. (1984). Gene sequence and predicted amino-acid sequence of the MotA protein, a membrane-associated protein required for flagellar rotation in *Escherichia coli*. *J. Bacteriol.* **143,** 991–999.

DeMot, R., and Vanderleyden, J. (1994). The C-terminal sequence conservation between OmpA-related outer membrane proteins and MotB suggests a common function in both gram-positive and gram-negative bacteria, possibly in the interaction of these domains with peptidoglycan. *Mol. Microbiol.* **12,** 333–334.

DePamphilis, M. L., and Adler, J. (1971). Fine structure and isolation of the hook-basal body complex of flagella from *Escherichia coli* and *Bacillus subtilis*. *J. Bacteriol.* **105,** 384–395.

Duke, T. A. J., LeNovere, N., and Bray, D. (2001). Conformational spread in a ring of proteins: A stochastic approach to allostery. *J. Mol. Biol.* **308,** 541–553.

Eberl, L., Christiansen, G., Molin, S., and Givskov, M. (1996). Differentiation of *Serratia liquefaciens* into swarm cells is controlled by the expression of the *flhD* master operon. *J. Bacteriol.* **178,** 554–559.

Elston, T. C., and Oster, G. (1997). Protein turbines. I. The bacterial flagellar motor. *Biophys. J.* **73,** 703–721.

England, J. C., and Gober, J. W. (2001). Cell cycle control of cell morphogenesis in *Caulobacter*. *Curr. Opin. Microbiol.* **4,** 674–680.

Fan, F., and Macnab, R. M. (1996). Enzymatic characterization of FliI: An ATPase involved in flagellar assembly in *Salmonella typhimurium*. *J. Biol. Chem.* **271,** 31981–31988.

Francis, N. R., Irikura, V. M., Yamaguchi, S., DeRosier, D. J., and Macnab, R. M. (1992). Localization of the *Salmonella typhimurium* flagellar switch protein FliG to the cytoplasmic M-ring face of the basal body. *Proc. Natl. Acad. Sci. USA* **89,** 6304–6308.

Francis, N. R., Sosinsky, G. E., Thomas, D., and DeRosier, D. J. (1994). Isolation, characterization and structure of bacterial flagellar motors containing the switch complex. *J. Mol. Biol.* **235,** 1261–1270.

Fraser, G. M., Bennett, J. C. Q., and Hughes, C. (1999). Substrate-specific binding of hook-associated proteins by FlgN and FliT, putative chaperones for flagellum assembly. *Mol. Microbiol.* **32,** 569–580.

Fuhr, G., and Hagedorn, R. (1989). Dielectric motors: A new hypothesis for the bacterial flagella. *J. Theor. Biol.* **139,** 39–59.

Fujime, S., Maruyama, M., and Asakura, S. (1972). Flexural rigidity of bacterial flagella studied by quasielastic scattering of laser light. *J. Mol. Biol.* **68,** 347–359.

Garza, A. G., Biran, R., Wohlschlegel, J., and Manson, M. D. (1996). Mutations in *motB* suppressible by changes in stator or rotor components of the bacterial flagellar motor. *J. Mol. Biol.* **258,** 270–285.

Gonzalez-Pedrajo, B., Fraser, G. M., Minamino, T., and Macnab, R. M. (2002). Molecular dissection of *Salmonella* FliH, a regulator of the ATPase FliI and the type III flagellar protein export pathway. *Mol. Microbiol.* **45,** 967–982.

Gosink, K. K., and Hase, C. C. (2000). Requirements for conversion of the Na^+-driven flagellar motor of *Vibrio cholerae* to the H^+-driven motor of *Escherichia coli*. *J. Bacteriol.* **182,** 4234–4240.

Harshey, R. M., and Toguchi, A. (1996). Spinning tails: Homologies among bacterial flagellar systems. *Trends Microbiol.* **4,** 226–231.

Hirano, T., Yamaguchi, S., Oosawa, K., and Aizawa, S.-I. (1994). Roles of FliK and FlhB in determination of flagellar hook length in *Salmonella typhimurium*. *J. Bacteriol.* **176,** 5439–5449.

Hirano, T., Minamino, T., and Macnab, R. M. (2001). The role in flagellar rod assembly of the N-terminal domain of *Salmonella* FlgJ, a flagellum-specific muramidase. *J. Mol. Biol.* **312,** 359–369.

Hirano, T., Minamino, T., Namba, K., and Macnab, R. M. (2003). Substrate specificity classes and the recognition signal for *Salmonella* type III flagellar export. *J. Bacteriol.* **185,** 2485–2492.

Hirota, N., and Imae, Y. (1983). Na^+-driven flagellar motors of an alkalophilic *Bacillus* strain YN-1. *J. Biol. Chem.* **258,** 10577–10581.

Homma, M., Komeda, Y., Iino, T., and Macnab, R. M. (1987a). The *flaFIX* gene product of *Salmonella typhimurium* is a flagellar basal body component with a signal peptide for export. *J. Bacteriol.* **169,** 1493–1498.

Homma, M., Ohnishi, K., Iino, T., and Macnab, R. M. (1987b). Identification of flagellar hook and basal body gene products (FlaFV, FlaFVI, FlaFVII, and FlaFVIII) in *Salmonella typhimurium*. *J. Bacteriol.* **169,** 3617–3624.

Homma, M., Kutsukake, K., Hasebe, M., Iino, T., and Macnab, R. M. (1990). FlgB, FlgC, FlgF and FlgG: A family of structurally related proteins in the flagellar basal body of *Salmonella typhimurium*. *J. Mol. Biol.* **211,** 465–477.

Hughes, K. T., Gillen, K. L., Semon, M. J., and Karlinsey, J. E. (1993). Sensing structural intermediates in bacterial flagellar assembly by export of a negative regulator. *Science* **262,** 1277–1280.

Iino, T. (1985). Genetic control of flagellar morphogenesis in *Salmonella*. *In* "Sensing and Response in Microorganisms" (M. Eisenbach and M. Balaban, Eds.), pp. 83–92. Elsevier, New York.

Ikebe, T., Iyoda, S., and Kutsukake, K. (1999). Structure and expression of the *fliA* operon of *Salmonella typhimurium*. *Microbiology* **145,** 1389–1396.

Irikura, V. M., Kihara, M., Yamaguchi, S., Sockett, H., and Macnab, R. M. (1993). *Salmonella typhimurium fliG* and *fliN* mutations causing defects in assembly, rotation, and switching of the flagellar motor. *J. Bacteriol.* **175,** 802–810.

Jaques, S., Kim, Y. K., and McCarter, L. L. (1999). Mutations conferring resistance to phenamil and amiloride, inhibitors of sodium-driven motility of *Vibrio parahaemolyticus*. *Proc. Natl. Acad. Sci. USA* **96,** 5740–5745.

Jones, C. J., and Macnab, R. M. (1990). Flagellar assembly in *Salmonella typhimurium*: Analysis with temperature-sensitive mutants. *J. Bacteriol.* **172,** 1327–1339.

Jones, C. J., Macnab, R. M., Okino, H., and Aizawa, S.-I. (1990). Stoichiometric analysis of the flagellar hook-(basal body) complex of *Salmonella typhimurium*. *J. Mol. Biol.* **212,** 377–387.

Kamiya, R., and Asakura, S. (1977). Flagellar transformations at alkaline pH. *J. Mol. Biol.* **108,** 513–518.

Kanto, S., Okino, H., Aizawa, S.-I., and Yamaguchi, S. (1991). Amino acids responsible for flagellar shape are distributed in terminal regions of flagellin. *J. Mol. Biol.* **219,** 471–480.

Karlinsey, J. E., Pease, A. J., Winkler, M. E., Bailey, J. L., and Hughes, K. T. (1997). The *flk* gene of *Salmonella typhimurium* couples flagellar P- and L-ring assembly to flagellar morphogenesis. *J. Bacteriol.* **179,** 2389–2400.

Karlinsey, J. E., Tsui, H.-C. T., Winkler, M. E., and Hughes, K. T. (1998). Flk couples *flgM* translation to flagellar ring assembly in *Salmonella typhimurium*. *J. Bacteriol.* **180,** 5384–5397.

Karlinsey, J. E., Shugo Tanaka, S., Bettenworth, V., Yamaguchi, S., Boos, W., Aizawa, S.-I., and Hughes, K. T. (2000). Completion of the hook-basal body of the *Salmonella typhimurium* flagellum is coupled to FlgM secretion and *fliC* transcription. *Mol. Microbiol.* **37,** 1220–1231.

Katayama, E., Shiraishi, T., Oosawa, K., Baba, N., and Aizawa, S.-I. (1996). Geometry of the flagellar motor in the cytoplasmic membrane of *Salmonella typhimurium* as determined by stereo-photogrammetry of quick-freeze deep-etch replica images. *J. Mol. Biol.* **255,** 458–475.

Khan, I. H., Reese, T. S., and Khan, S. (1992). The cytoplasmic component of the bacterial flagellar motor. *Proc. Natl. Acad. Sci. USA* **89,** 5956–5960.

Khan, S., and Berg, H. C. (1983). Isotope and thermal effects in chemiosmotic coupling to the flagellar motor of *Streptococcus*. *Cell* **32,** 913–919.

Khan, S., Dapice, M., and Reese, T. S. (1988). Effects of *mot* gene expression on the structure of the flagellar motor. *J. Mol. Biol.* **202,** 575–584.

Khan, S., Dapice, M., and Humayun, I. (1990). Energy transduction in the bacterial flagellar motor: Effects of load and pH. *Biophys. J.* **57,** 779–796.

Khan, S., Khan, I. H., and Reese, T. S. (1991). New structural features of the flagellar base in *S. typhimurium* revealed by rapid-freeze electron microscopy. *J. Bacteriol.* **173,** 2888–2896.

Kihara, M., Minamino, T., Yamaguchi, S., and Macnab, R. M. (2001). Intergenic suppression between the flagellar MS ring protein FliF of *Salmonella* and FlhA, a membrane component of its export apparatus. *J. Bacteriol.* **183,** 1655–1662.

Kleutsch, B., and Lauger, P. (1990). Coupling of ion flow and rotation in the bactgerial flagellar motor: Stochastic simulation of a microscopic model. *Eur. J. Biophys.* **18,** 175–191.

Ko, M., and Park, C. (2000). Two novel flagellar components and H-NS are involved in the motor function of *Escherichia coli*. *J. Mol. Biol.* **303,** 371–382.

Kojima, S., and Blair, D. F. (2001). Conformational change in the stator of the bacterial flagellar motor. *Biochemistry* **40,** 13041–13050.

Kojima, S., Asai, Y., Atsumi, T., Kawagishi, I., and Homma, M. (1999). Na^+-driven flagellar motor resistant to phenamil, an amiloride analog, caused by mutations in putative channel components. *J. Mol. Biol.* **285,** 1537–1547.

Kojima, S., Shoji, T., Asai, Y., Kawagishi, I., and Homma, M. (2000). A slow-motility phenotype caused by substitutions at residue Asp31 in the PomA channel component of a sodium-driven flagellar motor. *J. Bacteriol.* **182,** 3314–3318.

Kubori, T., Shimamoto, N., Yamaguchi, S., Namba, K., and Aizawa, S.-I. (1992). Morphological pathway of flagellar assembly in *Salmonella typhimurium*. *J. Mol. Biol.* **226,** 433–446.

Kubori, T., Matsushima, Y., Nakamura, D., Uralil, J., Lara-Tejero, M., Sukhan, A., Galan, J. E., and Aizawa, S.-I. (1998). Supramolecular structure of the *Salmonella typhimurium* type III protein secretion system. *Science* **280,** 602–605.

Kutsukake, K. (1994). Excretion of the anti-sigma factor through a flagellar substructure couples flagellar gene expression with flagellar assembly in *Salmonella typhimurium*. *Mol. Gen. Genet.* **243,** 605–612.

Kutsukake, K. (1997a). Autogenous and global control of the flagellar master operon *flhD*, in *Salmonella typhimurium*. *Mol. Gen. Genet.* **254,** 440–448.

Kutsukake, K. (1997b). Hook-length control of the export-switching machinery involves a double-locked gate in *Salmonella typhimurium* flagellar morphogenesis. *J. Bacteriol.* **179,** 1268–1273.

Kutsukake, K., and Iino, T. (1994). Role of the FliA–FlgM regulatory system on the transcriptional control of the flagellar regulon and flagellar formation in *Salmonella typhimurium*. *J. Bacteriol.* **176,** 3598–3605.

Kutsukake, K., Minamino, T., and Yokoseki, T. (1994). Isolation and characterization of FliK-independent flagellation mutants from *Salmonella typhimurium*. *J. Bacteriol.* **176,** 7625–7629.

Kutsukake, K., Ikebe, T., and Yamamoto, S. (1999). Two novel regulatory genes, *fliT* and *fliZ*, in the flagellar regulon of *Salmonella*. *Genes Genet. Syst.* **74,** 287–292.

Larsen, S. H., Adler, J., Gargus, J. J., and Hogg, R. W. (1974a). Chemomechanical coupling without ATP: The source of energy for motility and chemotaxis in bacteria. *Proc. Natl. Acad. Sci. USA* **71,** 1239–1243.

Larsen, S. H., Reader, R. W., Kort, E. N., Tso, W.-W., and Adler, J. (1974b). Change in direction of flagellar rotation is the basis of the chemotactic response in *E. coli*. *Nature* **249,** 74–77.

Lauger, P. (1977). Ion transport and rotation of bacterial flagella. *Nature* **268,** 360–362.

Lauger, P. (1988). Torque and rotation rate of the bacterial flagellar motor. *Biophys. J.* **53,** 53–65.

Li, C., Louise, C. J., Shi, W., and Adler, J. (1993). Adverse conditions which cause lack of flagella in *Escherichia coli*. *J. Bacteriol.* **175,** 2229–2235.

Liu, J. Z., Dapice, M., and Khan, S. (1990). Ion selectivity of the *Vibrio alginolyticus* flagellar motor. *J. Bacteriol.* **172,** 5236–5244.

Liu, X., and Matsumura, P. (1994). The FlhD/FlhC complex, a transcriptional activator of the *Escherichia coli* flagellar class II operons. *J. Bacteriol.* **176,** 7345–7351.

Liu, X., and Matsumura, P. (1995). An alternative sigma factor controls transcription of flagellar class-III operons in *Escherichia coli*: Gene sequence, overproduction, purification and characterization. *Gene* **164,** 81–84.

Lloyd, S. A., and Blair, D. F. (1997). Charged residues of the rotor protein FliG essential for torque generation in the flagellar motor of *Escherichia coli*. *J. Mol. Biol.* **266,** 733–744.

Lloyd, S. A., Tang, H., Wang, X., Billings, S., and Blair, D. F. (1996). Torque generation in the flagellar motor of *Escherichia coli*: Evidence of a direct role for FliG but not for FliM or FliN. *J. Bacteriol.* **178,** 223–231.

Lloyd, S. A., Whitby, F. G., Blair, D. F., and Hill, C. P. (1999). Structure of the C-terminal domain of FliG, a component of the rotor in the bacterial flagellar motor. *Nature* **400,** 472–475.

Lowe, G., Meister, M., and Berg, H. C. (1987). Rapid rotation of flagellar bundles in swimming bacteria. *Nature* **325,** 637–640.

Lux, R., Kar, N., and Khan, S. (2000). Overproduced *Salmonella typhimurium* flagellar motor switch complexes. *J. Mol. Biol.* **298,** 577–583.

Macnab, R. (1992). Genetics and biogenesis of bacterial flagella. *Annu. Rev. Genet.* **26,** 129–156.

Macnab, R. M. (1999). The bacterial flagellum: Reversible rotary propellor and type III export apparatus. *J. Bacteriol.* **181,** 7149–7153.

Macnab, R. M. (2003). How bacteria assemble flagella. *Annu. Rev. Microbiol.* **57,** 77–100.

Macnab, R. M., and Koshland, D. E. J. (1972). The gradient-sensing mechanism in bacterial chemotaxis. *Proc. Natl. Acad. Sci. USA* **69,** 2509–2512.

Macnab, R. M., and Ornston, M. K. (1977). Normal- to-curly flagellar transitions and their role in bacterial tumbling: Stabilization of an alternative quaternary structure by mechanical force. *J. Mol. Biol.* **112,** 1–30.

Magariyama, Y., Sugiyama, S., Muramoto, K., Maekawa, Y., Kawagishi, I., Imae, Y., and Kudo, S. (1994). Very fast flagellar rotation. *Nature* **371,** 752.

Makishima, S., Komoriya, K., Yamaguchi, S., and Aizawa, S.-I. (2001). Length of the flagellar hook and the capacity of the type III export apparatus. *Science* **291,** 2411–2413.

Manson, M. D., Tedesco, Berg, H. C., Harold, F. M., and van der Drift, C. (1997). A protonmotive force drives bacterial flagella. *Proc. Natl. Acad. Sci. USA* **74,** 3060–3064.

Manson, M. D., Tedesco, P., and Berg, H. C. (1980). Energetics of flagellar rotation in bacteria. *J. Mol. Biol.* **138,** 541–561.

Marykwas, D. L., and Berg, H. C. (1996). A mutational analysis of the interaction between FliG and FliM, two components of the flagellar motor of *Escherichia coli*. *J. Bacteriol.* **178,** 1289–1294.

Mathews, M. A. A., Tang, H. L., and Blair, D. F. (1998). Domain analysis of the FliM protein of *Escherichia coli*. *J. Bacteriol.* **180,** 5580–5590.

McCarter, L. L. (1994a). MotX, the channel component of the sodium-type flagellar motor. *J. Bacteriol.* **176,** 5988–5998.

McCarter, L. L. (1994b). MotY, a component of the sodium-type flagellar motor. *J. Bacteriol.* **176,** 4219–4225.

Meister, M., Lowe, G., and Berg, H. C. (1987). The proton flux through the bacterial flagellar motor. *Cell* **49,** 643–650.

Meister, M., Caplan, S. R., and Berg, H. C. (1989). Dynamics of a tightly coupled mechanism for flagellar rotation. *Biophys. J.* **55,** 905–914.

Mimori, Y., Yamashita, I., Murata, K., Fujiyoshi, Y., Yonekura, K., Toyoshima, C., and Namba, K. (1995). The structure of the R-type straight flagellar filament of *Salmonella* at 9 Å resolution by electron cryomicroscopy. *J. Mol. Biol.* **249,** 69–87.

Minamino, T., and Macnab, R. M. (1999). Components of the *Salmonella* flagellar export apparatus and classification of export substrates. *J. Bacteriol.* **181,** 1388–1394.

Minamino, T., and Macnab, R. M. (2000a). FliH, a soluble component of the type III flagellar export apparatus of *Salmonella*, forms a complex with FliI and hinhibits its ATPase activity. *Mol. Microbiol.* **37,** 1494–1503.

Minamino, T., and Macnab, R. M. (2000b). Domain structure of FlhB, a flagellar export component responsible for substrate-specificity switching. *J. Bacteriol.* **182,** 4906–4914.

Minamino, T., Iino, T., and Kutsukake, K. (1994). Molecular characterization of the *Salmonella typhimurium flhB* operon and its protein products. *J. Bacteriol.* **176,** 7630–7637.

Minamino, T., Doi, H., and Kutsukake, K. (1999a). Substrate specificity switching of the flagellum-specific export apparatus during flagellar morphogenesis in *Salmonella typhimurium*. *Biosci. Biotechnol. Biochem.* **63,** 1301–1303.

Minamino, T., Gonzalez-Pedrajo, B., Yamaguchi, K., Aizawa, S.-I., and Macnab, R. M. (1999b). FliK, the protein responsible for flagellar hook length control in *Salmonella*, is exported during hook assembly. *Mol. Microbiol.* **34,** 295–304.

Minamino, T., Chu, R., Yamaguchi, S., and Macnab, R. M. (2000a). Role of FliJ in flagellar protein export in *Salmonella*. *J. Bacteriol.* **182,** 4207–4215.

Minamino, T., Yamaguchi, S., and Macnab, R. M. (2000b). Interaction between FliE and FlgB, a proximal rod component of the flagellar basal body of *Salmonella*. *J. Bacteriol.* **182,** 3029–3036.

Morgan, D. G., Macnab, R. M., Francis, N. R., and DeRosier, D. J. (1993). Domain organization of the subunit of the *Salmonella typhimurium* flagellar hook. *J. Mol. Biol.* **229,** 79–84.

Morgan, D. G., Owen, C., Melanson, L. A., and DeRosier, D. J. (1995). Structure of bacterial flagellar filaments at 11 Å resolution: Packing of the α-helices. *J. Mol. Biol.* **249,** 88–110.

Muramoto, K., and Macnab, R. M. (1998). Deletion analysis of MotA and MotB, components of the force-generating unit in the flagellar motor of *Salmonella*. *Mol. Microbiol.* **29,** 1191–1202.

Muramoto, K., Sugiyama, S., Cragoe, E. J. J., and Imae, Y. (1994). Successive inactivation of the force-generating units of sodium-driven bacterial flagellar motors by a photoreactive amiloride analog. *J. Biol. Chem.* **269,** 3374–3380.

Muramoto, K., Makashima, S., Aizawa, S.-I., and Macnab, R. M. (1998). Effect of cellular level of Flik on flagellar hook and filament assembly in *Salmonella typhimurium*. *J. Mol. Biol.* **277,** 871–882.

Nambu, T., and Kutsukake, K. (2000). The *Salmonella* FlgA protein, a putative periplasmic chaperone essential for flagellar P ring formation. *Microbiology* **146,** 1171–1178.

Nambu, T., Minamino, T., Macnab, R. M., and Kutsukake, K. (1999). Peptidoglycan-hydrolyzing activity of the FlgJ protein, essential for flagellar rod formation in *Salmonella typhimurium*. *J. Bacteriol.* **181,** 1555–1561.

Nishimura, A., and Hirota, Y. (1989). A cell division regulatory mechanism controls the flagellar regulon in *Escherichia coli.*. *Mol. Gen. Genet.* **216,** 340–346.

Nolling, J., Breton, G., Omelchenko, M. V., Makarova, K. S., Zeng, Q., Gibson, R., Lee, H. M., Dubois, J., Qiu, D., and Hitti, J. (2001). Genome sequence and comparative analysis of the solvent-producing bacterium *Clostridium acetobutylicum*. *J. Bacteriol.* **183,** 4823–4838.

Okabe, M., Yakushi, T., Kojima, M., and Homma, M. (2002). MotX and MotY, specific components of the sodium-driven flagellar motor, colocalize to the outer membrane in *Vibrio alginolyticus*. *Mol. Microbiol.* **46,** 125–134.

Oosawa, F., and Hayashi, S. (1986). The loose coupling mechanism in molecular machines of living cells. *Adv. Biophys.* **22,** 151–183.

Oosawa, F., and Masai, J. (1982). Mechanism of flagellar motor rotation in bacteria. *J. Phys. Soc. Jpn.* **51,** 631–664.

Oosawa, K., Ueno, T., and Aizawa, S.-I. (1994). Overproduction of the bacterial flagellar switch proteins and their interactions with the MS ring complex in vitro. *J. Bacteriol.* **176,** 3683–3691.

Patterson-Delafield, J., Martinez, R. J., Stocker, B. A. D., and Yamaguchi, S. (1973). A new *fla* gen in *Salmonella typhimurium—flaR*—and its mutant phenotype—superhooks. *Arch. Mikrobiol.* **90,** 107–120.

Pruss, B. M., and Matsumura, P. (1996). A regulator of the flagellar regulon of *Escherichia coli, flhD*, also affects cell division. *J. Bacteriol.* **178,** 668–674.

Pruss, B. M., and Matsumura, P. (1997). Cell cycle regulation of flagellar genes. *J. Bacteriol.* **179,** 5602–5604.

Pruss, B. M., and Wolfe, A. J. (1994). Regulation of acetyl phosphate synthesis and degradation, and the control of flagellar expression in *Escherichia coli*. *Mol. Microbiol.* **12,** 973–984.

Qualding, C., and Stocker, B. A. D. (1962). An environmentally induced transition from the flagellated to the non-flagellated state in *Salmonella typhimurium*: The fate of parental flagella at cell division. *J. Gen. Microbiol.* **28,** 257–270.

Ryu, W. S., Berry, R. M., and Berg, H. C. (2000). Torque-generating units of the flagellar motor of *Escherichia coli* have a high duty ratio. *Nature* **403,** 444–447.

Samatey, F. A., Imada, K., Nagashima, S., Vonderviszt, F., Kumasaka, T., Yamamoto, M., and Namba, K. (2001). Structure of the bacterial flagellar protofilament and implications for a switch for supercoiling. *Nature* **410,** 331–337.

Samuel, A. D., and Berg, H. C. (1995). Fluctuation analysis of rotational speeds of the bacterial flagellar motor. *Proc. Natl. Acad. Sci. USA* **92,** 3502–3506.

Samuel, A. D. T., and Berg, H. C. (1996). Torque-generating units of the bacterial flagellar motor step independently. *Biophys. J.* **71,** 918–923.

Sato, K., and Homma, M. (2000a). Functional reconstitution of the Na^+-driven polar flagellar motor component of *Vibrio alginolyticus*. *J. Biol. Chem.* **275,** 5718–5722.

Sato, K., and Homma, M. (2000b). Multimeric structure of PomA, a component of the Na^+-driven polar flagellar motor of *Vibrio alginolyticus*. *J. Biol. Chem.* **275,** 20223–20228.

Schoenhals, G. J., and Macnab, R. M. (1999). FliL is a membrane-associated component of the flagellar basal body of Salmonella. *Microbiology* **145,** 1769–1775.

Sharp, L. L., Zhou, J., and Blair, D. F. (1995a). Features of MotA proton channel structure revealed by tryptophan-scanning mutagenesis. *Proc. Natl. Acad. Sci. USA* **92,** 7946–7950.

Sharp, L. L., Zhou, J., and Blair, D. F. (1995b). Tryptophan-scanning mutagenesis of MotB, an integral membrane protein essential for flagellar rotation in *Escherichia coli.*. *Biochemistry* **34,** 9166–9171.

Shi, W., Zhou, Y., Wild, J., Adler, J., and Gross, C. A. (1992). DnaK, DnaJ, and GrpE are required for flagellum synthesis in *Escherichia coli*. *J. Bacteriol.* **174,** 6256–6263.

Shi, W., Li, E., Louise, C. J., and Adler, J. (1993). Mechanism of adverse conditions causing lack of flagella in *Escherichia coli*. *J. Bacteriol.* **175,** 2236–2240.

Shin, W., and Park, C. (1995). Modulation of flagellar expression in *Escherichia coli* by acetyl phosphate and the osmoregulator, OmpR. *J. Bacteriol.* **177,** 4696–4702.

Shioi, J.-I., Matsuura, S., and Imae, Y. (1980). Quantitative measurements o protonmotive force and motility in *Bacillus subtilis*. *J. Bacteriol.* **144,** 891–897.

Silverman, M., and Simon, M. (1974a). Flagellar rotation and the mechanism of bacterial motility. *Nature* **249,** 73–74.

Silverman, M., and Simon, M. (1974b). Characterization of *Escherichia coli* flagellar mutants that are insensitive to catabolite repression. *J. Bacteriol.* **120,** 1196–1203.

Silverman, M. R., and Simon, M. I. (1972). Flagellar assembly mutants in *Escherichia coli*. *J. Bacteriol.* **112,** 986–993.

Slonczewski, J., Rosen, B. P., Alger, J. R., and Macnab, R. M. (1981). pH homeostasis in *Escherichia coli*: Measurement by ^{31}P nuclear magnetic resonance of methylphosphonate and phosphate. *Proc. Natl. Acad. Sci. USA* **78,** 6271–6275.

Sockett, H., Yamaguchi, S., Kihara, M., Irikura, V. M., and Macnab, R. M. (1992). Molecular analysis of the flagellar switch protein FliM of *Salmonella typhimurium*. *J. Bacteriol.* **174,** 793–806.

Sosinsky, G. E., Francis, N. R., DeRosier, D. J., Wall, J. S., Simon, M. N., and Hainfeld, J. (1992). Mass determination and estimation of subunit stoichiometry of the bacterial hook-basal body flagellar complex of *Salmonella typhimurium* by scanning transmission electron microscopy. *Proc. Natl. Acad. Sci. USA* **89,** 4801–4805.

Stader, J., Matsumura, P., Vacante, D., Dean, G. E., and Macnab, R. M. (1986). Nucleotide sequence of the *Escherichia coli motB* gene and site-limited incorporation of its product into the cytoplasmic membrane. *J. Bacteriol.* **166,** 244–252.

Stolz, B., and Berg, H. C. (1991). Evidence for interactions between MotA and MotB, torque-generating elements of the flagellar motor of *Escherichia coli*. *J. Bacteriol.* **173,** 7033–7037.

Suzuki, T., and Komeda, Y. (1981). Incomplete flagellar structures in *Escherichia coli* mutants. *J. Bacteriol.* **145,** 1036–1041.

Suzuki, T., Iino, T., Horiguchi, T., and Yamaguchi, S. (1978). Incomplete flagellar structures in nonflagellate mutants of *Salmonella typhimurium*. *J. Bacteriol.* **133,** 904–915.

Tang, H., Braun, T. F., and Blair, D. F. (1996). Motility protein complexes in the bacterial flagellar motor. *J. Mol. Biol.* **261,** 209–221.

Thomas, D., Morgan, D. G., and DeRosier, D. J. (2001). Structures of bacterial flagellar motors from two FliF–FliG gene fusion mutants. *J. Bacteriol.* **183,** 6404–6412.

Thomas, D. R., Morgan, D. G., and DeRosier, D. J. (1999). Rotational symmetry of the C ring and mechanism for the flagellar rotary motor. *Proc. Natl. Acad. Sci. USA* **96,** 10134–10139.

Togashi, F., Yamaguchi, S., Kihara, S. M., Aizawa, S.-I., and Macnab, R. M. (1997). An extreme clockwise bias mutation in *fliG* of *Salmonella typhimurium* and its suppression by slow-motile mutations in *motA* and *motB*. *J. Bacteriol.* **179,** 2994–3003.

Toker, A. S., and Macnab, R. M. (1997). Distinct regions of bacterial flagellar switch protein FliM interact with FliG, FliN and CheY. *J. Mol. Biol.* **273,** 623–634.

Tomoyasu, T., Ohkishi, T., Ukyo, Y., Tokumitsu, A., Takaya, A., Suzuki, M., Sekiya, K., Matsui, H., Kutsukake, K., and Yamamoto, T. (2002). The ClpXP ATP-dependent protease regulates flagelllum synthesis in *Salmonella enterica* serovar *Typhimurium*. *J. Bacteriol.* **184,** 645–653.

Trachtenberg, S., and DeRosier, D. J. (1987). Three-dimensional structure of the frozen-hydrated flagellar filament: The left-handed filament of *Salmonella typhimurium*. *J. Mol. Biol.* **195,** 581–601.

Trachtenberg, S., and DeRosier, D. J. (1991). A molecular switch: Subunit rotations involved in the right-handed to left-handed transitions of *Salmonella typhimurium* flagellar filaments. *J. Mol. Biol.* **220,** 67–77.

Ueno, T., Oosawa, K., and Aizawa, S.-I. (1992). M ring, S ring and proximal rod of the flagellar basal body of *Salmonella typhimurium* are composed of subunits of a single protein, FliF. *J. Mol. Biol.* **227,** 672–677.

Vogler, A. P., Homma, M., Irikura, V. M., and Macnab, R. M. (1991). *Salmonella typhimurium* mutants defective in flagellar filament regrowth and sequence similarity of FliI to F_0F_1, vacuolar, and archaebacterial ATPase subunits. *J. Bacteriol.* **173,** 3564–3572.

Walz, D., and Caplan, S. R. (2000). An electrostatic mechanism closely reproducing observed behavior in the bacterial flagellar motor. *Biophys. J.* **78,** 626–651.

Washizu, M., Kurahashi, Y., Iochi, H., Kurosawa, O., Aizawa, S.-I., Kudo, S., Magariyama, Y., and Hotani, H. (1993). Dielectrophoretic measurement of bacterial motor characteristics. *IEEE Trans. Ind. Appl.* **29,** 286–294.

Welch, M., Oosawa, K., Aizawa, S.-I., and Eisenbach, M. (1993). Phosphorylation-dependent binding of a signal molecule to the flagellar switch of bacteria. *Proc. Natl. Acad. Sci. USA* **90,** 8787–8791.

Williams, A. W., Yamaguchi, S., Togashi, F., Aizawa, S.-I., and Macnab, R. M. (1996). Mutations in *fliK* and *flhB* affecting flagellar hook and filament assembly in *Salmonella typhimurium*. *J. Bacteriol.* **178,** 2960–2970.

Wu, J., and Newton, A. (1997). Regulation of the *Caulobacter* flagellar gene hierarchy, not just for motility. *Mol. Microbiol.* **24,** 233–239.

Yamaguchi, S., Aizawa, S.-I., Kihara, M., Isomura, M., Jones, C. J., and Macnab, R. M. (1986a). Genetic evidence for a switching and energy-transducing complex in the flagellar motor of *Salmonella typhimurium*. *J. Bacteriol.* **168,** 1172–1179.

Yamaguchi, S., Fujita, H., Ishihara, A., Aizawa, S.-I., and Macnab, R. M. (1986b). Subdivision of flagellar genes of *Salmonella typhimurium* into regions responsible for assembly, rotation, and switching. *J. Bacteriol.* **166,** 187–193.

Yokoseki, T., Kutsukake, K., Ohnishi, K., and Iino, T. (1995). Functional analysis of the flagellar genes in the *fliD* operon of *Salmonella typhimurium*. *Microbiology* **141,** 1715–1722.

Yokota, T., and Gots, J. S. (1970). Requirement of adenosine 3′,5′-cyclic phosphate for flagellum formation in *Escherichia coli* and *Salmonella typhimurium*. *J. Bacteriol.* **103,** 513–516.

Yorimitsu, T., Sowa, Y., Ishijima, A., Yakushi, T., and Homma, T. (2002). The systematic substitutions around the conserved charged residues of the cytoplasmic loop of Na^+-driven flagellar motor component PomA. *J. Mol. Biol.* **320,** 403–413.

Yoshida, S., Sugiyama, S., Hojo, Y., Tokuda, H., and Imae, Y. (1990). Intracellular Na^+ kinetically interferes with the rotation of the Na^+-driven flagellar motors of *Vibrio alginolyticus*. *J. Biol. Chem.* **265,** 20346–20350.

Young, H. S., Dang, H., Lai, Y., DeRosier, D. J., and Khan, S. (2003). Variable symmetry in *Salmonella typhimurium* flagellar motors. *Biophys. J.* **84,** 571–577.

Zhao, R., Pathak, N., Jaffe, H., Reese, T. S., and Khan, S. (1996). FliN is a major structural protein of the C-ring in the *Salmonella typhimurium* flagellar basal body. *J. Mol. Biol.* **261,** 195–208.

Zhou, J., and Blair, D. F. (1997). Residues of the cytoplasmic domain of MotA essential for torque generation in the bacterial flagellar motor. *J. Mol. Biol.* **273,** 428–439.

Zhou, J., Fazzio, R. T., and Blair, D. F. (1995). Membrane topology of the MotA protein of *Escherichia coli*. *J. Mol. Biol.* **251,** 237–242.

Zhou, J., Lloyd, S. A., and Blair, D. F. (1998a). Electrostatic interactions between rotor and stator in the bacterial flagellar motor. *Proc. Natl. Acad. Sci. USA* **95,** 6436–6441.

Zhou, J., Sharp, L. L., Tang, H. L., Lloyd, S. A., Billings, S., Braun, T. F., and Blair, D. F. (1998b). Function of protonatable residues in the flagellar motor of *Escherichia coli*: A critical role for Asp 32 of MotB. *J. Bacteriol.* **180,** 2729–2735.

Apoptosis in Plants: Specific Features of Plant Apoptotic Cells and Effect of Various Factors and Agents

B. F. Vanyushin, L. E. Bakeeva, V. A. Zamyatnina, and N. I. Aleksandrushkina
Belozersky Institute of Physico Chemical Biology, Lomonosov Moscow State University, Moscow 119992, Russia

Apoptosis is an integral part of plant ontogenesis; it is controlled by cellular oxidative status, phytohormones, and DNA methylation. In wheat plants apoptosis appears at early stages of development in coleoptile and initial leaf of 5- to 6-day-old seedlings. Distinct ultrastructural features of apoptosis observed are (1) compaction and vacuolization of cytoplasm in the apoptotic cell, (2) specific fragmentation of cytoplasm and appearance in the vacuole of unique single-membrane vesicles containing active organelles, (3) cessation of nuclear DNA synthesis, (4) condensation and margination of chromatin in the nucleus, (5) internucleosomal fragmentation of nuclear DNA, and (6) intensive synthesis of mitochondrial DNA in vacuolar vesicles. Peroxides, abscisic acid, ethylene releaser ethrel, and DNA methylation inhibitor 5-azacytidine induce and stimulate apoptosis. Modulation of the reactive oxygen species (ROS) level in seedling by antioxidants and peroxides results in tissue-specific changes in the target date for the appearance and the intensity of apoptosis. Antioxidant butylated hydroxytoluene (BHT) reduces the amount of ROS and prevents apoptosis in etiolated seedlings, prolongs coleoptile life span, and prevents the appearance of all apoptotic features mentioned. Besides, BHT induces large structural changes in the organization of all cellular organelles and the formation of new unusual membrane structures in the cytoplasm. BHT distorts mitosis and this results in the appearance of multiblade polyploid nuclei and multinuclear cells. In roots of etiolated wheat seedlings, BHT induces differentiation of plastids with the formation of chloro(chromo)plasts. Therefore, ROS controlled by BHT seems to regulate mitosis, trigger apoptosis, and control plastid differentiation and the organization of various cellular structures formed by endocytoplasmic reticulum.

International Review of Cytology, Vol. 233
0074-7696/04 $35.00

KEY WORDS: Aging, Antioxidant, Apoptosis, BHT, PCD, Phytohormone, Plant, Plastid Differentiation.

Life is a great surprise. I do not see why death should not be an even greater one.
Vladimir Nabokov (1899–1977), novelist

I. Introduction

The life of any multicellular organism is accompanied, every day, by the death of some of its many cells. Various unfavorable environmental factors and agents may be responsible for this event; the cell death is mainly fortuitous. On the other hand, the fate of certain cells and tissues in the organism is strongly predetermined; their death is encoded in the genome, it proceeds at the proper developmental stage, and it is a requisite condition and an obligatory constituent part of ontogenesis. This genetically predetermined cell death was initially described as normal physiological death (Vorontsova and Liozner, 1955) or "regulated" programmed death (Lockshin and Williams, 1964) and its main features were described relatively long ago (Glücksmann, 1951; Vanyushin and Berdyshev, 1977). In particular, the significance of natural, genetically determined cell death in the regulation of cell populations during ontogenesis was clearly demonstrated by British embryologists (Kerr *et al*., 1972), who described in detail the specific morphological features of cells and tissues during this particular sort of cell death, and they coined the term *apoptosis* to describe and specify this biological phenomenon. Along with apoptosis as a genetically programmed terminal stage of cellular differentiation, some other varieties of programmed cell death exist in plants and animals, and they occur under the influence of various environmental factors (pathogens, chemical and physical agents) as a result of activation of specific internal triggers of cell suicide. Therefore, the term *programmed cell death* (PCD) is more general as compared with apoptosis, which emphasizes mainly the idea of cell death as a normal function of an organism (Lockshin and Zakeri, 2001). It was concluded that the mechanisms of PCD in plants bear a certain relation to those of apoptosis, and some processes, such as nucleic acid degradation, are superficially similar to aspects of the senescence syndrome (Thomas *et al*., 2003).

Along with PCD the programmed death of the entire organism or certain organs does exist. It was suggested that these phenomena be called phenoptosis and organoptosis, respectively (Skulachev, 2001, 2002). Phenoptosis was observed in animals and plants. This process is especially clear and

dramatically pronounced in Pacific salmon (fish die after spawning), and it is accompanied by an increase in steroid hormone content and sharp global DNA demethylation in all tissues (Berdyshev *et al.*, 1967). It seems that steroid hormones are involved in the triggering of phenoptosis in this fish; fish with gonads removed do not die when control spawning individuals die, and their life span is essentially increased (Vanyushin and Berdyshev, 1977). Phenoptosis is common among cereals. These plants die after flowering. We believe that, as in animals, phenoptosis in plants is controlled by hormones (phytohormones) triggering the PCD genes. The problem of relation and interdependency between phenoptosis, organoptosis, and apoptosis is of special interest. It would be easy to draw a chain: apoptosis → organoptosis → phenoptosis. In addition, mitoptosis (programmed death of mitochondria; Skulachev, 2002), placed at the beginning of this death chain, seems convincing. Aging and death are often due to mitoptosis and accumulation of apoptotic cells (Skulachev, 1999); the massive neuron apoptosis observed in patients with Alzheimer's disease may result in phenoptosis (patient death). Nevertheless, we are not inclined yet to place definite arrows indicating the directions in this chain. In fact, the interrelations between these processes may be more complicated and less predictable. For instance, it cannot be ruled out that organoptosis in one organ (coleoptile in wheat) might trigger apoptosis in another organ (leaf).

In plants, genetically programmed death of entire organs (leaves, petals, fruits) is designated *senescence* (Hadfield and Bennett, 1997). The coleoptile death in cereals due to PCD is a good example of organoptosis in plants (Vanyushin, 2001). PCD is responsible for elimination of unpollinated ovules and the collapse of the nucellus cells at the final stage of seed maturation, disintegration of the plasmodial tapetum cells in anthers, elimination of suspensor cells connecting the embryo to the mother plant, and dissolution of the aleurone layers in germinating grains of cereals. It is a delicate key instrument for formation of vascular xylem system and aerenchyma, root cap renovation, and shaping of leaf lobes and perforations. Like in animals, PCD is involved in the elimination of certain cells during plant embryogenesis. Two broad phases were observed in Norway spruce somatic embryogenesis (Filonova *et al.*, 2000). The first phase is represented by proliferating proembryogenic masses (PEMs). The second phase encompasses development of somatic embryos, which arise from PEMs. There are two successive waves of PCD, which are implicated in the transition from PEMs to somatic embryos and in correct embryonic pattern formation, respectively. The first wave of PCD is responsible for the degradation of PEMs when they give rise to somatic embryos. PCD in PEM cells and embryo formation are closely interlinked processes, both stimulated on withdrawal or partial depletion of auxins and cytokinins. The second wave of PCD eliminates terminally differentiated embryo-suspensor cells during early embryogeny. During the

dismantling phase of PCD, PEM and embryo-suspensor cells exhibit progressive autolysis, resulting in the formation of a large central vacuole (Filonova *et al.*, 2000). Autolytic degradation of the cytoplasm is accompanied by lobing and budding-like segmentation of the nucleus. Nuclear DNA undergoes fragmentation into both large fragments of about 50 kb and multiples of approximately 180 bp. The tonoplast rupture is delayed until lysis of the cytoplasm and organelles, including the nucleus, is almost complete. The protoplasm then disappears, leaving a cellular corpse represented by only the cell wall (Filonova *et al.*, 2000).

Although apoptosis is an obligatory integral part of plant ontogenesis, it can be prematurely induced (or suppressed) by various single or combined environmental factors of physical, chemical, and biological nature. This includes heat and cold, salt stress, hypoxia, ultraviolet (UV) light irradiation, nutrition deficiency, reactive oxygen species (ROS), metal ions (in particular, calcium), different chemicals (especially, prooxidants and antioxidants), phytohormones and other signal molecules, and various pathogens (viruses and microorganisms, including plant pathogenic bacteria and fungi). Of course, these factors are responsible for essential changes observed in the cellular metabolism that result in reorganization of cell structure and functioning. Nevertheless, fine mechanisms of influence of these agents and factors on apoptosis in plants are mostly unknown. There is no doubt that plant PCD is controlled by these factors, and the cell is often ready to die for the benefit of an entire organism.

Some peculiar and specific features and regularities of apoptosis in plants are described in this article, which cannot present a comprehensive elucidation of the many complicated problems associated with PCD in the plant kingdom. An interested reader may find intriguing details of plant PCD in various reviews (Ameisen, 2002; Dröge, 2002; Fath *et al.*, 2000; Fukuda, 1996, 2000; Gietl and Schmid, 2001; Greenberg, 1996, 1997; Heath, 1998, 2000; Hoeberichts and Woltering, 2003; Inada *et al.*, 2002; Lam and del Pozo, 2000; Lam *et al.*, 1999, 2001; McCabe and Lever, 2000; Neill *et al.*, 2002a,b; Pennell and Lamb, 1997; Ranganath and Nagashree, 2001; Rubinstein, 2000; Wu and Cheung, 2000; Young and Gallie, 2000; Zhivotovsky, 2002).

II. Main Characteristics of Apoptosis

A. Comparative Characteristics of Apoptosis in Eukaryotes

Although it has long been implied that, as in animals, apoptosis should be present in plants (Vanyushin and Berdyshev, 1977), study of the morphological characteristics and molecular mechanisms of apoptosis in plants still

lags behind such studies in animals. In particular, this may be associated with the keen interest in clinical investigations of apoptosis, as distortions of apoptosis are shown to be of crucial significance in the manifestation of many "molecular" diseases including cancer, Alzheimer's disease, aging, and others (Fadeel *et al.*, 1999).

Until more recently it was not known how apoptosis is manifested in plants, or the apoptotic marks most specific for these organisms. Now it is known that, in general, most features and mechanisms of apoptosis in plants and animals are similar (Ashkenazi and Dixit, 1998; Beers, 1997; Gilchrist, 1997, 1998; Greenberg, 1996; Groover *et al.*, 1997; Jiang *et al.*, 1999). Some apoptotic factors in animal and plant cells are even interchangeable: apoptotic changes in isolated plant nuclei may proceed in animal cell-free systems (Jiang *et al.*, 1999) and vice versa (Zhao *et al.*, 1999). In cells of *Arabidopsis thaliana* (Gallois *et al.*, 1997), pea (Orzaez and Granell, 1997a), and rice (Tanaka *et al.*, 1997) an antiapoptotic gene homologous to animal *dad1* (Sugimoto *et al.*, 1995) was detected. Activity of this gene decreases with plant aging (Gallois *et al.*, 1997; Orzaez and Granell, 1997a); the plant gene introduced into *ts* mutant hamster cells prohibits the triggering of apoptosis at permissive temperature (Gallois *et al.*, 1997; Tanaka *et al.*, 1997). Thus, the plant *dad*-encoded protein effectively prevents apoptosis in animal (hamster) cells.

As in animals, the exposure of phosphatidylserine on the outer membrane surface as an early indicator of apoptosis seems also to occur in plant cells (O'Brien *et al.*, 1997). PCD was activated in carrot cells cultured at low cell concentrations (Fewer than 10^4 cells/ml) and it was accompanied by condensation and shrinkage of cytoplasm and nucleus and DNA fragmentation (McCabe *et al.*, 1997). At this low cell density, DNA synthesis both in plant and animal cell cultures is limited to formation of Okazaki fragments with no subsequent ligation (Vanyushin, 1984). Therefore, in plants, like in animals, PCD may be controlled by social signaling. Human *bcl-2*, *bcl-xl*, nematode *ced-9*, and baculovirus *op-iap* antiapoptotic genes effectively function in transgenic tobacco plants and their expression confers heritable resistance to fungal phytopathogens: because of these genes, pathogen-induced apoptosis-like PCD does not occur in transgenic tobacco (Dickman *et al.*, 2001).

On the other hand, *bax*, a death-promoting member of the Bcl-2 family of animal proteins, triggered cell death in tobacco plants when expressed from a tobacco mosaic virus (TMV) vector (Lacomme and Cruz, 1999). A protein homologous to Bcl-2 was detected in the leaves of tobacco plants; the protein was mainly associated with mitochondria, plastids, and nuclei (Dion *et al.*, 1997). Expression of murine *Bax* gene in transgenic *Arabidopsis* plants triggered lethality. The *Arabidopsis (Bax inhibitor-1*) gene was isolated and transgenic plants with both *Bax* and *AtBI-1* under different promoters were generated. The *Arabidopsis* plants overexpressing Bax protein under the

control of a dexamethasone-inducible promoter exhibited, after dexamethasone treatment, marked cell death at the whole-plant level, cell shrinkage, membranous destruction, and other apoptotic phenotypes. Plants expressing both *Bax* and *AtBI-1* were able to maintain growth on dexamethasone treatment (Kawai-Yamada *et al.*, 2001). This is direct genetic evidence that the plant antiapoptotic protein AtBI-1 is biologically active in suppressing mammalian *Bax* action. In addition, transient cotransfection of Bax with Bax inhibitor BnBI-1 (from oilseed rape, *Brassica napus* L.) or NtBI-1 (from tobacco) in human embryonic kidney 293 cells revealed that both proteins can substantially inhibit apoptosis induced by Bax overexpression (Bolduc *et al.*, 2003). The plant *oxy5* gene, introduced and expressed in HeLa cells, effectively controls tumor necrosis factor (TNF)-induced apoptosis (Janicke *et al.*, 1998). A gene encoding a protein similar (56% identity) to the human protein PIRIN, a nuclear factor reported to interact with the human oncogene *Bcl-3*, was found in tomato cells (Orzaez *et al.*, 2001). All these facts show that the mechanisms of apoptosis are conserved and similar in plants and animals.

Unfortunately, data on apoptosis in plants are still fragmentary, and various apoptotic factors and pathways in these organisms were found mainly by analogy with that known for animal cells. Nevertheless, apoptosis in plants has many specific features that are not observed in animals. In contrast to animals, apoptotic cells in plants, because of their solid cell walls, do not disappear completely, and they take part in the formation of vascular bundles (Fukuda, 1996, 1997) and aerenchyma (Gunawardena *et al.*, 2001). Apoptotic bodies typical among animals were not detected in the cells of intact plants, but spherical fragments of protoplasts of similar appearance were observed in aging cell cultures (Groover *et al.*, 1997).

B. Morphological and Biochemical Features of Apoptosis in Plants

1. Overview

Apoptosis in plants is manifested in a set of specific changes in cell structure and morphology: chromatin condensation and margination with subsequent decay of the nucleus and internucleosomal nDNA fragmentation; huge vacuoles are formed in the cells (Bakeeva *et al.*, 1999; Groover and Jones, 1999; Kirnos *et al.*, 1997a; Liljeroth and Bryngelsson, 2001; O'Brien *et al.*, 1998a,b; Zamyatnina *et al.*, 2002a,b). The initial step of chromatin condensation occurs before DNA degradation, and it is considered a reversible step in the early stage of apoptosis; the loss of reversibility of chromatin condensation may be a critical point in the cascade of further irreversible changes during apoptosis (O'Brien *et al.*, 1998a,b). Apoptosis-inducing

agents (camptothecin, okadaic acid, salicylic acid, hydrogen peroxide, and calcium ionophore A23187) induce chromatin condensation in tobacco (*Nicotiana plumbaginifolia*) cells (O'Brien *et al*., 1998a). Destruction of tonoplast and vacuolization of cytoplasm usually precedes destruction of the nucleus and mitochondria (Fukuda, 2000). Disruption of cytoskeleton occurs in the early stages of apoptosis (Skalamera and Heath, 1998). In apoptotic cells in roots of maize during aerenchyma formation induced by ethylene or hypoxia, chromatin condensation detectable by electron microscopy is preceded by cytoplasmic changes including plasma membrane invagination and formation of vesicles, in contrast to mammalian apoptosis, in which chromatin condensation is assumed to be the first detectable apoptotic event (Gunawardena *et al*., 2001). Degradation of nuclear DNA (nDNA) occurs near or after vacuole collapse (Groover *et al*., 1997).

In terms of cytological events, Fukuda (2000) categorized at least three types of PCD in plants: (1) apoptosis-like cell death, (2) cell death occurring during leaf senescence, and (3) PCD in which the vacuole plays a central role, as it was observed in *Zinnia* differentiating tracheary elements. Apoptosis-like cell death is accompanied by rapid disruption of nucleus, incomplete degradation of cell organelles, and then low recovery of cell contents. The senescence type of cell death in leaves (Smart, 1994) and other organs proceeds slowly. In this cell death the disruption of the nucleus and vacuole occurs at the end of cell death after thorough degradation of chloroplasts. PCD in which disruption of vacuoles plays an essential role is placed between apoptotic cell death and leaf senescence-type cell death (Fukuda, 2000) in speed of cell death and degree of recovery of cell contents. In cereals even in one and the same organ (coleoptile, leaf) the combination of features of, at least, the first two types of plant PCD may be observed (Vanyushin, 2001).

Apoptotic degradation of DNA in chromatin is due mainly to the action of endonucleases induced by proteases called caspases (a family of cysteine proteases specific for target sites containing aspartate residues) (del Pozo and Lam, 1998). The endonucleases first attack DNA in the regions of rosette loops with liberation of relatively long fragments (50–300 kb). It was observed in tobacco plants as a result of hypersensitive response (Mittler and Lam, 1997; Mittler *et al*., 1997a,b), in apoptotic endosperm cells of developing maize and wheat grains (Young and Gallie, 2000), and BY-2 tobacco cells undergoing cold stress (Koukalova *et al*., 1997). This DNA breakage detected by pulse-field electrophoresis confirmed that processing of maize endosperm genome from 300- to 50-kb fragments occurs between 4 and 16 days after pollination (Young and Gallie, 2000), a period that precedes visible cell death (Young *et al*., 1997). DNA breakage can be detected *in situ* by a terminal deoxynucleotidyl transferase-mediated dUTP nick-end labeling (TUNEL) procedure that reveals DNA 3′ -OH groups (Gavrieli *et al*., 1992). Internucleosomal DNA fragmentation then proceeds, resulting

in the formation of fragments with chain length multiples to about 160–180 bp. It is suggested that initial DNA degradation occurs before cell death whereas the appearance of nucleosome-size DNA fragments follows cell death (Young and Gallie, 2000).

The specific internucleosomal DNA fragmentation was observed in aging wheat coleoptile and initial leaf (Kirnos *et al*., 1997a, 1999a,b), leaves of wheat, barley, and rye (Liljeroth and Bryngelsson, 2002), endosperm of forming maize and wheat seeds (Young and Gallie, 2000; Young *et al*., 1997), endosperm of germinating castor beans (Schmid *et al*., 1999), degenerating nucellus during the early stages of wheat grain development (Dominguez *et al*., 2001), aging cells of carrot cell cultures (LoSchiavo *et al*., 2000; McCabe *et al*., 1997), aging *Arabidopsis thaliana* plants (Callard *et al*., 1996), *Zinnia* and other plants during xylogenesis (Thelen and Northcote, 1989) and differentiation of vascular elements (Beers, 1997; Fukuda, 1996, 1997; Groover and Jones, 1999; Woffenden *et al*., 1998), cucumber cotyledons after heat shock (Balk *et al*., 1999), tobacco cells on cold stress (Koukalova *et al*., 1997), maize root cells triggered by cold stress (Ning *et al*., 2002), root cortex of soybean root necrosis mutants (Kosslak *et al*., 1997), primary roots of both *Arabidopsis thaliana* wild type and sos 1 (salt overly sensitive) mutant seedlings during salt-induced PCD (Huh *et al*., 2002), barley aleurone during seed germination (Bethke *et al*., 1999; Wang *et al*., 1996), developing barley anthers (Wang *et al*., 1999), aging pea carpels (Orzaez and Granell, 1997a,b), oat plants treated with the toxin victorin produced by the causal agent of victoria blight of oats, *Cochliobolus victoriae* (Navarre and Wolpert, 1999), aging petunia petals after flower pollination (Xu and Hanson, 2000), senescent leaves of *Philodendron hastatum*, *Epipremnum aureum*, *Bauhinia purpurea, Delonix regia*, and *Butea monosperma* (Yen and Yang, 1998), induced temperature-sensitive lethal cells of interspecific hybrids from the cross *Nicotiana suaveolens* × *N. tabacum* (Yamada *et al*., 2001), tapetal cells of sunflower plants carrying the PET1-CMS mitochondrial mutation (Balk and Leaver, 2001), haploid megagametophyte of white spruce (*Picea glauca*) seeds during post germinative seedling growth (He and Kermode, 2003), and in various plants infected with various pathogens (Mittler and Lam, 1995, 1997; Wang *et al*., 1996). DNA fragments (50 kb) were formed during PCD in tobacco cells infected with tobacco mosaic virus, but typical internucleosomal nDNA fragmentation (laddering) was not observed (Mittler *et al*., 1997a). DNA fragmentation in wheat and barley roots is indicative of programmed root cortical cell death (Liljeroth and Bryngelsson, 2001).

Unlike some initial reversible phases of apoptosis in plants (O'Brien *et al*., 1998), internucleosomal DNA fragmentation seems to be irreversible and it is one of the terminal apoptotic stages; deep DNA degradation by nonspecific terminal nucleases then follows; similarly to animals, in plant apoptotic cells

the terminal Ca^{2+}-activated nucleases (Xu and Hanson, 2000) rapidly attack single- and double-stranded DNA fragments formed. An increased Ca^{2+} content is typical for plant apoptotic cells. cDNAs for these terminal nucleases were already obtained from barley endosperm or *Zinnia* cells from forming vascular structural elements (Aoyagi *et al*., 1998). Intensive DNA degradation seems to be important for effective elimination of "wrong" DNA that might be formed in apoptotic cells in order to prevent its migration to other cells. On the other hand, this is a way to use DNA products as a suitable nucleic acid material by normal functioning cells in plant developing organs.

Cereal seedlings are unique and useful models for investigation of apoptosis in plants. Their growth may be easily synchronized and, at least, five cycles of synchronous replication of nDNA were observed in an initial leaf during the first 7-day period of seedling development (Kirnos *et al*., 1983). Coleoptile in cereals functions for a relatively short period at the early stage of ontogenesis, and it dies quickly as the seedlings grow and develop. Global nDNA synthesis in coleoptile ceases after a few synchronous replication cycles and this cessation seems to correspond to the beginning of apoptosis in nondividing cells (Kirnos *et al*., 1983, 1999a,b). Discrete peaks of total DNA synthesis in entire leaf at the early stage of wheat seedling development (Fig. 1) seem to correspond to cell cycles in basal meristematic leaf area. It is useful for biochemists, as it allows consideration, in terms of DNA, of an entire organ in an intact developing plant organism as a single cell and to investigate what happens, in particular, with DNA methylation in a cell cycle (Kirnos *et al*., 1995). Contrary to initial leaf, the nuclear DNA increase in coleoptile stops on day 4 of seedling life (Fig. 1); thus, the stopping of nDNA ($\rho = 1.700$ g/cm^3) synthesis in coleoptile is strictly arranged temporally in a program functioning at an early stage of seedling development. This is an obligatory beginning step of apoptosis and organoptosis. Soon after that the apoptotic DNA fragmentation in coleoptile becomes consistently detectable (Fig. 2). There is no nDNA replication; only mitochondrial DNA (mtDNA) ($\rho = 1.718$ g/cm^3) continues to be synthesized in coleoptile. It is possible that apoptosis in various plant organs of one and the same plant is somehow coordinated and that it depends on the number of cell divisions in the basal (meristematic) part of coleoptile and leaf. When apoptosis proceeds in the coleoptile it is also detectable in a proximal part of an initial leaf (Fig. 2). Unfortunately, it is unknown how the apoptotic signal is transmitted from cell to cell. A new *H52* gene found in tomato plants encodes transcription factor protein *HD*-Zip, which seems to control apoptotic signal expansion in plant leaves (Mayda *et al*., 1999). In plants with a suppressed *H52* gene, unlike control plants, apoptosis is not limited to single cells but captures all leaves with activation of pathogen-related genes and a strong increase in ethylene and salicylic acid (Mayda *et al*., 1999).

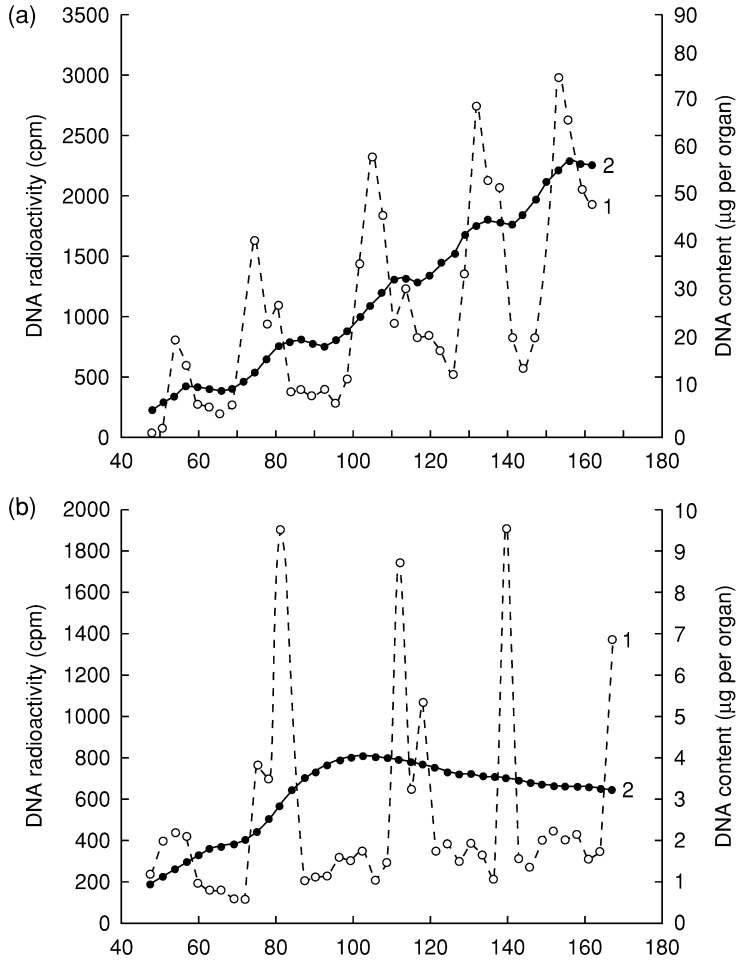

FIG. 1 DNA synthesis in an initial leaf (a) and coleoptile (b) of etiolated wheat seedlings. Curve 1, DNA radioactivity (cpm); curve 2, DNA content (μg per organ); abscissa, seedling age (h) (Kirnos *et al.*, 1983).

As already mentioned, in young wheat seedlings internucleosomal DNA fragmentation was also clearly observed in the initial leaf but it was detected only in the apical (i.e., most senescent) leaf part (Bakeeva *et al.*, 2001; Kirnos *et al.*, 1999b). This could testify to the fact that along with aging coleoptile apoptosis also appears in young developing initial leaf. This conclusion was quite unexpected and even unlikely because apoptosis was usually observed only in senescent but not young leaves (Nooden *et al.*, 1997; Yen and Yang,

1998). Besides, apoptosis is known to be typical for leaf aging and dying (Nooden *et al*., 1997). DNA extracted from leaves of 3-week-old wheat but not barley plants showed internucleosomal fragmentation (Liljeroth and Bryngelsson, 2001, 2002). To be sure that we are actually dealing with apoptosis in initial leaf, along with the observation of nuclear DNA fragmentation (Bakeeva *et al*., 2001) some other evidence of apoptosis at the level of the ultrastructural organization of the cell, at least, was also needed.

2. Ultrastructural Features of Apoptotic Parenchyma Cells in Coleoptile and Apical Area of Initial Leaf of Etiolated Wheat Seedling

a. Cytoplasm The volume of protoplasts in apoptotic cells of aging wheat coleoptile is significantly decreased; the cell component consists of a narrow layer located near the cell wall (Kirnos *et al*., 1999a). Polymorphous suspended cytoplasmic bodies (vesicles) were first detected in gigantic cell vacuoles of aging coleoptile (Fig. 3A). These structures are covered with a single membrane, and their interior is filled with cytoplasm containing one or more mitochondria (Bakeeva *et al*., 1999). In young coleoptiles (3-day-old seedlings) similar bodies were observed rarely, only in the cells of the extreme apical part of the coleoptile, which is the most senile part of the organ. These bodies contain plastids, mitochondria, or both (Fig. 3A and C). Despite the presence of vesicles in the cell vacuole in young coleoptiles there was no marked heavy mitochondrial DNA (H-mtDNA) synthesis, in contrast to that in old coleoptiles. Similar bodies were observed later in cytoplasm of maize root cells during aerenchyma formation induced by hypoxia or ethylene (Gunawardena *et al*., 2001).

Serial sectioning revealed the process of formation of vesicles detected in the cell vacuole: tonoplast forms protrusions filled with cytoplasm, and some mitochondria are transferred there (Fig. 4A–D) (Kirnos *et al*., 1997a). These outgrowths are separated later and, as a result, suspended polymorphous bodies covered with a membrane and containing mitochondria appear in vacuoles (Bakeeva *et al*., 1999; Kirnos *et al*., 1997a). This process is most intensive in parenchymal cells of the middle zone of aging coleoptile. There is practically no protoplast in the cells of the apical zone of such coleoptiles; in this zone only certain cells with an electron-dense tonoplast layer located near the cell wall and sometimes containing condensed mitochondria occur (Kirnos *et al*., 1997a).

A fraction consisting of unusual closed membrane vesicles was isolated first from homogenates of senescent wheat coleoptiles by differential centrifugation (Kirnos *et al*., 1997a). Electron microscopy investigation of the fraction showed that it is a suspension of specific subcellular particles with an unusual mode of organization. Like in an intact plant, these particles are single-membrane structures filled with cytoplasmic matrix and they contain

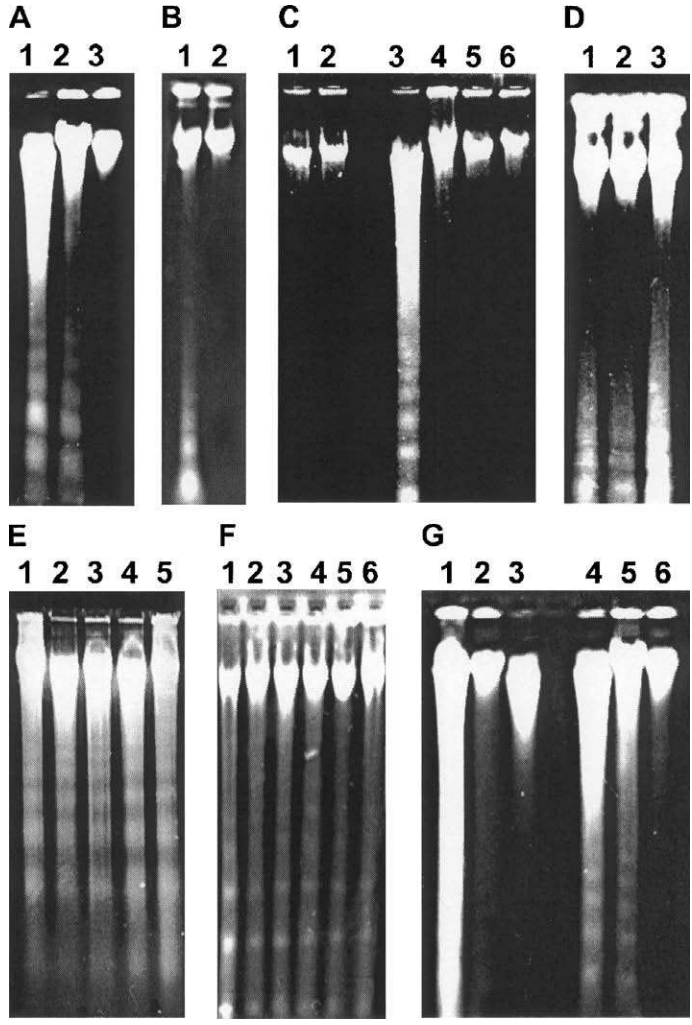

FIG. 2 Electropherograms of DNA isolated from coleoptiles (leaves) of etiolated wheat seedlings. (A) DNA from coleoptiles of control (grown on water) seedlings of various age: lane 1, 8-day-old seedlings; lane 2, 6-day-old seedlings; lane 3, 4-day-old seedlings. (B) DNA from initial leaf of control 8-day-old seedlings: lane 1, apical leaf part (1.0-cm-long stretch); lane 2, basal leaf part (1.0-cm-long stretch). (C) DNA from coleoptiles of: lane 1, 4-day-old seedlings grown in the presence of BHT (50 mg/liter); lane 2, 6-day-old seedlings grown in the presence of BHT (50 mg/liter); lane 3, control 8-day-old seedlings grown on water; lane 4, 8-day-old seedlings grown in the presence of BHT (1 mg/liter); lane 5, 8-day-old seedlings grown in the presence of BHT (10 mg/liter); lane 6, 8-day-old seedlings grown in the presence of BHT (50 mg/liter). (D) DNA from coleoptiles of 8-day-old seedlings. Seedlings were grown in the presence of: lane 1, 10^{-5} *M* 3,5-di-*tert*-butyltoluene; lane 2, 10^{-5} *M* ascorbic acid (sodium ascorbate), pH 5.5; lane 3, control (seedlings grown on water). (E) DNA from coleoptiles of

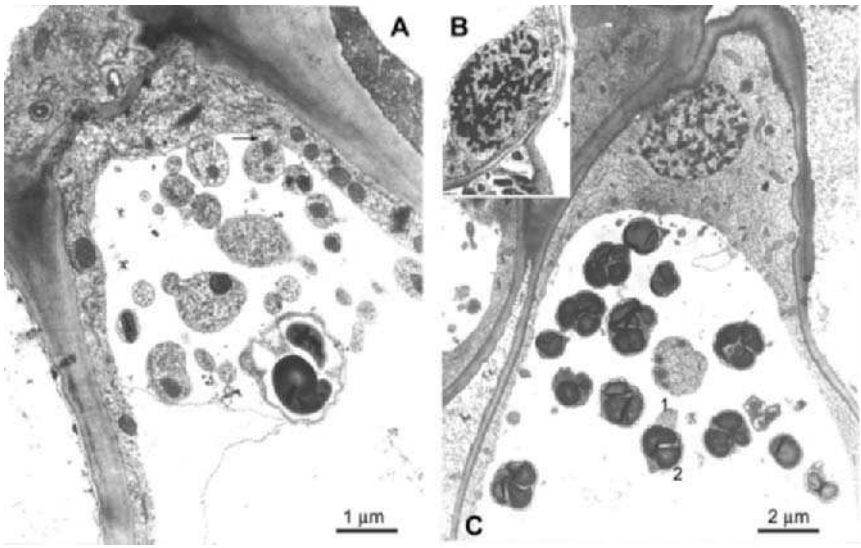

FIG. 3 Structure of parenchymal cells in the apical part of the coleoptile of a 3-day-old etiolated wheat seedling. (A) Cell fragment. Vesicles formed are seen in the cellular vacuole (arrow) (Bakeeva *et al.*, 1999). (B) Nucleus with marginated chromatin (neighboring cell). (C) Cell fragment. Vesicles containing subcellular organelles are seen in a vacuole: Mitochondrion (1) and plastid (2) (Zamyatnina *et al.*, 2002b).

one or more mitochondria (Fig. 4E and F). Sometimes ribosomes and microtubules may also be seen in these vesicles. Thus, isolated, unusually fast-sedimenting particles (Bakeeva *et al.*, 1999; Kirnos *et al.*, 1999a) are not artifacts, but do exist in an intact plant. They are most common in cells of old coleoptiles.

In plants, like in animals, aging is accompanied by an essential increase in the amount of mitochondrial DNA. In aging plant organs synthesis of heavy mitochondrial DNA (H-mtDNA, $\rho = 1.718$ g/cm^3) occurs mainly in the

8-day-old seedlings grown on water (lane 1, control) or for the last 6 days in the presence of 10^{-5} *M* phytohormones such as the following: lane 2, gibberellin (GA_3); lane 3, 6-benzylaminopurine; lane 4, 2,4-D; lane 5, fusicoccin C. (F) DNA from coleoptiles of cut wheat seedlings; lanes 1–4, 6-day-old seedlings were grown on water for 6 days and then were cut and incubated for 2 days in the presence of 10^{-5} *M* phytohormones: lane 1, abscisic acid; lane 2, 2,4-D; lane 3, 6-benzylaminopurine; lane 4, gibberellin (GA_3). Lane 5, DNA from coleoptiles of intact 8-day-old seedlings grown on water (control); lane 6, DNA from coleoptiles of control 6-day-old seedlings that were cut and then incubated on water for an additional 2 days. (G) DNA from coleoptiles of wheat seedlings grown in the presence of 5-azacytidine (100 μg/ml; lanes 1–3) or on water (lanes 4–6). Seedling age: lanes 1 and 4, 8 days; lanes 2 and 5, 6 days; lanes 3 and 6, 4 days (Bakeeva *et al.*, 2001).

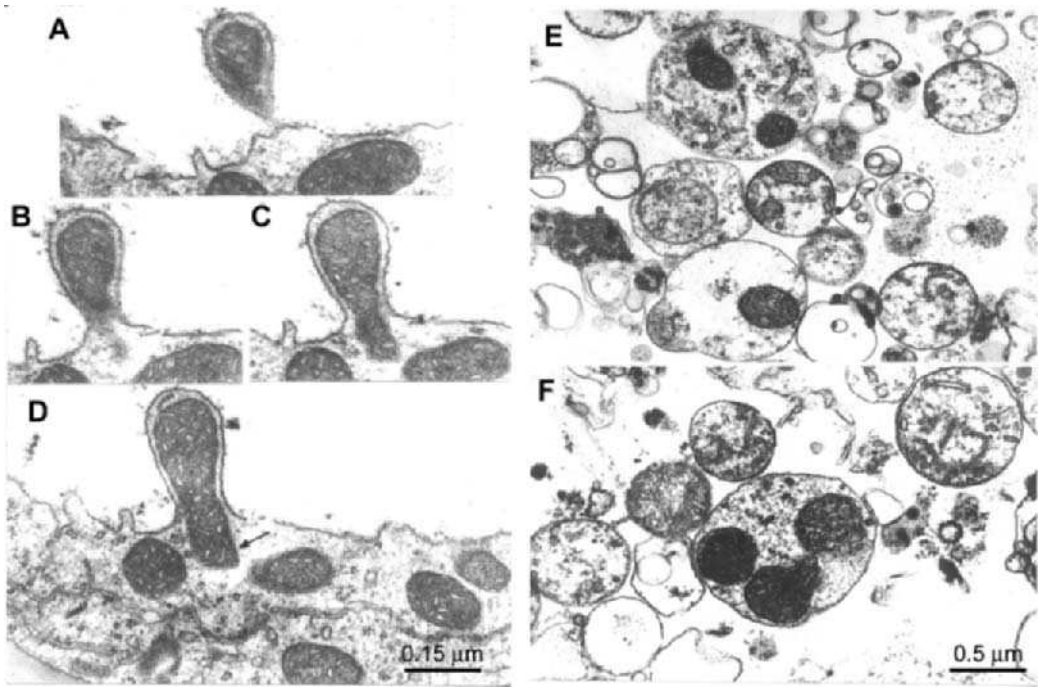

FIG. 4 Vesicle forming in the vacuole of a coleoptile parenchymal cell of an 8-day-old etiolated wheat seedling. (A–D) Serial sections. Arrow shows tonoplast protrusion and a mitochondrion displaced into a forming vesicle (Kirnos *et al*., 1999a). (E and F) Fractions of subcellular particles (vesicles) isolated from coleoptiles of 8-day-old wheat seedlings (Bakeeva *et al*., 1999).

vesicles described (Bakeeva *et al*., 1999). After incubation of seedlings in the presence of [^{3}H]thymidine the peak of radioactivity incorporated into DNA with buoyant density corresponding to that of newly formed H-mtDNA was observed in the fast-sedimenting vesicles containing mitochondria but not in free mitochondria (Bakeeva *et al*., 1999). H-mtDNA does not contain 5-methylcytosine (Kirnos *et al*., 1997a), but it has N^6-methyladenine (Vanyushin *et al*., 1988). Synthesis of H-mtDNA strongly increases with seedling age, it is specific for various higher plants including angiosperms and archegoniates (Kirnos *et al*., 1992a), and the amount of this DNA may correspond to 10–15% of that of nuclear DNA (Kirnos *et al*., 1997b). A strong increase in mtDNA content in the absence of nuclear DNA replication was also observed in aging animal cells; in *in vitro*-grown fibroblasts it is H_2O_2 dose dependent (Lee *et al*., 2000).

Vacuolar vesicles isolated from aging wheat coleoptiles contain a unique adenine DNA-methyltransferase (Fedoreyeva and Vanyushin, 2002). In the presence of *S*-adenosyl-L-methionine the enzyme *de novo* methylates the first adenine residue in the TGATCA sequence in single- or double-stranded DNA substrates, but it prefers single-stranded structures. This wheat adenine DNA-methyltransferase (*wadmtase*) is a Mg^{2+}- or Ca^{2+}-dependent enzyme with a maximum activity at pH 7.5–8.0. *wadmtase* seems to be responsible for mitochondrial DNA modification that might be involved in the regulation of replication of mitochondria in plants (Fedoreyeva and Vanyushin, 2002).

Similar to free mitochondria, the vesicles consume oxygen intensively. The respiration rates of vesicular and free mitochondria are similar; they correspond to 145 $\pm$ 15 and 160 $\pm$ 20 μM O_2/min per milligram of protein, respectively. Inhibitors of the respiration chain selectively decreased the respiration rate of mitochondria of both kinds. For example, myxothiazol (Q-cycle inhibitor) at a concentration of 2×10^{-6} *M* suppressed the respiration of vesicles and free mitochondria by 77 and 67%, respectively. The CN-insensitive (alternative) oxidation pathway was inhibited by 2 m*M* butylhydroxamic acid in vesicles and free mitochondria by 18% and 11%, respectively. Cyanide (2 m*M*) added after myxothiazol additionally decreased the residual respiration rate of both fractions by 15–20%. The content and composition of cytochromes in vesicles and the mitochondrial fraction isolated from coleoptiles of 8-day-old seedlings are similar (Bakeeva *et al*., 1999). The vesicle fraction contains about 2-fold more Ca^{2+} (195 nmol/mg protein) compared with free mitochondria (83 nmol/mg protein). It may be because vesicles are localized inside the vacuole, which could be a sort of depot for excessive Ca^{2+}. It also cannot be ruled out that the products of pronounced apoptotic degradation of nuclear DNA in these aging coleoptiles may accumulate in such vacuoles and form there the pool of precursors for superproduction of H-mtDNA in vesicles. Thus, in addition to free mitochondria some population of mitochondria in plants may exist and function in special

suspended vesicles formed by vacuolar membranes in undividing cells. The principal specific feature of mitochondria of these vesicles in senescent cells only is the strong synthesis of heavy GC-enriched mitochondrial DNA (H-mtDNA, GC = 56–58%). Synthesis of H-mtDNA starts at a certain moment in plant ontogenesis during aging of the individual organ (Kirnos *et al.*, 1997a). The biological meaning of intensive H-mtDNA synthesis in aging plant organs is still unclear. In any case, aging associated with apoptosis in wheat coleoptile cells is accompanied by formation of mitochondria that intensively synthesize H-mtDNA in special vesicles located in vacuoles. Unfortunately, the true functional role of H-mtDNA and the vesicles described is still unknown. It may be assumed that the new form of cytoplasm organization (vesicles) observed may to some extent discriminate between mitochondria and preserve their structure and activity, and, in particular, their ability to synthesize H-mtDNA in the process of cell aging and death.

Cells with obvious ultrastructural features of apoptosis were observed by electron microscopy in sections of the apical part of the initial leaf in 5-day-old etiolated wheat seedlings. A large central vacuole and a narrow, electron-dense, wall-located tonoplast layer are specific to such cells (Fig. 5).

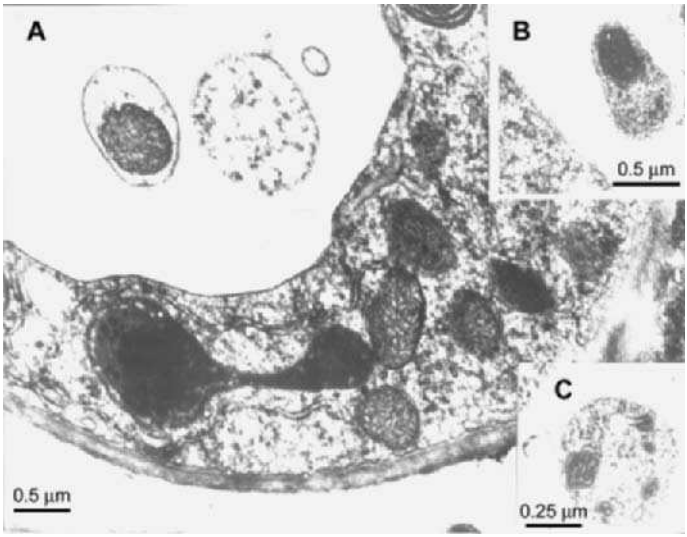

FIG. 5 Fragments of parenchymal cells of the apical part of an initial leaf of etiolated wheat seedlings of various age. (A) Fragment of the leaf cell of a 5-day-old wheat seedling. A vesicle containing an electron-dense mitochondrion is seen in the vacuole. (B) Vesicle with electron-dense mitochondrion in vacuole in the cell of the initial leaf of an 8-day-old etiolated wheat seedling grown in the presence of BHT (50 mg/liter). (C) Vesicle containing an electron-dense mitochondrion in the vacuole of a cell in an initial leaf of an 8-day-old etiolated wheat seedling grown on water (control plant) (Zamyatnina *et al.*, 2002b).

The cytoplasm in these cells does not have any visible signs of destruction; it contains many elements of Golgi apparatus, endoplasmic reticulum, and all main cellular organelles—nuclei, mitochondria, plastids, and ribosomes. Ribosomes are represented by polyribosomal complexes or they are associated with membranes of the endoplasmic reticulum. The main population of plastids in these cells is represented by chloroplasts with a relatively well-developed thylakoid system. Amyloplasts were also observed among plastids. In the cytoplasm of these cells, mitochondria with electron-dense structure are present; similar mitochondria are specific for apoptotic animal cells (James *et al*., 1993). The condensed ultrastructure of mitochondria in the cells of the initial leaf of wheat seedling may also be considered an index of developing apoptosis. In addition, myelin-like structures appear in the cytoplasm of cells of the apical part of the initial leaf in 5-day-old seedling. This also testifies to the development of the aging process in the initial leaf.

As in coleoptile apoptotic cells, single-membrane vesicles containing subcellular organelles were observed in vacuoles of apoptotic cells of the initial leaf. In leaf apoptotic cells these vesicles contain mainly plastids, not mitochondria as in the cells of aging coleoptile (Fig. 3A). Vesicles containing mitochondria were also observed in the initial leaf (Fig. 5), but less frequently compared with coleoptile. It is worth mentioning that vesicles containing plastids were observed only in apoptotic cells with a narrow tonoplast layer or almost without tonoplast.

Thus, formation in the cellular vacuole of vesicles with subcellular organelles is a specific feature that is common among apoptotic plant cells. It occurs in functionally different and specialized plant organs (tissues) such as leaf and coleoptile. This amazing event observed in the apoptotic plant cell—the separation of some parts of the cytoplasm with organelles as closed single-membrane vesicles and their escape into the cellular vacuole—seems to some extent similar to blebbing of apoptotic animal cells. Fragmentation of the cytoplasm is one of the main ultrastructural features of apoptosis in animals. But this similarity is only apparent. In contrast to blebs as elements of rapid reorganization and decay of the cytoplasm in animals, the vacuolar vesicles in an apoptotic plant cell seem to play other functional roles. First of all, the plant vesicles observed differ from all known specific cellular depots where rapid degradation of cellular structures and biopolymers takes place. They have nothing in common morphologically and functionally with ricinosomes discovered in senescing plant tissues, the specific organelles delivering large amounts of a papain-type cysteine endopeptidase at the final stages of cellular disintegration (Gietl and Schmid, 2001). Marks of degradation were never observed in the subcellular structures located in Ca^{2+}-enriched vesicles in wheat coleoptile cells. Nor were there signs of degradation in plastids and mitochondria in the vacuolar vesicles of cells of the wheat initial leaf (Fig. 5). It seems that conditions for organelle survival in

vesicles are even more comfortable than in other cytoplasmic compartments of the apoptotic plant cell. As mentioned already, mitochondria in these vesicles have intact structures and they consume oxygen actively (Bakeeva *et al.*, 1999). This obviously cannot be a property of degenerating subcellular organelles. Besides, active replication of mtDNA in the cells of aging coleoptile takes place in these vesicles (Bakeeva *et al.*, 1999) in spite of concomitant degradation of the apoptotic cell. Therefore, the vesicles observed seem to shelter and preserve some share of segregated organelles, at least, for some period during the process of apoptotic death of the cell. One cannot rule out that the strong replication of mtDNA in vesicles observed is due to alienation of vesicular mitochondria from the nucleus compared with free (nonvesicular) mitochondria and loss of the nuclear control for replication of this mtDNA. But the true sense and possible biological significance of these peculiar events are still unknown. In any case, in the cells of aging coleoptile and developing initial leaf of wheat seedlings the individual populations of organelles containing DNA are formed as a result of the fragmentation of the cytoplasm in the process of apoptosis. These organelles (mitochondria) are able to synthesize their own DNA under conditions of DNA degradation in the nucleus. The material of degrading nuclear DNA seems to be used for the synthesis of this mtDNA. It might be that some part of the mitochondrial and plastid DNAs newly formed in vesicles of the apoptotic cell does not perish but somehow migrates to neighboring cells. In this particular case, the age (apoptotic) superproduction of mtDNA in plants (Kirnos *et al.*, 1992a, 1997b, 1999a,b) could be quite appropriate. The transposition of mtDNA (mainly plasmid-like circular molecules of various contour lengths) (Kirnos *et al.*, 1992b) or plastid DNA from cell to cell has not yet been described. Nevertheless, this cannot be ruled out because plant cells are easily transformed by bacterial plasmid DNA and active intercellular transport of viral infections occurs in plants.

b. Nucleus Marked condensation and margination of chromatin are seen in the nuclei of apoptotic cells in the apical part of coleoptile (Fig. 3B) and initial leaf (Zamyatnina *et al.*, 2002b) in 3- to 5-day-old etiolated wheat seedlings. These visible apoptotic changes in chromatin organization may be associated with nuclear lamina solubilization and proteolytic degradation of lamins in plant nucleus preceding the domain and internucleosomal fragmentation of nuclear DNA (Sun *et al.*, 1999b).

Apoptotic DNA fragmentation in the coleoptile cells of an intact etiolated wheat seedling is a strongly programmed event in ontogenesis, and it appears clearly on the sixth day of seedling life (Fig. 2A, lane 2); in 8-day-old seedlings this process is strongly pronounced (Fig. 2A, lane 1). Apoptotic DNA fragmentation was also detected in the apical part of the initial leaf blade (Fig. 2B, lane 1), that is, in the oldest leaf zone with nondividing cells. This contrasts with the situation in coleoptile, where most cells are

synchronously involved in apoptosis. Thus, the aging of organs (initial leaf, coleoptile) in developing wheat seedlings, like leaf aging in other plants (Yen and Yang, 1998), is accompanied by apoptosis.

c. Conclusions The distinct features of apoptosis in coleoptile and the initial leaf of etiolated wheat seedlings are (1) compaction and vacuolization of cytoplasm in the apoptotic cell, (2) specific fragmentation of cytoplasm and appearance in the vacuole of unique single-membrane vesicles containing active organelles, (3) cessation of nuclear DNA synthesis, (4) condensation and margination of chromatin in the nucleus, (5) internucleosomal fragmentation of nDNA, and (6) intensive synthesis of mitochondrial DNA in vacuolar vesicles. Similar apoptotic events and features were observed in wheat seedlings grown in normal day light. These specific features of apoptotic cells observed in developing wheat seedlings seem to serve as markers of apoptosis in plants in general.

III. ROS-Induced Apoptosis in Plants

A. Oxidative Status and Apoptosis

Plants are constantly subjected to oxidative stress due, in particular, to photosynthesis, a powerful oxygen-producing process. The concentration of molecular oxygen in leaves may be high, and a significant part of the O_2 converts to reactive oxygen species (ROS)—superoxide anion, hydrogen peroxide, and hydroxyl radical. In addition, in mitochondria ROS are generated actively as undesirable side products of oxidative energy metabolism. Superoxide anion is formed by the univalent reduction of triplet-state molecular oxygen ($^3O_2$). This process is mediated by enzymes such as NAD(P)H oxidases and xanthine oxidase or nonenzymatically by redox-reactive compounds such as the semiubiquinone compound of the mitochondrial electron transport chain (Dröge, 2002). There are many ways to enzymatically or nonenzymatically inactivate ROS in plants. Active plant superoxide dismutases (SODs) convert superoxide into hydrogen peroxide. In biological tissues superoxide can also be converted nonenzymatically into the nonradical species hydrogen peroxide and singlet oxygen ($^1O_2$). In the presence of reduced transition metals (e.g., ferrous or cuprous ions), hydrogen peroxide can be converted into highly reactive hydroxyl radical (•OH). This event is extremely dangerous for any living cell, and in plants there exists an effective alternative transformation of hydrogen peroxide into water by the enzymes catalase or glutathione peroxidase. In animals an excessive and/or sustained

increase in ROS production has been implicated in premature aging and pathogenesis of many diseases (cancer, diabetes mellitus, atherosclerosis, ischemia, and other diseases). The well-known free radical theory of aging (Harman, 1956) is true and common for plants as well as for other organisms.

Along with their destructive effect, ROS have important signal functions in the cell: they control the cell cycle and trigger programmed cell death (PCD) in plants (Jabs, 1999). For example, H_2O_2 serves as a main signal of regulation of the cell cycle and PCD in plants; it stimulates a rapid inflow into cells of Ca^{2+} (Levine *et al.*, 1996), an ion playing the role of a secondary pro-apoptotic signal. H_2O_2 activates cell death and defense gene expression in birch leaves (Pellinen *et al.*, 2002).

H_2O_2 induces various morphological cell death features (cell shrinkage, chromatin condensation, and DNA fragmentation) in cultured tobacco BY-2 cells (Houot *et al.*, 2001). H_2O_2 and salicylic acid (SA) treatment of tobacco cells caused a rapid rise in intracellular ROS accumulation accompanied by induction of many apoptotic genes that, when prevented by antioxidant treatment, resulted in inhibition of gene induction (Maxwell *et al.*, 2002). Transgenic tobacco cells lacking alternative oxidase show increased susceptibility to three different death-inducing compounds (H_2O_2, SA, and the protein phosphatase inhibitor cantharidin) in comparison with wild-type cells. Death induced by H_2O_2 or SA occurs by a mitochondria-dependent pathway characterized by cytochrome *c* release from mitochondria. Conversely, death induced by cantharidin occurs by a pathway without any obvious mitochondrial involvement. Thus, plants maintain both mitochondria-dependent and -independent pathways of PCD (Robson and Vanlerberghe, 2002).

In *Arabidopsis* plants H_2O_2 activates genes for specific mitogen-activated protein kinases (MAP kinases) that are responsible for inactivation of auxin signals (Kovtun *et al.*, 2000). Therefore, oxidative stress may result in elimination of some phytohormonal signals.

ROS play a central role in the activation and propagation of pathogen-induced PCD in plants. Virally induced PCD in tobacco cells is accompanied by suppression of cytosolic ascorbate peroxidase, a key H_2O_2-detoxifying enzyme; therefore, H_2O_2 increases in infected cells and PCD is accelerated (Mittler *et al.*, 1998). Both exogenous H_2O_2 and bacterial elicitor harpin induce PCD in *Arabidopsis* cell suspension cultures; PCD induced by H_2O_2 is accompanied by expression of plant resistance (PR) genes encoding phenylalanine ammonia-lyase and glutathione-*S*-transferase (Desikan *et al.*, 1998). Superoxide accumulates in the cells of *lsd1 Arabidopsis* plant mutants and induces their apoptosis (Jabs *et al.*, 1996). ROS-dependent *isd1* gene of negative control for pathogen-induced apoptosis, was found in *Arabidopsis*; this gene encodes a zinc finger-containing protein that seems to be a transcription factor (Dietrich *et al.*, 1997).

H_2O_2 induces synthesis of many PR proteins and formation of ethylene and salicylic acid in tobacco plants (Chamnongpol *et al.*, 1998). Pathogen-induced PCD was diminished at low partial oxygen pressure (Mittler *et al.*, 1996); on the other hand, in the cells of transgenic plants in which the gene encoding endogenous catalase is inhibited (Chamnongpol *et al.*, 1998), PCD and the synthesis of PR proteins are strongly enhanced. The PR genes were mostly activated at sublethal ROS doses, but there was no visible PCD induction (Chamnongpol *et al.*, 1998). In plants (Keller *et al.*, 1998), like in animals, NADPH-oxidase is involved in ROS formation. Small GTP-binding *rac* protein with GTPase activity inhibits plant NADPH-oxidase and PCD induction (Kawasaki *et al.*, 1999). *OsRac1* gene expressed in transgenic rice plants suppresses ROS formation and PCD induced by caliculin A (inhibitor of protein phosphatase I) and phytopathogenic fungus (Kawasaki *et al.*, 1999).

The hypersensitive response, formation of lipid peroxides and PCD, of leaf cells is strongly enhanced but formation of phenolics (probably natural antioxidants) is diminished in transgenic tobacco plants with expressed transcription factor gene *AmMYB308*. This phenotype with premature aging may be reverted to initial wild type by addition of phenolic precursors to cell culture (Tamagnone *et al.*, 1998). This shows that natural phenolics, like flavones, carotenoids, ascorbic acid, α-tocopherol, and other antioxidants, play an essential protective role in plants; they diminish the risk of premature cell death. Synthetic antioxidants (BHT) may induce synthesis of natural antioxidants, probably carotenoids, in etiolated wheat seedlings (Shorning *et al.*, 1999).

ROS formation and induction of PCD (similar to plant and animal PCD) were increased in cells of the dinoflagellate *Peridinium gatunense* grown under CO_2 deficiency in water; ROS-induced cell death was inhibited by saturation of medium with CO_2, and it was also suppressed by catalase and cysteine protease inhibitor E-64 (Vardi *et al.*, 1999).

les22, encoding one of the enzymes of porphyrin metabolism in maize, is involved in the formation of heme, which is essential for the functioning of catalase and ascorbate peroxidase. Inactivation of this gene results in strong accumulation of ROS that induce pathogen-independent apoptosis (Hu *et al.*, 1998). As result of this gene mutation the cells produce a photoreactivated intermediate that generates ROS under intensive illumination. Gene *lls1*, encoding a protein destroying phenolics, also takes part in the regulation of apoptosis in maize (Gray *et al.*, 1997); pathogen-independent apoptosis proceeds in cells lacking this protein (enzyme). It was noticed that H_2O_2-induced death of soybean cells is strongly suppressed in the presence of inhibitors of poly(ADP-ribose)-polymerase, an enzyme essential for realization of the apoptotic process (Amor *et al.*, 1998).

oxy5 was induced in *Arabidopsis thaliana* plants subjected to oxygen stress (Janicke *et al.*, 1998). Expression of this plant gene in transformed bacteria

makes them resistant to oxygen stress. Plant cell death induced by oxygen stress is similar to TNF-induced apoptosis in animal cells. After *oxy5* was introduced into TNF-sensitive HeLa D98 cells they transformed into TNF-resistant cells with low ROS levels and high manganese SOD activity (Janicke *et al.*, 1998). Thus, plant protein may control TNF-induced apoptosis in animal cells.

ATAO1, encoding copper-dependent aminooxidase, was found in *Arabidopsis* plants (Moller and McPherson, 1998). This enzyme catalyzes oxidation of diamines (putrescine and others) with formation of respective aldehydes, ammonia, and hydrogen peroxide that stimulate apoptosis. Regulation of polyamine content in plants may be an important element in the control of apoptosis as polyamines are known to trigger mitochondria-dependent apoptosis in animals. The air pollutant ozone increases formation of $O_2^{\bullet -}$ and H_2O_2 and it stimulates PCD in plants (Pellinen *et al.*, 1999).

Thus, the nature of the ROS, and the sources and metabolic pathways of ROS formation in plant cells, are quite different. Maintaining internal oxidative status, as a sort of homeostatic ROS balance, in plant cells is of crucial importance for the life of the entire plant and induced death.

B. ROS and Antioxidants in a Wheat Seedling Life

The development of etiolated wheat seedling is accompanied by cyclic changes in the rate of $O_2^{\bullet -}$ production both in the entire intact seedling and in its separate organs (leaf, coleoptile) (Shorning *et al.*, 2000). The first increase in the rate of $O_2^{\bullet -}$ production is clearly observed during days 2–4 of seedling development, and then the rate of $O_2^{\bullet -}$ production decreases to the initial level. It then increases again for 2 days to a new maximum (Fig. 6). An increase in $O_2^{\bullet -}$ production in the first 4 days of seedling development correlates with an increase in DNA (Fig. 7A) and protein (Fig. 7B) contents in the coleoptile. DNA content reaches a maximum with the first maximum of superoxide anion ($O_2^{\bullet -}$) formation (Shorning *et al.*, 2000). The second peak of increased $O_2^{\bullet -}$ production, observed on day 6 or 7 of seedling development, coincides with a decrease in DNA and protein contents and apoptotic internucleosomal nuclear DNA fragmentation in the coleoptile.

Incubation of seedlings in the presence of the antioxidant BHT (ionol) diminishes the amount of ROS detected (Fig. 6) and it strongly affects seedling development but does not influence the increase in DNA and protein contents for the initial 4 days of seedling life. It slows down the subsequent age-dependent decrease in protein content (Fig. 7B) and fully prevents the age-dependent decrease in DNA content (Fig. 7A) in the coleoptile. Efficient prevention of apoptosis by BHT, correlating with BHT inhibition of ROS formation in wheat coleoptiles, shows that ROS may in fact trigger apoptosis in seedling tissues.

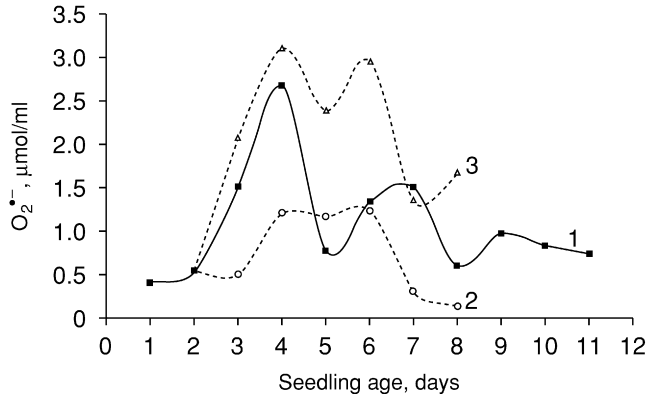

FIG. 6 Amount of $O_2^{\bullet-}$ detected in medium after incubation of intact etiolated wheat seedlings for 1 h in the presence of Triton X-100 (1 mg/ml): curve 1, control seedlings grown on water; curve 2, seedlings grown in the presence of 2.3×10^{-4} *M* BHT; curve 3, seedlings grown in the presence of 10^{-4} *M* benzyl chloride. To evaluate the amount of $O_2^{\bullet-}$ evolved into the medium, the differential spectrum of reduced tetranitro blue tetrazolium chloride was registered in samples with or without the addition of superoxide dismutase (1 μg/ml). Two wheat seedlings were placed in each of two cuvettes containing 4 ml of incubation medium and incubated at 25°C in daylight for 1 h. Absorption of reduced tetranitro blue tetrazolium chloride was measured at 530 nm. Abscissa, seedling age starting from seed imbibition (days); ordinate, the amount of $O_2^{\bullet-}$ evolved for 1 h (Shorning *et al.*, 2001).

1. Influence of BHT on Wheat Seedling Growth and Morphology

BHT significantly affects seedling growth and development. Moderate growth retardation by BHT was clearly observed even at concentrations 1–10 mg/liter (Bakeeva *et al.*, 2001). But at 50 mg/liter (2.27×10^{-4} *M*), the retardation of growth by BHT is expressed most strongly. Other xenobiotics (3,5-di-*tert*-butyltoluene, benzyl chloride) did not show a similar effect: wheat seedlings grown in the presence of these compounds at the same maximal concentration as for BHT did not differ morphologically from control plants (Shorning *et al.*, 1999). In animals (Vanyushin *et al.*, 1998) a marked reversible physiological effect of BHT on activation and induction of various processes, including DNA methylation and others, is most clearly seen at similar BHT concentrations (50 mg/kg body mass).

Coleoptile growth stops in 6-day-old control seedlings, and then the coleoptile length decreases (Shorning *et al.*, 1999); this is associated with coleoptile aging that coincides with intense apoptotic internucleosomal fragmentation of nuclear DNA (Kirnos *et al.*, 1999) and the appearance in the cytoplasm of specific vesicles containing mitochondria intensively producing heavy mitochondrial DNA (Bakeeva *et al.*, 1999). In contrast to control, in seedlings grown in the presence of BHT coleoptile growth did not stop during

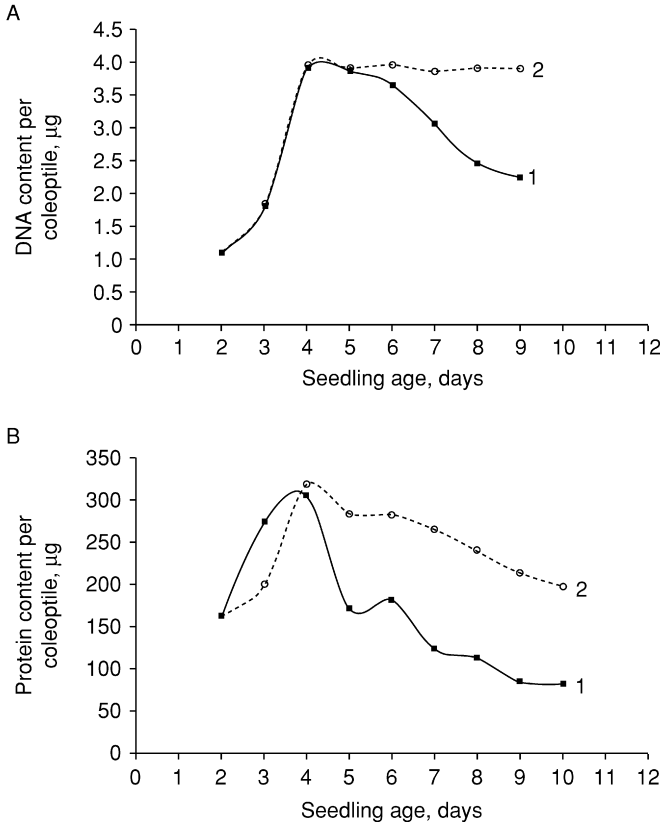

FIG. 7 DNA (A) and protein (B) content in wheat coleoptiles: Curve 1, coleoptiles of control seedlings (grown on water); curve 2, coleoptiles of seedlings grown in the presence of 2.3×10^{-4} *M* BHT. The DNA and protein amounts are given in micrograms per coleoptile (Shorning *et al.*, 2001).

the entire incubation period (11 days) (Shorning *et al.*, 1999). BHT inhibits aging of the coleoptile and postpones its programmed death by more than 30%. Thus, similarly to animals, BHT is an effective geroprotector in plants.

2. Influence of BHT on Content and Synthesis of DNA in Coleoptiles

In contrast to control etiolated plants, the decrease with age in DNA content in coleoptiles did not occur during the entire observation period of a few days when seedlings were grown in the presence of BHT (Fig. 7A). Thus, in the presence of BHT the decay of DNA is evidently postponed and the coleoptile

life span should be increased by at least 4 days, that is, by 30% (Kirnos *et al.*, 1992a,b, 1997a,b; Vanyushin *et al.*, 1988).

The synthesis of specific heavy mitochondrial DNA (H-mtDNA) in coleoptiles of control wheat seedling begins on the fourth day of seedling life, during the first maximum of $O_2^{\bullet -}$ formation. H-mtDNA is enriched with GC base pairs ($\rho = 1.718$ g/cm^3) when compared with nuclear DNA ($\rho = 1.700$ g/cm^3) and it consists mainly of circular molecules of various contour lengths (Kirnos *et al.*, 1992b). The increase in the amount of mtDNA coincides with the apoptotic fragmentation of DNA in the nucleus, and it may serve as an additional sign of apoptosis in plants. Unfortunately, the nature of the signal to increase the synthesis of H-mtDNA is unknown. ROS formed in the cell could be a good candidate for such signals because, during the growth of seedlings in the presence of BHT, that is, under conditions in which ROS are mostly inactivated, specific vacuolar vesicles containing mitochondria were not formed and the synthesis of H-mtDNA was not observed.

3. Influence of BHT on Apoptotic DNA Fragmentation in Wheat Coleoptiles

In contrast to control plants, in etiolated wheat seedlings grown in the presence of BHT at 1–50 mg/liter apoptotic DNA fragmentation does not occur (Fig. 2C, lanes 4–6). This means that BHT effectively prevents apoptosis in the coleoptile cells of etiolated wheat seedling. The non antioxidant BHT analog 3,5-di-*tert*-butyltoluene, lacking the hydroxyl group, does not prevent apoptotic DNA fragmentation at the same maximal concentration as used for BHT (Fig. 2D, lane 1). In contrast to BHT, seedlings growing in the presence of ascorbic acid do not escape from apoptosis in the coleoptile (Fig. 2D, lane 2); ascorbic acid has no influence on seedling growth and development even at relatively high concentrations (1 g/liter; 5.7×10^{-3} *M*) (Shorning *et al.*, 1999). It is most probably that, in contrast to BHT, ascorbic acid is not sufficiently hydrophobic to effectively penetrate into the plastid and mitochondrial membranes and thus to inactivate ROS formed in these organelles.

4. BHT-Induced Changes in Intracellular Structures

The growing of etiolated seedlings in the presence of BHT results in strong changes in all cellular organelles and the appearance of a few new and anomalous structures in the cell. In the coleoptile cells of etiolated seedlings grown in the presence of BHT, but not in control plants, gigantic multibladed nuclei of irregular shape are present (Fig. 8A). On the basis of ultrastructural parameters, these nuclei are polyploid. Multinuclear cells were often seen in coleoptiles and roots of 3- and 8-day-old etiolated wheat seedlings grown in the presence of BHT. This is due to incomplete cytokinesis that follows division of the nucleus. Cell lamina and then the cell wall are only partially

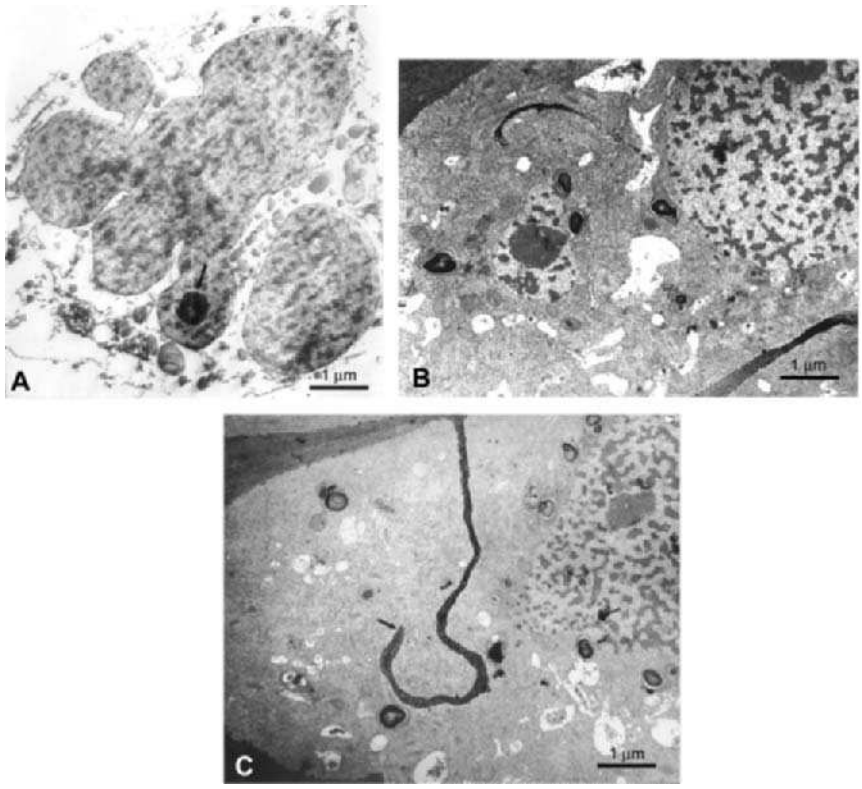

FIG. 8 Ultrastructure of cells in the coleoptile of a 3-day-old etiolated wheat seedling grown in the presence of BHT (50 mg/liter). (A) Multibladed nucleus; arrow shows a nucleolus. (B) Binuclear cell. (C) Defective cell wall (arrow) (Zamyatnina *et al.*, 2002b, 2003).

formed (Fig. 8B and C). The cell wall divides the cell only up to two-thirds or one-half its length; sometimes it is not formed at all. Multinuclear cells formed under the influence of BHT were observed earlier in onion roots (Alekperov *et al.*, 1975). Thus, BHT does not inhibit nuclear DNA synthesis (replication) (Fig. 7A), but it does suppress nuclear and cell divisions. The retarding effect of BHT on seedling growth may be due to inhibition of both cell elongation (Shorning *et al.*, 2000) and cell division.

In roots of etiolated wheat seedlings, BHT induces the formation and differentiation of plastids that are not typical of roots, in general, or of roots of etiolated plants, in particular. These unusual plastids newly formed in roots of BHT-induced etiolated wheat seedlings (Fig. 9A) have some properties typical of chromoplasts, or they are, in fact, chromoplasts. Induced differentiation of chloroplasts into chromoplasts is accompanied by intense synthesis and accumulation of such carotenoids as lycopene,

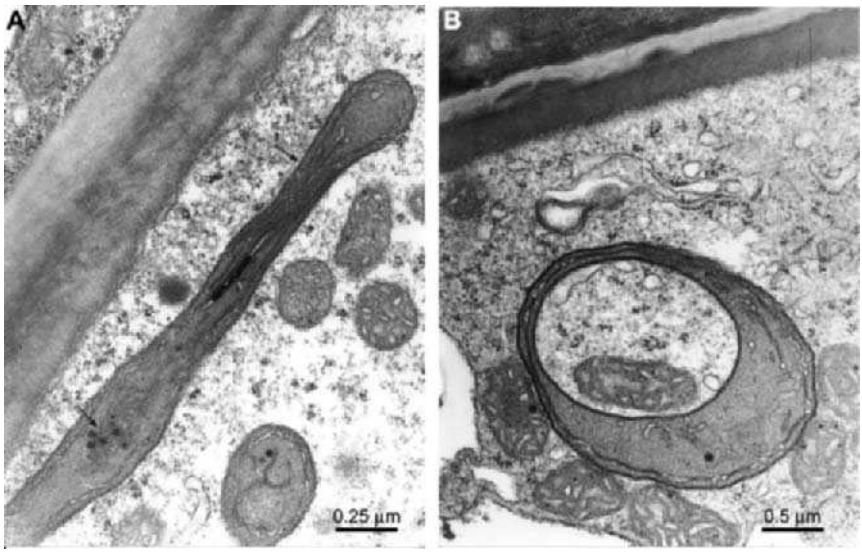

FIG. 9 Ultrastructure of plastids formed in a 3-day-old etiolated wheat seedling grown in the presence of BHT (50 mg/liter). (A) Long plastid with membrane system (1) and a prolamellar body (2) formed in the root. (B) An unusual circular plastid in a coleoptile cell. Mitochondrion is seen inside the plastid. Such plastids were never observed in organs of control plants (Zamyatnina *et al*., 2002b, 2003).

rhodoxanthin, astaxanthin, capsanthin, capsorubin, and others (Bouvier *et al*., 1998) that are effective antioxidants. Agents inducing the formation of ROS (menadione, *tert*-butylhydroperoxide, paraquat) or prooxidants (diamide, buthionine sulfoximine) or inhibition of catalase activity strongly increase the transcription of many genes responsible for synthesis of carotenoids (Bouvier *et al*., 1998). In roots BHT induced strong synthesis of pigments, probably carotenoids (Shorning *et al*., 1999), and it behaves like the prooxidants mentioned. It cannot be ruled out that under some conditions, depending on the oxygen concentration in different tissues and cells, BHT might be acting as a prooxidant. However, there is no doubt that BHT modulates ROS content in plant cells, and ROS may be agents of positive or negative control for plastid differentiation and carotenoid synthesis.

Plastids that are seen in coleptiles of control etiolated seedlings are relatively nondifferentiated plastids that may be related to the leukoplast group. The ultrastructure of plastids in wheat seedlings grown in the presence of BHT is drastically changed: the shape of the plastids becomes irregular and they most often have unusual closed circular structures (Fig. 9B). The membrane structure of these plastids is underdeveloped, the plastids do not or contain only a small number of thylakoids, and the main plastid volume is

filled with matrix that often contains starch deposits. Large circular-form plastids are also present in roots of seedlings grown in the presence of BHT, but not in control plants. It is worth mentioning that mitochondria are constantly seen inside such circular plastids. It is probable that under conditions of decreased ROS content due to BHT (Shorning *et al.*, 2000) some specific and probably symbiotic relations between these functionally and morphologically different cellular organelles may originate.

The overall plastid population formed in roots under the influence of BHT has a clearly unusual structure; these plastids have doubled membranes and they contain two main components—a membrane system corresponding to an underdeveloped thylakoid system and the matrix. Along with the membrane system mentioned, membrane vesicles fused with each other to form prolamellar bodies can be seen (Fig. 9A). In control etiolated wheat seedlings, these organelles were never observed.

Under the influence of BHT, mitochondria are less structurally changed compared with all other cellular organelles. Only the general morphology of mitochondria is changed in the coleoptile cells of 3-day-old seedlings grown with BHT. These mitochondria are gigantic long organelles, but their internal ultrastructure is not changed, and it is similar to the structure of mitochondria in control plants. Marked changes in mitochondrial ultrastructure induced by BHT were detected only in the root cells of 8-day-old seedlings: the mitochondrial matrix is electron transparent, and cristae are broken (not shown).

Significant deviations from the well-known conception of the ultrastructure of the Golgi complex are revealed on investigation of this complex in the coleoptile cells of seedling grown with BHT (Fig. 10A). The dictyosome (the main component of the Golgi complex) forms in the middle part of the chamber covered with membrane and is filled with closed membrane particles. Parts of dictyosome cisterns remain open into this chamber (Fig. 10B). It is known that formation of the cell wall depends on the activity of the Golgi complex. This complex participates in both synthesis and transportation of material that is needed for the formation of the cell wall. In addition, the Golgi complex takes part in the formation of the plasma membrane. Observed defects in cell wall formation and the distortion of cell division might be due to changes in the structure of the Golgi complex induced by BHT.

BHT also induces significant anomalies in the structure of endoplasmic reticulum of coleoptile parenchymal cells of etiolated wheat seedlings. Specific closed double-membrane structures formed around various cellular organelles by membranes of the endoplasmic reticulum were detected in coleoptiles of 3-day-old etiolated wheat seedlings grown in the presence of BHT. A closed double-membrane structure containing a few Golgi complexes is shown in Fig. 10B. An unusual closed membrane structure with cytoplasm of different density and a mitochondrion located in the center were

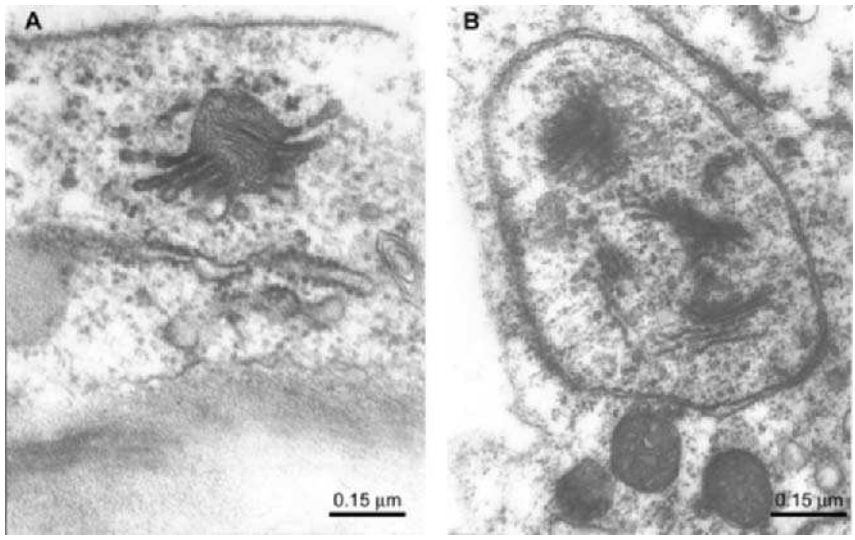

FIG. 10 Golgi apparatus and unusual cytoplasmic structure in the coleoptile of a 3-day-old etiolated wheat seedling grown in the presence of BHT (50 mg/liter). (A) Ultrastructure of the Golgi complex changed under the influence of BHT. (B) Cytoplasmic structure formed by membranes of the endoplasmic reticulum under the influence of BHT. This unusual structure contains a gathering of dictyosomes (Zamyatnina *et al.*, 2002b, 2003).

also observed (Bakeeva *et al.*, 2001). Chamber continuity of these closed membrane bodies is organized by membranes of the rough and smooth endoplasmic reticulum. The endoplasmic reticulum can be considered as relatively labile membrane system that can be changed and differentiated in correspondence with its functions. BHT affects strongly the organization of these cellular structures, and ROS controlled by the antioxidant seem to participate in the differentiation of the cellular membrane structures (Golgi apparatus and others).

Thus, BHT inhibits the growth of etiolated wheat seedlings, changes the morphology of their organs, prolongs the coleoptile life span, and prevents the appearance of specific marks of aging. In particular, in coleoptile BHT prevents the age-dependent decrease in the content of total DNA and protein, the apoptotic internucleosomal fragmentation of nuclear DNA, the appearance in cellular vacuoles of specific vesicles with mitochondria actively replicating mtDNA and the formation of heavy ($\rho = 1.718$ g/cm^3) mtDNA in them.

In contrast to coleoptile, in the initial leaf of 8-day-old etiolated wheat seedling BHT does not inhibit formation in the cellular vacuole of specific apoptotic vesicles containing subcellular organelles (Fig. 5) and it does not

block internucleosomal apoptotic DNA fragmentation in the nucleus. As in control 8-day-old seedlings (Fig. 5C), specific vesicles containing mitochondria were observed in the cellular vacuoles in the initial leaf of same-age seedlings grown in the presence of BHT (Fig. 5B). These vesicles occur there even more often than in the leaf of control seedlings grown in the absence of BHT. Thus, the effect of BHT on apoptosis in etiolated wheat seedlings has tissue-specific character. In contrast to coleoptile, BHT does not inhibit, but does slightly stimulate, apoptosis in the initial leaf. It is more probable that this is due to different concentrations of intracellular oxygen in the leaf and coleoptile. Despite the fact that the plants were grown in darkness, they were taken out of the dark for relatively short periods (few minutes) once a day when water or respective solutions of chemical were changed; these short light exposures were probably sufficient for some photosynthesis producing oxygen in the leaf cells (the initial leaf in seedlings grown under these conditions had weak yellow-greenish color compared with colorless coleoptile). At least, well-differentiated plastids with developed membrane structure in the cells of the initial leaf were seen. It is known that BHT and its derivatives may have prooxidant properties under increased partial oxygen pressure (Bolton and Thompson, 1991; Dwyer-Niedl *et al*., 1998). This may be due to the fact that under relatively high concentrations of molecular oxygen BHT is oxidized by a single-electron mechanism to the respective carcinogenic BHT quinone that generates superoxide anion under specific conditions (Smirnova *et al*., 2002). This seems to be responsible for a significant carcinogenic effect of BHT in animal tissues enriched with oxygen, such as lungs and others (Bolton and Thompson, 1991; Dwyer-Niedl *et al*., 1998). Besides, it may to some extent explain the fact that at the same concentration BHT has less retardant effect on wheat seedlings grown in the light (under condition of high formation of oxygen due to photosynthesis). Actually, BHT does not prevent apoptosis in green seedlings grown in the light. Thus, BHT can act as antioxidant as well as prooxidant both in plant and animal cells. Strong BHT action inducing plastid differentiation (Bakeeva *et al*., 2001) and formation of pigments (Shorning *et al*., 1999) in roots of etiolated wheat seedlings seems to be associated with its prooxidant activity and it is similar to the influence of typical prooxidants on the formation of carotenoids in the cells of pepper plants (Bouvier *et al*., 1998).

The multiple actions of BHT on etiolated plants seem to be due primarily to its antioxidative rather than its xenobiotic properties, because BHT strongly diminishes the superoxide content in etiolated wheat seedlings, whereas other xenobiotics used at the same concentrations are physiologically inert. Therefore, it can be concluded that ROS controlled by BHT trigger apoptosis and structural reorganization of the cytoplasm with formation of specific vacuolar vesicles and mtDNA synthesis in them. It seems that proper modulation of the ROS level by BHT in the cell is responsible for the changes

and distortions of organelle structure observed and for the appearance of new subcellular structures. This corresponds, in general, to idea that ROS effectively control apoptosis and mitosis. ROS as powerful secondary messengers also regulate the differentiation of plastids and the Golgi apparatus; they control cellular differentiation and plant growth and development.

5. Peroxides Stimulate Apoptosis

Peroxides such as H_2O_2 and cumene hydroperoxide (10^{-3} *M*) unambiguously stimulated apoptosis (DNA fragmentation) in coleoptile and induced it in an initial leaf when in an initial leaf of control seedlings apoptosis was not yet detected (Zamyatnina *et al.*, 2002b). There were no changes in the morphology of seedlings grown in the presence of these peroxides. Strong internucleosomal fragmentation and degradation of coleoptile nDNA under the influence of hydrogen peroxide were found in 5-day-old wheat seedlings. It is interesting that, at the same time, formation of endogenous superoxide anion in coleoptile cells is minimal (Fig. 6). It seems that "forcible" maintenance of high oxidative status by peroxides in a period of natural minimal ROS content is a supersensitive element of the triggering and intensification of apoptotic DNA fragmentation. Plant sensitivity to induction of apoptosis by peroxides seems to be associated with the natural cycles of ROS formation in seedlings, and it is different at various stages of early ontogenesis. Actually, hydrogen peroxide and cumene hydroperoxide start to induce DNA fragmentation already by day 4 of seedling life (Zamyatnina *et al.*, 2002b). In control plants apoptotic DNA fragmentation in the initial leaf was observed only on day 8 of seedling life (Zamyatnina *et al.*, 2002b). In a leaf H_2O_2 stimulates apoptosis approximately 24 h earlier than in coleoptile (Zamyatnina *et al.*, 2002b). This seems to be due in part to higher oxygen and/or Fe^{2+} contents in photosynthesizing leaf than in coleoptile (peroxides are the source of the reactive radical •OH in the presence of Fe^{2+} or in the light). In so far as hydrogen peroxide speeds up apoptosis in the initial leaf, it should promote leaf aging. In fact, peroxides induce aging in plants (Jabs, 1999).

Thus, modulation of the ROS level in seedlings by peroxides and antioxidants results in tissue-specific change in the target date for the appearance as well as intensity of apoptosis.

IV. Phytohormonal Control of Apoptosis

Phytohormones play a crucial role in the control of realization of entire developmental program in plants. There are some data showing that phytohormones may control and regulate apoptosis as a terminal stage of

cellular differentiation and in this particular way they may also modulate organoptosis and phenoptosis in plants.

When 2-day-old etiolated wheat seedlings were further grown in the presence of 10^{-5} *M* fusicoccin, 2,4-D, 6-benzylaminopurine (BA), or gibberellin (GA_3), these treatments did not substantially affect apoptotic DNA fragmentation in the coleoptile: it occurred approximately at the same time and was similarly extensive as in control seedlings (Fig. 2E). BA, GA_3, and 2,4-D did not substantially inhibit apoptotic DNA fragmentation in the coleoptile when excised 6-day-old shoots were exposed to these plant growth regulators (PGR) for a further 48 h (Fig. 2F). But when excised shoots of etiolated seedlings were exposed to 10^{-5} *M* abscisic acid (ABA), internucleosomal DNA fragmentation in the coleoptile was more extensive (Fig. 2F, lane 1) than in control shoots (Fig. 2F, lane 6). Thus, ABA sharply promoted apoptotic DNA fragmentation in the coleoptile of wheat seedlings. Unlike this stimulation of apoptosis in wheat coleoptiles, ABA inhibited apoptosis in developing barley anthers (Wang *et al.*, 1999) and in the aleurone layer of germinating barley grains (Wang *et al.*, 1996). In contrast, gibberellin induced apoptosis in the barley aleurone layer (Bethke *et al.*, 2000) but did not affect it in wheat coleoptile (Fig. 2E and F). Thus, the effects of various phytohormones on apoptosis in cereals are tissue specific. ABA-treated aleurone protoplasts can be kept alive for more than 6 months, whereas GA treatment of protoplasts induces the death of most cells in a few days (Fath *et al.*, 2000). On the other hand, in a daylily ABA addition hastens petal senescence (Rubinstein, 2000). Mechanisms for the promotion or inhibition of apoptosis by ABA are unknown. It is possible that ABA may influence the timing of PCD through regulation of ethylene biosynthesis, and a balance between ethylene and ABA is essential to onset of cell death in maize endosperm (Young and Gallie, 2000). ABA is supposed to induce such changes in cell metabolism that result in the accumulation of free radicals or activation of the cell antioxidant systems (Greenberg, 1996; Vanyushin, 2001). This suggestion does not contradict the evidence that changes in cell oxidative status affect apoptosis induction (Jabs, 1999; Shorning *et al.*, 2000; Vanyushin, 2001). A sharp stimulation of apoptosis by ABA, which was demonstrated for wheat coleoptiles (Fig. 2F, lane 1), is the opposite of the inhibitory effect of the antioxidant BHT (Bakeeva *et al.*, 2001). It might be that ABA triggers formation of reactive oxygen species. In barley aleurone, gibberellin suppressed the effect of ABA on apoptosis, whereas cytokinin and auxin did not influence apoptotic DNA fragmentation (Wang *et al.*, 1996), as in wheat coleoptiles.

Gibberellic acid triggers PCD in isolated cereal aleurone layers or protoplasts; cell death in barley aleurone occurs only after cells become highly vacuolated and is manifested by a loss of plasma membrane integrity; this is accompanied by strong activation of nucleases and proteases and rapid and extensive DNA degradation (Fath *et al.*, 2000).

Because cytokinins are believed to be rejuvenating phytohormones that stimulate the greening of senescing leaves and inhibit petal senescence, it would be reasonable to suppose that they must inhibit apoptosis, which, as mentioned earlier, accompanies plant organ senescence. However, any marked inhibitory effect of cytokinin on apoptosis in the coleoptiles of wheat seedlings was not observed (Fig. 2E, lane 3; Fig. 2F, lane 3). Similarly, this effect was not observed in the aleurone layer of germinating barley grains (Wang *et al*., 1996). Taking into account an apparent tissue specificity in the hormonal activity, in particular in their action on apoptosis, we believe that the cytokinin rejuvenating effect (leaf greening) is related mainly to their action on plastids. Nevertheless, it was shown that at high concentrations cytokinins (BA) block cell proliferation and induce PCD in both carrot (*Daucus carota*) and *Arabidopsis thaliana* cell cultures (Carimi *et al*., 2003). The cell death was accompanied by chromatin condensation, oligonucleosomal DNA degradation (laddering), and release of cytochrome *c* from mitochondria. In carrot cells, this induction takes approximately 24 h, with proliferating cells being more sensitive than quiescent cells. Abscisic acid and 2,4-D protect cells against the cytokinin-induced death. PCD in the form of DNA laddering was also seen in plants treated with cytokinins. This process was accompanied by accelerated senescence in the form of leaf yellowing (Carimi *et al*., 2003). The cytokinin isopentenyladenosine activates caspase-like proteases and induces apoptosis in tobacco BY-2 cells (Mlejnek and Prochazka, 2002).

When etiolated seedlings were grown in the presence of the ethylene releaser ethrel, noticeable DNA fragmentation was observed in the entire leaf and coleoptile in as little as 5 days after germination, whereas no fragmentation was detected in control seedlings of a similar age (Vanyushin *et al*., 2002). Ethrel-induced DNA fragmentation became more extensive with an increase in the ethrel concentration from 10^{-5} to 10^{-2} *M*. In addition, not only apoptotic internucleosomal DNA fragmentation but also deeper DNA degradation occurred in the ethrel-treated seedlings. It seems likely that this extensive degradation was caused by ethrel-induced endonucleases. The level of endonucleolytic activity in the ethrel-treated seedlings was increased severalfold as compared with control seedlings (Fedoreyeva *et al*., 2003). Thus, the ethylene releaser ethrel triggered and accelerated apoptotic DNA fragmentation and its further degradation in leaves and coleoptiles of etiolated wheat seedlings. This observation (Vanyushin *et al*., 2002) is in agreement with data indicating that a ''senescence hormone,'' ethylene, induces and stimulates apoptosis in plants. Ethylene released from ethrel exerted such an effect, for example, in protoplasts derived from carrot cells (Zhou *et al*., 1999). Ethylene was produced in maize endosperm during two developmental phases, the first phase coinciding with the onset of visible PCD in endosperm and the second phase correlating with increased nuclease

activity and the appearance of DNA fragments (Young *et al.*, 1997). Internucleosomal DNA fragmentation in cereal endosperm followed the peak of ethylene production (Young and Gallie, 1999). Suppression of ethylene production retarded apoptotic DNA fragmentation but could not prevent PCD in cereal endosperm (Young and Gallie, 1999). The application of exogenous ethylene throughout seed development resulted in earlier and more extensive cell death and internucleosomal DNA fragmentation in wheat and maize endosperm (Young and Gallie, 1999, 2000). In maize roots, hypoxia accelerated ethylene evolution, which triggered apoptosis; an oxygen-storing aerenchyma was produced as a result (Campbell and Drew, 1983; Drew *et al.*, 1979; Gunawardena *et al.*, 2001; He *et al.*, 1996). Ethylene sensitivity in various plants is most probably due to amount, competence, and activity of respective ethylene receptors (Young and Gallie, 2000). Ethylene controls processes of plant apoptosis and senescence via regulation of specific gene expression (Vanyushin, 2001).

Fusicoccin is a mighty plant growth regulator. The molecular mechanisms of its action are not fully elucidated, but it is evident that membranes of plant cells and membrane-bound proteins are principal targets of fusicoccin activity. In particular, fusicoccin activates plasmalemmal H^+-ATPase and induces specific binding of known regulatory 14–3–3 proteins with the plasmalemma (Vanyushin, 2001). These proteins can regulate apoptosis in mammalian cells. It is not inconceivable that they can fulfill a similar function in plants as well. Therefore, the formation of specific complexes between fusicoccin and these proteins might influence the apoptosis-controlling functions of regulatory 14–3–3 proteins in plant cells. In experiments with etiolated wheat seedlings, exogenous fusicoccin hardly affected apoptotic DNA fragmentation in coleoptiles (Fig. 2E, lane 5) although a fusicoccin-stimulating effect on DNA fragmentation was expected.

There are some data indicating that brassinosteroids, the steroid-type phytohormones, seem to take part in regulation of PCD accompanying tracheary element differentiation in *Zinnia* cells (Yamamoto *et al.*, 1997).

Apoptosis modulation by phytohormones may be mediated by their regulation of DNA methylation/demethylation, which is responsible for the induction of genes encoding apoptogenic proteins and/or possible repression of antiapoptotic genes.

V. DNA Methylation and Apoptosis

That an organism has a developmental program implies the regulated repression and derepression of corresponding genes. It has been suggested that programmed cell death is related to the derepression of definite terminal

genes inducing senescence and death (Vanyushin and Berdyshev, 1977). DNA methylation is one of the mechanisms for gene inactivation in plants (Kirnos *et al.*, 1995; Vanyushin and Kirnos, 1988; Vanyushin, 1984). Phytohormones control this process; they provide for specific DNA demethylation, which is required for expression of most genes. DNA methylation in plants was shown to be tissue specific (Kirnos *et al.*, 1995; Vanyushin and Kirnos, 1988; Vanyushin, 1984). The level of DNA methylation lowers with age considerably. Therefore, age-dependent DNA demethylation is somehow related to senescence and it may also be concerned with the genes encoding apoptogenic proteins (factors). It was directly shown that DNA demethylation, which resulted from the loss or inhibition of methyltransferase activity, triggers apoptosis in mammalian cells (Jackson-Grusby *et al.*, 2001; Stancheva *et al.*, 2001). Aging in plants is associated with demethylation and activation of some specific genes and, in particular, genes encoding polygalacturonase and cellulase, which are responsible for fruit ripening (Hadfield *et al.*, 1993).

In plants the DNA-demethylating agent, 5-azacytidine, induces the expression of diverse genes (Vanyushin *et al.*, 1990), including genes controlling flowering (Finnegan *et al.*, 1998). When plants were grown in the presence of 5-azacytidine, there was no need in their vernalization for flowering induction (Finnegan *et al.*, 1998). However, unlike the specific action of phytohormones on DNA methylation and gene activation (Kirnos *et al.*, 1986; Kirnos *et al.*, 1995; Vanyushin and Kirnos, 1988; Vanyushin, 1984), the effects of 5-azacytidine are random. Nevertheless, 5-azacytidine induced flowering. Although 5-azacytidine is known to induce apoptosis in animal cells (Hossain *et al.*, 1997; Hsiao *et al.*, 1996; Nakayama *et al.*, 1999; Saitoh *et al.*, 1995), the effects of this demethylating agent on apoptosis in plants were not studied.

5-Azacytidine sharply accelerated apoptotic DNA fragmentation in the coleoptiles of intact wheat seedlings exposed to this compound (Fig. 2G, lane 1). Earlier, it was established that the level of DNA methylation in such seedlings was distinctly lowered (Aleksandrushkina *et al.*, 1989). Thus, 5-azacytidine-accelerated DNA fragmentation can be caused by DNA demethylation and, correspondingly, by derepression and induction of various apoptogenic factors, including, for example, caspases, endonucleases, regulatory proteins, and so on. On the other hand, severe DNA degradation in wheat seedlings kept on 5-azacytidine can also be related to the increased availability of demethylated DNA in the chromatin to nucleases. The chromatin, which was formed in the presence of 5-azacytidine, is known to be less compact because H1 histone, responsible for compaction of chromatin, cannot bind to demethylated DNA.

Thus, it is not inconceivable that the activation of apoptosis by some plant growth regulators can be caused by their effects on DNA methylation and, thus, on the known induction (derepression) of genes encoding apoptogenic

proteins and/or the repression of genes preventing apoptosis (Hoeberichts *et al.*, 2001).

VI. Concluding Remarks

Different forms of genetically programmed cell death (PCD) exist in plants (apoptosis-like, vacuolar collapse, and slow leaf-aging type). Apoptosis is an integral part of plant ontogenesis and it is controlled by phytohormones and DNA methylation. Apoptosis in plants is, on the whole, similar to that in animals. It is accompanied by specific changes in cell morphology and in the structure of nucleus and cytoplasm, by activation of nucleases and caspases, and by an increase in mtDNA synthesis and domain and internucleosomal DNA fragmentation. Specific apoptotic fragmentation of cytoplasm with formation of vesicles in the cell vacuole is to some extent reminiscent of apoptotic cell blebbing in animals, but this sort of blebbing is directed inside the cell (into the vacuole), not outside the cell, as in animals. As in animals, Ca^{2+} controls apoptosis in plants. PCD may be induced by many unfavorable factors including oxidative stress. In particular, PCD is a part of the plant hypersensitive response during an attack by various pathogens (viral, bacterial, and fungal infections) that is usually accompanied by a strong increase in the formation of reactive oxygen species (ROS). ROS control both apoptosis and mitosis, and they are the secondary messengers that also regulate differentiation of plastids and Golgi apparatus. It is known that mitochondria play a key role in the initiation of some forms of apoptosis in plants: an induced release of cytochrome *c* and other protein factors from mitochondria results in apoptosis in plant cells similarly to that in animals. ROS trigger, but antioxidants suppress or even prevent, apoptosis in plants.

Apoptosis is essential for plant development; it is involved in forming the plant vascular system, in particular. It is known that in animals the inhibition of apoptosis blocks embryogenesis, and it seems that a similar process also takes place in plants. Future knowledge about the molecular mechanisms of apoptosis may provide effective tools for the control of plant growth and development.

Acknowledgments

Research described in this chapter was supported by the Russian Foundation for Basic Research (Grant 02–04–48005) and by the Ministry of Industry, Science, and Technologies (Grant NSH-1019.2003.4).

References

Alekperov, U. K., Abutalybov, M. G., and Askerov, I. T. (1975). Multipolar mitoses and multinuclearity on the antioxidant ionol effect in onion roots. *Tsitologiya* **17,** 101–103.

Aleksandrushkina, N. I., Kirnos, M. D., Rotaenko, E. P., and Vanyushin, B. F. (1989). Inhibition of nuclear DNA synthesis and methylation by 5-azacytidine during successive cell cycles in dividing cells of the first leaf of etiolated wheat seedlings. *Biokhimiya* **54,** 355–360.

Ameisen, J. C. (2002). On the origin, evolution, and nature of programmed cell death: A timeline of four billion years. *Cell Death Differ.* **9,** 367–393.

Amor, Y., Babiychuk, E., Inze, D., and Levine, A. (1998). The involvement of poly(ADP-ribose) polymerase in the oxidative stress responses in plants. *FEBS Lett.* **440,** 1–7.

Aoyagi, S., Sugiyama, M., and Fukuda, H. (1998). BEN1 and ZEN1 cDNAs encoding S1-type DNases that are associated with programmed cell death in plants. *FEBS Lett.* **429,** 134–138.

Ashkenazi, A., and Dixit, V. M. (1998). Death receptors: Signaling and modulation. *Science* **281,** 1305–1308.

Bakeeva, L. E., Kirnos, M. D., Aleksandrushkina, N. I., Kazimirchyuk, S. B., Shorning, B. Y., Zamyatnina, V. A., Yaguzhinsky, L. S., and Vanyushin, B. F. (1999). Subcellular reorganization of mitochondria producing heavy DNA in aging wheat coleoptiles. *FEBS Lett.* **457,** 122–125.

Bakeeva, L. E., Zamyatnina, V. A., Shorning, B. Yu., Aleksandrushkina, N. I., and Vanyushin, B. F. (2001). Effect of the antioxidant ionol (BHT) on growth and development of etiolated wheat seedlings: Control of apoptosis, cell division, organelle ultrastructure, and plastid differentiation. *Biochemistry (Moscow)* **66,** 850–859.

Balk, J., and Leaver, C. L. (2001). The PET1-CMS mitochondrial mutation in sunflower is associated with premature programmed cell death and cytochrome *c* release. *Plant Cell* **13,** 1803–1818.

Balk, J., Leaver, C. J., and McCabe, P. F. (1999). Translocation of cytochrome *c* from the mitochondria to the cytosol occurs during heat-induced programmed cell death in cucumber plants. *FEBS Lett.* **463,** 151–154.

Beers, E. P. (1997). Programmed cell death during plant growth and development. *Cell Death Differ.* **4,** 649–661.

Bethke, P. C., Lonsdale, J. E., Fath, A., Jones, R. L., Young, T. E., and Gallie, D. R. (2000). Regulation of programmed cell death in maize endosperm by abscisic acid. *Plant Mol. Biol.* **42,** 397–414.

Bolduc, N., Ouellet, M., Pitre, F., and Brisson, L. F. (2003). Molecular characterization of two plant BI-1 homologues which suppress Bax-induced apoptosis in human 293 cells. *Planta* **216,** 377–386.

Bolton, J. L., and Thompson, J. A. (1991). Oxidation of butylated hydroxytoluene to toxic metabolites: Factors influencing hydroxylation and quinone methide formation by hepatic and pulmonary microsomes. *Drug Metab. Dispos.* **19,** 467–472.

Bouvier, F., Backhaus, R. A., and Camara, B. (1998). Induction and control of chromoplast-specific carotenoids genes by oxidative stress. *J. Biol. Chem.* **273,** 30651–30659.

Callard, D., Axelos, M., and Mazzolini, L. (1996). Novel molecular markers for late phases of the growth cycle of *Arabidopsis thaliana* cell-suspension cultures are expressed during organ senescence. *Plant Physiol.* **112,** 705–715.

Campbell, R., and Drew, M. C. (1983). Electron microscopy of gas space (aerenchyma) formation in adventitious roots of *Zea mays* L. subjected to oxygen shortage. *Planta* **157,** 350–357.

Carimi, F., Zottini, M., Formentin, E., Terzi, M., and Lo Schiavo, F. (2003). Cytokinins: New apoptotic inducers in plants. *Planta* **216,** 413–421.

Chamnongpol, S., Willekens, H., Moeder, W., Langebartels, C., Sandermann, H., Van Montagu, M., Inze, D., and Van Camp, W. (1998). Defense activation and enhanced pathogen tolerance induced by H_2O_2 in transgenic tobacco. *Proc. Natl. Acad. Sci. USA.* **95,** 5818–5823.

del Pozo, O., and Lam, E. (1998). Caspases and programmed cell death in the hypersensitive response of plants to pathogens. *Curr. Biol.* **8,** 1129–1132.

Desikan, R., Reynolds, A., Hancock, J. T., and Neill, S. J. (1998). Harpin and hydrogen peroxide both initiate programmed cell death but have differential effects on defence gene expression in *Arabidopsis* suspension cultures. *Biochem. J.* **330,** 115–120.

Dickman, M. B., Park, Y. K., Oltersdorf, T., Li, W., Clemente, T., and French, R. (2001). Abrogation of disease development in plants expressing animal antiapoptotic genes. *Proc. Natl. Acad. Sci. USA.* **98,** 6957–6962.

Dietrich, R. A., Richberg, M. H., Schmidt, R., Dean, C., and Dangl, J. L. (1997). A novel zinc finger protein is encoded by the *Arabidopsis* LSD1 gene and functions as a negative regulator of plant cell death. *Cell* **88,** 685–694.

Dion, M., Chamberland, H., St-Michel, C., Plante, M., Darveau, A., Lafontaine, J. G., and Brisson, L. F. (1997). Detection of a homologue of bcl-2 in plant cells. *Biochem. Cell. Biol. (Biochim. Biol. Cellulaire)* **75,** 457–461.

Dominguez, F., Moreno, J., and Cejudo, F. J. (2001). The nucellus degenerates by a process of programmed cell death during the early stages of wheat grain development. *Planta* **213,** 352–360.

Drew, M. C., Jackson, M. B., and Giffard, S. (1979). Ethylene-promoted adventitious rooting and development of cortical air spaces (aerenchyma) in roots may be response to flooding in *Zea mays* L. *Planta* **147,** 83–88.

Dröge, W. (2002). Free radicals in the physiological control of cell function. *Physiol. Rev.* **82,** 47–95.

Dwyer-Nield, L. D., Thompson, J. A., Peljak, G., Squier, M. K., Barker, T. D., Parkinson, A., Cohen, J. J., Dinsdale, D., and Malkinson, A. M. (1998). Selective induction of apoptosis in mouse and human lung epithelial cell lines by the *tert*-butyl hydroxylated metabolite of butylated hydroxytoluene: A proposed role in tumor promotion. *Toxicology* **130,** 115–127.

Fadeel, B., Orrenius, S., and Zhivotovsky, B. (1999). Apoptosis in human disease: A new skin for the old ceremony? *Biochem. Biophys. Res. Commun.* **266,** 699–717.

Fath, A., Bethke, P., Lonsdale, J., Meza-Romero, R., and Jones, R. (2000). Programmed cell death in cereal aleurone. *Plant Mol. Biol.* **44,** 255–266.

Fedoreyeva, L. I., and Vanyushin, B. F. (2002). N^6-Adenine DNA-methyltransferase in wheat seedlings. *FEBS Lett.* **514,** 305–308.

Fedoreyeva, L. I., Aleksandrushkina, N. I., Dunaevsky, Y. E., Belozersky, M. A., and Vanyushin, B. F. (2003). Effect of the ethylene producer ethrel and antioxidant ionol (BHT) on the proteolytic apparatus in coleoptiles of wheat seedlings during apoptosis. *Biochemistry (Moscow)* **68,** 464–469.

Filonova, L. H., Bozhkov, P. V., Brukhin, V. B., Daniel, G., Zhivotovsky, B., and von Arnold, S. (2000). Two waves of programmed cell death occur during formation and development of somatic embryos in the gymnosperm, Norway spruce. *J. Cell Sci.* **113,** 4399–4411.

Finnegan, E. J., Genger, R. K., Kovac, K., Peacock, W. J., and Dennis, E. S. (1998). DNA methylation and the promotion of flowering by vernalization. *Proc. Natl. Acad. Sci. USA* **95,** 5824–5829.

Fukuda, H. (1996). Xylogenesis: Initiation, progression and cell death. *Annu. Rev. Plant Physiol. Plant Mol. Biol.* **47,** 299–325.

Fukuda, H. (1997). Tracheary element differentiation. *Plant Cell* **9,** 1147–1156.

Fukuda, H. (2000). Programmed cell death of tracheary elements as a paradigm in plants. *Plant Mol. Biol.* **44,** 245–253.

Gallois, P., Makishima, T., Hecht, V., Despres, B., Laudie, M., Nishimoto, T., and Cooke, R. (1997). An *Arabidopsis thaliana* cDNA complementing a hamster apoptosis suppressor mutant. *Plant J.* **11,** 1325–1331.

Gavrieli, Y., Sherman, Y., and Ben-Sasson, S. A. (1992). Identification of programmed cell death *in situ* via specific labeling of nuclear DNA fragmentation. *J. Cell Biol.* **119,** 493–501.

Gietl, C., and Schmid, M. (2001). Ricinisomes: An organelle for developmentally regulated programmed cell death in senescing plant tissues. *Naturwissenschaften* **88,** 49–58.

Gilchrist, D. G. (1997). Mycotoxins reveal connection between plants and animals in apoptosis and ceramide signaling. *Cell Death Differ.* **4,** 689–698.

Gilchrist, D. G. (1998). Programmed cell death in plant disease: The purpose and promise of cellular suicide. *Annu. Rev. Phytopathol.* **36,** 393–414.

Glücksmann, A. (1951). Cell deaths in normal vertebrate ontogeny. *Biol. Rev. Camb. Phil. Soc.* **26,** 59–86.

Gray, J., Close, P. S., Briggs, S. P., and Johal, G. S. (1997). A novel suppressor of cell death in plants encoded by the *Lls1* gene of maize. *Cell* **89,** 25–31.

Greenberg, J. T. (1996). Programmed cell death: A way of life for plants. *Proc. Natl. Acad. Sci. USA.* **93,** 12094–12097.

Greenberg, J. T. (1997). Programmed cell death in plant–pathogen interactions. *Annu. Rev. Plant Physiol. Plant Mol. Biol.* **48,** 525–545.

Greenberg, J. T., Guo, A., Klessig, D. F., and Ausubel, F. M. (1994). Programmed cell death in plants: A pathogen-triggered response activated coordinately with multiple defense functions. *Cell* **77,** 551–563.

Groover, A., and Jones, A. M. (1999). Tracheary element differentiation uses a novel mechanism coordinating programmed cell death and secondary cell wall synthesis. *Plant Physiol.* **119,** 375–384.

Groover, A., DeWitt, N., Heidel, A., and Jones, A. (1997). Programmed cell death of plant tracheary elements: Differentiating *in vitro*. *Protoplasma* **196,** 197–211.

Gunawardena, A. H. L. A. N., Pearce, D. M., Jackson, M. B., Hawes, C. R., and Evans, D. E. (2001). Characterisation of programmed cell death during aerenchyma formation induced by ethylene or hypoxia in roots of maize (*Zea mays* L.). *Planta* **212,** 205–214.

Hadfield, K. A., and Bennett, A. B. (1997). Programmed senescence of plant organs. *Cell Death Differ.* **4,** 662–670.

Hadfield, K. A., Dandekar, A. M., and Romani, R. J. (1993). Demethylation of ripening specific genes in tomato fruit. *Plant Sci.* **92,** 13–18.

Harman, D. (1956). Aging: A theory based on free radical and radiation chemistry. *J. Gerontol.* **11,** 298–300.

He, C. J., Morgan, P. W., and Drew, M. C. (1996). Transduction of an ethylene signal is required for cell death and lysis in the root cortex of maize during aerenchyma formation induced by hypoxia. *Plant Physiol.* **112,** 463–472.

He, X., and Kermode, A. R. (2003). Nuclease activities and DNA fragmentation during programmed cell death of megagametophyte cells of white spruce (*Picea glauca*) seeds. *Plant Mol. Biol.* **51,** 509–521.

Heath, M. C. (1998). Apoptosis, programmed cell death and hypersensitive response. *Eur. J. Plant Pathol.* **104,** 117–124.

Heath, M. C. (2000). Hypersensitive response-related death. *Plant Mol. Biol.* **44,** 321–334.

Hoeberichts, F. A., and Woltering, E. J. (2003). Multiple mediators of plant programmed cell death: Interplay of conserved cell death mechanisms and plant-specific regulators. *Bioessays* **25,** 47–57.

Hoeberichts, F. A., Orzaez, D., van der Plas, L. H., and Woltering, E. J. (2001). Changes in gene expression during programmed cell death in tomato cell suspensions. *Plant Mol. Biol.* **45,** 641–654.

Hossain, M. M., Takashima, A., Nakayama, H., and Doi, K. (1997). 5-Azacytidine induces toxicity in PC12 cells by apoptosis. *Exp. Toxicol. Pathol.* **49,** 201–206.

Houot, V., Etienne, P., Petitot, A. S., Barbier, S., Blein, J. P., and Suty, L. (2001). Hydrogen peroxide induces programmed cell death features in cultured tobacco BY-2 cells, in a dose-dependent manner. *J. Exp. Bot.* **52,** 1721–1730.

Hsiao, W. L., Mendosa, G., Kothari, N. H., and Fan, H. (1996). Comparison of transformation by manganese sulfate and 5-azacytidine in Rat 6 cells overexpressing the c-*myc* oncogene. *Carcinogenesis* **17,** 2771–2777.

Hu, G., Yalpani, N., Briggs, S. P., and Johal, G. S. (1998). A porphyrin pathway impairment is responsible for the phenotype of a dominant disease lesion mimic mutant of maize. *Plant Cell* **10,** 1095–1105.

Huh, G. H., Damsz, B., Matsumoto, T. K., Reddy, M. P., Rus, A. M., Ibeas, J. I., Narasimhan, M. L., Bressan, R. A., and Hasegawa, P. M. (2002). Salt causes ion disequilibrium-induced programmed cell death in yeast and plants. *Plant J.* **29,** 649–659.

Inada, N., Sakai, A., Kuroiwa, H., and Kuroiwa, T. (2002). Three-dimensional progression of programmed death in the rice coleoptile. *Int. Rev. Cytol.* **218,** 221–258.

Jabs, T. (1999). Reactive oxygen intermediates as mediators of programmed cell death in plants and animals. *Biochem. Pharmacol.* **57,** 231–245.

Jabs, T., Dietrich, R. A., and Dangl, J. L. (1996). Initiation of runaway cell death in an *Arabidopsis* mutant by extracellular superoxide. *Science* **273,** 1853–1856.

Jackson-Grusby, L., Beard, C., Possemato, R., Tudor, M., Fambrough, D., Csankovszki, G., Dausman, J., Lee, P., Wilson, C., Lander, E., and Jaenish, R. (2001). Loss of genomic methylation causes p53-dependent apoptosis and epigenetic deregulation. *Nat. Genet.* **27,** 31–39.

James, T. N., Terasaki, F., Pavlovich, E. R., and Vikhert, A. M. (1993). Apoptosis and pleomorphic micromitochondriosis in the sinus nodes surgically excised from five patients with the long QT syndrome. *J. Lab. Clin. Med.* **122,** 309–323.

Janicke, R. U., Porter, A. G., and Kush, A. (1998). A novel *Arabidopsis thaliana* protein protects tumor cells from tumor necrosis factor-induced apoptosis. *Biochim. Biophys. Acta.* **1402,** 70–78.

Jiang, Z. F., Zhu, S., Sun, Y. L., and Zhai, Z. H. (1999). Induction of apoptosis in purified animal and plant nuclei by *Xenopus* egg extracts. *Cell Res.* **9,** 79–90.

Kawai-Yamada, M., Jin, L., Yoshinaga, K., Hirata, A., and Uchimiya, H. (2001). Mammalian *Bax*-induced plant cell death can be down-regulated by overexpression of *Arabidopsis* Bax inhibitor-1 (AtBI-1). *Proc. Natl. Acad. Sci. USA* **98,** 12295–12300.

Kawasaki, T., Henmi, K., Ono, E., Hatakeyama, S., Iwano, M., Satoh, H., and Shimamoto, K. (1999). The small GTP-binding protein Rac is a regulator of cell death in plants. *Proc. Natl. Acad. Sci. USA* **96,** 10922–10926.

Keller, T., Damude, H. G., Werner, D., Doerner, P., Dixon, R. A., and Lamb, C. (1998). A plant homolog of the neutrophil NADPH oxidase gp91phox subunit gene encodes a plasma membrane protein with Ca^{2+} binding motifs. *Plant Cell* **10,** 255–266.

Kerr, J. F. R., Wyllie, A. H., and Currie, A. R. (1972). Apoptosis: A basic biological phenomenon with wide-ranging implication. *Br. J. Cancer* **26,** 239–257.

Kirnos, M. D., Volkova, S. A., Ganicheva, N. I., Kudryashova, I. B., and Vanyushin, B. F. (1983). Synchronous DNA synthesis in coleoptile and initial leaf of etiolated wheat seedlings: Nature and ratio between nuclear and mitochondrial DNAs synthesis. *Biokhimiya* **48,** 1587–1595.

Kirnos, M. D., Artyukhovskaya, N. A., Aleksandrushkina, N. I., Ashapkin, V. V., and Vanyushin, B. F. (1986). Phytohormone effect on the nuclear DNA methylation during replication and post-replication in the S-phase of the cell cycle in the initial leaf of etiolated wheat seedlings. *Biokhimiya* **51,** 1875–1885.

Kirnos, M. D., Aleksandrushkina, N. I., Goremykin, V. V., Kudryashova, I. B., and Vanyushin, B. F. (1992a). ''Heavy'' mitochondrial DNA in higher plants *Biokhimiya* **57,** 1566–1573.

Kirnos, M. D., Aleksandrushkina, N. I., Zagorskaya, G. Ya., Kireev, I. I., and Vanyushin, B. F. (1992b). Superproduction of heavy minicircular mitochondrial DNA in aging wheat coleoptiles. *FEBS Lett.* **298,** 109–112.

Kirnos, M. D., Aleksandrushkina, N. I., Vlasova, T. I., and Vanyushin, B. F. (1995). Structural and functional arrangement of methylation of replicating genome. *Mol. Biol.* **29,** 1242–1257.

Kirnos, M. D., Aleksandrushkina, N. I., and Vanyushin, B. F. (1997a). Apoptosis in the cells of the first leaf and coleoptile in wheat seedlings: Internucleosomal DNA fragmentation and the synthesis of ''heavy'' oligonucleosome-size fragments of DNA *Biochemistry (Moscow)* **62,** 1008–1014.

Kirnos, M. D., Aleksandrushkina, N. I., Shorning, B. Y., Bubenshchikova, S. N., and Vanyushin, B. F. (1997b). Overproduction of ''heavy'' DNA ''in non-dividing cells of the aging coleoptile in wheat seedlings during apoptosis *Biochemistry (Moscow)* **62,** 1579–1589.

Kirnos, M. D., Aleksandrushkina, N. I., Bakeeva, L. E., Kazimirchyuk, S. B., Shorning, B. U., Alekseeva, V. A., Yaguzhinsky, L. S., and Vanyushin, B. F. (1999a). Unusual fast sedimenting mitochondria producing heavy DNA in the cells of aging coleoptiles of wheat seedlings. *Biochemistry (Moscow)* **64,** 307–317.

Kirnos, M. D., Aleksandrushkina, N. I., Shorning, B. Y., Kudryashova, I. B., and Vanyushin, B. F. (1999b). Internucleosomal fragmentation and DNA synthesis in wheat seedlings. *Russ. J. Plant Physiol.* **46,** 48–57.

Kosslak, R. M., Chamberlin, M. A., Palmer, R. G., and Bowen, B. A. (1997). Programmed cell death in the root cortex of soybean root necrosis mutants. *Plant J.* **11,** 729–745.

Koukalova, B., Kovarik, A., Fajkus, J., and Siroky, J. (1997). Chromatin fragmentation associated with apoptotic changes in tobacco cells exposed to cold stress. *FEBS Lett.* **414,** 289–292.

Kovtun, Y., Chiu, W.-L., Tena, G., and Sheen, J. (2000). Functional analysis of oxidative stress-activated mitogen-activated protein kinase cascade in plants. *Proc. Natl. Acad. Sci. USA* **97,** 2940–2945.

Lacomme, C., and Cruz, S. S. (1999). Bax-induced cell death in tobacco is similar to the hypersensitive response. *Proc. Natl. Acad. Sci. USA* **96,** 7956–7961.

Lam, E., and del Pozo, O. (2000). Caspase-like protease involvement in the control of plant cell death. *Plant Mol. Biol.* **44,** 417–428.

Lam, E., Pontier, D., and del Pozo, O. (1999). Die and let live: Programmed cell death in plants. *Curr. Opin. Plant Biol.* **2,** 502–507.

Lam, E., Kato, N., and Lawton, M. (2001). Programmed cell death, mitochondria and the plant hypersensitive response. *Nature* **411,** 848–853.

Lee, H.-C., Yin, P.-H., Lu, C.-Y., Chi, C.-W., and Wei, Y.-H. (2000). Increase of mitochondria and mitochondrial DNA in response to oxidative stress in human cells. *Biochem. J.* **348,** 425–432.

Levine, A., Pennell, R. I., Alvarez, M. E., Palmer, R., and Lamb, C. (1996). Calcium-mediated apoptosis in a plant hypersensitive disease resistance response. *Curr. Biol.* **6,** 427–437.

Liljeroth, E., and Bryngelsson, T. (2001). DNA fragmentation in cereal roots indicative of programmed root cortical cell death. *Physiol. Plant.* **111,** 365–372.

Liljeroth, E., and Bryngelsson, T. (2002). Earlier onset of DNA fragmentation in leaves of wheat compared to barley and rye. *Hereditas.* **136,** 108–115.

Lockshin, R. A., and Williams, C. M. (1964). Programmed cell death. II. Endocrine potentiation of the breakdown of the intersegmental muscles of the silkmoths. *J. Insect Physiol.* **10,** 643–649.

Lockshin, R. A., and Zakeri, Z. (2001). Programmed cell death and apoptosis: Origins of the theory. *Nat. Rev.* **2,** 545–550.

LoSchiavo, F., Baldan, B., Compagnin, D., Ganz, R., Mariani, P., and Terzi, M. (2000). Spontaneous and induced apoptosis in embryogenic cell cultures of carrot (*Daucus carota* L.) in different physiological states. *Eur. J. Cell Biol.* **79,** 294–298.

Mayda, E., Tornero, P., Conejero, V., and Vera, P. (1999). A tomato homeobox gene (HD-zip) is involved in limiting the spread of programmed cell death. *Plant J.* **20,** 591–600.

Maxwell, D. P., Nickels, R., and McIntosh, L. (2002). Evidence of mitochondrial involvement in the transduction of signals required for the induction of genes associated with pathogen attack and senescence. *Plant J.* **29,** 269–279.

McCabe, P. F., and Leaver, C. J. (2000). Programmed cell death in cell cultures. *Plant Mol. Biol.* **44,** 359–368.

McCabe, P. F., Levine, A., Meijer, P. J., Tapon, N. A., and Pennel, R. I. (1997). A programmed cell death pathway activated in carrot cells cultured at low cell density. *Plant J.* **12,** 267–280.

Mittler, R., and Lam, E. (1995). Identification, characterization, and purification of a tobacco endonuclease activity induced upon hypersensitive response cell death. *Plant Cell* **7,** 1951–1962.

Mittler, R., and Lam, E. (1997). Characterization of nuclease activities and DNA fragmentation induced upon hypersensitive response cell death and mechanical stress. *Plant Mol. Biol.* **34,** 209–221.

Mittler, R., Shulaev, V., Seskar, M., and Lam, E. (1996). Inhibition of programmed cell death in tobacco plants during pathogen-induced hypersensitive response at low oxygen pressure. *Plant Cell* **8,** 1991–2001.

Mittler, R., Del Pozo, O., Meisel, L., and Lam, E. (1997a). Pathogen-induced programmed cell death in plants, a possible defense mechanism. *Dev. Genet.* **21,** 279–289.

Mittler, R., Simon, L., and Lam, E. (1997b). Pathogen-induced programmed cell death in tobacco. *J. Cell Sci.* **110,** 1333–1344.

Mittler, R., Feng, X., and Cohen, M. (1998). Post-transcriptional suppression of cytosolic ascorbate peroxidase expression during pathogen-induced programmed cell death in tobacco. *Plant Cell* **10,** 461–473.

Mlejnek, P., and Prochazka, S. (2002). Activation of caspase-like proteases and induction of apoptosis by isopentenyladenosine in tobacco BY-2 cells. *Planta* **215,** 158–166.

Moller, S. G., and McPherson, M. J. (1998). Developmental expression and biochemical analysis of the *Arabidopsis atao 1* gene encoding an H_2O_2-generating diamine oxidase. *Plant J.* **13,** 781–791.

Morel, J. B., and Dangl, J. L. (1997). The hypersensitive response and the induction of cell death in plants. *Cell Death Differ.* **4,** 671–683.

Nakayama, H., Kajikawa, S., Shinozuka, J., Su, W. P., and Doi, K. (1999). Possible involvement of DNA methylation in 5-azacytidine-induced neuronal cell apoptosis. *Histol. Histopathol.* **14,** 143–150.

Navarre, D. A., and Wolpert, T. J. (1999). Victorin induction of an apoptotic/senescence-like response in oats. *Plant Cell* **11,** 237–249.

Neill, S., Desikan, R., Clarke, A., Hurst, R. D., and Hancock, J. T. (2002a). Hydrogen peroxide and nitric oxide as signalling molecules in plants. *J. Exp. Bot.* **53,** 1237–1247.

Neill, S., Desikan, R., and Hancock, J. (2002b). Hydrogen peroxide signalling. *Curr. Opin. Plant Biol.* **5,** 388–395.

Ning, S. B., Song, Y. C., and Damme, P. P. (2002). Characterization of the early stages of programmed cell death in maize root cells by using comet assay and the combination of cell electrophoresis with annexin binding. *Electrophoresis* **23,** 2096–2102.

Nooden, L. D., Guiamet, J. J., and John, I. (1997). Senescence mechanisms. *Physiol. Plant* **101,** 746–753.

O'Brien, I. E. W., Reutelingsperger, C. P. M., and Holdaway, K. M. (1997). Annexin-V and TUNEL use in monitoring the progression of apoptosis in plants. *Cytometry* **29,** 28–33.

O'Brien, I. E. W., Baguley, B. C., Murray, B. G., Morris, B. A. M., and Ferguson, I. B. (1998a). Early stages of the apoptotic pathway in plant cells are reversible. *Plant J.* **13,** 803–814.

O'Brien, I. E. W., Murray, B. G., Baguley, B. C., Morris, B. A. M., and Ferguson, I. B. (1998b). Major changes in chromatin condensation suggest the presence of an apoptotic pathway in plant. *Exp. Cell Res.* **241,** 46–54.

Orzaez, D., and Granell, A. (1997a). The plant homologue of the defender against apoptotic death gene is down-regulated during senescence of flower petals. *FEBS Lett.* **404,** 275–278.

Orzaez, D., and Granell, A. (1997b). DNA fragmentation is regulated by ethylene during carpel senescence in *Pisum sativum*. *Plant J.* **11,** 137–144.

Orzaez, D., de Jong, A. J., and Woltering, E. J. (2001). A tomato homologue of the human protein PIRIN is induced during programmed cell death. *Plant Mol. Biol.* **46,** 459–468.

Pellinen, R., Palva, T., and Kangasjarvi, J. (1999). Subcellular localization of ozone-induced hydrogen peroxide production in birch (*Betula pendula*) leaf cells. *Plant J.* **20,** 349–356.

Pellinen, R. I., Korhonen, M. S., Tauriainen, A. A., Palva, E. T., and Kangasjarvi, J. (2002). Hydrogen peroxide activates cell death and defense gene expression in birch. *Plant Physiol.* **130,** 549–560.

Pennell, R., and Lamb, C. (1997). Programmed cell death in plants. *Plant Cell* **9,** 1157–1168.

Ranganath, R. M., and Nagashree, N. R. (2001). Role of programmed cell death in development. *Int. Rev. Cytol.* **202,** 159–242.

Robson, C. A., and Vanlerberghe, G. C. (2002). Transgenic plant cells lacking mitochondrial alternative oxidase have increased susceptibility to mitochondria-dependent and -independent pathways of programmed cell death. *Plant Physiol.* **129,** 1908–1920.

Rubinstein, B. (2000). Regulation of cell death in flower petals. *Plant. Mol. Biol.* **44,** 303–318.

Saitoh, F., Hiraishi, K., Adachi, M., and Hozumi, M. (1995). Induction by 5-aza-2′-deoxycytidine, an inhibitor of DNA methylation, of Le^y antigen, apoptosis and differentiation in human lung cancer cells. *Anticancer Res.* **15,** 2137–2143.

Schmid, M., Simpson, D., and Gietl, C. (1999). Programmed cell death in castor bean endosperm is associated with the accumulation and release of a cysteine endopeptidase from ricinosomes. *Proc. Natl. Acad. Sci. USA* **96,** 14159–14164.

Shorning, B. Y., Poleshchuk, S. V., Gorbatenko, I. Y., and Vanyushin, B. F. (1999). The antioxidant effect on plant growth and development. *Izv. RAN. Ser. Biol.* **1,** 30–38.

Shorning, B. Y., Smirnova, E. G., Yaguzhinsky, L. S., and Vanyushin, B. F. (2000). Necessity of superoxide production for development of etiolated wheat seedlings. *Biochemistry (Moscow)* **65,** 1357–1361.

Skalamera, D., and Heath, M. C. (1998). Changes in cytoskeleton accompanying infection-induced nuclear movements and the hypersensitive response in plant cells invaded by rust fungi. *Plant J.* **16,** 191–200.

Skulachev, V. P. (1999). Mitochondrial physiology and pathology: Concepts of programmed death of organelles, cells and organisms. *Mol. Aspects Med.* **20,** 139–184.

Skulachev, V. P. (2001). The programmed death phenomena, aging, and the samurai law of biology. *Exp. Gerontol.* **36,** 995–1024.

Skulachev, V. P. (2002). Programmed death phenomena: From organelle to organism. *Ann. N. Y. Acad. Sci.* **959,** 214–237.

Smart, C. M. (1994). Gene expression during leaf senescence. *New Phytol.* **126,** 419–448.

Smirnova, E. G., Lyubimov, Y. I., Malinina, T. G., Lyubimova, E. Y., Aleksndrushkina, N. I., Vanyushin, B. F., and Yaguzhinsky, L. S. (2002). BHT (ionol) produces superoxide-anion. *Biochemistry (Moscow)* **67,** 1539–1544.

Stancheva, I., Hensey, C., and Meehan, R. R. (2001). Loss of the maintenance methyltransferase, xDnmt1, induces apoptosis in *Xenopus* embryos. *EMBO J.* **20,** 1963–1973.

Sugimoto, A., Hozak, R. R., Nakashima, T., Nishimoto, T., and Rothman, J. H. (1995). dad-1, an endogenous programmed cell death suppressor in *Caenorhabditis elegans* and vertebrates. *EMBO J.* **14,** 4434–4441.

Sun, Y. L., Zhao, Y., Hong, X., and Zhai, Z.-H. (1999a). Cytochrome *c* release and caspase activation during menadione-induced apoptosis in plants. *FEBS Lett.* **462,** 317–321.

Sun, Y. L., Zhu, H. Z., Zhou, J., Dai, Y. R., and Zhai, Z. H. (1999b). Menadione-induced apoptosis and the degradation of lamin-like proteins in tobacco protoplasts. *Cell. Mol. Life Sci.* **55,** 310–316.

Tamagnone, L., Merida, A., Stacey, N., Plaskitt, K., Parr, A., Chang, C. F., Lynn, D., Dow, M. J., Roberts, K., and Martin, C. (1998). Inhibition of phenolic acid metabolism results in precocious cell death and altered cell morphology in leaves of transgenic tobacco plants. *Plant Cell* **10,** 1801–1816.

Tanaka, Y., Makishima, T., Sasabe, M., Ichinose, Y., Shiraishi, T., Nishimoto, T., and Yamada, T. (1997). *dad-1*: A putative programmed cell death suppressor gene in rice. *Plant Cell Physiol.* **38,** 379–383.

Thelen, M. P., and Northcote, D. H. (1989). Identification and purification of a nuclease from *Zinnia elegans* L.: A potential marker for xylogenesis. *Planta* **179,** 181–195.

Thomas, H., Ougham, H. J., Wagstaff, C., and Stead, A. D. (2003). Defining senescence and death. *J. Exp. Bot.* **54,** 1127–1132.

Vanyushin, B. F. (1984). Replicative DNA methylation in animals and higher plants. *Curr. Top. Microbiol. Immunol.* **108,** 99–114.

Vanyushin, B. F. (2001). Apoptosis in plants. *Usp. Biol. Khim.* **41,** 3–38.

Vanyushin, B. F., and Berdyshev, G. D. (1977). "Molecular and Genetic Mechanisms of Aging" pp. 3–295. Meditsina Press, Moscow.

Vanyushin, B. F., and Kirnos, M. D. (1988). DNA methylation in plants. *Gene* **74,** 117–121.

Vanyushin, B. F., Alexandrushkina, N. I., and Kirnos, M. D. (1988). N^6-Methyladenine in mitochondrial DNA of higher plants. *FEBS Lett.* **233,** 397–399.

Vanyushin, B. F., Sevost'yanova, S. S., Kirnos, M. D., and Saidova, N. S. (1990). Increase in protein content in wheat seeds induced by 5-azacytidine: An inhibitor of DNA methylation. *Izv. Akad. Nauk SSSR Ser. Biol.* **1,** 75–83.

Vanyushin, B. F., Lopatina, N. G., Wise, C. K., Fullerton, F. R., and Poirier, L. A. (1998). Butylated hydroxytoluene modulates DNA methylation in rats. *Eur. J. Biochem.* **256,** 518–527.

Vanyushin, B. F., Shorning, B. Y., Seredina, A. V., and Aleksandrushkina, N. I. (2002). Influence of phytohormones and 5-azacytidine on apoptosis in etiolated wheat seedlings. *Russ. J. Plant Physiol.* **49,** 558–564.

Vardi, A., Berman-Frank, I., Rozenberg, T., Hadas, O., Kaplan, A., and Levine, A. (1999). Programmed cell death of the dinoflagellate *Peridinium gatunense* is mediated by CO_2 limitation and oxidative stress. *Curr. Biol.* **9,** 1061–1064.

Vorontsova, M. A., and Liozner, L. D. (1955). "Physiological Regeneration" pp. 3–508. Sovjet Science Press, Moscow.

Wang, M., Oppedijk, B. J., Lu, X., van Duijn, B., and Schilperoort, R. A. (1996). Apoptosis in barley aleurone during germination and its inhibition by abscisic acid. *Plant Mol. Biol.* **32,** 1125–1134.

Wang, M., Hoekstra, S., van Bergen, S., Lamers, G. E., Oppedijk, B. J., van der Heijden, M. W., de Priester, W., and Schilperoort, R. A. (1999). Apoptosis in developing anthers and the role of ABA in this process during androgenesis in *Hordeum vulgare* L. *Plant Mol. Biol.* **39,** 489–501.

Woffenden, B. J., Freeman, T. B., and Beers, E. P. (1998). Proteasome inhibitors present tracheary element differentiation in *Zinnia* mesophyll cell cultures. *Plant Physiol.* **118,** 419–430.

Wu, H.-M., and Cheung, A. Y. (2000). Programmed cell death in plant reproduction. *Plant Mol. Biol.* **44,** 267–281.

Xu, Y., and Hanson, M. R. (2000). Programmed cell death during pollination-induced petal senescence in *Petunia*. *Plant Physiol.* **122,** 1323–1333.

Yamada, T., Marubashi, W., and Niwa, M. (2001). Facile induction of apoptosis into plant cells associated with temperature-sensitive lethality shown on interspecific hybrid from the cross *Nicotiana suaveolens* × *N. tabacum*. *Plant Cell Physiol.* **42,** 204–213.

Yamamoto, R., Demura, T., and Fukuda, H. (1997). Brassinosteroids induce entry into the final stage of tracheary element differentiation in cultured *Zinnia* cells. *Plant Cell Physiol.* **38,** 980–983.

Yen, C. H., and Yang, C. H. (1998). Evidence for programmed cell death during leaf senescence in plants. *Plant Cell Physiol.* **39,** 922–927.

Young, T. E., and Gallie, D. R. (1999). Analysis of programmed cell death in wheat endosperm reveals differences in endosperm development between cereals. *Plant Mol. Biol.* **39,** 915–926.

Young, T. E., and Gallie, D. R. (2000). Programmed cell death during endosperm development. *Plant Mol. Biol.* **42,** 397–414.

Young, T. E., Gallie, D. R., and DeMason, D. A. (1997). Ethylene-mediated programmed cell death during maize endosperm development of *Su* and *sh2* genotypes. *Plant Physiol.* **115,** 737–751.

Zamyatnina, V. A., Bakeeva, L. E., Aleksandrushkina, N. I., and Vanyushin, B. F. (2002a). Apoptosis in etiolated wheat seedlings. 1. Specific ultrastructure of apoptotic cell. *Russ. J. Plant Physiol.* **49,** 1–11.

Zamyatnina, V. A., Bakeeva, L. E., Aleksandrushkina, N. I., and Vanyushin, B. F. (2002b). Apoptosis in the initial leaf of etiolated wheat seedlings: Influence of the antioxidant ionol (BHT) and peroxides. *Biochemistry (Moscow)* **67,** 212–221.

Zamyatnina, V. A., Bakeeva, L. E., Aleksandrushkina, N. I., and Vanyushin, B. F. (2003). Apoptosis in etiolated wheat seedlings. 2. Effects of the antioxidant butylated hydroxytoluene and peroxides. *Russ. J. Plant Physiol.* **50,** 251–260.

Zhao, Y., Jiang, Z. F., Sun, Y. L., and Zhai, Z. H. (1999). Apoptosis of mouse liver nuclei induced in the cytosol of carrot cells. *FEBS Lett.* **448,** 197–200.

Zhivotovsky, B. (2002). From the nematode and mammals back to the pine tree: On the diversity and evolution of programmed cell death. *Cell Death Differ.* **9,** 867–869.

Zhou, J., Zhuo, H. Z., and Dai, Y. R. (1999). Effect of ethrel on apoptosis in carrot protoplasts. *Plant Growth Regul.* **27,** 119–123.

This Page Intentionally Left Blank

Cell Biology of Leydig Cells in the Testis

Syed G. Haider
Institute of Anatomy II, Heinrich Heine University, D-40225 Düsseldorf, Germany

This article reviews results on differentiation, structure, and regulation of Leydig cells in the testes of rodents and men. Two different populations—fetal and adult Leydig cells—can be recognized in rodents. The cells in these two populations are different in ultrastructure, life span, capacity for androgen synthesis, and mechanisms of regulation. A brief survey on the origin, ontogenesis, characterization of precursors, ultrastructure, and functional markers of fetal and adult Leydig cells is presented, followed by an analysis of genes in Leydig cells and the role of luteinizing hormone and its receptor, steroidogenic acute regulatory protein, hydroxysteroid dehydrogenases, androgen and its receptor, anti-Müllerian hormone, estrogens, and thyroid hormones. Various growth factors modulate Leydig cell differentiation, regeneration, and steroidogenic capacity, for example, interleukin 1α, transforming growth factor β, inhibin, insulin-like growth factors I and II, vascular endothelial growth factor, and relaxin-like growth factor. Retinol and retinoic acid increase basal testosterone secretion in adult Leydig cells, but decrease it in fetal Leydig cells. Resident macrophages in the interstitial tissue of the testis are important for differentiation and function of Leydig cells. Apoptosis of Leydig cells is involved in the regulation of Leydig cell number and can be induced by cytotoxins. Characteristics of aging Leydig cells in rodents seem to be species specific. 11β-Hydroxysteroid dehydrogenase protects testosterone synthesis in the Leydig cells of stressed rats. Last, the following aspects of human Leydig cells are briefly described: origin, differentiation, triphasic development, aging changes, pathological changes, and gene mutations leading to infertlity.

KEY WORDS: Testis, Leydig cells, Leydig cell precursors, Differentiation, Steroidogenesis, Hydroxysteroid dehydrogenases, Growth factors, Apoptosis.

I. Introduction

Reviews on Leydig cells have been published on various aspects, for example, origin, proliferation, and differentiation of fetal and adult Leydig cells; their functional maturation, endocrine regulation, and communicating functions; as well as their endocrine, paracrine, and autocrine regulation (Dufau, 1988; Habert *et al*., 2001; Huhtaniemi and Bartke, 2001; Huhtaniemi *et al*., 1984; Lejeune *et al*., 1998; Mendis-Handagama and Ariyaratne, 2001; Saez, 1994; Tähkä, 1986). The book *The Leydig Cells*, edited by Payne, Hardy, and Russell (1996), is an excellent source of information and a bibliography of important research papers on various aspects of Leydig cells that have been published since the discovery of these cells by Franz Leydig (1850). The aim of the present review is to present the current state of knowledge on the cell biology of Leydig cells, with particular emphasis on morphological aspects of differentiation and functional maturation; also, advances in gene analysis, and apoptosis of Leydig cells, are included herein. The article reviews results on the differentiation and maturation of Leydig cells in rodents, particularly in rats, as this species has been extensively studied. Human Leydig cells are described separately at the end of this review (Section V).

II. Differentiation of Leydig Cells

Two morphologically and functionally different populations of Leydig cells can be recognized in the rat testis: (1) fetal Leydig cells (FLCs; see Figs. 1–3) and (2) adult Leydig cells (ALCs; see Fig. 4) (Ariyaratne *et al*., 2000a; Haider and Servos, 1998; Haider *et al*., 1986; Hardy *et al*., 1989; Kuopio *et al*., 1989b; Lording and de Kretser, 1972; Majdic *et al*., 1998). Table I summarizes the ultrastructural characteristics of these two cell types and mentions the common features as well as the differences between FLCs and ALCs.

FIG. 1 (a) Fetal day 14.5. A precursor of rat fetal Leydig cells with tubulovesicular mitochondria and a lipid droplet (thin arrow) in the interstitium; lamina propria (thick arrow) of a seminiferous cord (Sc). At right below is a portion of a fetal Leydig cell with lipid droplets. Bar: 1 μm. Original magnification, ×9000. (b) Fetal day 16.5. A large, round fetal Leydig cell surrounded in semicircular pattern by an adjacent fetal Leydig cell. Lipid droplets (arrows); cell contacts between the two fetal Leydig cells (arrowheads). Bar: 1 μm. Original magnification, ×12,000. (c) Fetal day 16.5. Ultrastructure of tubulovesicular mitochondria in a fetal Leydig cell with two desmosome-like cell contacts (arrows) with an adjacent fetal Leydig cell. Bar: 1 μm. Original magnification, ×27,000.

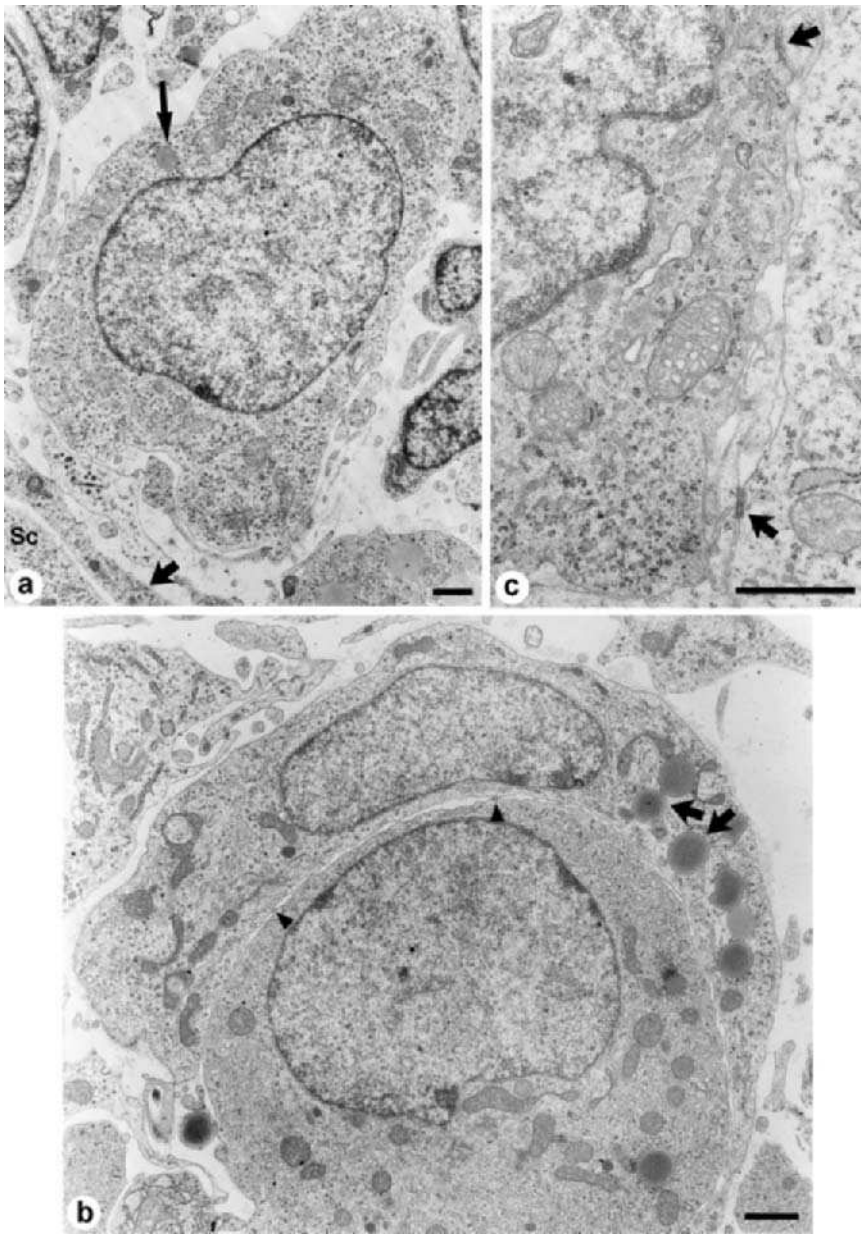
Sc
a
c
b

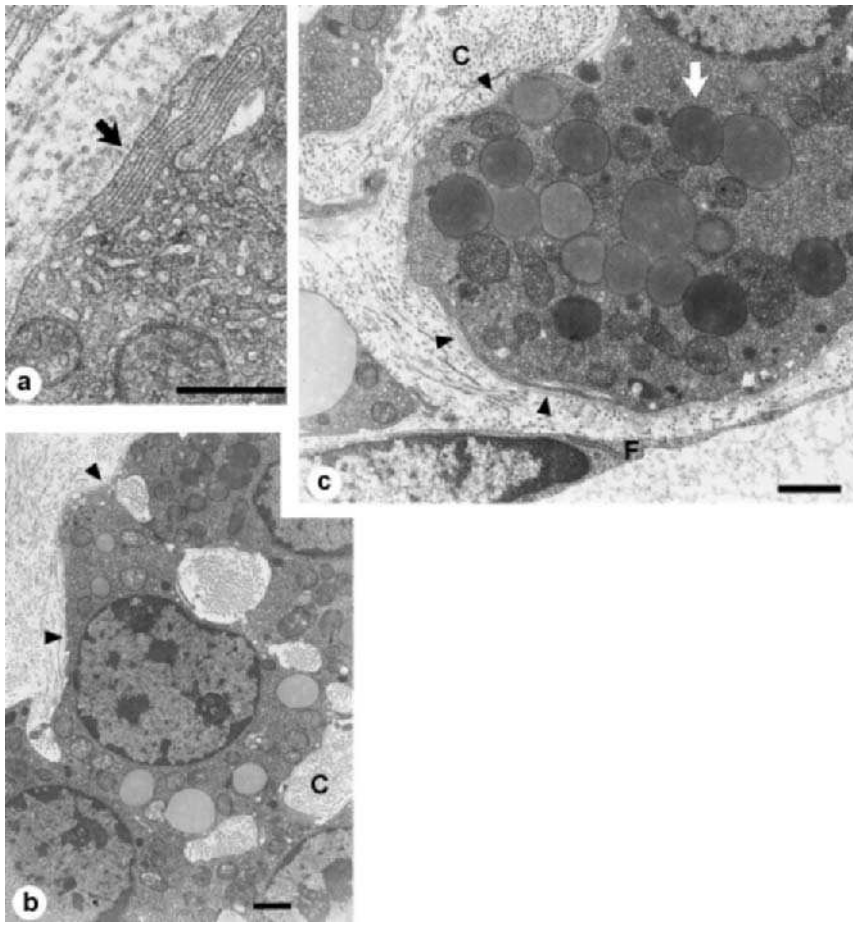

FIG. 2 Fetal day 18. Rat testis. Details of the ultrastructure of fetal Leydig cells. (a) Finger-like flat protrusions at the cell membrane (arrow); the protrusions consist constantly of 50- to 60-nm-thick processes with a 25-nm-wide space between the two adjacent processes. These processes contain cross-sections of cytoskeletal filaments and lie piled on each other between two adjacent fetal Leydig cells or between a fetal Leydig cell and the collagen fibers within a cluster of fetal Leydig cells. Bar: 0.5 μm. Original magnification, ×51,000. (b) Nuclei of four fetal Leydig cells in a cluster surrounded by basal lamina (arrowheads), which is also present around the cells within the cluster. The intercellular spaces are filled with collagen fibers (C). Bar: 1 μm. Original magnification, ×8000. (c) A portion of a fetal Leydig cell within a cluster with a fibroblast (F) lying at the periphery of the cluster. The basal lamina (arrowheads) surrounds the Leydig cell completely. The Leydig cell contains mitochondria with tubulovesicular cristae, SER, and large round lipid droplets (open arrow). Collagen fibers (C). Bar: 1 μm. Original magnification, ×14,000.

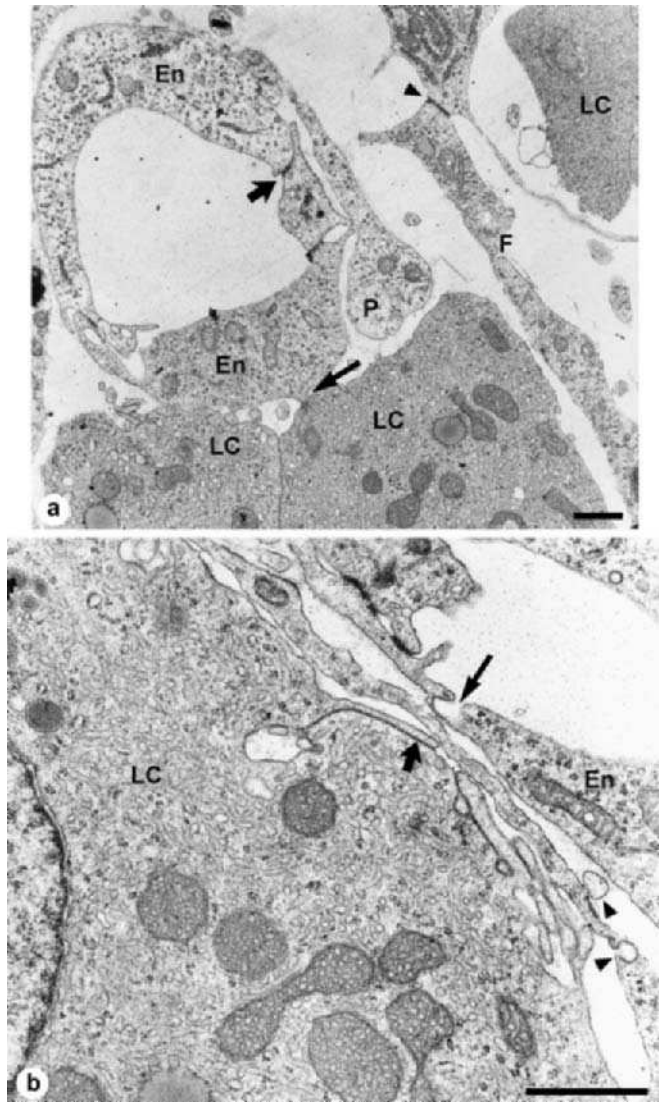

FIG. 3 Fetal day 18.5. Rat testis. (a) Three fetal Leydig cells (LC) in perivascular region around a fenestrated interstitial blood capillary. Vascular endothelial cells (En); a pericyte (P); a perivascular fibroblast (F); a direct cell contact between a fetal Leydig cell and the vascular endothelial cell (thin arrow); a cell contact between the two neighboring vascular endothelial cells (thick arrow); a membrane-thickened cellular contact between the two adjacent fibroblasts (arrowhead). Bar: 1 μm. Original magnification, ×12,000. (b) A perivascular fetal Leydig cell (LC) in close vicinity of a vascular endothelial cell (En); membranous interdigitation between the Leydig cell and the blood capillary (thick arrow); Omega figures (arrowheads) and a wide fenestration (arrow) of the blood capillary. Bar: 1 μm. Original magnification, ×30,000.

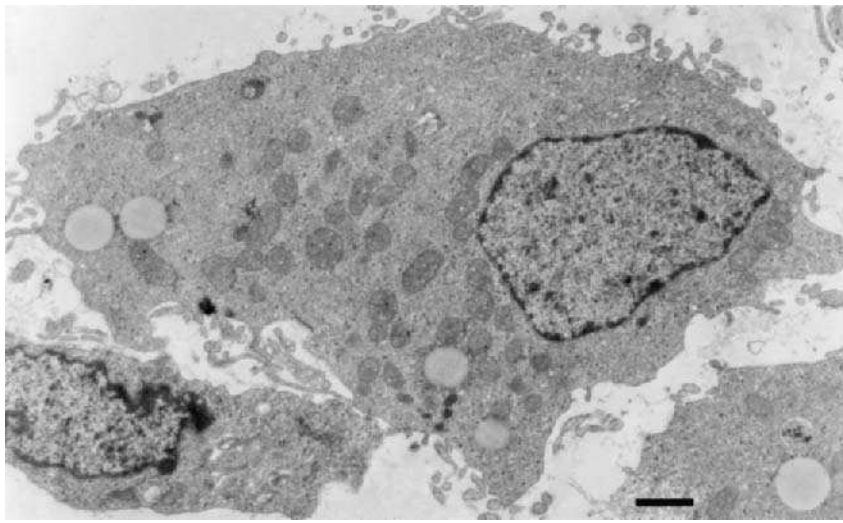

FIG. 4 Postnatal day 35. Ultrastructure of an adult Leydig cell in rat. A large amount of SER, many mitochondria with tubulovesicular cristae, and only a few small lipid droplets are the main features. Below, left: A portion of a neighboring fibroblast. Bar: 1 μm. Original magnification, ×11,000.

A. Fetal Leydig Cells

Table II shows the time of first morphological appearance of various tissues in male fetal gonad and mesonephros of rat, as revealed by electron microscopy. Mesonephros with mesenchymal fibroblasts is observed from fetal day (fd) 12 onward. The precursors for FLCs (Fig. 1a) originate from the mesenchymal fibroblasts. Fetal day 14.5 seems to be the turning point for the differentiation of FLC precursors for the following two reasons: (1) *ultrastructure*: the oval-shaped FLC precursors contain smooth endoplasmic reticulum (SER), mitochondria of tubulovesicular type, and a few small lipid droplets (Fig. 1a); they are clearly distinguishable from the normal mesenchymal fibroblasts, which are largely spindle-shaped, with elongated nucleus, rough endoplasmic reticulum (RER), and do not contain tubulovesicular mitochondria, SER, and lipid droplets; and (2) from fd 14.5 onward these cells express luteinizing hormone (LH) receptor and synthesize 3β-hydroxysteroid dehydrogenase (3β-HSD) (Haider *et al.*, 1986; Huhtaniemi and Pelliniemi, 1992; Majdic *et al.*, 1998; Ziegler *et al.*, 1983). The beginning of the formation of testicular cords is observed for the first time on fd 14.5. The peritubular cells of mesenchymal origin build the wall of the testicular cords. The formation of testicular cords starts first at the cortex of the gonad and progresses gradually toward the hilus near

TABLE I
Ultrastructural Features of Fetal and Adult Leydig Cells: A Comparison[a]

Features	In fetal LC	In adult LCs	Common in both types
Nucleus	Round with smooth membranes	Elliptic or round with curly membranes	Thick euchromatin, numerous nuclear pores
Smooth ER			Present in abundance
RER	Largely absent	Only a few	
Mitochondria			Tubulovesicular cristae
Golgi apparatus	Small to moderate size	Large and well differentiated	
Lipid droplets	Numerous; diameter, 0.9 μm	A few; diameter, 0.5 μm	
Cell contacts	With other FLCs	With ALCs and fibroblasts	25-nm space contacts with adjacent LCs
Microvilli			Accumulation in localized spaces
Surface	Numerous, finger-like protrusions	A few, small protrusions	
Basal lamina	Present, of various thickness	Absent	
Arranged	In clusters	Not exclusively in clusters	

Abbreviations: ALC, adult Leydig cell; ER, endoplasmic reticulum; FLC, fetal Leydig cell; RER, rough endoplasmic reticulum. [a]References: Haider (unpublished data); Haider *et al.* (1995); Kuopio *et al.* (1989a,b).

the mesonephros (Fig. 5). On fd 16 many FLCs can be observed in the interstitium with distinct ultrastructural features for a steroid-building cell. The FLCs are now large and round with a round nucleus, an abundance of SER, tubulovesicular mitochondria, and many lipid droplets (Fig. 1b). The FLCs build clusters for the first time on fd 16, are surrounded by a basal lamina and at the outermost boundary by a sheath of spindle-shaped fibroblasts. The temporal coincidence of FLC differentiation with the formation of testicular cords on fd 16 is clear. It can be speculated that the peritubular fibroblasts contribute to the trigger mechanisms that initiate FLC differentiation via local growth factors (Skinner, 1991).

TABLE II
Time of First Appearance of Structures in Fetal Testis and Mesonephros in Rat and of Identification of Substances in Fetal Leydig Cells[a]

	Fetal day					
	10	12.5	14.5	15.5	16.5	18.5
Mesonephros	–/–	Present	Present	Present	Present	Present
Germinal epithelium	–/–	Present	Present	Present	Present	Present
Gonadal anlage	–/–	–/–	Present	Testis	Testis	Testis
Sertoli cells	–/–	Precursors	Precursors	Precursors	Present	Present
Mesenchymal fibroblasts	Present	Present	Present	Present	Present	Present
Testicular cords	–/–	–/–	–/–	Only a few	In cortex	Many
FLC precursors	–/–	–/–	Only a few	Increasing	Many	Many
FLCs	–/–	–/–	–/– (?)	Present	7.7×10^3	16.1×10^3
Basal lamina around FLCs					Present	Present
LH receptor in FLCs				+	+	++
3β-HSD in FLCs			+	+	++	+++
SF-1 in FLCs				+	++	++
Inhibin in FLCs			+	++	+++	+++
AR in peritubular cells				–/–	+	++

Abbreviations: AR, androgen receptor; 3β-HSD, 3β-hydroxysteroid dehydrogenase; LH, luteinizing hormone; SF-1, steroidogenic factor 1. [a]References: Byskov (1986); Habert *et al.* (2001); Haider *et al.* (1986); Majdic and Saunders (1996); Majdic *et al.* (1995, 1997, 1998); Ziegler *et al.* (1983).

On fd 16, the FLCs show an even, moderate intensity of 3β-HSD. These cells are exclusively arranged in large compact clusters in the interstitial spaces or triangles between the seminiferous cords. The cells and their nuclei are large, and round in shape. The cytoplasm contains SER, mitochondria with tubular as well as saccular cristae (''tubulovesicular''), a small to moderately sized Golgi apparatus, and many lipid droplets of various sizes (average diameter, 0.9 μm). Cell contacts are observed between adjacent FLCs but not between an FLC and the surrounding fibroblast. The cell membrane possesses numerous characteristic flat, finger-like, polyhedral, and interdigitating protrusions; these protrusions contain cytoskeletal filaments and show a constant thickness of 50–60 nm, with a 25-nm-wide space between the membranes of two adjacent protrusions (Fig. 2a). These

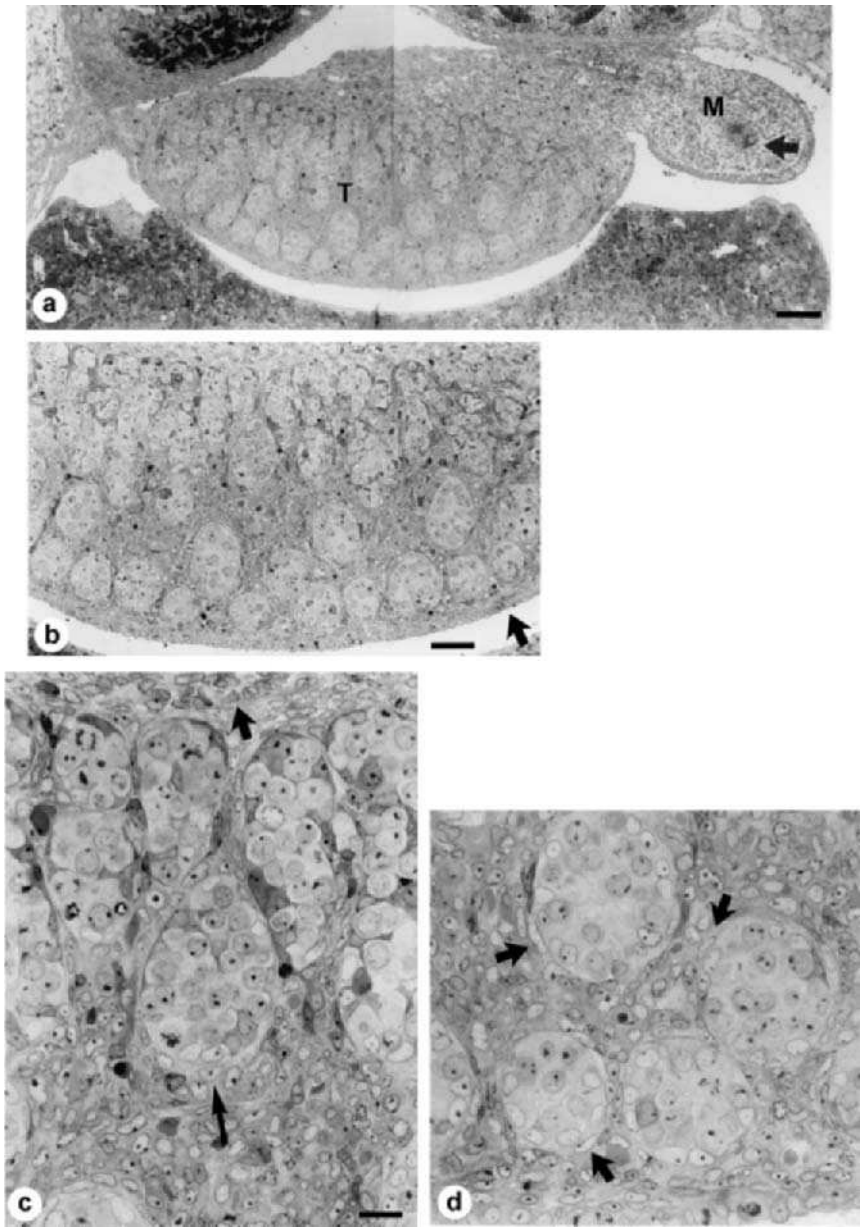

FIG. 5 Fetal day 16. (a) Rat testis (T) and mesonephros (M) with wolffian duct (arrow). Bar: 80 μm. (b) Magnification of a portion of testis in (a). Tunica albuginea (arrow). Bar: 55 μm. (c) Magnification of a portion from the upper half of (b); flat and spindle-shaped mesenchymal fibroblasts from mesonephros (thick arrow). The process of formation of testicular cords is here visible but not completed, a peritubular fibroblast (thin arrow). Bar [also for (d)]: 15 μm. (d) Magnification of a portion from the lower half of (b); the formation of testicular cords is here completed; peritubular fibroblasts (arrows).

protrusions either touch similar protrusions from an adjacent FLC or surround the collagen fiber bundles lying between the FLCs of a cluster. The FLCs are surrounded by a continuous basal lamina of various thickness (Fig. 2b and c). Kuopio *et al.* (1989a) were the first to show the basal membrane around rat FLCs and to demonstrate the presence of laminin and collagen type IV in the basal membrane. After birth, the basal membrane becomes discontinuous. A membrane cleft, consistently 25 nm in width, is present between neighboring FLCs. The FLC clusters are regularly surrounded by at least one layer of fibroblasts, which are joined together via cytoplasmic extensions. The fibroblasts in this sheath were designated by Kuopio *et al.* (1989b) as "envelope cells." Within an FLC cluster, bundles of collagen fibers are observed frequently between the individual FLCs (Fig. 2b).

The exact trigger mechanism—hormonal as well as nonhormonal—for the differentiation of FLCs is not known. There are reports providing evidence that the differentiation and proliferation of FLCs are independent of pituitary gonadotropins (Baker and O'Shaughnessy, 2001; Majdic *et al.*, 1998; O'Shaughnessy *et al.*, 1998). The proliferation of FLCs remains largely unaffected in rats treated with an antiandrogen, cyproterone acetate, during prenatal and postnatal phases (Haider *et al.*, 1983). Androgen receptor is present in the peritubular cells and not in FLCs from fd 17 onward (Majdic *et al.*, 1995). The steroidogenic factor SF-1 is present in 3β-HSD-positive FLCs from fd 17.5 onward (Majdic and Saunders, 1996). The α subunit of inhibin is expressed in rat FLCs from fd 14.5 onward; the high intensity during the fetal period decreases postnatally (Majdic *et al.*, 1997).

Another factor, which has been mentioned often in the literature, is the rapid proliferation of vascular endothelial cells in the interstitium, visible already on fd 12 to 14 and with a maximum degree on fd 16 (for references see Byskov, 1986). Growth factors from endothelial cells may contribute to FLC differentiation (see Section II.B for ALCs). Special cell contacts between perivascular FLCs and the endothelial cells of blood capillaries are often observed (Fig. 3a and b). These capillaries are fenestrated (Fig. 3). Gap junctions and special desmosome-like cell contacts are observed between adjacent FLCs (Fig. 3). No information is available concerning whether macrophages provide growth factors or other stimuli to initiate or regulate FLC differentiation. The peak of FLC proliferation lies between fd 18 and fd 19 (Ziegler *et al.*, 1983). Androgens from FLCs are required for gonadogenesis, formation of ALC precursors, differentiation and morphogenesis of the male genital tract, and sexual "male imprinting" of the brain.

Two sources for the precursors of FLCs have been reported in the literature: (1) mesenchymal fibroblasts from the mesonephros (Fig. 5)

and (2) mesenchymal fibroblasts from the gonadal ridge (Buher *et al.*, 1993; Byskov, 1986; de Kretser and Kerr, 1994; Merchant-Larios and Moreno-Mendoza, 1998; Merchant-Larios *et al.*, 1993; Nishino *et al.*, 2001). Most of these authors agree, however, on the mesonephros as an origin for FLC precursors. There are reports, showing coelomic epithelium as an additional source (''not the major source'') for FLC precursors in mouse; the coelomic epithelium produces a low level of SF-1, thus contributing to FLC differentiation (Brennan *et al.*, 2003). Employing two neural crest reporter lines, Brennan *et al.* (2003) found no evidence for a significant contribution of the neural crest to the differentiation of FLCs in mouse.

Another point, which has been controversial, is the ultimate fate of the FLC. According to some reports, FLCs are not identifiable at the light microscopic level after postnatal day (pnd) 30 (Haider *et al.*, 1983, 1986; Kuopio *et al.*, 1989b). However, there are reports, showing the presence of FLCs in rat until pnd 90 (Ariyaratne *et al.*, 2000a; Kerr and Knell, 1988). Ontogenesis of the enzymes 3β-HSD, 3α-HSD, and 17β-HSD in the FLC has been reported by various authors (Dupont *et al.*, 1993; Haider *et al.*, 1986; Schäfers *et al.*, 2001), using enzyme histochemical and immune histochemical methods. Kuopio *et al.* (1989b) described three consecutive development stages in prepubertal rats: (1) fetal (FLCs in the fetal testis), (2) early juvenile (FLCs during neonatal–early juvenile life), and (3) juvenile–adult (adult cells before and after puberty). At the electron microscopic level Haider and Servos (1998) showed the presence of 3β-HSD in the membranes, predominantly the outer membrane, of SER in FLCs. Figure 6 summarizes the main events in the differentiation of FLCs in rat.

B. Adult Leydig Cells

Hardy *et al.* (1989) subdivided the postnatal differentiation of rat Leydig cells into three stages: (1) *progenitor stage*: Leydig cells originate from mesenchyme-like fibroblasts (pnd 14–28) and produce androsterone as the predominant androgen end product; (2) *immature stage*: Leydig cells produce small amounts of testosterone on about pnd 35 and metabolize most of this testosterone, the predominant androgen end product being 5α-androstane-3α, 17β-diol; and (3) *mature stage*: Leydig cells actively produce testosterone as androgen end product and are fully functional in the sexually mature animal, by pnd 90 (Hardy *et al.*, 1990; Shan and Hardy, 1992; Shan *et al.*, 1995, 1997). Figure 7 schematically represents the main steps in the differentiation of ALCs in rat.

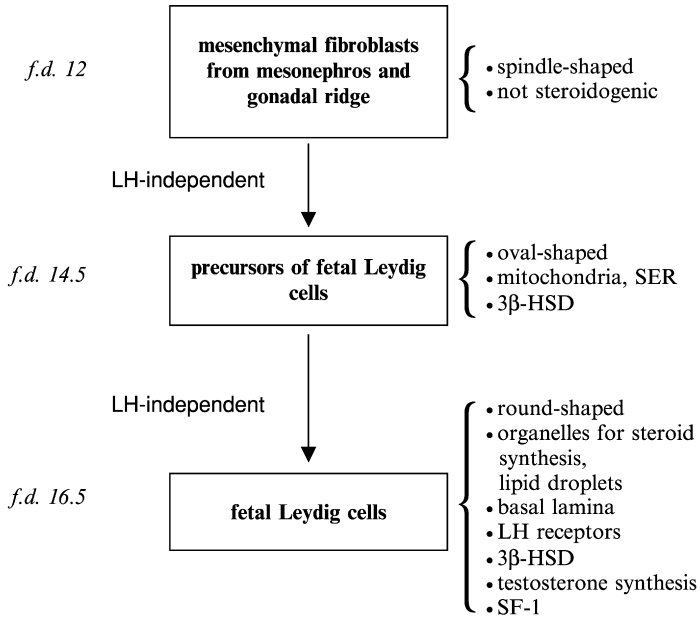

FIG. 6 Schematic diagram of the differentiation of fetal Leydig cells in rat (for references see text).

1. ALC Precursors

The earliest appearance of ALCs in rat testis has been reported as pnd 10 by Ariyaratne *et al.* (2000a) and pnd 13 by Haider *et al.* (1995). Fibroblasts lying in the outer peritubular layer (Fig. 8a) as well as in the perivascular region (Fig. 9a) are the precursors of ALCs ("progenitors" in the classification of Hardy *et al.*, 1989), as shown by the presence of 3β-HSD in these cells at the electron microscopic level (Haider and Servos, 1998). Peritubular fibroblasts in the outer layer of the lamina propria (also known as boundary tissue) and perivascular fibroblasts show ultrastructural features typical of a fibroblast. However, from pnd 10 to pnd 13—at the earliest—and thereafter, these cells contain in addition organelles typical of steroid-synthesizing cells, that is, SER, tubulovesicular mitochondria, and lipid droplets (Fig. 8a). Autoradiographic double-labeling experiments with [^{3}H]thymidine and [^{14}C]thymidine revealed that these precursors of ALCs show the highest labeling index and a duration of DNA synthesis (S phase) of 10 h from pnd 9 to 23 (Fig. 10). The ALC precursors show the highest proliferative capacity. The absolute number of fibroblasts shows a peak on pnd 13 and then decreases gradually with age (Haider *et al.*, 1995). These precursors of

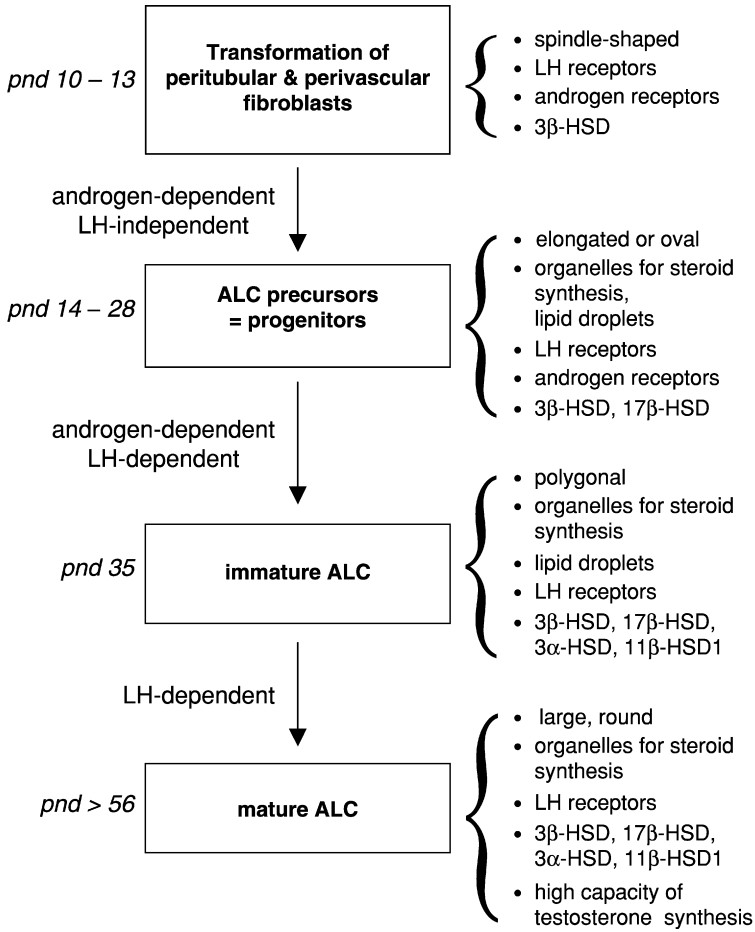

FIG. 7 Schematic diagram of the differentiation of adult Leydig cells in rat (for references see text).

ALCs contain LH receptors, androgen receptors, 3β-HSD, 3α-HSD, and 17β-HSD (Ge *et al.*, 1996).

2. Immature and Mature ALCs

The transition of precursors into ALCs is also reflected by changes in form and shape: precursors are thin and spindle-shaped; as they mature, their size increases gradually and their shape changes from slender to oval and then finally to large and round. On about pnd 30 ALCs are located around the

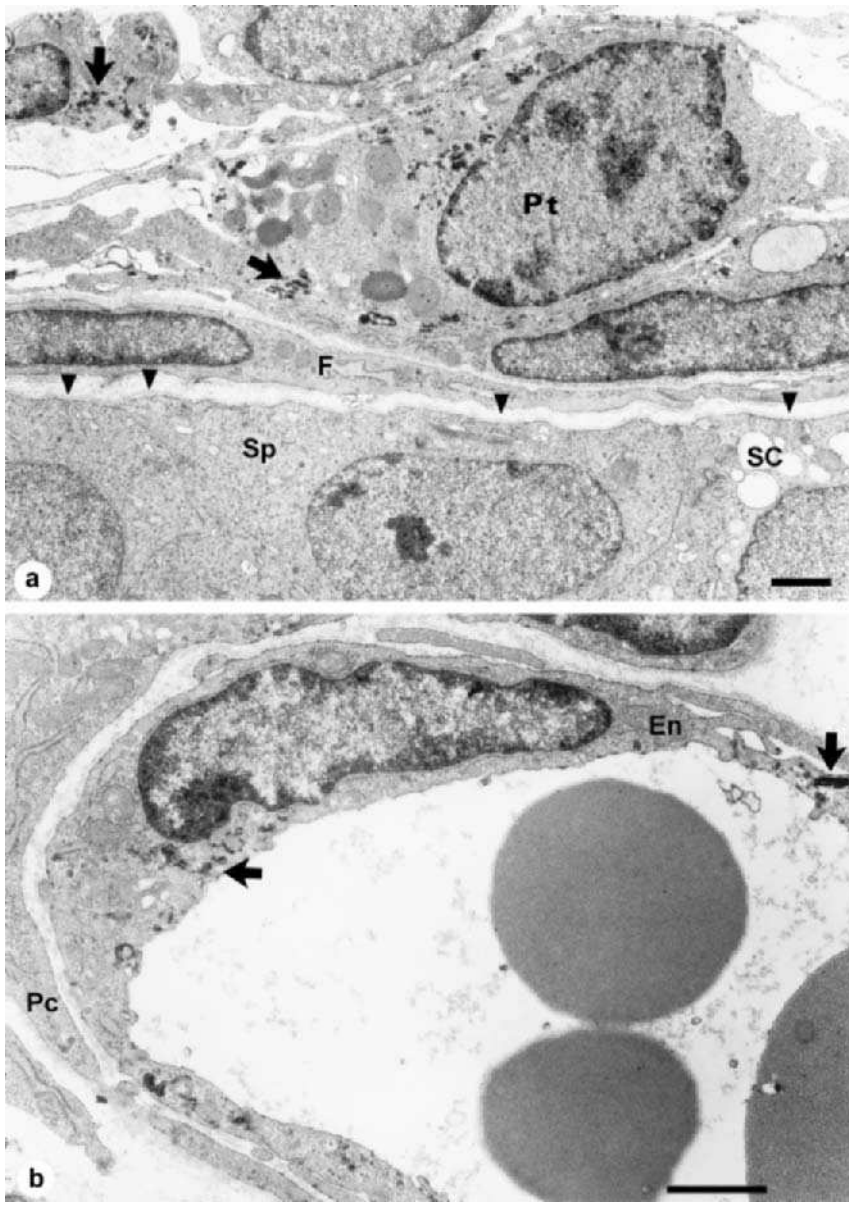

FIG. 8 Postnatal day 15. Rat testis. (a) Localization of 3β-HSD at electron microscopic level in a peritubular precursor (Pt) of an adult Leydig cell. The enzymatic reaction product is localized in the form of electron-dense granules on the membranes of SER (arrow) of the precursor cell. No enzymatic reaction product in a peritubular fibroblast (F), a Sertoli cell (SC), and a spermatogonia (Sp). Basal lamina (arrowheads) surrounding the seminiferous cord. Bar: 1 μm.

seminiferous tubules homogeneously, and perivascularly in close association with interstitial blood capillaries. The nuclei are large and round with condensed euchromatin and with one or two nucleoli. The cytoplasm contains large amounts of SER, a high number of tubulovesicular mitochondria, a well-differentiated Golgi apparatus, and small lipid droplets (average diameter, 0.5 μm) (Fig. 4). Unlike FLCs, ALCs are not surrounded by a basal membrane and are not always surrounded by an "envelope" of fibroblasts.

Microvilli are present only focally in large number; occasionally small membrane protrusions are observed. ALCs are connected with adjacent ALCs and fibroblasts by cell contacts with a constant 25-nm cleft (Table I). The cells contain LH receptors, 3β-HSD, 3α-HSD, and 17β-HSD and from pnd 30 onward also 11-βHSD type 1 (Dupont *et al.*, 1993; Ge *et al.*, 1997b, 1999; Haider *et al.*, 1986; Hardy *et al.*, 1989; Mendis-Handagama and Ariyaratne 2001; Neumann *et al.*, 1993; Schäfers *et al.*, 2001; Teerds *et al.*, 1999). Early ALCs (after the immature phase and before the mature phase) seem to possess 40% of the testosterone-secreting capacity of mature ALCs and the greatest capacity for secreting androstenedione, when compared with immature and mature ALCs in postnatal testis, as demonstrated by Mendis-Handagama and Ariyaratne (2001). The prime intratesticular function of androgens from ALCs is to initiate, maintain, and regulate the process of spermatogenesis.

3. EDS in Analysis of Leydig Cell Differentiation

Research work using the substance ethane dimethanesulfonate (EDS, a methane sulfonic ester of ethylene glycol, ethane-1,2-dimethanesulfonate) has markedly extended our knowledge on the differentiation of ALCs. EDS has been successfully used as an antagonist of ALCs, particularly to study the mode of regeneration of newly built Leydig cells after the destruction of ALCs by EDS in prepubertal or adult rats (Molenaar *et al.*, 1985; Morris, 1996; Risbridger and Davis, 1994; Taylor *et al.*, 1998; Teerds *et al.*, 1989, 1999). A single intraperitoneal injection of EDS at a dose of 75 to 100 mg/kg body weight is sufficient to induce ALC destruction after 12 h and leads to complete destruction after 72 h in rat. The changes in ALCs are as follows: vesiculation in the SER; focal hypertrophy of the Golgi apparatus; clumping,

Original magnification, ×12,000. (b) 3β-HSD on the membranes of SER (arrows) in a vascular endothelial cell (En). The reaction was observed only focally in nearly 12% of the interstitial fields. No reaction product in the pericyte (Pc) and erythrocytes. Bar: 1 μm. Original magnification, ×20,000. (Reproduced with kind permission of the publisher, Springer-Verlag, Heidelberg, Germany; from Haider and Servos (1998) *Anat. Embryol.* **198,** 101–110.)

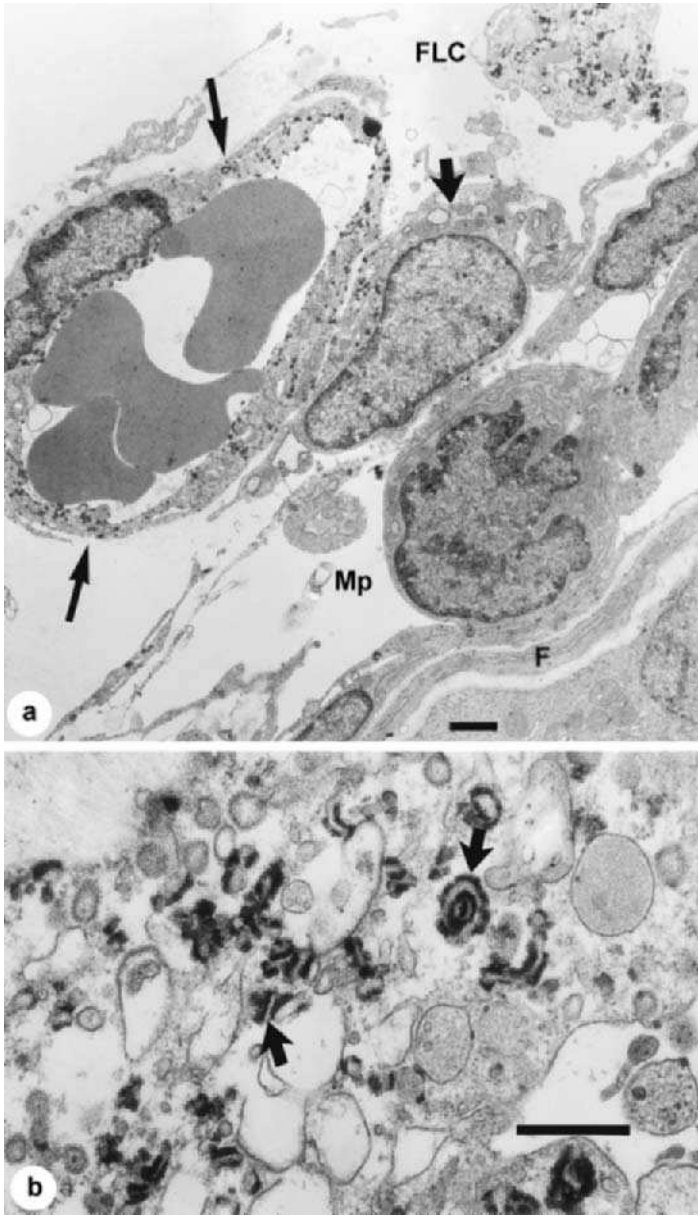

FIG. 9 Rat testis. Postnatal day 15. Electron microscopic localization of 3β-HSD. (a) Electrondense reaction product is present on the SER membranes in a fetal Leydig cell (FLC), a perivascular precursor of an adult Leydig cell (thick arrow) and in the vascular endothelial cell (arrows). The reaction is not present in the macrophage (Mp) and in the fibroblast (F). Bar: 1 μm. Original magnification, ×8000. (b) Distinct localization of the enzyme on the SER membranes (arrows) in a fetal Leydig cell. Bar: 0.5 μm. Original magnification, ×40,000. (Reproduced with kind permission of the publisher, Springer-Verlag, Heidelberg, Germany; from Haider and Servos (1998). *Anat. Embryol*. **198,** 101–110.)

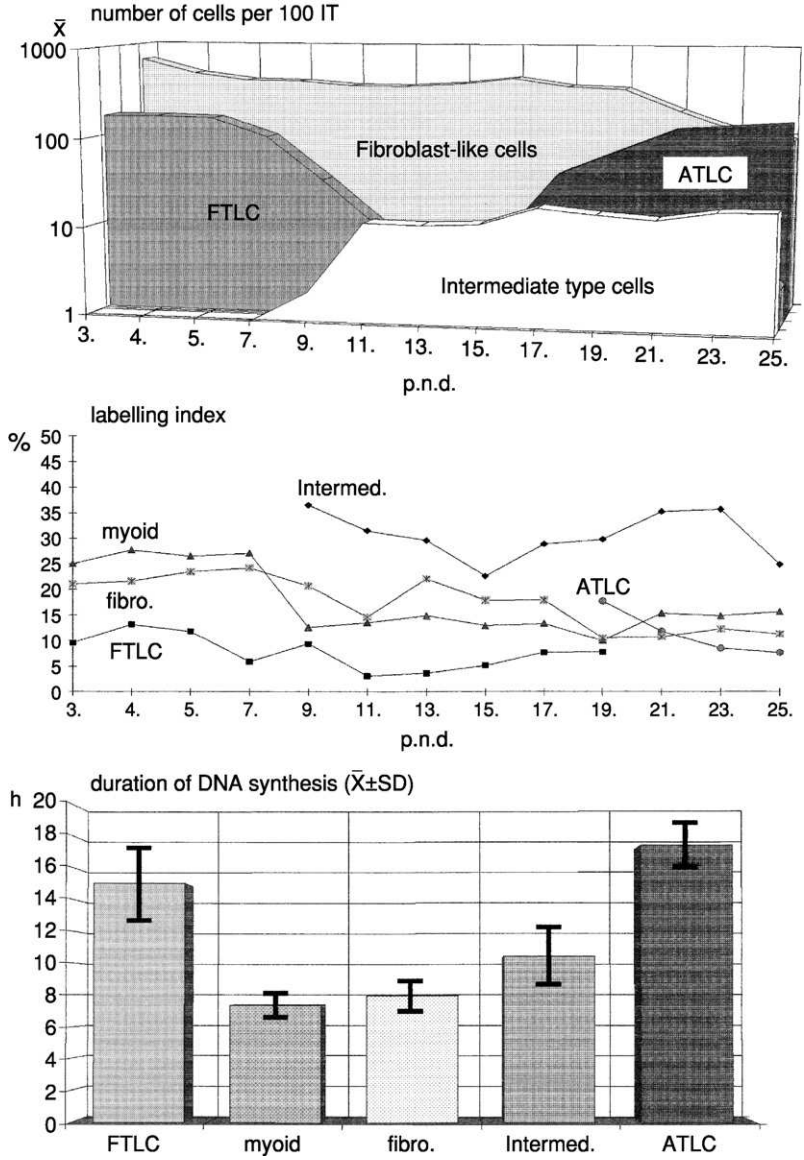

FIG. 10 Cell number, labeling index, and duration of DNA synthesis of various cell types in rat testis interstitium from pnd 3 to 25. *Top*: Absolute number of fetal Leydig cells (FTLCs), fibroblasts/fibrocytes, ALC precursors (intermediate type cells), and adult Leydig cells (ATLCs). *Middle*: Labeling index in percentage as determined by [^{3}H]thymidine incorporation. The precursors for adult Leydig cells—here termed "intermediate"—show the highest labeling index. *Bottom*: Duration of DNA synthesis. Interstitial fibroblasts (here shown as "fibro") and peritubular cells (here shown as "myoid") show the lowest duration of DNA synthesis.

condensation, and margination of nuclear chromatin; and phagocytic activity by interstitial macrophages. All these hallmarks suggest that ALCs are indeed capable of apoptosis (see Section IV). These studies have shown that the mode of formation of newly built ALCs after EDS treatment is strikingly similar to the process of differentiation of ALCs from peritubular and perivascular fibroblasts, as reported above. Fibroblasts in the interstitial tissue are precursors for ALCs newly built after EDS treatment. These precursors show ultrastructural features similar to those of ALC precursors from pnd 10 to 20. Also, the pattern of androgen production in ALCs newly built after EDS treatment and that of immature LCs are similar, as both these cell types preferably synthesize 5α-androstane-3α, 17β-diol, an androgen that is not built by mature ALCs after pnd 65. Strong gonadotropic stimulation precedes the formation of LCs after EDS treatment as well as the differentiation of ALC precursors from postnatal fibroblasts. Pretreatment with human chorionic gonadotropin (hCG) protects the Leydig cells from the cytotoxic effects of EDS. Teerds *et al.* (1999) used the following markers for precursor and developing Leydig cells in an EDS study: the LH receptor, 3β-HSD immunoreactivity, transforming growth factor α (TGF-α), and a new marker for Leydig cell maturation, relaxin-like factor (RLF); LH receptor immunoreactivity was found in Leydig cell-depleted testes 3 and 8 days after EDS treatment. Positive (precursor) cells had a mesenchymal-like morphology. Fifteen days after EDS administration the first new Leydig cells were observed. These authors suggest that the adult EDS-treated rat can serve as a model for studying the ALC development that normally occurs in the prepubertal rat testis. Using EDS in rat, Sriraman *et al.* (2003) evaluated the relative roles of LH and follicle-stimulating hormone (FSH) in the regulation of differentiation of ALCs; depriving EDS-treated rats of endogenous FSH led to a significant decrease in serum testosterone and *in vitro* response to hCG by the Leydig cells. In addition, the data of these authors show that the repopulation of precursor Leydig cells is independent of LH; LH is, however, obligatory for the functional differentiation of ALCs.

There is evidence that immature rat Leydig cells are intrinsically less sensitive to EDS than mature ALCs (Kelce *et al.*, 1991). In contrast to this report, a single intraperitoneal injection of EDS (100 mg/kg body weight) into 20-day-old rat destroyed (24 h later) FLCs as well as immature ALCs completely, as the counting of 3β-HSD-positive Leydig cells yielded; the decrease in the number of lipid droplet-containing cells in the interstitial spaces was 55% after 24 h, and 94% after 72 h (Haider, unpublished results). It seems that EDS does not kill ALCs exclusively but also FLCs. Further studies are necessary to clarify this controversy.

4. Role of Androgens in ALC Differentiation

Androgens are required for the onset of ALC differentiation (precursor stage and immature stage). LH stimulates the later stages of ALC development, that is, the transformation of immature into mature ALCs (Fig. 7). Hardy *et al.* (1990) were the first to provide experimental evidence that androgens are required for the differentiation of ALC precursors; they observed a significant increase in testosterone secretion from Leydig cells, cultured *in vitro* from 21-day-old rats, in the presence of LH plus dihydrotestosterone (DHT); by contrast, LH or DHT alone was without significant effect. These authors concluded that LH alone is insufficient but that androgen and LH induce ALC precursors to produce testosterone. O'Shaughnessy *et al.* (2002b) observed failure of normal ALC development in androgen receptor-deficient mice; the data showed that in the absence of androgen receptors, FLC function is normal, but there is a developmental failure of ALC maturation, with cells acquiring only partial characteristics of the ALC population. These results support the evidence, put forward by Hardy *et al.* (1990), that androgens are indeed required for the differentiation of ALC precursors. This is also in accordance with the observation that treatment with the antiandrogen cyproterone acetate does not impair the proliferation of FLCs but delays the development of ALC precursors and of immature ALCs (Haider *et al.*, 1983). The proliferative activity of ALCs seems to be largely limited to the prepubertal period (Ge *et al.*, 1996; Russell *et al.*, 1995); ALCs lose their proliferative capacity during postnatal differentiation. A decline in cyclin A_2 and an increase in cyclin G_1 are associated with this loss, and hormonal factors regulate Leydig cell proliferation in a stage-specific manner, that is, progenitor → immature → mature (Ge and Hardy, 1997). A few reports have shown the mitotic division of Leydig cells in rat and mouse; however, mitosis seems to play only a minor role in ALC proliferation (Mendis-Handagama, 1991; Russell *et al.*, 1995).

C. Roles of Genes in Leydig Cells

Studies on genes in Leydig cells would help explain the differentiation, dedifferentiation, and death of these cells in various phases of life. Desert hedgehog signaling was shown to be necessary for fetal Leydig cell development in mouse (Yao *et al.*, 2002). Clark *et al.* (2000) showed that the Desert hedgehog gene is required in mouse testis for the formation of ALCs and for normal development of peritubular cells and seminiferous tubules. O'Shaughnessy *et al.* (2002a) published elegant studies on gene expression in Leydig cells during development in mouse and observed five developmental patterns (Figs. 11 and 12): (1) mRNA species encoding P450

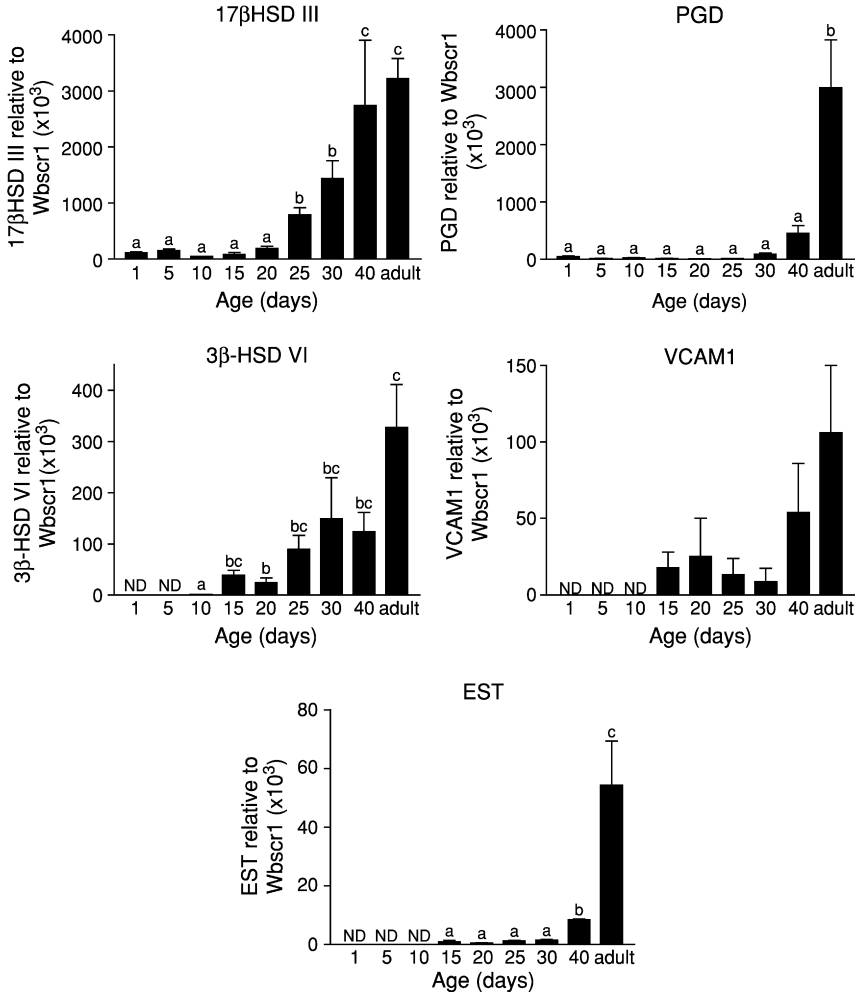

FIG. 11 Expression of 17β-HSD III, PGD-synthetase, 3β-HSD VI, VCAM1, and EST (estrogen sulfotransferase) mRNA levels during development in mouse testis interstitial tissue. (Reproduced with kind permission of the authors and the publisher, Society for the Study of Reproduction; from O'Shaughnessy *et al.* (2002). *Biol. Reprod.* **66,** 966–975.)

side chain cleavage ($P450_{scc}$), $P450_{c17}$, relaxin-like factor (RLF), glutathione *S*-transferase 5-5 (GST5-5) StAR protein, LH receptor, and epoxide hydrolase (EH). These genes were expressed in FLCs as well as ALCs and increased in expression around puberty toward a maximum in the adult; (2) mRNA species encoding 3β-HSD VI, 17β-HSD III, vascular cell adhesion molecule 1, estrogen sulfotransferase, and prostaglandin D (PGD)-synthetase. These

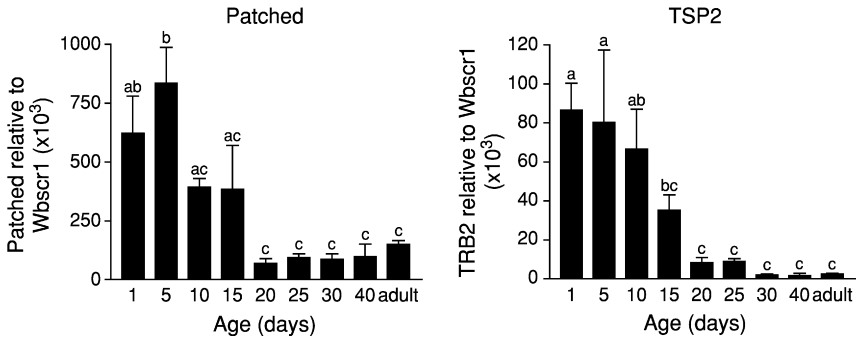

FIG. 12 Expression of *Ptc* (patched gene) and *TRB2* (thrombospondin 2) mRNA levels during development in mouse testis interstitial tissue. (Reproduced with kind permission of the authors and the publisher, Society for the Study of Reproduction; from O'Shaughnessy *et al.* (2002). *Biol. Reprod.* **66,** 966–975.)

genes were expressed only in ALCs (Fig. 11); (3) a pattern containing patched and thrombospondin 2 (TSP2) was shown predominantly by FLCs during the fetal and neonatal phases (Fig. 12); (4) mRNA species encoding 5α-reductase 1 and 3α-HSD showed a peak of expression around puberty; and (5) little developmental change was observed in the expression of mRNA species encoding sulfonylurea receptor 2 and 3β-HSD 1. To sum up, five genes (3β-HSD VI, 17β-HSD III, vascular cell adhesion molecule 1, estrogen sulfotransferase, and PGD-synthetase) were expressed in ALCs and not in FLCs. One gene (TSP2) may be expressed only in FLCs and not in ALCs. Brennan *et al.* (2003) studied the role of platelet-derived growth factor (PDGF) in mouse fetal testis organogenesis. These authors showed that *Pdgfr*-$\alpha^{-/-}$ XY gonads displayed disruptions in the organization of the vasculature and in the partitioning of interstitial and testis cord compartments; and severe reductions in characteristic XY proliferation, mesonephric cell migration, and fetal Leydig cell differentiation. Brennan *et al.* (2003) concluded that PDGFR-α mediates testis cord organization and fetal Leydig cell development in the XY gonad.

Data on mouse cDNAs and structural genes that encode steroidogenic enzymes in Leydig cells have helped increase understanding of the regulation of expression of these enzymes at the molecular level (Payne and Youngblood, 1995). An excellent update on the 3β-HSD/isomerase gene family in Leydig cells and in other tissues has been published by Labrie *et al.* (1996). Ge and Hardy (1998) observed variation in the end product of androgen biosynthesis and metabolism during postnatal differentiation of rat Leydig cells; the data indicate that steroidogenic enzyme gene expression is not induced simultaneously, but through sequential changes in testosterone biosynthetic and metabolizing enzyme activities, resulting

in different androgen end products being secreted by Leydig cells during pubertal development. Studies on the mutations of gonadotropin and of their receptors in human patients are of great clinical importance to clarify the pathogenesis of some disturbances in fertility (Themmen and Huhtaniemi, 2000; see Section X).

III. Hormones and Receptors in Leydig Cells

A. LH and LH Receptors

LH is the prime inducer of ALC differentiation, and is particularly important for the stages of immature and mature ALCs (Ge *et al*., 1996; Habert *et al*., 2001). LH is the most important hormone for the maintenance of high rates of ALC proliferation (Benton *et al*., 1995; Habert *et al*., 2001; Huhtaniemi *et al*., 1984). Bortolussi *et al*. (1990) reported on the Leydig cell number and gonadotropin receptors in rat testis from birth to puberty. Earlier reports established that the administration of LH or hCG induced an increase in the number and size of Leydig cells in both young and adult rats (Ewing and Zirkin, 1983; Molenaar *et al*., 1986).

Studies show that different endocrine mechanisms regulate the differentiation of FLCs and ALCs (Figs. 6 and 7). O'Shaughnessy *et al*. (1998) showed that the fetal development of Leydig cell activity in mouse is independent of pituitary gonadotropin function. Using hypogonadal mice (*hpg*), which lack circulating gonadotropins, Baker and O'Shaughnessy (2001) demonstrated that the fetal development of Leydig cells and Sertoli cells is independent of gonadotropins and that the normal differentiation and proliferation of the adult Leydig cell population (starting about day 10 after parturition) is dependent on the presence of gonadotropins. Also, Migrenne *et al*. (2001) confirmed this finding in rat tissue, that is, that FLCs are LH independent for their functional differentiation; however, these authors found that FLCs are LH dependent for their activity, as decapitation reduced testosterone concentrations in plasma and in testis *in vivo*, and basal testosterone secretion of testes *ex vivo*. This suggests that LH is required to maintain the physiological activity of Leydig cells during late fetal life.

Setchell *et al*. (2003) reported that concentrations of LH reaching testicular interstitial fluid were only about one-tenth of that measured in circulation, presumably because the endothelial cells restrict access of the hormone to the interstitial fluid. This indicated that either Leydig cells are extremely sensitive to LH stimulation or that testicular endothelial cells modulate the action of LH on Leydig cells. Ghinea *et al*. (1994) described receptor-mediated

transendothelial transport of LH in rat testis; they found LH/hCG receptors not only in Leydig cells, but also in endothelial cells. Misrahi *et al.* (1996) examined the transport of hCG in rat testicular microvasculature and reported that LH/hCG receptors are present in endothelial cells and are involved in hormone transcytosis through these cells (Ghinea and Milgrom, 1995). 3β-HSD reaction was shown in SER membranes of a few vascular endothelial cells at the electron microscopic level on pnd 15 in the interstitial tissue of rat testis (Haider and Servos, 1998). These 3β-HSD-positive endothelial cells were usually located in the vicinity of 3β-HSD-positive Leydig cells. Of all interstitial fields, counted in the corresponding cryostat sections, 12% showed this focal presence of 3β-HSD in the endothelial cells. Whether acute regulation of steroidogenesis by blood-borne LH is involved in the paracrine relationship between Leydig cells and vascular endothelial cells should be the subject of future studies. These reports show that vascular endothelial cells are indeed involved in the mediation of Leydig cell steroid biosynthesis; the exact mechanism of this regulation is still unknown.

Confirming the interaction between Leydig cells and vascular endothelial cells, Collin and Bergh (1996) reported the presence of immunoreactive vascular endothelial growth factor (irVEGF) in Leydig cells and in macrophages of rat testis; the authors concluded that Leydig cells secret angiogenic factors and that they are the source of inflammation mediators produced in testis after hCG treatment (see also Section III).

Prince *et al.* (1998) studied the effect of blockade of the hypothalamic–pituitary–testicular (HPT) axis with a gonadotropin-releasing hormone (GnRH) antagonist (antide) on the neonatal population of Leydig cells in the new world primate, the common marmoset. After treatment Leydig cells became atrophic and exhibited irregular nuclei. The SER was greatly diminished in quantity and distribution. SER tubules were relatively unbranched and not anastomosing as in controls. The tubular elements of mitochondrial cristae were rarely evident; only a few lipid droplets were observed. The two features of control Leydig cells, that is, membranofibrillar inclusion and basal laminae, remained prominent in the cells of treated animals. The authors concluded that gonadotrophic hormones are primary regulators of neonatal Leydig cell development in primates; and cell regression and not apoptosis is the cause of inhibition. The role of FSH in the regulation of Leydig cell function has been the subject of various studies. Baker *et al.* (2003) studied this aspect, using two mouse models with null mutations in either FSH β subunit or FSH receptor; the authors concluded that Sertoli cells regulate the development of Leydig cell number and that constitutive activity within FSH receptor knockout mice is sufficient to stimulate this process; the presence of the hormone itself is not required when circulating LH levels are adequate.

B. Steroidogenesis in Leydig Cells

A schematic diagram (Fig. 13) summarizes in a simplified form the most important steps needed for testosterone biosynthesis from cholesterol in Leydig cells. Cholesterol esters are first stored in lipid droplets. Abundant peroxisomes are present in the steroid-producing cells and are involved in the β-oxidation of fatty acids, and in the biosynthesis and metabolism of cholesterol. Peroxisomes contain thiolase and mevalonate kinase, two enzymes necessary for the initial steps of cholesterol synthesis. Mendis-Handagama *et al.* (1990a,b, 1992) were the first to provide evidence that the structure and function of peroxisomes in Leydig cells are influenced by LH. Also, a positive correlation is reported between testosterone production and the number and density of peroxisomes in Leydig cells (Ichihara *et al.*, 1993). The *in vitro* experiments of Bilinska and Litwin (1995) show the immunocytochemical presence of catalase, acyl-CoA oxidase, and 3-ketoacyl-CoA thiolase in the peroxisomes of mouse Leydig cells; these studies suggest that a decrease in testosterone secretion precedes reduction in peroxisome number in Leydig cells.

Cholesterol, the substrate for all steroid hormones, is transferred from cellular stores (e.g., lipid droplets or the plasma membrane) into the outer membrane of mitochondria by protein kinase A. There are two transport proteins involved in the transfer of cholesterol from the outer membrane to the inner membrane of mitochondria: (1) steroidogenic acute regulatory protein, and (2) peripheral-type benzodiazepine receptor.

1. Steroidogenic Acute Regulatory Protein

Steroidogenic acute regulatory protein (StAR) is an indispensible protein for regulating the acute production of steroids in gonads and adrenal glands in rat, mouse, sheep, and human (Stocco, 1996). StAR is rapidly synthesized by the cytosol in response to trophic hormones, and consists of 37- and 32-kDa precursors of a 30-kDa protein. StAR is required for the transfer of cholesterol from the outer to the inner mitochondrial membrane, the first and rate-limiting step in steroid hormone biosynthesis (Arakane *et al.*, 1998; Stocco, 1999). Kotula *et al.* (2001) (Fig. 14) demonstrated an immunofluorescent localization of StAR in the mitochondria of mouse Leydig cells *in vitro*. Oxidative stressors, such as reactive oxygen species, dissipate the mitochondrial membrane potential, resulting in the posttranscriptional inhibition of StAR expression and concomitant inhibition of steroid hormone synthesis; the maintenance of mitochondrial membrane potential is required for steroidogenesis (Diemer *et al.*, 2003). It seems that regulation of the StAR gene is controlled by the orphan nuclear receptor steroidogenic factor (SF-1). Mutations in the StAR gene lead to lipoid congenital adrenal

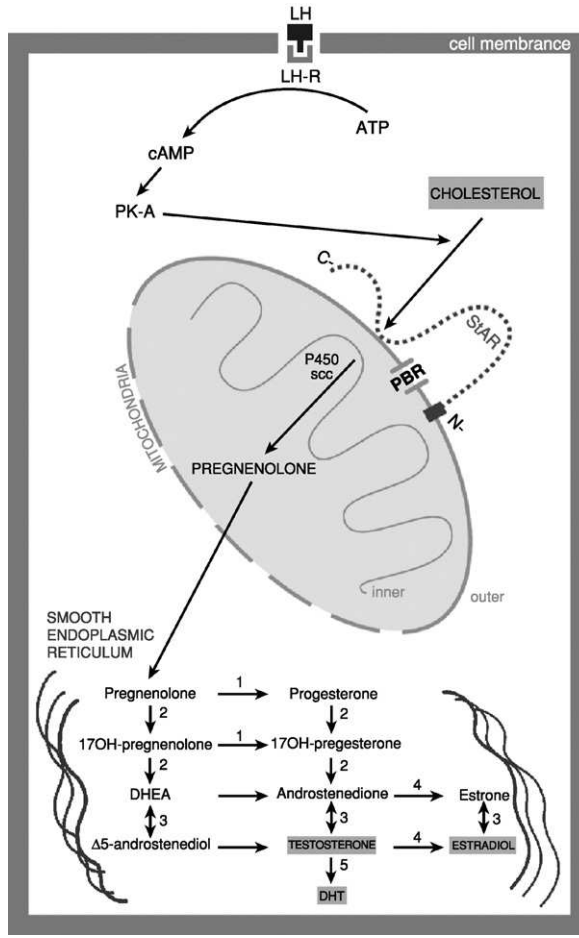

FIG. 13 A simplified summary of the important steps for steroidogenesis in Leydig cells. Luteinizing hormone (LH), on binding with the receptor (LH-R), induces the synthesis of cyclic AMP (cAMP) from ATP. cAMP catalyzes the synthesis of protein kinase A (PK-A), which is needed for the transport of cholesterol from the cytoplasmic pool to mitochondria. Steroidogenic acute regulatory protein (StAR) and peripheral benzodiazepine receptor (PBR) transfer cholesterol from the outer membrane to the inner mitochondrial membrane, where the enzyme P450 side-chain cleavage (P450scc) resides. The N terminus of StAR is connected with the site of mitochondrial import machinery at the outer mitochondrial membrane. The PBR protein functions probably as a channel for cholesterol. The enzyme P450scc converts cholesterol into pregnenolone, which is ultimately transferred to smooth endoplasmic reticulum, where the synthesis of testosterone takes place. DHEA, Dihydroepiandrosterone; DHT, dihydrotestosterone. Reaction 1, 3β-Hydroxysteroid dehydrogenase; reaction 2, cytochrome P450 17α-hydroxylase; reaction 3, 17β-hydroxysteroid dehydrogenase; reaction 4, cytochrome P450 aromatase; reaction 5, 5α-reductase. (Modified and redrawn from Chen *et al.*, 1996a; Habert *et al.*, 2001; Stocco, 1999.) (See also color insert.)

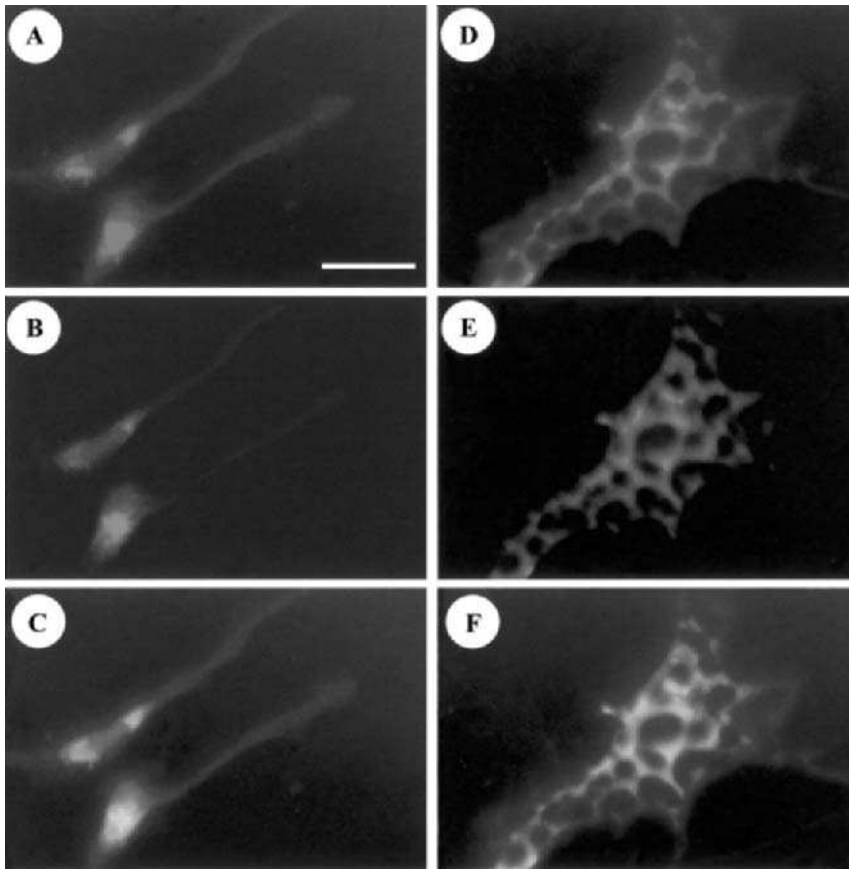

FIG. 14 Different localization of mitochondria (A and D) and the immunoreactive StAR protein (B and E) in cultured Leydig cells stimulated by hCG and testicular macrophage-conditioned medium. (C) and (F) represent digitized and superimposed images from (A and B) and (D and E), respectively, indicating the mitochondrial localization of StAR protein (asterisks). Bar: 20 μm. (Reproduced with kind permission of the senior author, Bilinska, and of the publisher of *Folia Histochemica et Cytobiologica*; from Kotula *et al*. (2001). *Folia Histochem. Cytobiol*. **39,** 169–170.) (See also color insert.)

hyperplasia, in which the patient builds virtually no steroid (for review see Stocco, 1999).

2. Peripheral-Type Benzodiazepine Receptor

Peripheral-type benzodiazepine receptor (PBR) is a mitochondrial protein involved in the transport of cholesterol from the outer to the inner

mitochondrial membrane. Molecular modeling of PBR suggests that it might function as a channel for cholesterol. PBR has a hydrophobic outer surface and hydrophilic interior core facilitating passage of amphiphilic cholesterol. Targeted disruption of the PBR gene in Leydig cells results in the arrest of cholesterol transport into mitochondria (Krueger and Papadopoulos, 1990; Papadopoulos, 1996, 2003). There is evidence for dynamic multistep interaction and protein-to-protein associations between StAR and PBR (West *et al.*, 2001) and between protein kinase A, StAR, and PBR (Hauet *et al.*, 2002). However, the exact mechanism by which cholesterol is shifted to the inner mitochondrial membrane is still unknown.

Steroidogenesis begins with enzymatic cleavage of the side chain of the substrate cholesterol to form pregnenolone. This reaction is catalyzed by the cholesterol side chain cleavage enzyme system (CSCC), which is located on the matrix side of the inner mitochondrial membrane. Pregnenolone is transferred to the membranes of smooth endoplasmic reticulum, which contain various HSD enzymes, necessary for ultimate conversion of pregnenolone into testosterone (Fig. 13).

3. Role of HSD Enzymes

The hydroxysteroid dehydrogenases (HSDs) are essential for steroidogenesis in Leydig cells (Habert *et al.*, 2001; Labrie *et al.*, 1996; Lejeune *et al.*, 1998; Payne and Youngblood, 1995; see Fig. 13). 3β-HSD, 17α-hydroxylase, and 17β-HSD are required for the synthesis of steroids. 11β-HSD, 3α-HSD, and 5α-reductase are also involved in the synthesis, as well as in the metabolism, of steroids.

The kinetics and ontogenesis of 3β-HSD, a key enzyme necessary for the synthesis of testosterone in Leydig cells, have been studied by several authors in rat (Dupont *et al.*, 1993; Haider *et al.*, 1986; Lording and de Kretser, 1972) and in mouse (Baker *et al.*, 1999). Leydig cells synthesize and maintain a high level of 17β-HSD type 4 (Carstensen *et al.*, 1996; Normand *et al.*, 1995). 17β-HSD4 oxidizes 5-androstene-3β,17β-diol to dehydroepiandrosterone, and estradiol to esterone. Ivell *et al.* (2003) demonstrated the differentiation-dependent expression of 17β-HSD type 10 in rodent testis; this isoform in FLCs continued to be expressed at a time when functionally FLCs begin to involute. Schäfers *et al.* (2001) described the postnatal ontogenesis of the oxidative reaction of 17β-HSD in rat Leydig cells, using enzyme histochemical methods (Fig. 15); for 17β-HSD, a peak for FLCs on pnd 16 and two peaks for ALCs on pnd 19 and 37 were observed. Between pnd 13 and 25 FLCs showed a higher intensity for 17β-HSD than did ALCs.

The enzyme 11β-HSD catalyzes the oxidation of corticosterone to the inactive metabolite 11-dehydrocorticosterone in rat Leydig cells (Ge and

Hardy, 2000; Ge *et al*., 1997a,b; Monder *et al*., 1994a,b; Phillips *et al*., 1989). Two isoforms of 11β-HSD have been established: type 1 (Seckl and Walker, 2001) and type 2 (Yang and Yu, 1994). Many studies show that rat Leydig cells contain 11β-HSD type 1 (Brereton *et al*., 2001; Ge *et al*., 1997b; Leckie *et al*., 1998). 11β-Dehydrogenase bioactivity in testis exceeds that of 11-oxoreductase (Waddell *et al*., 2003). According to Schäfers *et al*. (2001) 11β-HSD reaction is present from pnd 31 onward, first in a few ALCs and later in almost all these cells homogeneously; the reaction was completely absent in FLCs. The ontogenic curves of 17β-HSD and 11β-HSD show an inverse relationship (Fig. 15). 11β-HSD has been suggested as a marker for the functional maturity of ALCs in rats (Haider *et al*., 1990; Monder *et al*., 1994a,b; Phillips *et al*., 1989). The appearance of 11β-HSD correlates with the postnatal increase in Leydig cell number, testicular weight, total surface area of the intracellular membranes, and the content and secretion of testosterone by Leydig cells (Phillips *et al*., 1989). Neumann *et al*. (1993) showed a temporal coincidence of the first appearance of elongated spermatids in the seminiferous tubules and the first appearance of the histochemical reaction of 11β-HSD in Leydig cells of rats on pnd 35.

4. Androgens

ALCs produce androgens and are themselves the target of androgen action. Androgens also contribute to autocrine regulation of ALCs. Androgens inhibit testosterone production by ALCs (Hales and Payne, 1989). Shan *et al*. (1995) reported an intranuclear localization of androgen receptor (AR) in ALCs, particularly during the prepubertal phase. According to Shan *et al*. (1995), ALCs are maximally sensitive to androgen during puberty; AR mRNA was moderate on pnd 21, highest on pnd 35, and lowest on pnd 90. Shan *et al*. (1997) observed that androgen maximally stimulates AR levels in immature ALCs but is without significant effect in matured ALCs; in contrast AR levels in Sertoli cells are more sensitive to androgen regulation in adult than in immature animals. There are various lines of strong evidence showing that androgens are required for the onset of ALC differentiation (Hardy *et al*. 1990; O'Shaughnessy *et al*., 2002b). Whereas the AR level in the nuclei of adult Sertoli cells depends mainly on the level of androgen, in the case of ALCs and peritubular cells this androgen dependency is more limited (Zhu *et al*., 2000). Treatment with an antiandrogen, for example, flutamide, leads to distinct hypertrophy of ALCs, enlargement of the Golgi apparatus (Fig. 16a), a 4-fold increase in the number of mitochondria, and degenerative and dissolution processes in mitochondria (Fig. 16b–d; Haider *et al*., 1994).

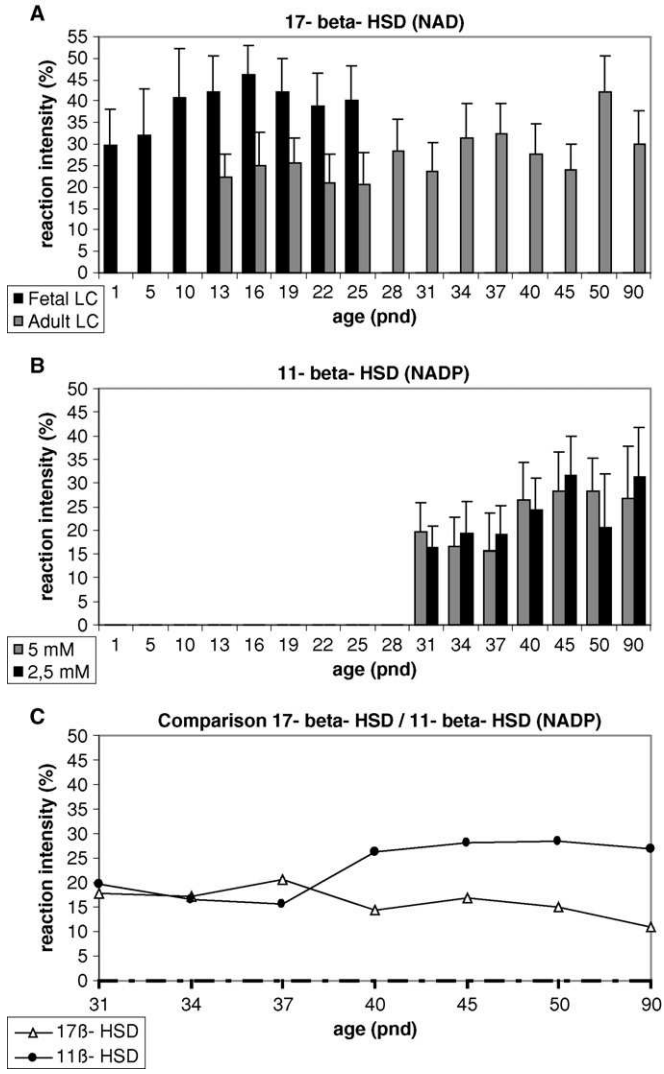

FIG. 15 (A) Histograms showing the semiquantitative measurement of the intensity of 17β-HSD reaction in rat Leydig cells; cofactor NAD; mean ± SD of total Leydig cell fields. (B) Histograms for the intensity of 11β-HSD in adult Leydig cells; cofactor, NADP; mean ± SD of total Leydig cells. (C) Comparison between the intensity of 17β-HSD and 11β-HSD. The values (17β-HSD versus 11β-HSD) on each postnatal day are significantly different ($p < 0.05$), with the exception of pnd 34. (Reproduced with kind permission of the authors and Kluwer Academic Publishers, the Netherlands; from Schäfers *et al.* (2001). *Histochem. J.* **33,** 585–595.)

5. Anti-Müllerian Hormone

Anti-Müllerian hormone (AMH), a glycoprotein homodimer belonging to the transforming growth factor β (TGF-β) family, is produced by Sertoli cells in rat from fd 14.5 until pubertal maturation, and is responsible for

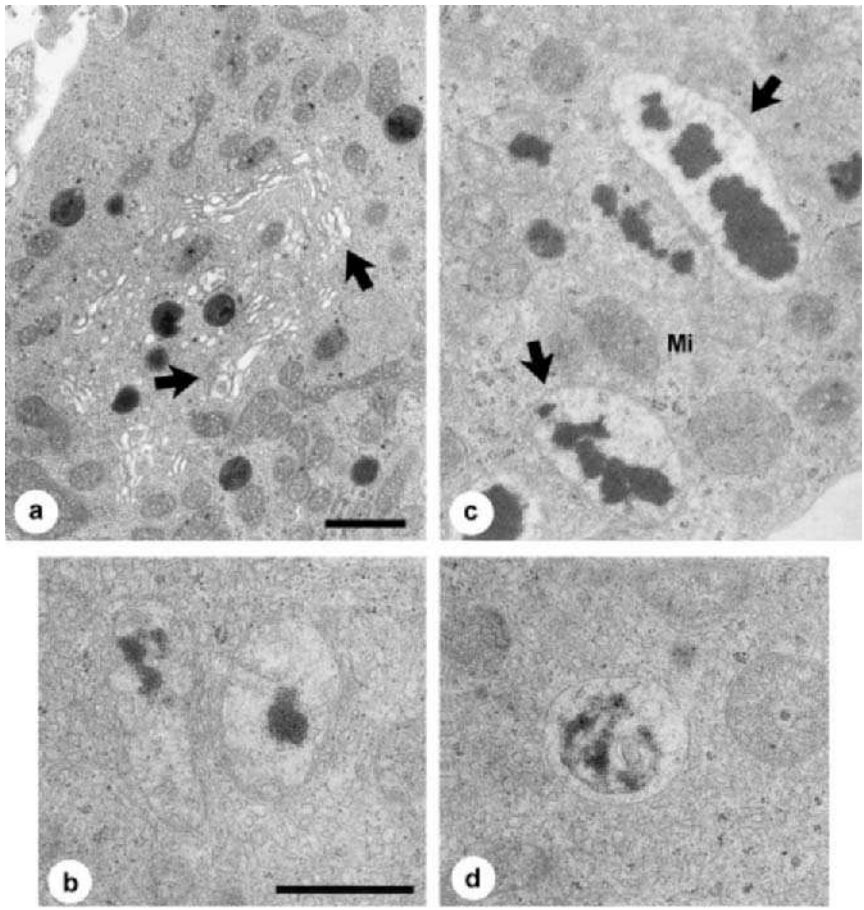

FIG. 16 Changes in Golgi apparatus and in mitochondria of an adult Leydig cell in rat, induced by treatment with the antiandrogen flutamide. (a) A marked (nearly 4-fold) enlargement of the Golgi apparatus; the saccules have lost the typical ladder-like arrangement and have been separated. Bar: 1 μm. Original magnification, ×14,000. (b) Transition of the condensed intramitochondrial mass into granulation. Bar [also valid for (c) and (d)]: 1 μm. Original magnification, ×25,000. (c) Condensation of intramitochondrial fluid (arrows). Some mitochondria (Mi) are intact. (d) Loss of the inner membrane of the mitochondria. (Reproduced with the kind permission of the publisher, Springer-Verlag, Heidelberg; from Haider *et al.* (1994). *Fertiliät* **10,** 42–47.)

the complete regression of Müllerian ducts in male fetuses (for review see Josso *et al.*, 1993). AMH appears to influence steroidogenesis in Leydig cells during the fetal and prepubertal periods, as shown by Rouiller-Fabre *et al.* (1998a). These authors provided the first experimental evidence that AMH inhibited LH-stimulated testosterone production by dispersed FLCs (from fd. 16 to 20) in culture in a dose-dependent manner; this inhibition resulted from a drop in the steroidogenic activity of each Leydig cell without affecting the number of 3β-HSD-positive cells. It seems that AMH, like other members of the TGF-β family, has an autocrine/paracrine effect on testicular steroidogenic function during the fetal and prepubertal periods. Racine *et al.* (1998) reported that AMH receptors in Leydig cells are responsible for its effects on steroidogenesis.

6. Estrogens

The male gonad can convert androgens into estrogens. The terminal enzyme responsible for this irreversible conversion is cytochrome P450 aromatase (P450arom) (for review see Carreau *et al.*, 1999). The P450arom gene is regulated in a cell-specific manner via the alternative use of promoters located in the first exons. The enzyme is present in the endoplasmic reticulum of steroidogenic cells in vertebrates. P450arom is present in immature and mature ALCs as well as in Sertoli cells in rat. In pig, ram, and human the enzyme is present mainly in Leydig cells (Carreau *et al.*, 1999). There are several lines of evidence for a physiological role of estrogens in the regulation of Leydig cell function. Genissel and Carreau (2001) demonstrated the presence of cAMP reponse-like elements (CREs) and the existence of androgen-responsive elements (AREs) on the P450arom gene in rat Leydig cells. Carreau *et al.* (2002) reported immunolocalization of P450arom in rat Leydig cells and in elongated spermatids. It seems that the regulation of P450arom and its enzymatic activity in rat ALCs are under LH (through cyclic AMP) and steroid control; in addition, some paracrine factors from the seminiferous tubules are involved herein, the germ cells probably exerting positive control in the production of P450arom in Leydig cells (Genissel *et al.*, 2001). Leyding cells express two estrogen receptor (ER) subtypes, ERα and ERβ, and have the capacity to convert testosterone to the natural estrogen 17β-estradiol. Thus Leydig cells are subject to estrogen as well as xenoestrogen and other hormone disruptors. These substances, which include environmental toxicants as well, cause adverse effects in the development and function of Leydig cells, impairing the fertility potential (Akingbemi *et al.*, 2001; Sharpe, 2001, 2003).

Atanassova *et al.* (1999) reported on the permanent effects of neonatal estrogen exposure in rats on spermatogenesis and Leydig cells in adulthood;

as indicated by gonadotropins and testosterone levels, the hypothalamic–pituitary axis and Leydig cells are probably more sensitive than Sertoli cells to reprogramming by estrogens neonatally. Using transgenic mice, Akingbemi *et al.* (2003) showed that abrogation of the ERα gene by targeted deletion or treatment with an antiestrogen increases Leydig cell steroidogenesis in association with elevations in the serum levels of LH, which presumably is the result of estrogen insensitivity at the level of the hypothalamus and/or pituitary gonadotropes; data suggest that ERα has a regulatory role in Leydig cell steroidogenic function. Zhou *et al.* (2002) demonstrated androgen receptors and ERα in the Leydig cells of adult mouse. ERα is present in Leydig cells and peritubular myoid cells in dog testis; however, in cat testis ERα is present only in Leydig cells (Nie *et al.*, 2002).

7. Thyroid Hormones

Summarizing the present knowledge on the effects of thyroid hormones on the differentiation and proliferation of ALCs, Mendis-Handagama and Ariyaratne (2001) write: "...thyroid hormone causes proliferation of mesenchymal cell precursors and acceleration of their differentiation into Leydig cell progenitors in addition to its effect of enhanced proliferation of progenitors and newly formed Leydig cells." Many reports suggest strongly that hypofunction or hyperfunction of the thyroid gland affects Leydig cell proliferation. In transient neonatal hypothyroid rats that were allowed to become euthyroid thereafter, testes contained twice the number of Leydig cells per testis compared with similarly aged controls on day 135; the Leydig cells were significantly smaller than in the controls (Mendis-Handagama and Sharma, 1994). Also, Hardy *et al.* (1996) reported increased proliferation of Leydig cells induced by neonatal hypothyroidism in rat. Ariyaratne *et al.* (2000b) studied the effects of thyroid hormones on Leydig cell regeneration in adult rat after EDS treatment; hypothyroidism prevented Leydig cell regeneration after EDS treatment, and hyperthyroidism led to an early onset of mesenchymal cell differentiation together with an increased number of Leydig cells as compared with controls on day 21 after treatment. The exact mechanism by which thyroid hormones increase the number of mesenchymal precursors of ALCs and support the differentiation of precursors into progenitors and thereafter into immature Leydig cells is unknown (Mendis-Handagama *et al.*, 1998) and should be the subject of future studies. Do they act by inhibiting AMH? Do they influence paracrine regulation between Sertoli cells and Leydig cells?

8. Testicular Innervation

Whether the innervation of testis plays a significant role in the regulation of testosterone synthesis in the Leydig cell, is only poorly understood (Mayerhofer, 1996). Lee *et al.* (2002) provided anatomic and functional evidence for a neural hypothalamic–testicular pathway that is independent of the pituitary; the authors showed that the injection of the transganglionic retrograde tracer pseudorabies virus into testes caused viral staining in the spinal cord, the brainstem, and the hypothalamus; this pathway seems to interfere with Leydig cell function independently of the pituitary. The inferior spermatic nerve seems to contribute to the regulation of hemicastration-induced testosterone elevation, as sectioning of the inferior, and not the superior, spermatic nerve suppresses this elevation (Frankel *et al.*, 1984). Zhu *et al.* (1998) studied denervation-induced nuclear changes in Leydig cells of hemicastrated adult rats; they did not observe any change in Leydig cell number or organelle number. The authors suggest that nuclear and heterochromatin-associated cellular activity might be inhibited by testicular denervation in hemicastrated rats. Anakwe *et al.* (1985) reported on the characterization of β-adrenergic binding sites on rodent Leydig cells. There is a report that histamine affects testicular steroid production in golden hamster (Mayerhofer *et al.*, 1989). However, there are many open questions in this field: is there any direct effect of testicular nerves on Leydig cell testosterone production? Does this control via nerves influence a paracrine aspect of Leydig cell regulation concerning other testicular compartments?

C. Regulation by Growth Factors

1. Interleukins, TGF-β, and Other Factors

a. Interleukins Leydig cell differentiation, proliferation, endocrine function, and regulation are modulated by various local factors and growth factors (for reviews see Saez, 1994; Sharpe, 1990; Skinner, 1991; Spiteri-Grech and Nieschlag, 1993; and see Fig. 17). Transforming growth factors (TGFs) and interleukin 1 regulate the proliferative activity of immature Leydig cells in culture (Avallet *et al.*, 1987; Khan *et al.*, 1992a,b). Interleukin 1α (IL-1α), a multifunctional polypeptide cytokine, acts as a systemic and paracrine messenger in endocrine and central nervous systems and as a growth factor (Gustafsson *et al.*, 1988; Pöllänen *et al.*, 1989; Syed *et al.*, 1988). Khan *et al.* (1992a) showed that interleukin 1 stimulates DNA synthesis in immature rat Leydig cells *in vitro*. Human Leydig cells and Sertoli cells produce interleukins 1 and 6 (Cudicini *et al.*, 1997). Calkins *et al.* (1988) demonstrated that 17K IL-1 inhibits rat Leydig cell steroidogenesis in

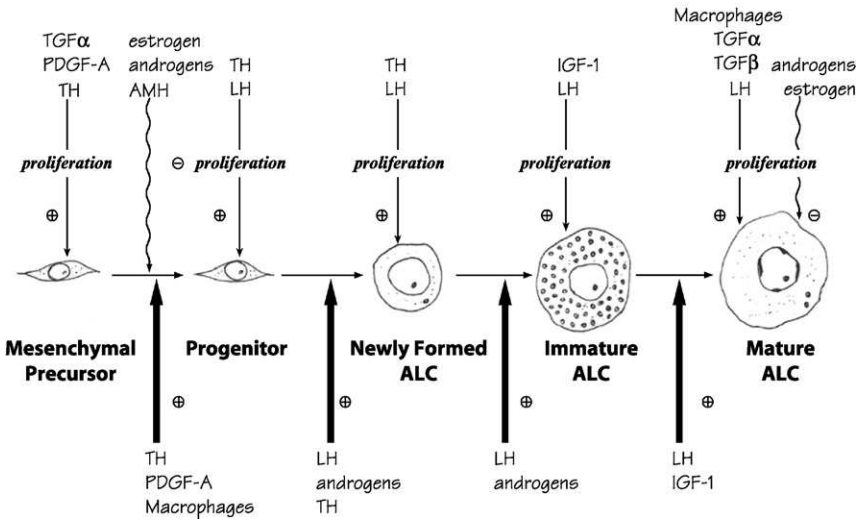

FIG. 17 Schematic representation summarizing the regulation of adult Leydig cell differentiation in postnatal testis. ALC, Adult Leydig cells; TH, thyroid hormone; ⊕, stimulation; ⊖, inhibition. (Reproduced by the kind permission of the authors and the publisher, Society for the Study of Reproduction; from Mendis-Handagama and Ariyaratna (2001). *Biol. Reprod.* **65,** 660–671.)

primary culture. Confirming these results, Sultana *et al*. (2000) regard IL-1 proteins as constitutive paracrine mediators in testis; they reported on molecular cloning and expression of a functionally different alternative splice variant of prointerleukin 1α from rat testis. When tested on hCG-stimulated Leydig cells *in vitro*, a dose-dependent inhibition of testosterone production was obtained with mature 17K IL-1α and at a lower potency with 32proIL-1α, whereas 24proIL-1α was inactive. Sultana *et al*. (2000) conclude that the functional difference between the two forms of proIL-α in the Leydig cell assay indicates alternative functions of the splice variant.

Svechnikov *et al*. (2001) studied the age-dependent stimulation of Leydig cell steroidogenesis by interleukin 1 isoforms; they showed that rat 17K IL-1-α, IL-1, 32K IL-1α precursor, and a 24K splice variant stimulated testosterone production by Leydig cells from 40-day-old, but not from 80-day-old, rats. Because Sertoli cells are the main constitutive source of IL-1α in the testis, the data from Svechnikov *et al*. (2001) support the hypothesis that Sertoli cells are involved in the regulation of Leydig cell streoidogenesis by release of IL-1α, acting as a paracrine messenger (Jonsson *et al*., 1999). Walch and Morris (2002) showed that the cyclooxygenase 2 pathway mediates IL-β regulation of IL-1α, IL-1β, and IL-6 mRNA levels in Leydig cell progenitors in rat testis.

b. TGF-β The growth factors that control Leydig cell functions also include TGF-β, which plays an important role in signal transduction for cell–cell interaction in testis, particularly as a potent inhibitor of Leydig cell functions (Avallet *et al*., 1987; Saez, 1994; Skinner, 1991). Three isoforms, TGF-β1, TGF-β2, and TGF-β3, have been identified in mammals. In FLCs, a moderate positive immunohistochemical reaction for TGF-β1 appears on fd 16.5 and becomes strong during late fetal life. Postnatally, FLCs show strong intensity until pnd 20; however, ALCs exhibit only weak staining on pnd 20 (Gautier *et al*., 1994). TGF-β1 inhibits basal and LH-stimulated testosterone secretion in fetal rat testes *in vitro* only on fd 13.5 and not in later stages of fetal life (Gautier *et al*., 1997). Olaso *et al*. (1997) demonstrated an immunohistochemical reaction for TGF-β2 in FLCs on fd 16.5; the intensity increases from fd 18.5 onward. A similar pattern was observed for TGF-β3 as well; TGF-β3 inhibited LH-stimulated testosterone production by FLCs from 20.5-day-old fetus *in vitro* (Olaso *et al*., 1999). This inhibitory effect was equal to that observed with TGF-β1 or TGF-β2. ALCs express TGF-β receptor type II strongly, and only weakly receptor type I (Olaso *et al*., 1998).

c. Inhibin Jarred *et al*. (1999) studied the localization of inhibin α, βA, and βB subunits during ovine testicular development from day 40 to 135 of gestation; fetal Leydig cells expressed all three inhibin subunits, but this was restricted to the period between 40 and 90 days of gestation; the data suggest that only activin ligands are produced by Leydig cells during late gestation. Several lines of evidence indicate that inhibin B is the testis-specific form; it regulates FSH secretion in pituitary and plays a paracrine/autocrine role in testis. Inhibin acts in testis possibly through inhibition of activin action by forming inhibitory complexes with type II activin receptors (Anderson and Sharpe, 2000).

Insulin-like growth factors I and II (IGF-I and IGF-II) are expressed differentially in FLCs and ALCs in rat testis. Rouiller-Fabre *et al*. (1998b) showed that IGF-I acts as a paracrine/autocrine factor in the differentiation and activity of FLCs. IGF-I is present in FLCs from fd 16.5 until fd 20.5 (Rouiller-Fabre *et al*., 1998b), and from pnd 15 onward in FLCs as well as in precursor, immature, and mature ALCs, with the highest level during puberty (Grizard *et al*., 1991; Haider, unpublished observations). In contrast, IGF-II is expressed in FLCs only from fd 21 until pnd 11 (Koike and Noumura, 1995). These results suggest that IGF-I and IGF-II are probably involved in different processes of Leydig cell differentiation; periods of IGF-I expression seem to coincide with periods of high testosterone production. Probably the main function of IGF-I is to induce immature ALCs into mature ALCs, as shown by studies on knockout IGF-null mice, which present lower production of testosterone and a low level of $P450_{c17}$ and

17-Ketosteroid reductase (17-KSR):17β-HSD enzymes, and the main steroids secreted by their Leydig cells are progesterone and androstenedione (Ge *et al*., 1996). Moore and Morris (1993) provided evidence for the involvement of IGF-I in the local control of steroidogenesis and DNA synthesis of Leydig cells in rat. IGF-I stimulates the proliferative capacity of ALC precursors and of immature ALCs; it does not affect mature ALCs (Ge and Hardy, 1997). IGF-I gene null mutation leads often to early mortality; in surviving animals the male reproductive system is usually infantile (Baker *et al*., 1996). Leydig cells are able to produce vascular endothelial growth factor (VEGF), and this process, mediated by cAMP-dependent protein kinase A, is under gonadotropic control (Anand *et al*., 2002). VEGF seems to participate in the paracrine regulation of the interaction between Leydig cells and neighboring vascular endothelial cells (Ergün *et al*., 1997, 1999).

There are reports about relaxin-like factor (RLF) as a major secretory product of Leydig cells in various mammalian species (for review see Ivell and Bathgate, 2002). The insulin-like factor (INSL3) gene is responsible for RLF production. A strong immune histochemical reaction of RLF is observed in FLCs as well as in ALCs, but only a weak reaction in prepubertal immature Leydig cells in rat and in hypertrophic or transformed Leydig cells. Studies in transgenic mice revealed that RLF plays a role in the second phase of testicular descent, acting on the gubernaculum. INSL3 knockout mice are cryptorchoid (Boockfor *et al*., 2001; Nef and Parada, 1999). Some authors used RLF as a marker for Leydig cell differentiation or function (Teerds *et al*., 1999); however, which aspect of differentiation or function is exactly marked by RLF is still unknown. The ontogenic expression of leptin receptor in rat Leydig cells shows a pattern similar to that of RLF expression (Caprio *et al*., 2003).

Excess vitamin A induces testicular lesions and spermatogenic disorders, and vitamin A deficiency causes early cessation of spermatogenesis and impairs testosterone secretion. Vitamin A (retinol) and its principal biologically active derivative, retinoic acid, are involved in Leydig cell function, in addition to the functions of Sertoli cells and germ cells. Livera *et al*. (2002) have summarized the relevant data on rodents. Leydig cells contain retinoic acid receptors and retinoic X receptors. The knockout of the receptor $RXR\beta^2$, present in Leydig cells in addition to Sertoli cells, induces sterility (Boulogne *et al*., 1999). The following reactions take place in the cytoplasm of rodents, Leydig cells:

$$\text{Retinol} \overset{\text{ADH}}{\leftrightarrow} \text{retinaldehyde} \overset{\text{retinol DH}}{\rightarrow} \text{retinoic acid}$$

where ADH is alcohol dehydrogenase and retinol DH is retinol dehydrogenase; for references, see Hardy *et al*. (2000) and Livera *et al*. (2002).

The retinoic acid is ultimately transported to the nucleus of Leydig cells, where it regulates most probably the transcriptional activity of retinoic acid nuclear receptors. In ALCs, retinoids increase basal testosterone secretion and expression of StAR and of the enzyme $P450_{c17}$, and decrease 3β-HSD and LH receptor synthesis. Surprisingly, basal testosterone secretion is decreased by retinoids in FLCs. The explanation for this opposite effect in FLCs and ALCs is unknown.

Barreiro *et al.* (2003) demonstrated the presence of ghrelin, the endogenous ligand for the growth hormone-secretagogue receptor in FLCs and ALCs in rat testis. The function of ghrelin is unknown. Leydig cells synthesize a large amount of oxytocin, which contributes to the contraction of smooth muscle cells in the lamina propria around seminiferous tubules and regulates their movement (Nicholson and Pickering, 1993).

2. Macrophage Growth Factors

Testicular macrophages can be described in two categories: (1) resting macrophages, which play a supportive role for Leydig cells, and (2) activated macrophages, which secrete on activation, for example, by bacterial inflammation, a host of inhibitory cytokines, that dramatically lower testosterone synthesis (for review see Hales, 2002). Resident macrophages constitute an integral part of the interstitial tissue in the testis of rat (Jonsson *et al.*, 2001; Miller *et al.*, 1983; Niemi *et al.*, 1986) and mouse (Hume *et al.*, 1984). Nearly 25% of all cells in the testicular interstitium of rat are macrophages, identified by using a vital dye (trypan blue or India ink) as well as macrophage membrane antigen MRC W3/25 (Niemi *et al.*, 1986). The macrophages are closely attached and mixed with Leydig cells; the macrophage density increases in cryptorchid and irradiated testis (Bergh, 1985). In an elegant series of experiments Gaytan *et al.* (1994a,b) provided evidence that interstitial resident macrophages are needed for Leydig cell differentiation in rat, as the selective depletion of macrophages prevents Leydig cell repopulation in EDS-treated rats. These authors selectively depleted macrophages in the right testes by an intratesticular injection of dichlormethylene diphosphonate-containing liposomes and studied the regeneration of Leydig cells in both testes after EDS treatment. The newly built ALCs were abundant in the left, macrophage-containing testes. However, the number of ALCs decreased in the macrophage-depleted right testes, clearly depending on the time elapsed between EDS treatment and macrophage depletion. The authors conclude that macrophages are needed for the differentiation of Leydig cells from mesenchymal precursors, as well as for the proliferative activity of newly formed Leydig cells, possibly through secretion of essential growth factors. In another set of experiments, Gaytan *et al.* (1995a) studied how macrophages respond to EDS-induced Leydig cell death; a 2-fold

increase in the number of macrophages was found on days 1–2 after EDS treatment in both sham-operated and short-term hypophysectomized rats. In long-term hypophysectomized rats, there was a delay in the increase in number of macrophages. It suggests that the phagocytic capacity of macrophages is diminished, particularly after long-term hypophysectomy. Testicular macrophages are also needed for the response of Leydig cells to gonadotropin treatment (Gaytan *et al.*, 1995b). Resident macrophages prevent the inflammatory reaction elicited by massive Leydig cell death, induced by EDS (Gaytan *et al.*, 1995c).

Testicular macrophages in rat produce 25-hydroxycholesterol (25-HC) and express 25-hydroxylase, the enzyme that converts cholesterol to 25-HC. 25-HC seems to be an important factor mediating the interaction between macrophages and neighboring Leydig cells, because it is efficiently converted to testosterone by Leydig cells. The production of 25-HC is negatively regulated by testosterone, which may be representative of a paracrine negative feedback loop (Lukyanenko *et al.*, 2003). 25-HC, produced by testicular macrophages during the early postnatal period (pnd 10, 20, and 40), influences the differentiation of Leydig cells *in vitro* (Chen *et al.*, 2002). Chronic exposure of Leydig cells to 25-HC increases basal production of testosterone but decreases LH-stimulated steroidogenesis at all ages. 25-HC increases 3β-HSD activity in both progenitor and immature Leydig cells. These data support the evidence of Gaytan *et al.* (1994b), that macrophages are needed for Leydig cell differentiation; the influence is mediated possibly via the secretion of 25-HC. Kmicikiewicz *et al.* (1999) studied the effects of testicular macrophages, macrophage-conditioned medium, and interleukin-1α on bank vole Leydig cell steroidogenesis. These authors found that Leydig cells from a long photoperiod produced more testosterone, and were sensitive to the stimulatory effect of both testicular macrophages and testicular macrophage-conditioned medium; they were also more sensitive to the inhibitory influence of IL-1α than were short-photoperiod animals.

IV. Apoptosis and the Effects of Aging and Stress in Leydig Cells

A. Apoptosis

Several reports suggest that ALCs are capable of engaging the programmed cell death pathway in response to certain stimuli, for example, EDS (Henriksen *et al.*, 1995; Tapanainen *et al.*, 1993). Morris *et al.* (1997) studied Leydig cell apoptosis in response to EDS after both *in vivo* and *in vitro* treatment; the early characteristics of apoptosis were cell shrinkage and the condensation of nuclear chromatin; the sign of later-stage apoptosis was the

formation of apoptotic bodies. Electrophoresis of DNA extracted from treated Leydig cells exhibited the laddering characteristic of the apoptotic process. The *in vivo* application of EDS caused a 20-fold increase in the number of apoptotic cells in interstitial cell preparations. The apoptosis-related gene products act in cohort: Bcl-2 and Bcl-x_L promote cell survival, while Bax promotes cell death often positively regulated by the tumor-suppressor gene *p53* (Daugas and Kroemer, 2000; Palaga and Osborne, 2002). Taylor *et al.* (1998) showed that EDS kills Leydig cells by apoptosis; however, the control of Leydig cell death does not involve p53 or Bcl-2 family members. Bax protein, although expressed in the interstitium, is not present in Leydig cells. Bcl-x_L in Leydig cells was only transiently increased after EDS treatment. Experimental data from the same group show that EDS-induced apoptosis of rat Leydig cells is a Fas-mediated process; both Fas receptor and Fas ligand proteins increased in Leydig cells after EDS treatment. Immunohistochemistry showed a strong intensity of Fas receptor and Fas ligand in Leydig cells in early stages of apoptosis; the intensity decreased as the nuclear morphology became more fragmented (Taylor *et al.*, 1999; Woolveridge *et al.*, 2001). Nandi *et al.* (1999) studied germ cell apoptosis in the testes of rats after testosterone withdrawal by EDS; the data suggest that Fas may play a role in the apoptotic death of germ cells that results from reduced intratesticular testosterone levels, and that testosterone may play a role in germ cell survival via its suppression of Fas. Employing double immunostaining for single-stranded DNA and the steroidogenic enzyme $P450_{c17}$, Yokoi *et al.* (1998) showed that FLCs in rat testis undergo apoptosis during the perinatal period, and the number of Leydig cells is regulated by both the rate of cell proliferation and apoptotic cell death.

B. Cell Aging

Chen *et al.* (1996a) have reviewed the literature on age-related changes in Leydig cells of rats and humans. It seems that changes in rat ALCs depend on the strain of rat used. Common in many strains is a decrease in testosterone associated with a decrease in LH (Geisthovel *et al.*, 1981; Steiner *et al.*, 1984). In Brown Norway rats the decrease in testosterone is associated with an increase in FSH and with an unchanged level of LH (Chen *et al.*, 1994). It seems that LH or hCG treatment does not reverse LH and testosterone levels completely; changes in Leydig cells rather than loss of these cause reduced steroidogenesis (Chen *et al.*, 1996a; Lin *et al.*, 1980). Total testicular 3β-HSD is reduced in aged Long Evans rats and in Wistar rats (Leathem and Albrecht, 1974), but not in Sprague-Dawley rats (Kaler and Neaves, 1981). Kim *et al.* (2002) studied age-related changes in the Leydig cells of Brown Norway rats: the absolute volume and the average number of Leydig

cells, and the steroidogenic ability of ALCs, decreased with age; serum LH and serum testosterone remained unchanged from month 3 until month 12 and decreased from month 19 onward. The ALC number per testis remained unchanged. The data from these authors led them to suggest that the decrease in Leydig cell function can be reversed nearly completely by treatment with LH and thyroxin (T_4). RLF is present in the FLCs and ALCs of rats; it is upregulated at puberty (Ivell and Bathgate, 2002). Hybridization analysis showed that in the testes of 2-year-old rats RLF/INSL3 mRNA was dramatically reduced compared with young animals; this was also confirmed by immunohistochemistry (Paust *et al.*, 2002). Chen *et al.* (1996b) treated old Brown Norway rats with EDS, which destroyed Leydig cells; the newly built Leydig cells restored high plasma testosterone in the old rats, indicating that the old hypothalamic–pituitary axis and the old testis environment were still intact. Chen and Zirkin (1999) showed that long-term suppression of Leydig cell steroidogenesis prevents Leydig cell aging; the authors administered contraceptive doses of testosterone to Brown Norway rats for 8 months, leading to the suppression of endogenous Leydig cell testosterone production; the ability to produce testosterone in the Leydig cells was rapidly restored after the end of treatment. Johnson and Neaves (1981) reported on the age-dependent changes in Leydig cells of stallions. The aspects of aging in human Leydig cells are mentioned in Section V.

C. Stress and Leydig Cells

Stress affects reproduction (Fenster *et al.*, 1997; Orr *et al.*, 1994). However, the mechanisms by which various stress stimuli affect reproductive functions in mammalian species are still not properly understood. One of the stress-impaired functional parameters in reproduction seems to be Leydig cell steroidogenesis (Hardy and Ganjam, 1997; Hardy *et al.*, 2002; Maric *et al.*, 1996; Monder *et al.*, 1994a,b). Stress-induced high levels of corticosterone seem to inhibit Leydig cell steroidogenesis by a glucocorticoid receptor-mediated mechanism (Hales and Payne, 1989). Several studies from the group of C. Monder provide evidence that 11β-HSD alleviates glucocorticoid-mediated inhibition of steroidogenesis in rat Leydig cells; the Leydig cells resist the inhibitory action of glucocorticoids on testosterone synthesis through oxidative inactivation of corticosterone by 11β-HSD (Monder *et al.*, 1994a,b). Leydig cells express glucocorticoid receptors and may also be targeted for direct inhibition of steroidogenesis by glucocorticoids. Hardy *et al.* (2002) published a report on the effects of psychosocial stress on steroidogenesis in rat Leydig cells and thereby the role of glucocorticoid metabolism in behavioral dominance. Employing a group housing

context called a visible burrow system for a highly aggressive subline of the Long-Evans rats, the male rats establish within few days a dominance hierarchy topped by a single dominant male that repeatedly attacks other males; the subordinate males show a reduction in aggression activity and sexual and social behavior, and an increase in defensive responses (Blanchard *et al*., 1995). Using this system, Hardy *et al*. (2002) observed a significant increase in LH and testosterone in dominant rats relative to control rats on day 4. Serum LH and testosterone were lower in subordinate animals on day 7, but testosterone alone was lower on day 14, suggesting that lowered LH secretion in subordinates may gradually be reversed by declines in androgen negative feedback. At all three time points serum corticosterone levels were higher in subordinate males compared with controls. In contrast, oxidative 11β-HSD activity in Leydig cells of dominant males was higher relative to controls and unchanged in subordinates (Fig. 18). The authors conclude that a failure of Leydig cells of subordinate males to compensate for increased glucocorticoid action during stress, by increasing 11β-HSD activity, potentiates a stress-mediated reduction in testosterone secretion. Furthermore, these data suggest an inhibition of the reproductive axis in subordinate males at the level of the pituitary.

V. Human Leydig Cells

Several studies on the morphology and ultrastructure of human Leydig cells during fetal (Codesal *et al*., 1990; Holstein *et al*., 1971; Kuopio *et al*., 1989a; Pelliniemi and Niemi, 1969), neonatal (Prince, 1985), prepubertal (Prince, 1984, 1990), and adult (Chemes, 1996; Christensen, 1975; Schulze, 1984) phases have been published.

The undifferentiated human gonade anlage appears in fetal week 6. Its differentiation in male leads to the formation of tunica albuginea, seminiferous cords and interstitial tissue at the end of fetal week 7. The interstitial tissue consists of mesenchymal fibroblasts, extracellular matrix, and small blood capillaries. Rarely, some large round cells with acidophilic cytoplasm appear during this stage; these cells were regarded as Leydig cell precursors by Holstein *et al*. (1971). The number of 3β-HSD-positive Leydig cells increases gradually and continuously. Leydig cells show a peak of development in week 19 of gestation, followed by a phase of quiescence (Haider *et al*., 2001). The absolute number and true counts of Leydig cells remain constant from weeks 17–19 of gestation; an 80% decrease is observed from week 22 onward (Fig. 19a). The numbers of interstitial fibrocytes and Leydig cells show an inverse relationship (Fig. 19b). From week 17, up to week 22, peritubular cells are arranged in two layers: an outer layer and an inner

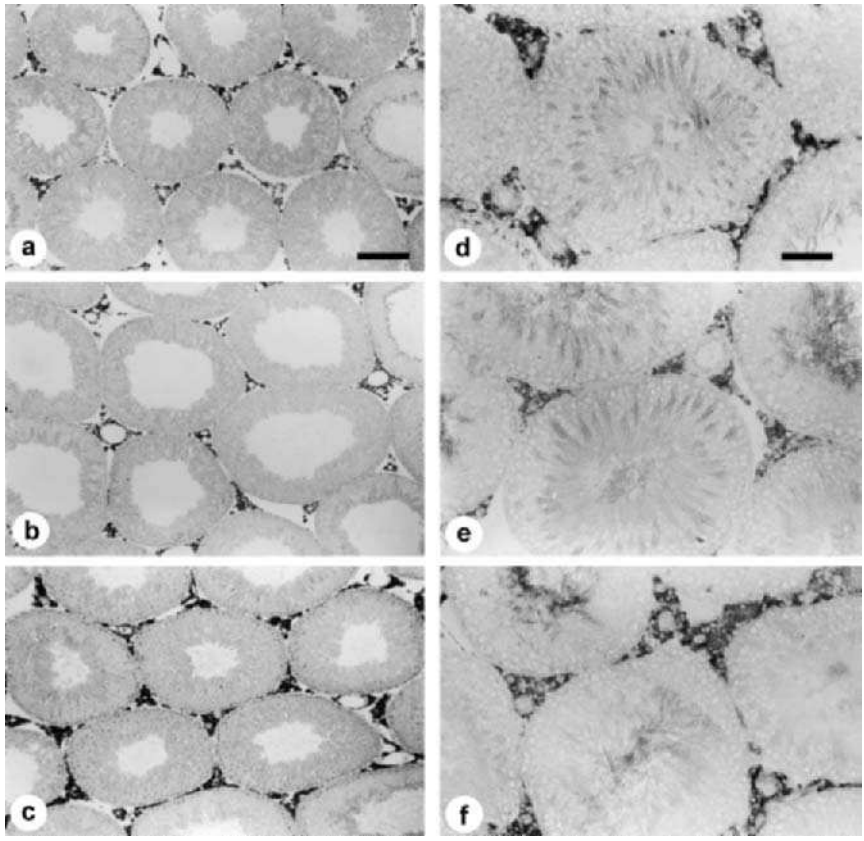

FIG. 18 Stress-induced changes in the patterns of the enzyme 11β-HSD in the Leydig cells of adult rat. Immunohistochemical staining in paraffin sections (a–c; bar, 125 μm) for type 1 11β-HSD and enzyme histochemical reaction in the cryostat sections (d–f; bar, 80 μm) for 11β-HSD. Control (a), subordinate (b), and dominant (c) rats after 14 days of VBS housing. The intensity of the immune reaction in dominant rats was higher compared with subordinates and controls. Control (d), subordinate (e), and dominant (f) rats after 4 days of VBS housing. The subordinates had a lower enzymatic reaction intensity compared with control and dominants. (Reproduced with the kind permission of the authors and of the publisher, Society for the Study of Reproduction; from Hardy *et al.* (2002). *Biol. Reprod.* **67,** 1750–1755.)

layer. The phase of quiescence coincided temporally with the existence of only an inner layer of peritubular cells (Fig. 19c).

It suggests that the cells of the outer layer of peritubular cells may probably serve as precursors for Leydig cells. Nuclei of Leydig cells showed only focally an androgen receptor (AR) immune reaction with weak to moderate intensity; only 17.8% of all Leydig cells—identified by a distinct 3β-HSD reaction—were positive for AR immune reaction. During this period (fetal

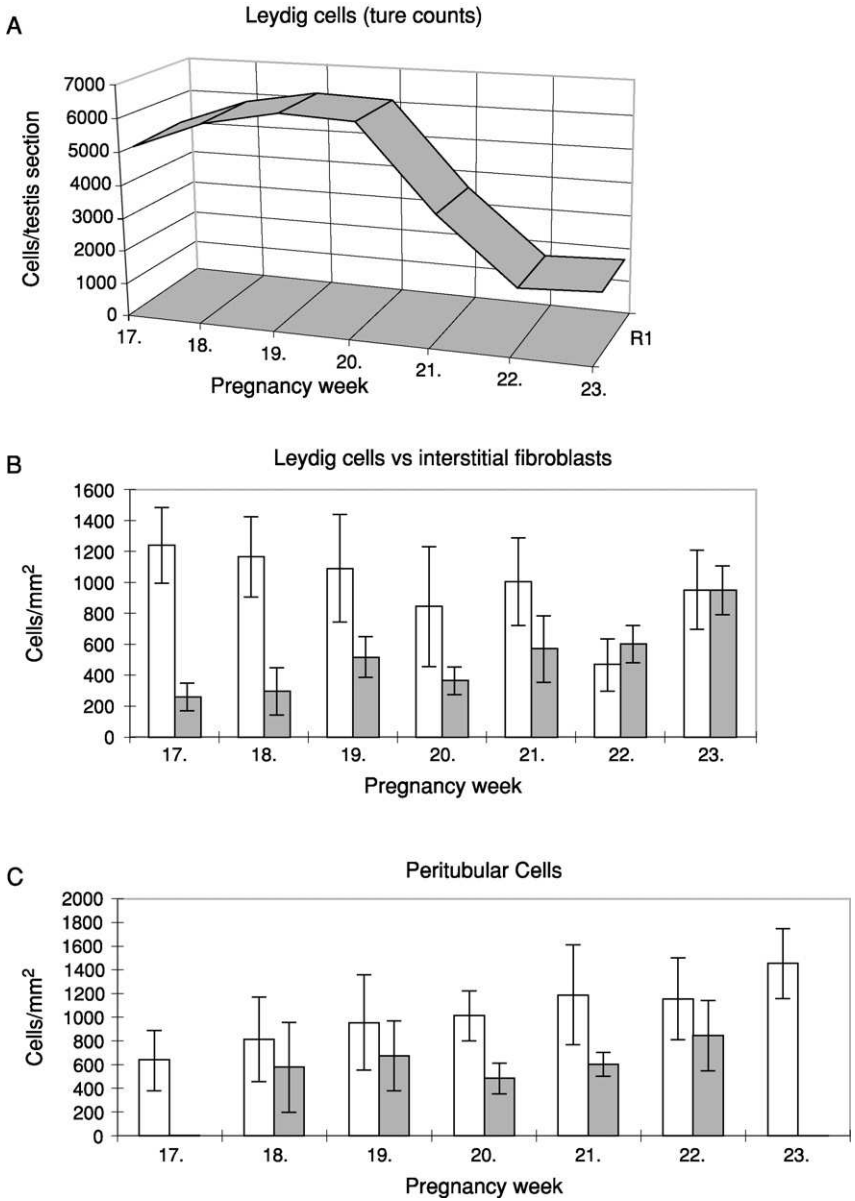

FIG. 19 Cell-counting data from human fetal testes. (A) True counts of 3β-HSD-positive Leydig cells per round cross-section from the middle region (maximum diameter) of the testis. (B) Leydig cells (open columns) and interstitial fibroblasts (shaded columns). Shown is the average number of cells per square millimeter (mean ± SD). (C) Peritubular cells in inner layer (open columns) and in outer layer (solid columns). Shown is the average number of cells per square millimeter (mean ± SD).

week 17 to fetal week 23) a specific strong intranuclear AR immune reaction is observed in the thin, slender peritubular cells in the testes of all fetuses. The androgen reaction is absent in Sertoli cells in all testes during this period. The peritubular cells build the first category of testicular cells, which express AR regularly. The period of quiescence shows various degrees of involution of Leydig cells and continues until birth. The dominant cell types in the interstitium are fibrocytes and mesenchymal fibroblasts. Neonatally, the differentiation of Leydig cells restarts either from the mesenchymal fibroblasts or from the previously involuted Leydig cells; this is still an unsolved matter. The peak of this neonatal proliferation of Leydig cells lies between months 2 and 3 (Prince, 1985).

Summarizing the literature and his own data, Prince (2001) proposed a triphasic nature of Leydig cell development in humans (Fig. 20). The arguments are convincing. The phases of highest proliferation of Leydig cells and thereby of maximum testosterone production are (1) 14–19 weeks of fetal life, (2) from the second to the third month after birth, and (3) from puberty throughout adult life (Reyes *et al*., 1974, Winter *et al*., 1976). The neonatal phase is dependent on reactivation of the hypothalamic–testicular axis. In contrast to biphasic LC development in rodents, primate and human LCs show a triphasic course of development. Also, in contrast to rodents, there is no evidence in humans of the simultaneous existence of two separate and

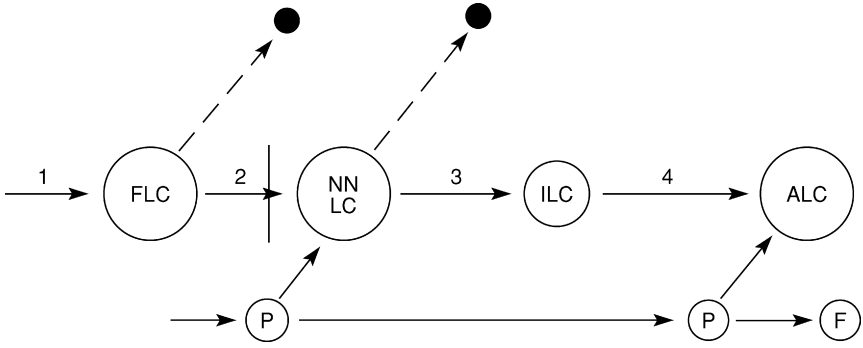

FIG. 20 Three phases of Leydig cell development in humans. Main horizontal axis: (1) Development of fetal Leydig cells (FLCs) from undifferentiated mesenchymal precursors; (2) regression of fetal Leydig cells with subsequent maturation into mature neonatal Leydig cells (NNLCs): the vertical line represents the birth, the broken line leading to a solid circle represents the cells that degenerate after the fetal phase; (3) regression of NNLCs: a component regresses to immature Leydig cells (ILCs), which are present throughout childhood; a broken line leading to a solid circle represents the NNLC component that degenerates; (4) maturation of ILCs at puberty into a segment of adult Leydig cells (ALCs). P, Precursor cells including primitive fibroblasts of interstitium and peritubular fibroblasts; F, fibroblastic cells of the adult interstitium. (Reproduced with the kind permission of the author and the publisher, Society of Endocrinology; from F. P. Prince (2001). *J. Endocrinol.* **168,** 213–216.)

distinct cell populations. Prince (2002) also pointed out the possible morphological diversity of mitochondrial cristae in human Leydig cells, and described the presence of "lamellar and tubular associations" of cristae and their possible implications for a steroid-producing cell. Kuopio *et al.* (1989a) reported the presence of a basement membrane around Leydig cells of the human fetus (weeks 14–24 of gestation).

VEGF, and its two receptors (Flt-1 and KDR), are present in normal human Leydig cells (Ergün *et al.*, 1997). Also endothelin, and its receptors A and B, are produced in human Leydig cells (Ergün *et al.*, 1999); the authors suggest that VEGF and endothelin are involved in paracrine and autocrine regulation of Leydig cells. Chemes *et al.* (1992) studied the capacity of testosterone secretion and responsiveness to hCG of mesenchymal cells isolated from human prepubertal testes of patients with androgen insensitivity syndrome; they demonstrated that immature Leydig cells precursors from mesenchymal fibroblasts are capable of testosterone synthesis and secretion. Addition of hCG increases testosterone secretion and promotes differentiation toward mature Leydig cells. Some studies on human Leydig cells have shown the presence of substances, that are also present in nerve cells, for example, substance P or neurofilament triplet proteins NF-L, NF-M, and NF-H (Davidoff *et al.*, 1999; Schulze *et al.*, 1987). According to these authors the data suggest a neuroendocrine nature of human Leydig cells (Davidoff *et al.*, 1993). These authors also proposed a possible neural origin of human Leydig cells; this hypothesis is, however, not justified by the data provided by this group.

Aged human Leydig cells are mostly vacuolated, multinucleated, and contain abundant lipid droplets (Paniagua *et al.*, 1986). They contain lipofuscin granules and cytoplasmic or intranuclear crystalline inclusions, less SER, and fewer mitochondria (Holstein *et al.*, 1988; Mori *et al.*, 1982; Paniagua *et al.*, 1991). The biologically available serum testosterone is decreased, as reviewed by Vermeulen (1991). The mechanisms of reduced steroidogenesis, discussed in the literature, are loss of Leydig cells, reduced production of testosterone by individual Leydig cells, deficits in the steroidogenic pathway, particularly of microsomal enzymes $P450_{SCC}$ and P450 17α-hydrolase, and also reduction of pregnenolone formation in mitochondria (Bélanger *et al.*, 1994; Chen *et al.*, 1996a; Nieschlag *et al.*, 1982; Takahashi *et al.*, 1983).

Histochemical studies on the enzymes in Leydig cells of patients (total $n = 71$) with andrological diseases revealed three patterns (Haider *et al.*, 1988): (1) *normal status* ($n = 42$): spermatogenesis was normal (plasma testosterone, >400 ng/100 ml). Moderate to strong intensity of the following enzymes was observed in the cytoplasm of Leydig cells: nonspecific esterases, secondary alcohol dehydrogenase, β-hydroxybutyric acid dehydrogenase, 3-βHSD, 17β-HSD, and 3α-HSD. The Leydig cells were arranged in clusters

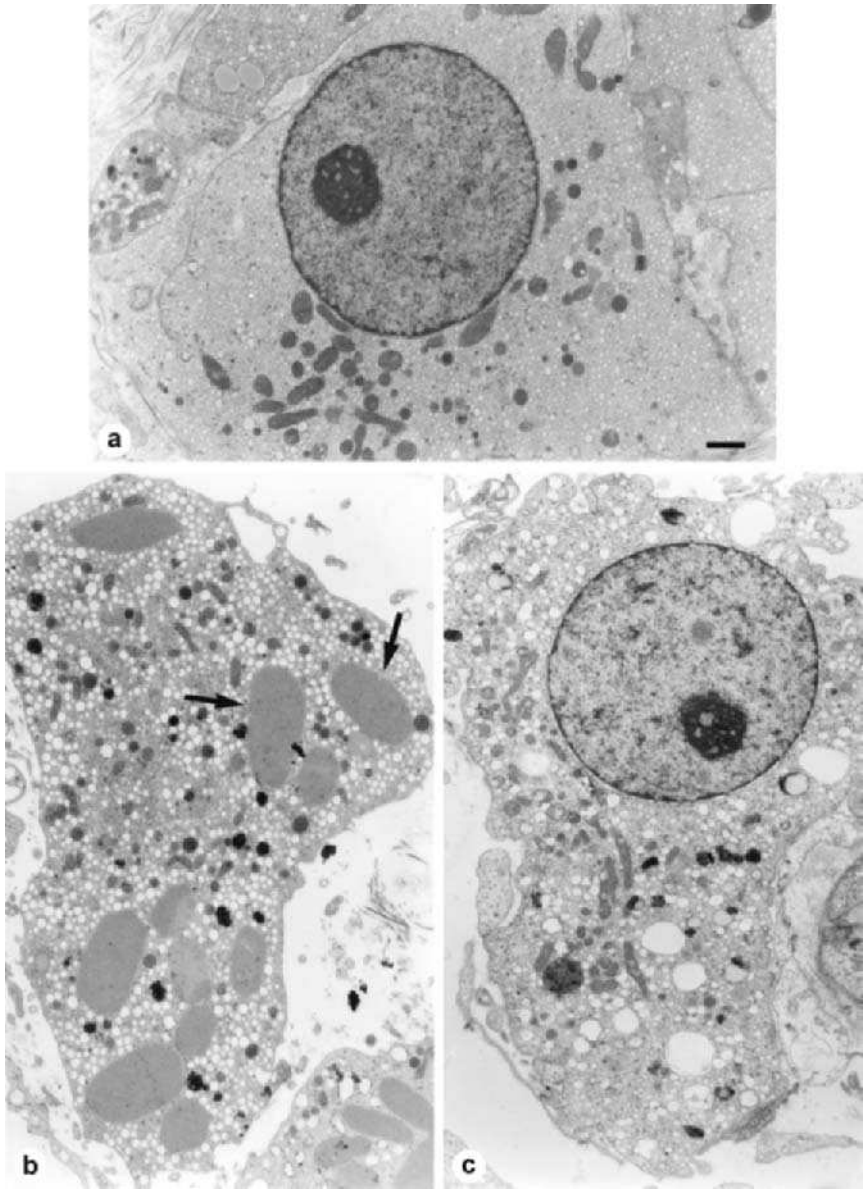

FIG. 21 Ultrastructure of Leydig cells in adult humans with infertility disorders. Bar [also valid for (b) and (c)]: 1 μm; original magnification, ×8000. (a) A man with normal spermatogenesis and normal histochemical status of steroidogenic enzymes in Leydig cells. The Leydig cell shown contains abundant SER and mitochondria with tubulovesicular cristae. (b) A Leydig cell from a patient with a partial stop of spermatogenesis and weak pathological status of steroidogenic enzyme histochemistry. Main changes: decrease in SER amount, only a few intact mitochondria and prominently a large number of Reinke's crystals (arrows), electron-dense

as well as in isolated form in the peritubular and perivascular regions. As shown in electron microscopic studies, the Leydig cells contained light cytoplasm, and an abundance of SER and tubulovesicular mitochondria (Fig. 21a); (2) *weak pathological status* ($n = 22$): Spermatogenesis was partially blocked, mostly at the level of secondary spermatocytes (plasma testosterone, 250–400 ng/100 ml). The Leydig cells showed reaction for nonspecific esterases, alcohol dehydrogenase, and β-hydroxybutyric acid dehydrogenase; however, the reaction for 3β-HSD, 17β-HSD, and 3α-HSD was weak or absent. The Leydig cells were arranged rarely in clusters; isolated Leydig cells were more often observed. The cytoplasm appeared dark and in some cells light. Only a few tubulovesicular mitochondria and a small amount of SER were observed. Electron-dense bodies of various sizes, vacuoles, and a conspicuously large number of Reinkes crystals with a typical network pattern were present (Fig. 21b). Sperm production in these patients was improved after 3 months of treatment with hCG-HMG, as shown by semen analysis; (3) *severe pathological status* ($n = 7$): Spermatogenesis was severely blocked at the level of spermatocytes or of spermatogonia (plasma testosterone, 100–350 ng/100 ml). All six enzymes, mentioned above, were either not detectable histochemically or showed only a weak signal in the Leydig cells. Clusters as well as isolated Leydig cells with the following features were observed: tubulovesicular mitochondria with signs of degeneration as well as complete dissolution, a moderate amount of SER with swelling of the ER membranes, only a few electron-dense bodies, numerous cytoplasmic vacuoles of different sizes, round or elongated vesicles at the cell membrane, and only a few Reinkes crystals (Fig. 21c). HCG-HMG treatment failed to improve sperm production in this group. There were no correlations between these three patterns and plasma LH or plasma FSH values.

Data on mutations of gonadotropin receptors in human male patients with infertility diseases have been published (for review see Themmen and Huhtaniemi, 2000). Liu *et al*. (1999) reported on Leydig cell tumors, caused by an activating mutation of the gene encoding the LH receptor. Inactivating mutations of the human LH receptor disrupt male differentiation, ranging from mild undervirilization to complete lack of genital masculinization (Themmen and Huhtaniemi, 2000). Summarizing the data on the mutations of LH, LH receptor, FSH, and FSH receptor in humans and the pathological

bodies, and small vacuoles in the cytoplasma. (c) A Leydig cell from a patient with complete stop of spermatogenesis at the level of spermatocytes and with severe pathological status of steroidogenic enzyme histochemistry. Main ultrastructural features: Mitochondria with signs of degeneration up to complete dissolution, swelling of SER membranes, numerous cytoplasmic vacuoles of various sizes, and electron-dense bodies in the cytoplasm. (For definition of histochemical status, see text.)

changes in infertile patients, Huhtaniemi and Bartke (2001) suggested a sexual dichotomy between LH (critically ''a male gonadotropin'') and FSH (critically ''a female gonadotropin'').

VI. Concluding Remarks

Research has provided important information about the differentiation, apoptotic death, and regeneration of Leydig cells. It is now established that mesenchymal fibroblasts build the precursors of Leydig cells. The differentiation of Leydig cells in rodents is biphasic and in humans it is triphasic.

There are, however, still several open questions. Data on the ultimate fate of FLCs in rodents are contradictory. Further studies are necessary to determine the exact mechanisms of cell death of Leydig cells: apoptosis, involution, or dedifferentiation. The apoptotic death of ALCs has been studied extensively. However, only a little information is available on FLC death. The mechanism leading to death of FLCs may possibly differ from that of ALCs. Our knowledge on the intracellular signalling system in Leydig cells is limited. Additional experiments are needed to explore the physiological rationale of high production of RLF in mature Leydig cells. Studies on the mediating or regulatory role played by the vascular endothelial cells in transport of LH to Leydig cells would help clarify the paracrine interaction between these two interstitial cell compartments. The indication of cross-talk between Leydig cells and testicular macrophages is becoming inreasingly clear. The functional hypogonadism in older male mammals is caused mainly by dedifferentiation of ALCs; however, the molecular mechanisms that lead to the reduced steroidogenic capacity of individual Leydig cells in aged rats are still unclear. Estrogens, xenoestrogens, and other hormone disruptors affect testosterone production in Leydig cells; this should be the target of future research in view of the immense implications for the clinical and applied sciences. Analysis of genes is a fascinating and highly promising field of research to attack more information about the reproductive biology of Leydig cells. Studies on the mutations of genes for gonadotropic hormones and their receptors as well as androgen and its receptor would offer key insights into the pathogenesis of various congenital infertility disturbances.

Acknowledgments

The data in this review was collected in cooperation with colleagues Ms. B. Hilscher, Prof. W. Hilscher, Prof. D. Passia, and Prof. N. Hofmann; research students G. Schwochau, A. Neumann, D. Laue, S. Tajtaraghi, B. G. Schlutius, B. A. Schäfers, R. Darbandi-Tonkabon,

N. Sabbari, F. J. Hensel, G. Overmeyer, and H. G. Ziegler; and technical assistants G. Servos, G. Berthold, M. Baasen, and U. Mockenhaupt. With deep thanks the author acknowledges their cooperation and help. The author also thanks Dr. M. P. Hardy (Population Council, Rockefeller University, New York, NY) for critical reading of the manuscript and valuable suggestions. This work was partially financed by the Deutsche Forschungsgemeinschaft (the German Research Council).

References

Akingbemi, B. T., Youker, R. T., Sottas, C. M., Ge, R., Katz, E., Klinefelter, G. R., Zirkin, B. R., and Hardy, M. P. (2001). Modulation of rat Leydig cell steroidogenic function by di(2-ethylhexyl)phthalate. *Biol. Reprod.* **65,** 1252–1259.

Akingbemi, B. T., Ge, R., Rosenfeld, C. S., Newton, L. G., Hardy, D. O., Catterall, J. F., Lubhan, D. B., Korach, K. S., and Hardy, M. P. (2003). Estrogen receptor-α gene deficiency enhances androgen biosynthesis in the mouse Leydig cell. *Endocrinology* **144,** 84–93.

Anakwe, O. O., Murphy, P. R., and Moger, W. H. (1985). Characterization of β-adrenergic binding sites on rodent Leydig cells. *Biol. Reprod.* **33,** 815–826.

Anand, R. J., Paust, H. J., Altenpohl, K., and Mukhopadhyay, A. K. (2002). Regulation of vascular endothelial growth factor production by Leydig cells in vitro: Role of protein kinase A and mitogen-activated protein kinase cascade. *Biol. Reprod.* **68,** 1663–1673.

Anderson, R. A., and Sharpe, R. M. (2000). Regulation of inhibin production in the human male and its clinical implications. *Int. J. Androl.* **23,** 136–359.

Arakane, F., Kallen, C. B., Watari, H., Foster, J. A., Sepuri, N. B. V., Pain, D., Stayrook, S. E., Lewis, M., Gerton, G. L., and Strauss, J. F. (1998). The mechanism of action of steroid acute regulatory protein (StAR). *J. Biol. Chem.* **273,** 16339–16345.

Ariyaratne, H. B., Mendis-Handagama, S. M. C., Hales, D. B., and Mason, J. I. (2000a). Studies of the onset of Leydig precursor cell differentiation in the prepubertal rat testis. *Biol. Reprod.* **63,** 165–171.

Ariyaratne, H. B. S., Mason, J. I., and Mendis-Handagama, S. M. L. C. (2000b). Effects of thyroid hormone on Leydig cell regeneration in the adult rat following ethane dimethane sulphonate treatment. *Biol. Reprod.* **63,** 1115–1123.

Atanassova, N., Mckinnell, C., Walker, M., Turner, K. J., Fischer, J. S., Morley, M., Miller, M. R., Groome, N. P., and Sharpe, R. M. (1999). Permanent effects of neonatal estrogen exposure in rats on reproductive hormone levels, Sertoli cell number, and the efficiency of spermatogenesis in adulthood. *Endocrinology* **140,** 5364–5373.

Avallet, O., Vigier, M., Perrad-Sapori, M. H., and Saez, J. M. (1987). Transforming growth factor-β inhibits Leydig cell functions. *Biochem. Biophys. Res. Commun.* **146,** 575–581.

Baker, J., Hardy, M. P., Zhou, J., Bondy, C., Lupu, F., Bellvé, A. R., and Efstratiadis, A. (1996). Effects of an IGF-I gene null mutation on mouse reproduction. *Mol. Endocrinol.* **10,** 903–918.

Baker, P. J., and O'Shaughnessy, P. J. (2001). Role of gonadotrophins in regulating numbers of Leydig and Sertoli cells during fetal and postnatal development in mice. *Reproduction* **122,** 227–234.

Baker, P. J., Sha, J. A., McBride, M. W., Peng, L., Payne, A. H., and O'Shaughnessy, P. J. (1999). Expression of 3-hydroxysteroid dehydrogenase type I and IV isoforms in the mouse testis during development. *Eur. J. Biochem.* **260,** 911–916.

Baker, P. J., Pakarinen, P., Huhtaniemi, I. T., Abel, M. H., Charlton, H. M., Kumar, T. R., and O'Shaughnessy, P. J. (2003). Failure of normal Leydig cell development in follicle-stimulating

hormone (FSH) receptor-deficient mice, but not FSHβ-deficient mice: Role for constitutive FSH receptor activity. *Endocrinology* **144,** 138–145.

Barreiro, M. L., Gaytan, F., Caminos, J. E., Pinilla, L., Casanueva, F. F., Aguilar, E., Dieguez, C., and Tena-Sempere, M. (2003). Cellular location and hormonal regulation of ghrelin expression in rat testis. *Biol. Reprod.* **67,** 1768–1776.

Bélanger, A., Candas, B., Dupont, L., Cusan, P., Diamond, J., Gomez, L., and Labrie, F. (1994). Changes in serum concentrations of conjugated and unconjugated steroids in 40- to 80-year old men. *J. Clin. Endocrinol. Metab.* **79,** 1086–1090.

Benton, L., Shan, L. X., and Hardy, M. P. (1995). Differentiation of adult Leydig cells. *J. Steroid Biochem. Mol. Biol.* **53,** 61–68.

Bergh, A. (1985). Effect of cryptorchidism on the morphology of testicular macrophages: Evidence for a Leydig cell–macrophage interaction in the rat testis. *Int. J. Androl.* **8,** 86–96.

Bilinska, B., and Litwin, J. A. (1995). Immunocytochemical demonstration of peroxisomes in cultured Leydig cells: A decrease in testosterone secretion precedes reduction of peroxisomes. *Eur. J. Histochem.* **39,** 273–280.

Blanchard, D. C., Spencer, R. L., Weiss, S. M., Blanchard, R. J., McEwen, B., and Sakai, R. R. (1995). Visible burrow system as a model of chronic social stress: Behavioral and neuroendocrine correlates. *Psychoneuroendocrinology* **20,** 117–134.

Boockfor, F. R., Fullbright, G., Büllesbach, E. E., and Schwabe, C. (2001). Relaxin-like factor (RLF) serum concentrations and gubernacular RLF receptor display in relation to pre- and neonatal development of rats. *Reproduction* **122,** 899–906.

Bortolussi, M., Zanchetta, R., Belvedere, P., and Colombo, L. (1990). Sertoli and Leydig cell numbers and gonadotrophin receptors in rat testis from birth to puberty. *Cell Tissue Res.* **260,** 185–191.

Boulogne, B., Levacher, C., Durand, P., and Habert, R. (1999). Retinoic acid receptors and retinoic X receptors in the rat testis during fetal and postnatal development: Immunolocalization and implication in the control of the number of gonocytes. *Biol. Reprod.* **61,** 1548–1557.

Brennan, J., Tilmann, C., and Capel, B. (2003). PDGFR-α mediates testis cord organization and fetal Leydig cell development in the XY gonad. *Genes Dev.* **17,** 800–810.

Brereton, P. S., van Driel, R. R., Suhaimi, F. B., Koyama, K., Dilley, R., and Krozowski, Z. (2001). Light and electron microscopy localization of the 11 β-hydroxysteroid dehydrogenase type I enzyme in the rat. *Endocrinology* **142,** 1644–1651.

Buher, M., Subin, G. U., and McLaren, A. (1993). Mesonephros contribution to testis differentiation in the fetal mouse. *Development* **117,** 273–281.

Byskov, A. (1986). Differentiation of mammalian embryonic gonad. *Physiol. Rev.* **66,** 77–112.

Calkins, J. H., Sigel, M. M., Nankin, H. R., and Lin, T. (1988). Interleukin-1 inhibits Leydig cell steroidogenesis in primary culture. *Endocrinology* **123,** 1605–1610.

Caprio, M., Fabbrini, E., Ricci, G., Basciani, S., Gnessi, L., Arizzi, M., Carta, A. R., De Martino, M. U., Isidori, A. M., Frajese, G. V., and Fabbri, A. (2003). Ontogenesis of leptin receptor in rat Leydig cells. *Biol. Reprod.* **68,** 1199–1207.

Carreau, S., Genissel, C., Bilinska, B., and Lavellet, J. (1999). Sources of estrogens in the testis and reproductive tract of the male. *Int. J. Androl.* **22,** 211–223.

Carreau, S., Bourguiba, S., Lambard, S., Galeraud-Denis, I., Genissel, C., and Levallet, J. (2002). Reproductive system: Aromatase and estrogens. *Mol. Cell. Endocrinol.* **193,** 137–143.

Carstensen, J. F., Tesdorpf, J. G., Kaufmann, M., Markus, M. M., Husen, B., Leenders, F., Jakob, F., de Launoit, Y., and Adamski, J. (1996). Characterization of 17β-hydroxysteroid dehydrogenase IV. *J. Endocrinol.* **150,** 3–12.

Chemes, H. E. (1996). Leydig cell development in humans. *In* "The Leydig Cell" (A. H. Payne, M. P. Hardy, and L. D. Russell, Eds.), pp. 175–201. Cache River Press, Vienna, IL.

Chemes, H., Gigorraga, C., Bergadá, C., Schteingart, H., Rey, R., and Pellizari, E. (1992). Isolation of human Leydig cell mesenchymal precursors from patients with the androgen insensitivity syndrome: Testosterone production and response to human chorionic gonadotropin stimulation in culture. *Biol. Reprod.* **46,** 793–801.

Chen, H., and Zirkin, B. R. (1999). Long-term suppression of Leydig cell steroidogenesis prevents Leydig cell aging. *Proc. Natl. Acad. Sci. USA* **96,** 14877–14881.

Chen, H., Hardy, M. P., Huhtaniemi, I., and Zirkin, B. R. (1994). Age-related decreased Leydig cell testosterone production in the Brown Norway rat. *J. Androl.* **15,** 551–557.

Chen, H., Luo, L., and Zirkin, B. R. (1996a). Leydig cell structure and function during aging. *In* "The Leydig cell" (A. H. Payne, M. P. Hardy, and L. D. Russell, Eds.), pp. 221–230. Cache River Press, Vienna, IL.

Chen, H., Huhtaniemi, I., and Zirkin, B. R. (1996b). Depletion and repopulation of Leydig cells in the testes in aging Brown Norway rats. *Endrocrinology* **137,** 3447–3452.

Chen, J. J., Lukyanenko, Y., and Huston, J. C. (2002). 25-Hydroxycholesterol is produced by testicular macrophages during the early postnatal period and influences differentiation of Leydig cells in vitro. *Biol. Reprod.* **66,** 1336–1341.

Christensen, A. K. (1975). Leydig Cells. *In* "Handbook of Physiology" (D. W. Hamilton and R. O. Greep, Eds.), Vol. 5, pp. 57–94. American Physiological Society, Washington, D.C.

Clark, A. M., Garland, K. K., and Russell, L. D. (2000). Desert hedgehog (*Dhh*) gene is required in the mouse testis for formation of adult-type Leydig cells and normal development of peritubular cells and seminiferous tubules. *Biol. Reprod.* **63,** 1825–1838.

Codesal, J., Regardera, J., Nistal, M., Regardera-Sejas, J., and Paniagua, R. (1990). Involution of human fetal Leydig cells: An immunohistochemical, ultrastructural and quantitative study. *J. Anat.* **172,** 103–114.

Collin, O., and Bergh, A. (1996). Leydig cells secrete factors which increase vascular permeability and endothelial cell proliferation. *Int. J. Androl.* **19,** 221–228.

Cudicini, C., Lejeune, H., Gomez, E., Bosman, E., Ballet, F., Saez, J., and Jegou, B. (1997). Human Leydig cells and Sertoli cells are producers of interleukin-1 and 6. *J. Clin. Endocr. Metab.* **82,** 1426–1433.

Daugas, E., and Kroemer, G. (2000). Apoptosis: Searching for the central executioner. *In* "Testis, Epididymis, and Technology in the Year 2000" (B. Jégou, C. Pineau, and J. Saez, Eds.), E. Schering Research Foundation Workshop, Suppl. 6, pp. 129–139. Springer-Verlag, Heidelberg, Germany.

Davidoff, M. S., Schulze, W., Middendorff, R., and Holstein, A. F. (1993). The Leydig cell of the human testis: A new member of the diffuse neuroendocrine system. *Cell Tissue Res.* **271,** 429–439.

Davidoff, M. S., Middendorff, R., Pusch, W., Müller, D., Wichers, S., and Holstein, A. F. (1999). Sertoli and Leydig cells of the human testis express neurofilament triplet proteins. *Histochem. Cell. Biol.* **111,** 173–187.

De Kretser, D. M., and Kerr, J. B. (1994). The cytology of the testis. *In* "The Physiology of Reproduction" (E. Knobil and J. D. Neil, Eds.), pp. 1177–1290. Raven Press, New York.

Diemer, T., Allen, J. A., Hales, K. H., and Hales, D. B. (2003). Reactive oxygen disrupts mitochondria in MA-10 tumor Leydig cells and inhibits steroidogenic acute regulatory (StAR) protein and steroidogenesis. *Endocrinology* **144,** 2882–2891.

Dufau, M. L. (1988). Endocrine regulation and communicating functions of the Leydig cell. *Annu. Rev. Physiol.* **50,** 483–508.

Dupont, E., Labrie, F., Luu-The, V., and Pelletier, G. (1993). Ontogeny of 3β-hydroxysteroid dehydrogenase Δ^5-Δ^4 isomerase (3β-HSDH) in rat testis as studied by immunocytochemistry. *Anat. Embryol.* **187,** 583–589.

Ergün, S., Kilic, N., Fiedler, W., and Mukhopadhyay, A. K. (1997). Vascular endothelial growth factor and its receptors in normal human testicular tissue. *Mol. Cell. Endocrinol.* **131,** 9–20.

Ergün, S., Harneit, S., Paust, H. J., Mukhopadhyay, A. K., and Holstein, A. F. (1999). Endothelin and endothelin receptors A and B in the human testis. *Anat. Embryol.* **199,** 207–214.

Ewing, L. L., and Zirkin, B. (1983). Leydig cell structure and steroidogenic function. *Recent Prog. Hormone Res.* **39,** 599–635.

Fenster, L., Katz, D. F., Wyrobek, A. J., Pieper, C., Rempel, D. M., Oman, D., and Swan, S. H. (1997). Effects of psychological stress on human semen quality. *J. Androl.* **18,** 194–202.

Frankel, A. I., Mock, E. J., and Chapman, J. C. (1984). Hypophysectomy and hemivasectomy can inhibit the testicular hemicastration response of the immature rat. *Biol. Reprod.* **30,** 804–808.

Gautier, C., Levacher, C., Avallet, O., Vigier, M., Rouiller-Fabre, Lecerf, L., Saez, J., and Habert, R. (1994). Immunohistochemical localization of transforming growth factor-β1 in the fetal and neonatal rat testis. *Mol. Cell. Endocrinol.* **99,** 55–61.

Gautier, C., Levacher, C., Saez, J., and Habert, R. (1997). Transforming growth factor β1 inhibits steroidogenesis in dispersed fetal testicular cells in culture. *Mol. Cell. Endocrinol.* **131,** 21–30.

Gaytan, F., Bellido, C., Morales, C., Reymundo, C., Aguilar, E., and van Rooijen, N. (1994a). Selective depletion of testicular macrophages and prevention of Leydig cells repopulation after treatment with ethylene dimethane sulphonate (EDS) in rat. *J. Reprod. Fertil.* **101,** 175–182.

Gaytan, F., Bellido, C., Morales, C., Reymundo, C., Aguilar, E., and Van Rooijen, N. (1994b). Effects of macrophage depletion at different times after treatment with ethylene dimethane sulfonate (EDS) on the regeneration of Leydig cells in the adult rat. *J. Androl.* **15,** 558–564.

Gaytan, F., Romero, J. L., Morales, C., Reymundo, C., Bellido, C., and Aguilar, E. (1995a). Response of testicular macrophages to EDS-induced Leydig cell death. *Andrologia.* **27,** 259–265.

Gaytan, F., Bellido, C., Morales, C., van Rooijen, N., and Aguilar, E. (1995b). Role of testicular macrophages in the response of Leydig cells to gonadotrophins in young hypophysectomized rats. *J. Endocrinol.* **147,** 463–471.

Gaytan, F., Bellido, C., Morales, C., Reymundo, C., Aguilar, E., and Rooijen, N. (1995c). Response to Leydig cell apoptosis in the absence of testicular macrophages. *J. Reprod. Immunol.* **29,** 81–94.

Ge, R. S., and Hardy, M. P. (1997). Decreased cyclin A_2 and increased cyclin G_1 levels coincide with loss of proliferative capacity in rat Leydig cells during pubertal development. *Endocrinology* **138,** 3719–3726.

Ge, R. S., and Hardy, M. P. (1998). Variation in the end products of androgen biosynthesis and metabolism during postnatal differentiation of rat Leydig cells. *Endocrinology* **139,** 3787–3795.

Ge, R. S., and Hardy, M. P. (2000). Initial predominance of the oxidative activity of type I 11β-hydroxysteroid dehydrogenase in primary rat Leydig cells and tranfected cell lines. *J. Androl.* **21,** 303–310.

Ge, R. S., Shan, L.-X., and Hardy, M. P. (1996). Pubertal development of Leydig cells. *In* "The Leydig Cell" (A. H. Payne, M. P. Hardy, and L. D. Russel, Eds.), pp. 160–173. Cache River Press, Vienna, IL.

Ge, R. S., Gao, H. B., Nacharaju, V. L., Gunsalus, G. L., and Hardy, M. P. (1997a). Identification of a kinetically distinct activity of 11β-hydroxysteroid dehydrogenase in rat Leydig cells. *Endocrinology* **138,** 2435–2442.

Ge, R. S., Hardy, D. O., Catterall, J. F., and Hardy, M. P. (1997b). Developmental changes in glucocorticoid receptor and 11β-hydroxysteroid dehydrogenase oxidative and reductive activities in rat Leydig cells. *Endocrinology* **138,** 5089–5095.

Ge, R. S., Hardy, D. O., Catterall, J. F., and Hardy, M. P. (1999). Opposing changes in 3α-hydroxysteroid dehydrogenase oxidative and reductive activities in rat Leydig cells during pubertal development. *Biol. Reprod.* **60,** 855–860.

Geisthovel, F., Brabant, G., Wickings, J., and Nieschlag, E. (1981). Changes in testicular hCG binding and Leydig cell function in rats throughout life. *Horm. Res.* **14,** 47–55.

Genissel, C., and Carreau, S. (2001). Regulation of the aromatase gene expression in mature rat Leydig cells. *Mol. Cell. Endocrinol.* **178,** 141–146.

Genissel, C., Levallet, J., and Carreau, S. (2001). Regulation of cytochrom P450 aromatase gene expression in adult rat Leydig cells: Comparison with estradiol production. *J. Endocrinol.* **168,** 95–105.

Ghinea, N., and Milgrom, E. (1995). Transport of protein hormones through the vascular endothelium. *J. Endocrinol.* **145,** 1–9.

Ghinea, N., Mai, T. V., Groyer-Picard, M. T., and Milgrom, E. (1994). How protein hormones reach their target cells? Receptor-mediated transcytosis of HCG through endothelial cells. *J. Cell. Biol.* **125,** 87–97.

Grizard, G., Fournet, M., Rigaudiere, N., Lombard-Vignon, N., and Grizard, J. (1991). Insulin binding to Leydig cells and insulin levels in testicular interstitial fluid at different stages of development in the rat. *J. Endocrinol.* **128,** 375–381.

Gustafsson, K., Söder, O., Pöllänen, P., and Ritzen, E. M. (1988). Isolation and partial characterization of an interleukin-like factor from rat testis interstitial fluid. *J. Reprod. Immunol.* **14,** 139–150.

Habert, R., Lejeune, H., and Saez, J. M. (2001). Origin, differentiation and regulation of fetal and adult Leydig cells. *Mol. Cell. Endocrinol.* **179,** 47–74.

Haider, S. G., and Servos, G. (1998). Ultracytochemistry of 3β-hydroxysteroid dehydrogenase in Leydig cell precursors and vascular endothelial cells of the postnatal rat testis. *Anat. Embryol.* **198,** 101–110.

Haider, S. G., Urban, A., Hilscher, B., Hilscher, W., and Passia, D. (1983). Cyproterone acetate induced changes in the behaviour of hydroxysteroid dehydrogenases in rat Leydig cells during perinatal development. *Andrologia* **15,** 498–506.

Haider, S. G., Passia, D., and Overmeyer, G. (1986). Studies on fetal and postnatal development of rat Leydig cells employing 3β-hydroxysteroid dehydrogenase activity. *Acta Histochem.* **32,** 197–202.

Haider, S. G., Passia, D., and Hofmann, N. (1988). Histochemical patterns of some enzymes in the Leydig cells of infertile patients. *Acta Histochem.* **36,** 427–433.

Haider, S. G., Passia, D., and Rommert, F. F. G. (1990). Histochemical demonstration of 11β-hydroxysteroid dehydrogenase as a marker for Leydig cell maturation in rat. *Acta Histochem.* **38,** 203–207.

Haider, S. G., Hettwer, H., Passia, D., and Servos, G. (1994). Ultrastructural and enzyme histochemical changes in the rat Leydig cell induced by an antiandrogen (Flutamide). *Fertilität* **10,** 42–47.

Haider, S. G., Laue, D., Schwochau, G., and Hilscher, B. (1995). Morphological studies on the origin of adult-type Leydig cells in rat testis. *It. J. Anat. Embryol.* **100**(Suppl.1), 535–541.

Haider, S. G., Berthold, G., and Darbandi, R. (2001). Differentiation of Leydig cells and peritubular cells in fetal human testis from 17th to 23rd postconceptional week. Abstract presented at VIIth Int. Congress of Andrology, June 15–19, Montreal, 2001. *J. Androl.* **2001**(Suppl.), 197.

Hales, D. B. (2002). Testicular macrophage modulation of Leydig cell steroidogenesis. *J. Reprod. Immunol.* **57,** 3–18.

Hales, D. B., and Payne, A. H. (1989). Glucocorticoid-mediated repression of P450scc mRNA and de novo synthesis in cultured Leydig cells. *Endocrinology* **124,** 2099–2104.

Hardy, D. O., Ge, R. S., Catterall, J. F., Hou, Y. T., Penning, T. M., and Hardy, M. P. (2000). Identification of the oxidative 3α-hydroxysteroid dehydrogenase activity of rat Leydig cells as type II retinol dehydrogenase. *Endocrinology* **141,** 1608–1617.

Hardy, M. P., and Ganjam, V. K. (1997). Stress, 11β-HSD, and Leydig cell function. *J. Androl.* **18,** 475–479.

Hardy, M. P., Zirkin, B. R., and Ewing, L. L. (1989). Kinetic studies on the development of the adult population of Leydig cells in testes of the pubertal rat. *Endocrinology* **124,** 762–770.

Hardy, M. P., Kelce, W. R., Klinefelter, G. R., and Ewing, L. L. (1990). Differentiation of Leydig cell precursors in vitro: A role for androgen. *Endocrinology* **127,** 488–490.

Hardy, M. P., Sharma, R. S., Arambepola, N. K., Sottas, C. M., Russel, L. D., Bunick, D., Hess, R. A., and Cooke, P. S. (1996). Increased proliferation of Leydig cells induced by neonatal hypothyroidism in the rat. *J. Androl.* **17,** 231–237.

Hardy, M. P., Sottas, C. M., Ge, R. S., McKittrick, C. R., Tamashiro, K. L., McEwen, B. S., Haider, S. G., Markham, C. M., and Blanchard, R. J. (2002). Trends of reproductive hormones in male rats during psychosocial stress: Role of glucocorticoid metabolism in behavioral dominance. *Biol. Reprod.* **67,** 1750–1755.

Hauet, T., Liu, J., Li, H., Gazouli, M., Culty, M., and Papadopoulos, V. (2002). PBR, StAR, and PKA: Partners in cholesterol transport in steroidogenic cells. *Endocr. Res.* **28,** 395–401.

Henriksen, K., Hakovirta, H., and Parvinen, M. (1995). Testosterone inhibits and induces apoptosis in rat seminiferous tubules in a stage specific manner: In situ quantification in squash preparations after administration of ethane dimethanesulphonate. *Endocrinology* **136,** 3285–3291.

Holstein, A. F., Wartenberg, H., and Vossmeyer, J. (1971). Zur Cytologie der pränatalen Gonadenentwicklung beim Menschen. II. Die Entwicklung der Leydigzellen im Hoden von Embryonen und Feten. *Z. Anat. Entwicklungsgeschichte* **135,** 43–66.

Holstein, A. F., Roosen-Runge, E. C., and Schirren, C. (1988). "Illustrated Pathology of Human Spermatogenesis." Grosse Verlag, Berlin.

Huhtaniemi, I., and Bartke, A. (2001). Perspective: Male reproduction. *Endocrinology* **142,** 2178–2183.

Huhtaniemi, I., and Pelliniemi, L. (1992). Fetal Leydig cells: Cellular origin, morphology, life span, and special functional features. *Proc. Soc. Exp. Biol. Med.* **201,** 125–140.

Huhtaniemi, I. T., Warren, D. W., and Catt, K. J. (1984). Functional maturation of rat testis Leydig cells. *Ann. N. Y. Acad. Sci.* **438,** 283–303.

Hume, D. A., Halpin, D., Charlton, H., and Gordon, S. (1984). The mononuclear phagocyte system of the mouse defined by immunohistochemical localization of antigen F4/80: Macrophage of endocrine organs. *Proc. Natl. Acad. Sci. USA* **81,** 4174–4177.

Ichihara, I., Kawamura, H., and Pelliniemi, L. J. (1993). Ultrastructure and morphometry of testicular Leydig cells and the interstitial components correlated with testosterone in aging rats. *Cell Tissue Res.* **271,** 241–255.

Ivell, R., and Bathgate, A. D. (2002). Reproductive biology of the relaxin-like factor (RLF/INSL3). *Biol. Reprod.* **67,** 699–705.

Ivell, R., Balvers, M., Anand, R. J. K., Paust, H. J., McKinnel, C., and Sharpe, R. (2003). Differentiation-dependent expression of 17β-hydroxysteroid dehydrogenase, type 10, in the rodent testis: Effect of aging in Leydig cells. *Endocrinology* **144,** 3130–3137.

Jarred, R. A., Cancilla, B., Richards, M., Groome, N. P., McNatty, K. P., and Risbridger, G. P. (1999). Differential localization of inhibin subunit proteins in the ovine testis during fetal gonadal development. *Endocrinology* **140,** 979–986.

Johnson, L., and Neaves, W. B. (1981). Age related changes in Leydig cell populations, seminiferous tubule and sperm production in stallions. *Biol. Reprod.* **24,** 703–712.

Jonsson, C. K., Zetterström, R. H., Holst, M., Parvinen, M., and Söder, O. (1999). Constitutive expression of interleukin-1-α messenger ribonucleic acid in rat Sertoli cells is dependent upon interaction with germ cells. *Endocrinology* **140,** 3755–3761.

Jonsson, C., Setchell, B., Martinelle, N., Svechnikov, K., and Söder, O. (2001). Endotoxin-induced interleukin-1 expression in testicular macrophages is accompained by down-regulation of the constitutive expression in Sertoli cells. *Cytokine* **14,** 283–288.

Josso, N., Cate, R. L., Picard, J. Y., Vigier, B., di Clemente, N., Wilson, C., Imbeaud, S., Pepinsky, R. B., Guerrier, D., Boussin, L., Legeai, L., and Carre-Eusebe, D. (1993). Anti-Müllerian hormone: The Jost factor. *Recent Prog. Horm. Res.* **48,** 1–59.

Kaler, L. W., and Neaves, W. B. (1981). The steroidogenic capacity of the aging rat testis. *J. Gerontol.* **36,** 398–404.

Kelce, W. R., Zirkin, B. R., and Ewing, L. L. (1991). Immature rat Leydig cells are intrinsically less sensitive than adult Leydig cells to ethane dimethanesulfonate. *Toxicol. Appl. Pharmacol.* **111,** 189–200.

Kerr, J. B., and Knell, C. M. (1988). The fate of fetal Leydig cells during the development of the fetal and postnatal rat testis. *Development* **103,** 535–544.

Khan, S. A., Khan, S. J., and Dorrington, J. H. (1992a). Interleukin-1 stimulates deoxyribonucleic acid synthesis in immature rat Leydig cells in vitro. *Endocrinology* **131,** 1853–1857.

Khan, S. A., Teerds, K., and Dorrington, J. H. (1992b). Growth factor requirements for DNA synthesis by Leydig cells from the immature rat. *Biol. Reprod.* **46,** 335–341.

Kim, I. S., Ariyaratne, H. B. S., and Mendis-Handagama, S. M. L. (2002). Changes in the testis interstitium of Brown Norway rats with aging and effects of luteinizing and thyroid hormones on the aged testes in enhancing the steroidogenic potential. *Biol. Reprod.* **66,** 1359–1366.

Kmicikiewicz, I., Wojtusiak, A., and Bilinska, B. (1999). The effect of testicular macrophages, macrophage-conditioned medium and interkleukin-1-α on bank vole Leydig cell steroidogenesis. *Exp. Clin. Endocrinol. Diabetes* **107,** 262–271.

Koike, S., and Noumura, T. (1995). Immunohistochemical localization of insulin-like growth factor II in the perinatal rat gonad. *Growth Regul.* **5,** 185–189.

Kotula, M., Koziel, E., Sadowska, M., Gancarczyk, M., and Bilinska, B. (2001). Immunofluorescent localization of the StAR protein in mitochondria of mouse Leydig cells in vitro. *Folia Histochem. Cytobiol.* **39,** 169–170.

Krueger, K. E., and Papadopoulos, V. (1990). Peripheral-type benzodiazepine receptors mediate translocation of cholesterol from the outer to inner mitochondrial membranes in adrenocortical cells. *J. Biol. Chem.* **265,** 15015–15022.

Kuopio, T., Paranko, J., and Pelliniemi, L. J. (1989a). Basement membrane and epithelial features of fetal-type Leydig cells in rat and human testis. *Differentiation* **40,** 198–206.

Kuopio, T., Tapanainen, J., Pelliniemi, L. J., and Huhtaniemi, I. (1989b). Developmental stages of fetal-type Leydig cells in prepubertal rats. *Development* **107,** 213–220.

Labrie, F., Simard, J., Luu-The, V., Be'langer, A., Pelletier, G., Moral, Y., Mebarki, R., Sanchez, F., Durocher, F., Turgeon, C., Labrie, Y., Rheaume, E., Labrie, C., and Lachance, Y. (1996). The 3β-hydroxysteroid dehydrogenase/isomerase gene family: Lessons from type II 3β-HSD congenital deficiency. *In* "Signal Transduction in Testicular Cells" (V. Hansson, F. O. Levy, and K. Taskén, Eds.), Schering Research Foundation Suppl. 2, pp. 185–218. Springer-Verlag, Heidelberg, Germany.

Leathem, J. H., and Albrecht, E. D. (1974). Effect of age on testis Δ^5-3β-hydroxysteroid dehydrogenase in the rat. *Proc. Soc. Exp. Biol. Med.* **145,** 1212–1214.

Leckie, C. M., Welberg, L. A., and Seckel, J. R. (1998). 11β-Hydroxysteroid dehydrogenase is a predominant reductase in intact rat Leydig cells. *J. Endocrinol.* **159,** 233–238.

Lee, S., Miselis, R., and Rivier, C. (2002). Anatomical and functional evidence for a neural–hypothalamic testicular pathway that is independent of the pituitary. *Endocrinology* **143,** 4447–4454.

Lejeune, H., Habert, R., and Saez, J. M. (1998). Origin, proliferation and differentiation of Leydig cells. *J. Mol. Endocrinol.* **20,** 1–25.

Leydig, F. (1850). Zur Anatomie der männlichen Geschlechtsorgane and Analdrüsen der Säugethiere. *Z. Wissenschaftliche Zool.* **2,** 1–57.

Lin, T., Murono, E., Osterman, J., Allen, D. O., and Nankin, H. R. (1980). The aging Leydig cell. I. Testosterone and adenosine 3′,5′-monophosphate response to gonadotropin stimulation in rats. *Steroids* **35,** 653–663.

Liu, G., Duranteau, L., Carel, J. C., Monroe, J., Doyle, D. A., and Shenker, A. (1999). Leydig cell tumors caused by an activating mutation of the gene encoding the luteinizing hormone receptor. *N. Engl. J. Med.* **341,** 1731–1736.

Livera, G., Rouiller-Fabre, V., Pairault, C., Levacher, C., and Habert, R. (2002). Regulation and perturbation of testicular functions by vitamin A. *Reproduction* **124,** 173–180.

Lording, D. W., and de Kretser, D. M. (1972). Comparative ultrastructural and histochemical studies of the interstitial cells of rat testis during fetal and postnatal development. *J. Reprod. Fertil.* **29,** 261–269.

Lukyanenko, Y., Chen, J. J., and Huston, J. C. (2003). Testosterone regulates 25-hydroxycholesterol production in testicular macrophages. *Biol. Reprod.* **67,** 1435–1438.

Majdic, G., and Saunders, P. T. K. (1996). Differential patterns of expression of DAX-1 and steroidogenic factor-1 (SF-1) in the fetal rat testis. *Endocrinology* **137,** 3586–3589.

Majdic, G., Millar, M. R., and Saunders, P. T. K. (1995). Immunolocalisation of androgen receptor to interstitial cells in fetal rat testes and to mesenchymal and epithelial cells of associated ducts. *J. Endocrinol.* **147,** 285–293.

Majdic, G., McNeilly, A. S., Sharpe, R. M., Evans, L. R., Groome, N. P., and Saunders, P. T. K. (1997). Testicular expression of inhibin and activin subunits and follistatin in the rat and human fetus and neonate and during postnatal development in the rat. *Endocrinology* **138,** 2136–2147.

Majdic, G., Saunders, P. T. K., and Teerds, K. J. (1998). Immunoexpression of the steroidogenic enzymes 3-β hydroxysteroid dehydrogenase and 17α-hydroxylase, $C_{17,20}$ lyase and the receptor for luteinizing hormone (LH) in the fetal rat testis suggests that the onset of Leydig cell steroid production is independent of LH action. *Biol. Reprod.* **58,** 520–525.

Maric, D., Kostic, T., and Kovacevic, R. (1996). Effects of acute and chronic immobilization stress on rat Leydig cell steroidogenesis. *J. Steroid Biochem. Mol. Biol.* **58,** 351–355.

Mayerhofer, A. (1996). Leydig cell regulation by catecholamines and neuroendocrine messengers. *In* "The Leydig cell" (A. H. Payne, M. P. Hardy, and L. D. Russell, Eds.), pp. 407–418. Cache River Press, Vienna, IL.

Mayerhofer, A., Bartke, A., Amador, A. G., and Began, T. (1989). Histamine affects testicular steroid production in the golden hamster. *Endocrinology* **125,** 560–562.

Mendis-Handagama, S. M. L. C. (1991). Mitosis in normal adult guinea pig Leydig cells. *J. Androl.* **12,** 240–243.

Mendis-Handagama, S. M. L. C., and Ariyaratne, H. B. S. (2001). Differentiation of the adult Leydig cell population in the postnatal testis. *Biol. Reprod.* **65,** 660–671.

Mendis-Handagama, S. M. L. C., and Sharma, O. P. (1994). Effects of neonatal administration of the reversible goitrogen propylthiouracil on the testis interstitium in adult rats. *J. Reprod. Fertil.* **100,** 85–92.

Mendis-Handagama, S. M. L. C., Watkins, P. A., Gelber, S. J., Scallen, T. J., Zirkin, B. R., and Ewing, L. L. (1990a). Luteinizing hormone causes rapid and transient changes in rat Leydig cell peroxisome volume and intraperoxisomal sterol carrier protein-2 content. *Endocrinology* **127,** 2947–2954.

Mendis-Handagama, S. M. L. C., Zirkin, B. R., Scallen, T. J., and Ewing, L. L. (1990b). Studies on peroxisomes of the adult rat Leydig cell. *J. Androl.* **11,** 270–278.

Mendis-Handagama, S. M. L. C., Watkins, P. A., Gelber, S. J., and Scallen, T. J. (1992). Leydig cell peroxisomes and sterol carrier protein-2 in luteinizing hormone-deprived rats. *Endocrinology* **131,** 2839–2845.

Mendis-Handagama, S. M. L. C., Ariyaratne, H. B. S., Teunissen van Manen, K. R., and Haupt, R. L. (1998). Differentiation of adult Leydig cells in the neonatal rat testis is arrested by hypothyroidism. *Biol. Reprod.* **59,** 351–357.

Merchant-Larios, H., and Moreno-Mendoza, N. (1998). Mesonephric stromal cells differentiate into Leydig cells in the mouse fetal testis. *Exp. Cell. Res.* **244,** 230–238.

Merchant-Larios, H., Moreno-Mendoza, N., and Buehr, M. (1993). The role of mesonephros in cell differentiation and morphogenesis of the mouse fetal testis. *Int. J. Dev. Biol.* **37,** 407–415.

Migrenne, S., Pairault, C., Racine, C., Livera, G., Geloso, A., and Habert, R. (2001). Luteinizing hormone dependent activity and luteinizing hormone-independent differentiation of rat fetal Leydig cells. *Mol. Cell. Endocrinol.* **172,** 193–202.

Miller, S. C., Bowman, B. M., and Rowland, H. G. (1983). Structure, cytochemistry, endocytic activity, and immunoglobulin (Fc) receptors of rat testicular interstitial tissue macrophages. *Am. J. Anat.* **168,** 1–13.

Misrahi, M., Beau, I., Ghinea, N., Vannier, B., Loosfelt, H., Meduri, G., Vu Hai, M. T., and Milgrom, E. (1996). The LH/CG and FSH receptors: Different molecular forms and intracellular traffic. *Mol. Cell. Endocrinol.* **125,** 161–167.

Molenaar, R., de Rooije, D. G., Rommerts, F. F. G., Reuvers, P. J., and van der Molen, H. J. (1985). Specific destruction of Leydig cells in mature rats after in vivo administration of ethane dimethyl sulfonate. *Biol. Reprod.* **33,** 1213–1222.

Molenaar, R., de Rooije, D. G., Rommerts, F. F. G., and van der Molen, H. J. (1986). Repopulation of Leydig cells in mature rats after selective destruction of the existent Leydig cells with ethylene dimethane sulfonate is dependent on luteinizing hormone and not follicle-stimulating hormone. *Endocrinology* **118,** 2546–2554.

Monder, C., Hardy, M. P., Blanchard, R. J., and Blanchard, D. C. (1994a). Reciprocal changes in plasma corticosterone and testosterone in stressed male rats maintained in a visible burrow system: Evidence for a mediating role of testicular 11β-hydroxysteroid dehydrogenase. *Endocrinology* **134,** 1193–1198.

Monder, C., Miroff, Y., Marandici, A., and Hardy, M. P. (1994b). 11β-Hydroxysteroid dehydrogenase alleviates glucocorticoid-mediated inhibition of steroidogenesis in rat Leydig cells. *Endocrinology* **134,** 1199–1204.

Moore, A., and Morris, F. D. (1993). The involvement of insulin-like growth factor-I in local control of steroidogenesis and DNA synthesis of Leydig and non-Leydig cells in the rat testicular interstitium. *J. Endocrinol.* **138,** 107–114.

Mori, H., Hiromoto, N., Nakahara, M., Shiraishi, T., and Matsumoto, K. (1982). Stereological analysis of Leydig cell ultrastructure in aged humans. *J. Clin. Endocrinol. Metab.* **55,** 634–641.

Morris, I. D. (1996). Leydig cell toxicology. *In* "The Leydig Cell" (A. H. Payne, M. P. Hardy, and L. D. Russell, Eds.), pp. 573–596. Cache River Press, Vienna, IL.

Morris, A. J., Taylor, M. F., and Morris, I. D. (1997). Leydig cell apoptosis in response to ethylene demethanesulphonate both in vivo and in vitro. *J. Androl.* **18,** 274–280.

Nandi, S., Banerjee, P. P., and Zirkin, B. R. (1999). Germ cell apoptosis in the testes of Sprague Dawley rats following testosterone withdrawal by ethane 1,2-dimethanesulfonate administration: Relationship to Fas? *Biol. Reprod.* **61,** 70–75.

Nef, S., and Parada, L. F. (1999). Cryptorchidism in mice mutant for INSL3. *Nat. Genet.* **22,** 295–299.

Neumann, A., Haider, S. G., and Hilscher, B. (1993). Temporal coincidence of the appearance of elongated spermatids and of histochemical reaction of 11β-hydroxysteroid dehydrogenase in rat Leydig cells. *Andrologia* **25,** 263–269.

Nicholson, H. D., and Pickering, B. T. (1993). Oxytocin, a male intragonadal hormone. *Regul. Peptides* **45,** 253–256.

Nie, R., Zhou, Q., Jassim, E., Saunders, P. T. K., and Hess, R. A. (2002). Differential expression of estrogen receptor α and β in the reproductive tract of adult male dogs and cats. *Biol. Reprod.* **66,** 1161–1168.

Niemi, M., Sharpe, R. M., and Brown, W. R. A. (1986). Macrophages in the interstitial tissue of the rat testis. *Cell Tissue Res.* **243,** 337–344.

Nieschlag, E., Lammers, U., Freischem, C. W., Langer, K., and Wickings, E. J. (1982). Reproductive functions in young fathers and grandfathers. *J. Clin. Endocrinol. Metabol.* **55,** 676–681.

Nishino, K., Yamanouchi, K., Naito, K., and Tojo, H. (2001). Characterization of mesonephric cells that migrate into the XY gonad during testis differentiation. *Exp. Cell Res.* **267,** 225–232.

Normand, T., Husen, B., Leenders, F., Pelczar, H., Baert, J., Begue, A., Flourens, A., Adamski, J., and de Launoit, Y. (1995). Molecular characterization of mouse 17β-hydroxysteroid dehydrogenase. *J. Steroid Biochem. Mol. Biol.* **55,** 541–548.

Olaso, R., Gautier, C., Levacher, C., Durand, P., Saez, J., and Habert, R. (1997). The immunohistochemical localization of transforming growth factor-β2 in the fetal and neonatal rat testis. *Mol. Cell. Endocrinol.* **126,** 165–172.

Olaso, R., Pairault, C., and Habert, R. (1998). Expression of type I and II receptors for transforming growth factor β in the adult rat testis. *Histochem. Cell. Biol.* **110,** 613–618.

Olaso, R., Pairault, C., Saez, J., and Habert, R. (1999). Transforming growth factor β3 in the fetal and neonatal rat testis: Immunolocalization and effect on fetal Leydig cell function. *Histochem. Cell. Biol.* **112,** 247–254.

Orr, T. E., Taylor, M. F., Bhattacharyya, A. K., Collins, D. C., and Mann, D. R. (1994). Immobilization stress disrupts testicular steroidogenesis in adult male rats by inhibiting the activities of 17α-hydroxylase and 17,20-lyase without affecting the binding LH/hCG receptors. *J. Androl.* **15,** 302–308.

O'Shaughnessy, P. J., Baker, P., Sohnius, U., Haavisto, A.-M., Charlton, H. M., and Huhtaniemi, I. (1998). Fetal development of Leydig cell activity in the mouse is independent of pituitary gonadotroph function. *Endocrinology* **139,** 1141–1146.

O'Shaughnessy, P. J., Willerton, L., and Baker, P. J. (2002a). Changes in Leydig cell gene expression during development in the mouse. *Biol. Reprod.* **66,** 966–975.

O'Shaughnessy, P. J., Johnsten, H., Willerton, L., and Baker, P. J. (2002b). Failure of normal adult Leydig cell development in androgen-receptor-deficient mice. *J. Cell Sci.* **115,** 3491–3496.

Palaga, T., and Osborne, B. (2002). The 3D's of apoptosis: Death, degradation and DIAPs. *Nat. Cell Biol.* **4,** E149–E151.

Paniagua, R., Amat, P., Nistal, M., and Martin, A. (1986). Ultrastructure of Leydig cells in human aging testes. *J. Anat.* **146,** 173–183.

Paniagua, R., Nistal, M., Sáez, F. J., and Fraile, B. (1991). Ultrastructure of the aging human testis. *J. Electron Microsc. Tech.* **19,** 241–260.

Papadopoulos, V. (1996). Peripheral-type benzodiazepine/diazepam binding inhibitor receptor: Biological role in steroidogenic cell function. *Endocr. Rev.* **14,** 222–240.

Papadopoulos, V. (2003). Peripheral benzodiazepine receptor: Structure and function in health and disease. *Ann. Pharm. Fr.* **61,** 30–50.

Paust, H. J., Wessels, J., Ivell, R., and Mukhopadhyay, A. K. (2002). The expression of RLF/INSL3 gene is reduced in Leydig cells of the aging rat testis. *Exp. Gerontol.* **37,** 1461–1467.

Payne, A. H., and Youngblood, G. L. (1995). Regulation of expression of steroidogenic enzymes in Leydig cells. *Biol. Reprod.* **52,** 217–225.

Payne, A. H., Hardy, M. P., and Russell, L. D. (1996). "The Leydig Cell." Cache River Press, Vienna, IL.

Pelliniemi, L. J., and Niemi, M. (1969). Fine structure of human foetal testis. *Cell Tissue Res.* **99,** 507–522.

Phillips, D. M., Lakshmi, V., and Monder, C. (1989). Corticosteroid 11β-dehydrogenase in rat testis. *Endocrinology* **125,** 209–216.

Pöllänen, P., Söder, O., and Parvinen, M. (1989). Interleukin-1α stimulation of spermatogonial proliferation in vivo. *Reprod. Fertil. Dev.* **1,** 85–87.

Prince, F. P. (1984). Ultrastructure of immature Leydig cells in human prepubertal testis. *Anat. Rec.* **209,** 165–176.

Prince, F. P. (1985). An ultrastructural and immunoperoxidase study of the neonatal human testis: Evidence of mature, testosterone producing Leydig cells and Leydig cell regression. *Anat. Rec.* **211,** 156A.

Prince, F. P. (1990). Ultrastructural evidence of mature Leydig cells and Leydig cell regression in the neonatal human testis. *Anat. Rec.* **228,** 405–417.

Prince, F. P. (2001). The triphasic nature of Leydig cell development in humans, and comments on nomenclature. *J. Endocrinol.* **168,** 213–216.

Prince, F. P. (2002). Lamellar and tubular associations of the mitochondrial cristae: Unique forms of the cristae present in steroid-producing cells. *Mitochondrion* **1,** 381–389.

Prince, F. P., Mann, D. R., and Fraser, H. M. (1998). Blockade of the hypothalamic–pituitary testicular axis with a GnRH antagonist in the neonatal marmoset monkey: Changes in Leydig cell ultrastructure. *Tissue Cell* **30,** 651–661.

Racine, C., Forest, M. G., Louis, F., Ferre, A., Huhtaniemi, I., Josso, N., and di Clement, N. (1998). Receptors for anti-mullerian hormone on Leydig cells are responsible for its effects on steroidogenesis and cell differentiation. *Proc. Natl. Acad. Sci. USA* **95,** 594–599.

Reyes, F. I., Boroditsky, R. S., Winter, J. S. D., and Faiman, C. (1974). Studies on human sexual development. II. Fetal and maternal serum gonadotropin and sex steroid concentrations. *J. Clin. Endocrinol. Metabol.* **38,** 612–617.

Risbridger, G. P., and Davies, A. (1994). Isolation of rat Leydig cells and precursor forms after administration of ethane dimethane sulfonate. *Am. J. Physiol.* **266,** E975–E979.

Rouiller-Fabre, V., Carmona, S., Abou Merhi, R., Cate, R., and Habert, R. (1998a). Effect of anti-mullerian hormone on Sertoli and Leydig cell functions in fetal and immature rats. *Endocrinology* **139,** 1213–1220.

Rouiller-Fabre, V., Lecref, L., Gautier, C., Saez, J. M., and Habert, R. (1998b). Expression and effect of insulin-like growth factor I on rat fetal Leydig cell function and differentiation. *Endocrinology* **139,** 2926–2934.

Russell, L. D., de France, L. R., Hess, R., and Cook, P. (1995). Characteristics of mitotic cells in developing and adult rat testes with observations on cell lineage. *Tissue Cell* **27,** 105–128.

Saez, J. M. (1994). Leydig cells: Endocrine, paracrine, and autocrine regulation. *Endocr. Rev.* **15,** 574–626.

Schäfers, B. A., Schlutius, B. G., and Haider, S. G. (2001). Ontogenesis of oxidative reaction of 17β-hydroxysteroid dehydrogenase and 11β-hydroxysteroid dehydrogenase in rat Leydig cells: A histochemical study. *Histochem. J.* **33,** 585–595.

Schulze, C. (1984). "Sertoli Cells and Leydig Cells in Man." Springer-Verlag, Heidelberg, Germany.

Schulze, W., Davidoff, M. S., and Holstein, A. F. (1987). Are Leydig cells of neural origin? Substance P-like immunoreactivity in human testicular tissue *Acta Endocrinol.* **115,** 373–377.

Seckl, J. R., and Walker, B. R. (2001). 11β-Hydroxysteroid dehydrogenase type I: A tissue-specific amplifier of glucocorticoid action. *Endocrinology* **142,** 1371–1376.

Setchell, B. P., Pakarinen, P., and Huhtaniemi, I. (2003). How much LH do the Leydig cells see? *J. Endocrinol.* **175,** 375–382.

Shan, L. X., and Hardy, M. P. (1992). Developmental changes in levels of luteinizing hormone receptor and androgen receptor in rat Leydig cells. *Endocrinology* **131,** 1107–1114.

Shan, L. X., Zhu, L. J., Bardin, W., and Hardy, M. P. (1995). Quantitative analysis of androgen receptor messenger ribonucleic acid in developing Leydig cells and Sertoli cells by in situ hybridization. *Endocrinology* **136,** 3856–3862.

Shan, L. X., Bardin, W., and Hardy, M. P. (1997). Immunohistochemical analysis of androgen effects on androgen receptor expression in developing Leydig and Sertoli cells. *Endocrinology* **138,** 1259–1266.

Sharpe, R. M. (1990). Intratesticular control of steroidogenesis. *Clin. Endocrinol.* **33,** 787–807.

Sharpe, R. M. (2001). Hormones and testis development and the possible adverse effects of environmental chemicals. *Toxicol. Lett.* **120,** 221–232.

Sharpe, R. M. (2003). The oestrogen hypothesis: Where do we stand now? *Int. J. Androl.* **26,** 2–15.

Skinner, M. K. (1991). Cell–cell interactions in the testis. *Endocr. Rev.* **12,** 45–77.

Spiteri-Grech, J., and Nieschlag, E. (1993). Paracrine factors relevant to the regulation of spermatogenesis: A review. *J. Reprod. Fertil.* **98,** 1–14.

Sriraman, V., Sairam, M. R., and Rao, A. J. (2003). Evaluation of relative roles of LH and FSH in regulation of differentiation of Leydig cells using an ethane 1,2-dimethylsulfonate-treated adult rat model. *J. Endocrinol.* **176,** 151–161.

Steiner, R. A., Bremner, W. J., Clifton, D. K., and Dorsa, D. M. (1984). Reduced pulsatile luteinizing hormone and testosterone secretion with aging in the male rat. *Biol. Reprod.* **31,** 251–258.

Stocco, D. M. (1996). Acute regulation of Leydig cell steroidogenesis. *In* "The Leydig Cell" (A. H. Payne, M. P. Hardy, and L. D. Russell, Eds.), pp. 241–258. Cache River Press, Vienna, IL.

Stocco, D. M. (1999). An update on the mechanism of action of the steroidogenic acute regulatory (StAR) protein. *Exp. Clin. Endocrinol. Diabetes* **107,** 229–235.

Sultana, T., Svechnikov, K., Weber, G., and Söder, O. (2000). Molecular cloning and expression of a functionally different alternative splice variant of prointerleukin-1α from the rat testis. *Endrocrinology* **141,** 4413–4418.

Svechnikov, K. V., Sultana, T., and Söder, O. (2001). Age-dependent stimulation of Leydig cell steroidogenesis by interleukin-1 isoforms. *Mol. Cell. Endocrinol.* **182,** 193–201.

Syed, V., Söder, O., Arver, S., Lidh, M., Khan, S., and Ritzen, E. M. (1988). Ontogeny and cellular origin of an interkeukin-1-like factor in the reproductive tract of the male rat. *Int. J. Androl.* **11,** 437–447.

Tähkä, K. M. (1986). Current aspects of Leydig cell function and its regulation. *J. Reprod. Fertil.* **78,** 367–380.

Takahashi, J., Higashi, Y., Lanasa, J. A., Yoshida, K. I., Winters, S. J., Oshima, H., and Troen, P. (1983). Studies of the human testis. XVIII. Simultaneous measurement of nine intrastesticular steroids: Evidence for reduced mitochondrial function in testis of elderly men. *J. Clin. Endocrinol. Metab.* **56,** 1178–1187.

Tapanainen, J. S., Tilly, J. L., Vihko, K. K., and Hsueh, A. J. W. (1993). Hormonal control of apoptotic cell death in the testis: gonadotrophins and androgens as testicular cell survival factors. *Mol. Endocrinol.* **7,** 643–650.

Taylor, M. F., Woolveridge, I., Metcalfe, A. D., Streuli, C. H., Hickman, J. H., and Morris, I. D. (1998). Leydig cell apoptosis in the rat testes after administration of the cytotoxine ethane dimethane sulphonate: Role of the Bcl-2 family members. *J. Endocrinol.* **157,** 317–326.

Taylor, M. F., de Boer-Brouwer, M., Woolveridge, I., Teerds, K. J., and Morris, I. D. (1999). Leydig cell apoptosis following the administration of ethane dimethane sulphonate to the adult male rat is a Fas-mediated process. *Endocrinology* **140,** 3797–3804.

Teerds, K. J., de Rooije, D. G., Rommerts, F. F. G., and Wensing, C. J. G. (1989). Proliferation and differentiation of possible Leydig cell precursors after destruction of the existing Leydig cells with ethane dimethyl sulphonate (EDS): The role of LH/human chorionic gonadotrophin. *J. Endocrinol.* **122,** 689–696.

Teerds, K. J., de Boer-Brouwer, M., Dorrington, J. H., Balvers, M., and Ivell, R. (1999). Identification of markers for precursor and Leydig cell differentiation in the adult rat testis following ethane dimethyl sulphonate administration. *Biol. Reprod.* **60,** 1437–1445.

Themmen, A. P. N., and Huhtaniemi, I. T. (2000). Mutations of gonadotropins and gonadotropin receptors: Elucidating the physiology and pathophysiology of pituitary–gonadal function. *Endocr. Rev.* **21,** 551–583.

Vermeulen, A. (1991). Clinical review 24: Androgens in the aging male. *J. Clin. Endocrinol. Metab.* **73,** 221–224.

Waddell, B. J., Hisheh, S., Krozowski, Z. S., and Burton, P. J. (2003). Localization of 11β-hydroxysteroid dehydrogenase types 1 and 2 in the male reproductive tract. *Endocrinology* **144,** 3101–3106.

Walch, L., and Morris, P. L. (2002). Cyclooxygenase 2 pathway mediates IL-1β regulation of IL-α, -1β, and IL-6 mRNA levels in Leydig cell progenitors. *Endocrinology* **143,** 3276–3283.

West, L. A., Horvat, R. D., Roess, D. A., Barisas, B. G., Juengel, J. L., and Niswender, G. D. (2001). Steroidogenic acute regulatory protein and peripheral-type benzodiazepine receptor associate at the mitochondrial membrane. *Endocrinology* **142,** 502–505.

Winter, J. S. D., Hughes, I. A., Reyes, F. I., and Faiman, C. (1976). Pituitary gonadal relations in infancy. 2. Patterns of serum gonadal steroid concentrations in man from birth to two years of age. *J. Clin. Endocrinol. Metabol.* **42,** 679–686.

Woolveridge, I., Taylor, M. F., Griffin, J., Ashcroft, H. P., Rommerts, F. F. G., and Morris, I. D. (2001). Apoptosis and related gene products in rat Leydig cell tumors and following regression induced by the cytotoxin ethane dimethanesulphonate. *Int. J. Androl.* **24,** 56–64.

Yang, K., and Yu, M. (1994). Evidence for distinct isoforms of 11β-hydroxysteroid dehydrogenase in the ovine liver and kidney. *J. Steroid Biochem. Mol. Biol.* **49,** 245–250.

Yao, H. H., Whoriskey, W., and Capel, B. (2002). Desert hedgehog/Patched 1 signaling specifies fetal Leydig cell fate in testis organogenesis. *Genes Dev.* **16,** 1433–1440.

Yokoi, H., Yamama, Y., Tsuruo, Y., Kawarada, Y., Miura, N., Sugiyama, T., and Ishimura, K. (1998). Leydig cells undergoing apoptosis in the perinatal rat testis. *Acta Histochem. Cytochem.* **31,** 355–361.

Zhou, Q., Nie, R., Prins, G. S., Saunders, P. T. K., Katzenellenbogen, B. S., and Hess, R. A. (2002). Localization of androgen and estrogen receptors in adult male mouse reproductive tract. *J. Androl.* **23,** 870–881.

Zhu, B. C., Cavicchia, J. C., and Chiocchio, S. R. (1998). Testicular denervation-induced nuclear changes in Leydig cell of hemicastrated adult rats. *Tissue Cell* **30,** 485–491.

Zhu, L. J., Hardy, M. P., Inigo, I. V., Huhtaniemi, I., Bardin, C. W., and Moo-Young, A. J. (2000). Effects of androgen on androgen receptor expression in rat testicular and epididymal cells: A quantitative immunohistochemical study. *Biol. Reprod.* **63,** 368–376.

Ziegler, H. G., Haider, S. G., Passia, D., and Hilscher, W. (1983). Enzyme histochemical and morphometrical studies on Δ^5-3β-hydroxysteroid dehydrogenase during the fetal and neonatal development of rat Leydig cells. *Andrologia* **15,** 392–397.

This Page Intentionally Left Blank

The Exocyst Complex in Polarized Exocytosis

Shu-Chan Hsu,* Daniel TerBush,† Mathew Abraham,‡ and Wei Guo‡
*Department of Cell Biology and Neuroscience, Rutgers University, Piscataway, New Jersey 08854
†Department of Biochemistry and Molecular Biology, Uniformed Services, University of the Health Sciences, Bethesda, Maryland 20814
‡Department of Biology, University of Pennsylvania, Philadelphia, Pennsylvania 19104

Note: Wei Guo is the corresponding author.

Exocytosis is an essential membrane traffic event mediating the secretion of intracellular protein contents such as hormones and neurotransmitters as well as the incorporation of membrane proteins and lipids to specific domains of the plasma membrane. As a fundamental cell biological process, exocytosis is crucial for cell growth, cell–cell communication, and cell polarity establishment. For most eukaryotic cells exocytosis is polarized. A multiprotein complex, named the exocyst, is required for polarized exocytosis from yeast to mammals. The exocyst consists of eight components: Sec3, Sec5, Sec6, Sec8, Sec10, Sec15, Exo70, and Exo84. They are localized to sites of active exocytosis, where they mediate the targeting and tethering of post-Golgi secretory vesicles for subsequent membrane fusion. Here we review the progress made in the understanding of the exocyst and its role in polarized exocytosis.

KEY WORDS: Membrane traffic, Exocytosis, Exocyst, Vesicle targeting, Vesicle tethering, Rab, Rho, Ral, Cell polarity.

I. Introduction

Polarized exocytosis is essential for a wide range of biological processes from neuronal growth cone formation to epithelial asymmetry establishment. Polarized exocytosis consists of at least three stages. First, Golgi-derived secretory

0074-7696/04 $35.00

vesicles are targeted to the vicinity of designated plasma membrane domains via microtubule- and/or actin-based transport systems. Second, after the vesicles arrive at their destinations, they are tethered to specific plasma membrane domains (Guo *et al.*, 2000; Pfeffer, 1999). Finally, interactions between vesicle and plasma membrane integral membrane proteins, termed v-SNAREs and t-SNAREs, respectively (SNARE, soluble *N*-ethylmaleimide-sensitive fusion attachment protein receptors), lead to the fusion of the secretory vesicle with the plasma membrane. This fusion event allows the secretion of vesicle contents and the incorporation of membrane proteins at specific plasma membrane domains. Studies suggest that the membrane addition at the specific sites on the plasma membrane is mediated by the exocyst, an evolutionarily conserved multiprotein complex. Here, we review our current understanding of the exocyst complex and its role in polarized exocytosis.

II. Discovery of the Exocyst Complex

The origins of the exocyst can be traced to a single genetic screen performed in *Saccharomyces cerevisiae* in the late 1970s (Novick and Schekman, 1979; Novick *et al.*, 1980). The screen identified 23 complementation groups of temperature-sensitive yeast mutants defective in secretion. These 23 genes could be divided into two basic groups. The first group consisted of 13 genes encoding proteins important for endoplasmic reticulum (ER)-to-Golgi and/or intra-Golgi membrane trafficking. The second group included 10 genes encoding proteins that function at a late stage in the exocytic pathway: after protein packaging into exocytic vesicles in Golgi but before vesicle fusion with the plasma membrane (Novick *et al.*, 1980, 1981). These 10 genes are known as the "late-acting" secretory genes and are named *SEC1*, *SEC2*, *SEC3*, *SEC4*, *SEC5*, *SEC6*, *SEC8*, *SEC9*, *SEC10*, and *SEC15*. Yeast cells containing late-acting *sec* mutations share a common phenotype when examined by thin-section electron microscopy: they accumulate 80- to 100-nm post-Golgi vesicles at the nonpermissive temperature (Novick *et al.*, 1980, 1981).

Almost all the late-acting *SEC* genes discovered in yeast now have homologs in higher organisms. Sec1 is homologous to fruitfly *Drosophilia melanogaster Rop* (Salzberg *et al.*, 1993), to nematode *Caenorhabditis elegans UNC18* (Gengyo-Ando *et al.* 1993), and to mammalian neuronal Sec1 or Muc18 (Garcia *et al.* 1994; Pevsner *et al.*, 1994). The Sec1 family proteins have been found to play a role in regulating SNARE protein interactions during membrane fusion (Jahn, 2002). Sec4 is the founding member of the Rab family of low molecular weight GTPases that function in many membrane-trafficking pathways (Salminen and Novick, 1987) and Sec2 is the guanine nucleotide exchange factor for Sec4 (Walch-Solimena *et al.*,

1997). Sec9 is the yeast homolog of SNAP-25, a neuronal t-SNARE (Brennwald *et al.*, 1994). The remaining six late-acting *SEC* genes all function as part of the exocyst complex as described below.

The earliest data indicating that a late-acting *SEC* gene product may be present in a high molecular weight complex came from the analysis of the Sec15 protein in yeast. Sec15 was shown to associate with a 19.5S particle, of which 25% was associated with the plasma membrane while the remainder was cytoplasmic (Bowser and Novick, 1991). Interestingly, overexpression of Sec15 resulted in a block in the secretory pathway and caused clustering of exocytic vesicles. These vesicles, however, failed to cluster in the *sec4-8* and *sec2-41* mutant background (Salminen and Novick, 1989). These functional data are the first evidence showing a link between a component of the exocyst complex and Sec4, a Rab GTPase essential for post-Golgi secretion. In rapid succession, Sec8 and Sec6 proteins were shown to coisolate with Sec15 in a high molecular weight complex consisting of at least eight polypeptides (Bowser *et al.*, 1992; TerBush and Novick, 1995). This complex was shown to be localized to sites of polarized exocytosis in yeast, indicating a possible role in vesicle targeting (TerBush and Novick, 1995). Importantly, the stability of this complex of eight subunits was found to be markedly disrupted in yeast strains containing *sec3-2*, *sec5-24*, *sec6-4*, *sec10-2*, and *sec15-1* alleles (TerBush and Novick, 1995). This brings up the possibility that the protein products of the *SEC3*, *SEC5*, and *SEC10* genes, the remaining members of the late-acting *SEC* genes, could be associated with Sec6, Sec8, and Sec15 in one multiprotein complex.

Yeast was not the only organism in which genetics identified an exocyst component. In a promoter trap screen for mouse strains with embryonic lethal mutations, The SA *bgeo4* gene (Friedrich and Soriano, 1991) was isolated and later shown to be homologous to exocyst *SEC8* (Friedrich *et al.*, 1997). SA *bgeo4* is also known as *spock* because its *in vivo* expression in transgenic animals resulted in a bright staining pattern in the telencephalon resembling Mr. Spock's facial expression. Mice homozygous for *spock* displayed markedly less mesoderm formation and showed arrest of development on embryonic day 6.5 (Friedrich and Soriano, 1991; Friedrich *et al.*, 1997). Because it is known that secretion of growth factors is important for mesoderm formation, this result is consistent with *spock* playing a role in exocytosis. No direct data supporting this hypothesis, however, were available (Friedrich *et al.*, 1997). While genetic screens identified genes coding for individual exocyst subunits, subsequent biochemical purification and characterization of these gene products enabled the discovery of these gene products as components of the exocyst complex as well as of additional exocyst subunits missed by the genetic methods.

Novick's group, taking advantage of molecular biology and yeast genetics, generated a yeast strain containing a c-*myc* epitope-tagged *SEC8* gene as the

sole copy of *SEC8*. With this strain, proteins associated with the Sec8 protein were isolated by large-scale coimmunoprecipitation from detergent extracts of yeast lysates. The exocyst complex proteins were then separated by sodium dodecyl sulfate–polyacrylamide gel electrophoresis (SDS–PAGE) and individual complex-specific bands were excised and concentrated by funnel tube gel electrophoresis (TerBush *et al.*, 2001). These bands were then separated for a second time by SDS–PAGE and concentrated. The protein present in each gel slice was then subjected to proteolysis, and the resulting peptides were separated by high-performance liquid chromatography. These peptides were then identified by Edman degradation peptide sequencing or by matching their mass against a peptide database of yeast proteins (TerBush *et al.*, 1996). In the latter case, this was possible because the complete yeast genome was available to provide a complete data set against which to compare the exocyst peptide masses. This approach identified Sec3, Sec5, Sec10, and Exo70 as proteins that coisolated with the previously identified Sec6, Sec8, and Sec15. This seven-protein complex was named the exocyst as all of the known components of this complex are required for exocytosis in yeast (TerBush *et al.*, 1996).

The search for mammalian exocyst complex was prompted by the timely realization of the conservation of the secretory pathway from yeast to mammals. It was observed that many proteins involved in the late stage of the yeast secretory pathway, such as the SNARE proteins, the SNARE-associated proteins, and the small GTPase rab family members, have homologs in mammals that participate in general exocytosis during membrane addition and in regulated exocytosis underlying neurotransmission (Bennet and Scheller, 1993; Bennet *et al.*, 1993). Curiously, there were six secretory proteins (Sec3, Sec5, Sec6, Sec8, Sec10, and Sec15) required for the late stage of the yeast secretory pathway, which had no identified mammalian homologs (Novick and Schekman, 1980). In fact, yeast genetic studies showed that overexpression of Sso1, a yeast homolog of the mammalian t-SNARE protein syntaxin, can suppress mutations in two of these secretory proteins, Sec3 and Sec15 (Aalto *et al.*, 1993). This observation suggests that at least two of these secretory proteins may act upstream of syntaxin.

By screening human genome expressed sequence tag (EST) databases with these yeast *Sec* proteins, Scheller's group was able to identify human infant brain ESTs homologous to *SEC6* and *SEC8* (Ting, 1995). These ESTs were then used to clone *rSec6* and *rSec8* genes from rat brain cDNA libraries (Ting *et al.*, 1995). Mammalian Sec6 and Sec8 comigrated on a continuous glycerol gradient at 17 svedberg, indicating that they are components of a 600- to 700-kDa complex. Subsequently, antibodies generated against rSec6p and rSec8p were used to monitor the purification of the rat brain rSec6/8 (exocyst) complex from rat brain lysate, using sequential column chromatography (Hsu *et al.*, 1996). The purified mammalian exocyst complex contained

Sec6 and Sec8, as well as six other proteins. Peptide sequencing of the additional six exocyst subunits showed that they are mammalian homologs of the yeast secretory proteins Sec3, Sec5, Sec10, and Sec15, as well as of two additional yeast proteins Exo70 and Exo84 (Brymora *et al*., 2001; Hsu *et al*., 1996; Kee *et al*., 1997; Matern *et al*., 2001).

What about Exo84 in yeast? It turns out that in yeast Exo84 runs at almost exactly the same molecular weight as that of a prominent C-terminal breakdown product of Sec3 (91 kDa) in SDS–polyacrylamide gels. When the yeast exocyst complex was isolated, peptide sequence identified only the Sec3 fragment on the gel. Using a database search, Guo *et al*. was able to identify the yeast Exo84 on the basis of the rat Exo84 sequence. Genetic analysis indicates that the yeast Exo84, like the other exocyst proteins, is essential for exocytosis (Guo *et al*., 1999b; Zhang and Guo, unpublished data).

Although there is limited sequence homology between mammalian and yeast exocyst subunits (approximately 17 to 24% sequence identity) (Brymora *et al*., 2001; Hazuka *et al*., 1997; Guo *et al*., 1997; Kee *et al*., 1997; Matern *et al*., 2001; Ting *et al*., 1995), it is interesting to note that both complexes contain eight subunits of similar molecular weights ranging from 70 to 140 kDa (Hsu *et al*., 1996; TerBush *et al*., 1996).

The purified mammalian exocyst complex has been visualized by quick-freeze/deep etch electron microscopy (Hsu *et al*., 1999). In the absence of fixation with glutaraldehyde, the complex shows variable conformations, usually as a set of four or six arms radiating outward from a central point. The arms are about 4–6 nm in width and 10–30 nm in length. After a brief fixation with glutaraldehyde, the exocyst complex adopts a much more uniform conformation, resembling the letter "T" or "Y." It has an elongated body about 30 nm long and 13 nm wide, with two arms approximately 15 nm long and 6 nm wide splaying outward from one end of this central body. The arms appear to attach to the body through a flexible hinge region, allowing the arms to extend from the body at varying angles. For comparison, the diameter of a synaptic vesicle is about 50 nm, demonstrating that the exocyst complex is a large macromolecule.

III. Characteristics of the Exocyst Complex

A. Organization

To understand the function of the exocyst, it is important to understand the molecular organization of this complex. Guo *et al*. (1999a) have subcloned the cDNAs for individual yeast exocyst components into the pcDNA3 expression vector and translated these proteins *in vitro* in rabbit reticulocyte

lysates. Coimmunoprecipitation experiments were then carried out on all pairwise combinations of cosynthesized exocyst proteins in order to identify the interactions between these subunits. The individual components were tagged with specific epitope sequences such as hemagglutinin (HA) and FLAG. The tagged proteins were immunoprecipitated with monoclonal antibodies against the epitope sequences and the precipitates were analyzed for the presence of the nontagged subunit. The results of this experiment showed that Sec5 interacts with Exo70, Sec10 interacts with Sec 15 (Roth *et al.*, 1998), Sec5 interacts with Sec6, Sec5 interacts with Sec3, and Sec6 interacts with Sec8. Analysis using the yeast two-hybrid assay confirmed most of these results (Guo *et al.*, 1999a). These binding results are also supported by genetics. For example, Sec10 is needed to link Sec15 to the remainder of the complex. In agreement, Sec15 was absent from the partial complex isolated from a *sec10-2* mutant strain (TerBush and Novick, 1995). The binding of Sec10/Sec15 to the rest of the exocyst is mediated by the interaction of Sec10 with Sec5. Sec5 also makes critical links to Exo70, Sec6, and Sec3. Sec5 therefore appears to be at the core of the complex. As supporting evidence to this model, loss of Sec5 function leads to the failure of Sec10, Sec15, Exo70, and the mutant Sec5 protein to coprecipitate with Sec8 (TerBush and Novick, 1995; TerBush *et al.*, 1996). The coprecipitation of Sec3 was reduced, suggesting that Sec5 also plays an important role linking Sec3 to Sec8, most likely through the association of Sec5 with Sec6 and Sec6 with Sec8.

Using a pairwise two-hybrid assay, Matern *et al.* (2001) studied the pairwise subunit–subunit interactions of the mammalian exocyst complex. Positive two-hybrid interactions were found between Sec15 and Sec10, Sec8 and Sec10, Sec5 and Sec6, and Sec6 and Exo70. There is also interaction between Sec3 and Sec5 and between Sec3 and Sec8. In addition to these strong two-hybrid interactions, numerous weak interactions were also detected. The existence of these weaker interactions brings up the possibility that the stability of the intact complex may be achieved through a series of higher order interactions not detectable by the pairwise protein interaction studies using the two-hybrid assay. While additional binding assays are still needed to support these data and identify new interaction partners, studies carried out so far have revealed similar subunit–subunit interaction pattern in both yeast and mammalian exocyst.

B. Subcellular Localization

In yeast, components of the exocyst complex are concentrated in subdomains of the plasma membrane that represent sites of active vesicle fusion (Finger *et al.*, 1998; Mondesert *et al.*, 1997; TerBush and Novick, 1995). These sites of active vesicle fusion relocate with the cell cycle. As cells enter the cycle,

exocyst subunits were found concentrated in the emerging bud. With further cell growth, the exocyst proteins were concentrated at the tip of the bud. When the daughter cell has grown to a certain size and their growth pattern has switched from apical to isotropic, the exocyst proteins were redistributed throughout the daughter plasma membrane. During cytokinesis, exocyst components reconcentrated first as one ring, and then as two rings at the neck that separates the mother cell and the bud. One of the components of the exocyst complex, Sec3, localized to these sites independently of ongoing secretion and of mutations in other components of the exocyst. These observations led to the proposal that Sec3 represents a spatial landmark for exocytosis and that it may be the component of the exocyst complex that is most proximal to the target membrane (Finger *et al*., 1998). It is interesting to note that during isotopic growth, disruption of septin affected the localization of Sec3 and Sec5 (Barral *et al*., 2000). Septins constitute a family of conserved GTPases implicated in many cell biological processes including cell division and cell polarization (Field and Kellog, 1999; Kartmann and Roth, 2001; Longtine *et al*., 1996; Mitchison and Field, 2002). This observation suggests that septins may play a role in restricting exocyst localization.

The subcellular localization of the mammalian exocyst complex seems to be much more complicated. With the cell biological approach, exocyst complex localization has been investigated by antibody detection of endogenous exocyst subunits and by green fluorescent protein (GFP) tagging of exogenously introduced exocyst subunits. Anti-exocyst subunit antibodies have detected two major exocyst subcellular distribution patterns in cells with no extensions or processes emanating from the cell body. In MDCK epithelial and pancreatic acinar cells, the Sec6 and Sec8 subunits were found to have both perinuclear and plasma membrane enrichment (Shin *et al*., 2000; Yeaman *et al*., 2001). In particular, plasma membrane–localized exocyst staining was enriched at the tight junction (Grindstaff *et al*., 1998; Yeaman *et al*., 2001) or the lateral membrane (Kreitzer *et al*., 2003) in MDCK cells. Sec10 also exhibited a similar tight junction enrichment (Lipschutz *et al*., 2000). When MDCK cells were treated with the calcium chelator EGTA to disrupt cell–cell contact among these cells, plasma membrane–localized Sec8 was found to redistribute into the cytoplasm (Grindstaff *et al*., 1998). Thus the plasma membrane localization of at least one exocyst subunit is dependent on cell polarity and/or cell-to-cell contact.

In cells with processes or extensions emanating from the cell body, the exocyst complex subunits have been found at the perinuclear region, as well as throughout the processes with enrichment at the tip of the processes. In neuroendocrine PC12 cells Exo70 localization was dependent on the differentiation state of the cell (Vega and Hsu, 2001). In undifferentiated PC12 cells, Exo70 displayed perinuclear enrichment. On the addition of nerve growth factor to promote neurite outgrowth, Exo70 was found distributing from the

perinuclear region into the growing neurite and became enriched in the growth cone. This nerve growth factor-induced Exo70 redistribution was dependent on the activation of the mitogen-activated protein (MAP) kinase pathway. Antibodies against four other exocyst subunits, Sec6, Sec8, Sec15, and Exo84, showed similar localization (Wang and Hsu, 2003). In cultured hippocampal neurons, Sec6 and Sec8 were also found in the cell body, axons, and dendrites (Hazuka *et al.*, 1999). In cultured kidney glomerular visceral epithelial cells known as podocytes, Sec6 and Sec8 were also found in the cell body, with enrichment at the terminus of podocyte processes (Simons *et al.*, 1999).

Localization of the exocyst complex was also assessed by monitoring GFP-tagged exocyst subunits (Matern *et al.*, 2001). When N- or C-terminal GFP fusion constructs of Sec3, Sec5, Sec8, Sec10, and Exo70 as well as the C-terminal GFP fusion construct of Sec15 were stably transfected into MDCK cells, all fusion proteins, except Exo70, displayed cytosolic distribution. This subcellular localization pattern may be due to the failure of GFP-tagged exocyst subunits to completely incorporate into the endogenous exocyst complex. Interestingly, GFP-tagged Exo70 showed plasma membrane enrichment. However, GFP–Exo70-expressing cells failed to establish stable cell-to-cell contact, suggesting that this construct may act as a dominant-negative construct. Overall, cell biological studies indicate that the exocyst complex is enriched at or recruited to distinct cellular locations and that this localization is dependent on cellular signals.

Localized exocyst enrichment in the cell is likely due to the anchoring or active recruitment of the exocyst complex by insoluble cellular structures. In agreement, sedimentation studies have shown that the majority of the exocyst complex cosedimented with an insoluble cellular fraction in rat brain (Hsu *et al.*, 1996). The question now is: what is the cellular structure that associates with the exocyst complex. The perinuclear localization of the exocyst complex suggests that it is associated with either the Golgi apparatus/network or the microtubule-organizing center. Both structures have perinuclear localization.

In MDCK cells, pharmacological, biochemical, and cell biological studies showed that the exocyst complex is localized to the trans-Golgi network at the perinuclear region and to the plasma membrane, where it colocalized with adhesion junction proteins including ZO-1, cortical actin, E-cadherin, α-catenin, and occludin (Grindstaff *et al.*, 1998; Yeaman *et al.*, 2001). Exocyst complex Sec6 and Sec8 subunits colocalized with vesicles carrying exocytic cargoes. Blockage of exocytosis inhibited recruitment of the exocyst complex to the plasma membrane. Treatments that block exocytosis, such as low temperature and expression of kinase-inactive protein kinase D, also caused the accumulation of exocyst subunits at the perinuclear region. Thus it was hypothesized that there is a steady state distribution of the exocyst complex between the trans-Golgi network and the plasma membrane. In addition, the

introduction of various monoclonal antibodies against Sec6 and Sec8 into permeabilized MDCK cells resulted in protein cargo accumulation either at the perinuclear region or near the plasma membrane, implicating that the exocyst complex may function at multiple stages in Golgi-to-plasma membrane vesicle trafficking. These results show that exocyst Sec6 and Sec8 subunits are recruited to specific plasma membrane domains via vesicle trafficking. They are consistent with studies in yeast in which the localization of GFP-tagged exocyst was also dependent on vesicle trafficking (Finger *et al.*, 1998; Guo *et al.*, 1999b).

In neuroendocrine PC12 cells, three lines of evidence suggest that the exocyst complex is associated with cytoskeletal elements such as septins and microtubules (Vega and Hsu, 2001, 2003). First, density gradient centrifugation study of brain and PC12 cell lysates showed that the majority of exocyst subunits Sec6, Sec8, and Exo70 comigrated with septins and microtubules, but not with Golgi, endosome, or plasma membrane proteins. Consistent with this result, the complex coimmunoprecipitated with septins and tubulin from both brain and PC12 cell lysates. In addition, the exocyst complex copurified with five septins, including septin2, through a lengthy purification process involving multiple column chromatography (Hsu *et al.*, 1999). Second, visualization of endogenous exocyst subunits and septin2 by monoclonal antibodies showed that both exocyst and septin2 have similar localization. They exhibited filamentous distribution emanating from the perinuclear region toward the plasma membrane (Vega and Hsu, 2003; Wang and Hsu, 2003). Septin2, like the exocyst complex, has also been shown to play a role in neurite outgrowth in PC12 cells (Vega and Hsu, 2003). Third, treatment of PC12 cells with microtubule-disrupting, but not Golgi-disrupting, drug dispersed both exocyst and septin2 perinuclear localization. These observations are consistent with findings in yeast in which exocyst subunits localization was also affected in septin-defective cells (Barral *et al.*, 2000).

The above-described results suggest that exocyst localization is dependent on the cellular structures with which it associates. Identification and characterization of exocyst associated proteins/cellular structure should provide important insights into the molecular events underlying exocyst function.

IV. Function and Regulation of the Exocyst Complex

A. Role of the Exocyst Complex in Exocytosis

Most of the exocyst subunits (Sec3, Sec5, Sec6, Sec8, Sec10, and Sec15) in yeast were first identified as *SEC* gene products because of their involvement in secretion (Novick *et al.*, 1980). Mutations in these genes resulted in

defective secretion as assayed by measuring the cell surface incorporation and intracellular accumulation of enzymes such as invertase. Furthermore, electron microscopic studies revealed the accumulation of 80-nm secretory vesicles in the mutant cells. Study of newly generated mutants in the other two genes, *EXO70* and *EXO84*, revealed similar phenotypes (TerBush and Guo, unpublished observation). In addition, genetic studies in yeast also demonstrated close genetic interactions among the exocyst components and other genes involved in secretion, such as Sso1 (Aalto *et al.*, 1993).

Insights into the biological functions of the exocyst complex in higher eukaryotes have been obtained by perturbing exocyst function in tissue culture cells or in whole organisms. In the MDCK epithelial cell line, the introduction of anti-exocyst Sec8 subunit monoclonal antibodies into streptolysin O-permeabilized cells perturbed protein targeting to the basolateral, but not to the apical, plasma membrane domain of these cells (Grindstaff *et al.*, 1998). Similarly, the inhibition of exocyst function with anti-exocyst Sec8 subunit monoclonal antibodies in pancreatic acinar primary cells also disrupted the delivery of calcium signaling proteins to the apical plasma membrane domains of these cells (Shin *et al.*, 2000). In the neuroendocrine PC12 cell line, the overexpression of an exocyst Sec10 deletion dominant-negative construct prevented neurite outgrowth (Vega and Hsu, 2001). Thus, perturbations in exocyst function affect protein targeting to specific plasma membrane domains to establish cell polarity and promote neurite outgrowth. In the mammalian system, the exocyst complex has also been shown to be required for vesicle trafficking. In fact, the exocyst complex is ubiquitously expressed, suggesting that it may be a core component of the vesicle-targeting machinery in every cell. Interestingly, the highest exocyst subunit expression is found in brain, an organ with highly polarized cells (Guo *et al.*, 1997; Kee *et al.*, 1997; Sjolinder *et al.*, 2002; Ting *et al.*, 1995). In mice with the exocyst subunit Sec8 knocked out, animals die shortly after the induction of gastrulation (Friedrich *et al.*, 1997). The early embryonic lethality suggests that exocyst function is essential for development. However, it is not clear whether the induction of lethality at gastrulation is a result of maternal contribution depletion or of the dispensability of exocyst function until the induction of gastrulation. The first possibility is consistent with observations in yeast, in which exocyst null mutants are nonviable.

In the case of exocyst subunit Sec5 knockout in the fruit fly *Drosophila melanogaster*, the organisms die as growth-arrested larva (EauClaire and Guo, 2003; Murthy *et al.*, 2003). The null alleles failed to grow and the neuromuscular junctions failed to develop completely. Furthermore, neurite outgrowth in culture is inhibited in *sec5* mutants once maternally supplied Sec5 is exhausted. Using a T cell transmembrane protein, CD8, as a plasma membrane protein marker, the authors showed that exocytosis at the plasma membrane was defective in *sec5* mutants, whereas the synthesis of

CD8 protein and the generation of CD8-containing vesicles were normal. This is similar to what was observed in temperature-sensitive yeast exocyst mutants. After temperature shift, the mutant cells accumulated secretory vesicles; and the exocytosis of cell wall enzyme markers such as invertase was blocked. In sharp contrast to the arrest of neurite growth and plasma membrane protein addition, the authors found that synaptic transmission continued to be robust despite the decline of maternal Sec5 protein. These results indicate that the exocyst complex is required for constitutive secretion where secretory vesicles are delivered from Golgi to the plasma membrane. It is not, however, necessary for regulated secretion in the form of neurotransmission where synaptic vesicles are tethered near the plasma membrane and undergo repeated local exocytosis and endocytosis cycles. Similarly, the depletion of exocyst Sec10 subunit in *Drosophila* by RNA interference (RNAi) also resulted in early postembryonic lethality (Andrews *et al*., 2002). However, tissue-specific Sec10 RNAi did not cause defect in neuromuscular junction formation. Neurotransmission in this organism was not perturbed. Instead, the ring gland, an organ specialized in hormone secretion, was affected. These results suggest that fruit fly Sec10 is required for hormone secretion but not for constitutive or regulated secretion underlying neurogenesis or neurotransmission. This discrepancy in exocyst subunit deletion studies brings up at least two possibilities. First, the Sec10 subunit is not essential for exocyst complex function in membrane addition or neurotransmission. However, it is necessary, on its own or as part of the exocyst complex, in mediating hormone secretion. Alternatively, there is more than one Sec10 isoform in *Drosophila*. The Sec10 isoform that is deleted in this RNAi study is not the isoform that is part of the exocyst complex. In fact, Northern blot analysis in mammalian tissues suggests that there may be different isoforms of Sec10 (Guo *et al*., 1997). Coimmunoprecipitation experiments using antibodies against the Sec10 isoforms may help verify this possibility.

It was discovered that the last four amino acids of exocyst subunits Sec6 and Sec8 contain consensus sequence for type 1 PDZ domain protein binding (Riefler *et al*., 2003; Sans *et al*., 2003). Through this consensus sequence Sec8 was found to interact with the postsynaptic density protein PSD-95 (Riefler *et al*., 2003), a member of the membrane-associated guanylate kinase (MAGUK) family that has been shown to participate in the assembly of synaptic signaling complexes at excitatory synapses (Fang and Zhang, 2002; Hung and Sheng, 2002). In addition, Sec8 has also been found to interact with the NMDA (*N*-methyl-D-aspartate) receptor through synapse-associated protein SAP-102 (Sans *et al*., 2003). NMDA receptor is a member of the ionotropic glutamate receptors that mediate most of the excitatory neurotransmission in the central nervous system (Dingledine *et al*., 1999). The Sec8/SAP-102/NMDA receptor interaction appears to have taken place at an early

stage in the vesicle trafficking pathway, possibly at the endoplasmic reticulum or the Golgi apparatus. Overexpression of a *sec8* mutant with deletion of its last four amino acids decreased NMDA-mediated current and surface expression, indicating that the Sec8/SAP-102/NMDA receptor interaction plays a role in regulating the delivery of the NMDA receptor to the cell surface. These results bring up the possibility that the exocyst complex may target a subset of proteins from the Golgi to the plasma membrane, using PDZ domain proteins as adaptors (Hoogenraad and Sheng, 2003).

B. Exocyst Regulation by Ras Superfamily of Small GTPases

Genetic and cell biological experiments showed that the exocyst complex is required for a multitude of cellular processes, all requiring protein targeting to specific plasma membrane domains. The question now is, what are the molecular mechanisms controlling the exocyst in protein targeting? The exocyst functions in mediating protein targeting, and is likely to be tightly regulated to promote precise protein/membrane addition to the plasma membrane. Identification of proteins that interact with the exocyst will help us to understand the regulation of this complex as well as of exocytosis. Research from both yeast and mammalian cells identified several members of the Ras family of small GTPases that interact and regulate the exocyst (for review, see Lipschutz and Mostov, 2002; Novick and Guo, 2002). Because the small GTPases have multiple effectors, exocyst function could be coordinated with other cellular processes also controlled by these G proteins.

1. Rab

The first GTP-binding protein found to associate with the exocyst was the yeast Sec4 protein, a member of the Rab branch of the Ras superfamily. In general, Rab proteins associate with specific membrane compartments during both exocytic and endocytic pathways and regulate vesicular transport at distinct stages along these pathways (Lazar *et al.*, 1997; Novick and Zerial, 1997). Sec4 is associated with secretory vesicles and is essential for vesicle transport from the Golgi apparatus to the cell surface. Exocyst subunit Sec15 was found to interact with the GTP-bound form of Sec4, but not with other yeast Rab proteins such as Ypt1. In addition, Sec15 interacts with Sec4ΔC (non prenylated) and Sec4L79 (GTP bound), but not Sec4I133 (nucleotide-free state) or Sec4V29 (probable GDP-bound state), suggesting that it prefers the GTP-bound form of Sec4 and that Sec4 prenylation is not required for its binding. Furthermore, the interaction with Sec15 with Sec4 requires the effector domain of Sec4p, because replacement of four amino

acids in this domain with the corresponding region of Ypt1, the closest homolog for Sec4 in yeast, abolished the interaction.

In addition to its interaction with Sec4, Sec15 also associates with secretory vesicles (Guo *et al*., 1999). Subcellular fractionation of yeast lysates demonstrated that Sec15 cofractionated with Sec4 and Snc (vesicle-bound v-SNAREs). Second, immunoelectron microscopy studies showed that both Sec4 and Sec15 colocalized with clusters of secretory vesicles that accumulate in response to Sec15 overproduction (Guo *et al*., 1999; Salminen and Novick, 1989). Sec4-GTP:Sec15 interaction may trigger further interactions between Sec15 and other exocyst components, eventually leading to docking and fusion of secretory vesicles with specific domains of the plasma membrane. Loss of Sec4 function left the exocyst in a partially assembled state (Guo *et al*., 1999b). Overproduction of Sec4, on the other hand, compensated for partial loss-of-function mutations in exocyst subunits. On the other hand, loss of either Sec4 function or Sec4 exchange protein Sec2 function prevented Sec15 overproduction-induced vesicle clustering (Salminen and Novick, 1989). These observations all support the hypothesis that the exocyst is a downstream effector of Sec4, possibly functioning in tethering vesicles that carry Sec4 in its GTP-bound state to the plasma membrane. In mammalian cells, there are several Rab proteins that, like Sec4, regulate exocytosis. It will be interesting to investigate whether any of these Rab proteins interact with the mammalian exocyst.

2. Rho

Given the proposed role of the exocyst in vesicle tethering, it is critical that this complex be properly positioned so that exocytosis will take place at the right site. In budding yeast, the exocyst was specifically localized to the bud tip or the mother/daughter connection, regions of active membrane addition during its life cycle. This polarized localization was lost in several *rho1* and *cdc42* mutant alleles (Guo *et al*., 2001; Zhang *et al*., 2001). The Rho GTP-binding proteins are master regulators of a wide range of cellular processes including cytoskeleton organization, cell polarization, gene transcription, and membrane traffic. The yeast Rho family consists of six members: Cdc42, Rho1, Rho2, Rho3, Rho4, and Rho5. The effect of Rho1 and Cdc42 on exocyst localization was not mediated through organization of the actin. Rather, the GTP-bound form of Rho1 and Cdc42 directly interacted with Sec3. Truncation of the Rho1/Cdc42-binding domain of Sec3 led to its depolarized localization in the cell. The availability of various *cdc42* mutant alleles has identified various cellular processes controlled by Cdc42. While GFP-tagged exocyst components were depolarized in several *cdc42* mutant alleles resulting in the mislocalization of GFP-tagged exocyst subunits (Zhang *et al*., 2001), one *cdc42* mutant allele also exhibited

accumulation of secretory vesicles in the cell (Adamo *et al.*, 2001). These mutant phenotypes implicate a role for Cdc42 in regulating exocytosis, both spatially and kinetically. Both Rho1 and Cdc42 interact with the N terminus of Sec3. In fact, these two proteins compete in their binding to Sec3 (Zhang *et al.*, 2001). Cdc42 is essential for the establishment of yeast polarity and Rho1 may be important for the maintenance of polarized growth (Yamochi *et al.*, 1994). Their interactions with the exocyst may help to restrict exocytosis to the site of polarized cell growth, where new plasma membrane components are added.

While Rho1 and Cdc42 interact with Sec3, Rho3, in its GTP-bound form, directly interacts with the exocyst protein Exo70 (Adamo *et al.*, 1999; Robinson *et al.*, 1999). *rho3* mutants exhibited depolarized actin as well as defects in exocytosis (Adamo *et al.*, 1999). However, there is no report of exocyst localization defects in these mutants. The role of Rho3 in exocytosis is probably kinetic in nature. Although different Rho proteins talk to the exocyst in different ways, all of these interactions may allow the Rho proteins to coordinate exocytosis with other Rho-dependent processes, such as actin organization, to achieve polarized yeast cell growth.

Rho proteins are involved in polarized exocytosis in mammalian cells (Kroschewski *et al.*, 1999; Musch *et al.*, 2001; Rogers *et al.*, 2003). One study demonstrated that the exocyst is a downstream effector of TC10, a Rho protein sharing sequence similarity with Cdc42. A yeast two-hybrid screen using constitutively active mutant of TC10 identified the exocyst component, Exo70 (Inoue *et al.*, 2003). Coimmunoprecipitation experiment further showed that TC10, but not other Rho proteins, preferably binds to the exocyst complex. Importantly, expression of the active form of TC10 in 3T3 cells promoted the recruitment of Exo70 to the plasma membrane, where the exocyst carries out its physiological function. Overexpression of full-length Exo70 in 3T3 adipocytes enhanced insulin-mediated glucose uptake. On the other hand, overexpression of the N-terminal portion of Exo70 (Exo70N) blocked glucose uptake. Exo70N did not affect the translocation of Glut4. Instead, it probably inhibited a step after Glut4-containing vesicles were transported to the plasma membrane. This study not only reveals a molecular connection between the exocyst and Rho protein in mammalian cells, but also provides evidence for the role of the exocyst in exocytosis at the vicinity of the plasma membrane. It was proposed that Glut4 exocytosis takes place in the lipid raft domains of the plasma membrane in 3T3 adipocytes (Saltiel and Pessin, 2002). On the other hand, it has also been shown that exocysts are spatially limited to the basolateral domain, which is not enriched with lipid rafts in MDCK cells (Grindstaff *et al.*, 1998; Kreitzer *et al.*, 2003; Yeaman *et al.*, 2001). While the plasma membrane is a primary site for exocyst function, more experiments are needed to further investigate the nature of the plasma membrane domains where the exocyst functions.

3. Ral

Yeast two-hybrid screens and *in vitro* protein-binding studies have revealed that exocyst subunit Sec5 interacts with a Ras family member, Ral, in mammalian cells (Brymora *et al.*, 2001; Moskalenko *et al.*, 2002; Polzin *et al.*, 2002; Sugihara *et al.*, 2002). Sec5 preferentially binds to the GTP-bound form of RalA, and the interaction domain has been mapped to the N terminus of Sec5p. The structure of the RalA-binding domain of Sec5 has been analyzed by crystallography and was shown to display an immunoglobulin-like β-sandwich structure that represents a novel interaction domain for an effector of a GTP-binding protein (Fukai *et al.*, 2003; Mott *et al.*, 2003). The Sec5–RalA interaction may modulate exocyst function by either regulating the formation of the complex or modulating the exocyst activity. In this regard, the disruption of Ral function has been shown to perturb exocyst complex assembly (Moskalenko *et al.*, 2002), an effect similar to that seen on the loss of Sec4 function in yeast (Guo *et al.*, 1999). The involvement of Ral in protein targeting and the secretory pathway may be, at least partially, through their regulation of exocyst function. Both expression of constitutively active RalA and inhibition of either the function or synthesis of RalA had a similar effect on protein export in epithelial cells. Proteins normally targeted to the basolateral surface of epithelial cells became randomly distributed between the apical and basolateral surfaces, while proteins normally targeted to the apical surface were unaffected (Moskalenko *et al.*, 2002). RalA has been shown to associate with regulated secretory compartments such as synaptic vesicles (Ngsee *et al.*, 1991) and secretory granules (Mark *et al.*, 1996). The RalA–exocyst interaction is also important in regulated exocytosis. Both expression of activated RalA and inhibition of RalA function were found to block the stimulated release of human growth hormone by the neuroendocrine PC12 cell line (Moskalenko *et al.*, 2002). In another study, expression of a dominant-negative form of RalA was shown to diminish the readily releasable pool of synaptic vesicles (Polzin *et al.*, 2002). Interestingly, Sugihara *et al.* (2002) found that injection of antibodies against Sec5 inhibited RalA and Cdc42-induced filopodia formation by a mechanism that is independent of the secretory pathway.

C. Role of the Exocyst in Protein Synthesis

When the human exocyst Sec10 subunit was overexpressed in MDCK cells, there was increased protein delivery to the basolateral, but not to the apical plasma membrane (Lipschutz *et al.*, 2000). Curiously, however, the transfected cells also exhibited an increase in protein synthesis for both basolateral and apical secretory proteins, with a concomitant increase in intracellular

vesicles. In addition, these cells showed morphological changes and are more prone to form cysts and tubules, a process reminiscent of the situation in autosomal dominant polycystic kidney disease (ADPKD) (Charron *et al.*, 2000a,b). These results bring to attention that exocyst function may be coordinated with the protein synthesis process, providing a link between protein synthesis and protein targeting to the plasma membrane.

In support of the above observations, an interaction between the exocyst and the β subunit of Sec61 (Seb1/Sbh1) was found in both yeast and mammalian cells (Lipschutz *et al.*, 2003; Toikkanen *et al.*, 2003). Sec61 complex is the main component of the endoplasmic reticulum translocon. Overexpression of subunits of Sec61 suppressed mutant alleles of the exocyst components in yeast. The interaction between these proteins suggests that there is a regulatory mechanism for exocyst function at both end points of the secretory pathway.

V. Conclusion and Future Directions

Although genetic, cell biological, and biochemical studies in various systems have shown that proper exocyst localization and function are important for protein and membrane trafficking from Golgi to the plasma membrane, it is still not clear how the exocyst carries out its function. Despite its large size, there are few recognizable sequence motifs on exocyst subunits to provide clues to the molecular mechanisms of this complex's function. The subcellular localization and molecular associations of the exocyst complex have been extensively studied. The results from these studies have given us valuable information about this complex. On the basis of these results, we have the following two speculations.

First, the exocyst may function as a member of the family of "tethering" proteins found in various stages of membrane traffic ranging from ER to Golgi transport to endocytosis (reviews for "tethering" proteins are provided by Guo *et al.*, 2000; Pfeffer, 1999; Short and Barr, 2002; Waters and Hughson, 2000; Whyte and Munro, 2002). This family of proteins may tether incoming vesicles to their targeting membrane and function before the docking and fusion events mediated by SNAREs. Although there is limited sequence homology among these proteins at different stages of membrane traffic, some similar mechanisms can be found. For example, most of these proteins interact (physically and/or functionally) with Rab proteins at specific stages. In essence, the exocyst can be regarded as a tethering complex that functions at the plasma membrane for tethering post-Golgi secretory vesicles. It interacts with the Rab protein Sec4 and may further interact with SNAREs for exocytosis. Ample genetic evidence links the exocyst to

SNARES; but what is the molecular basis for the connection between this vesicle-tethering complex and the downstream membrane-docking and fusion machinery? Answering this question is not only important for the studies of the exocyst, but also for our understanding of post-Golgi exocytosis. Because the exocyst functions upstream of "committed" docking and fusion, its vesicle-tethering function makes it is an ideal candidate to spatially, temporally, and/or kinetically control exocytosis. The eight components of the exocyst complex are therefore excellent targets for regulatory proteins. Although small GTPases have been found to interact with the exocyst, it is likely that other proteins also interact and regulate exocyst proteins.

Second, we propose that the exocyst may regulate vesicle trafficking at the vicinity of the plasma membrane by modulating cytoskeletal dynamics and/or vesicle transfer from microtubules to actin and finally to the plasma membrane. Currently few proteins, in addition to the microtubule, actin, and their associated motors, have been identified to play a role in this process (Goode *et al*., 2000). In neuroendocrine PC12 cells, the exocyst showed association with microtubules and septin proteins, especially septin2. On nerve growth factor activation of the MAP kinase pathway, both exocyst and septin2 were recruited, possibly in coordination with a subset of microtubules, from the microtubule-organizing center to the plasma membrane via filament-like structures. Once the exocyst is recruited to the vicinity of the plasma membrane, the exocyst may mediate vesicle transfer, by its direct or indirect association with the cytoskeletons, from microtubules to cortical actin or from cortical actin to the plasma membrane. It is also interesting to note that septins have been shown to coordinate with microtubules and actin through microtubule- and actin-associated proteins (Kinoshita *et al*., 1997, 2002; Nagata *et al*., 2003; Surka *et al*., 2002; Vega and Hsu, 2003), making them suitable candidates for communicating between microtubules and actin. Overall, current findings strongly suggest a role for exocyst function at the vicinity of the plasma membrane to ultimately allow the docking and fusion of vesicles with the plasma membrane. The regulation of exocyst localization by cellular signals, such as members of the Ras family of small GTPases, plays an important role in regulating the site and kinetics of exocyst function.

The exocyst was originally discovered in the budding yeast *Saccharomyces cerevisiae*. Genetic analyses carried out in this organism have proved particularly useful in identifying and characterizing the role of many proteins involved in the vesicle trafficking pathway, including the exocyst complex, in the spatial regulation of secretion and cell polarization. The apparently "simple" budding process requires a sophisticated system to temporally and spatially coordinate membrane traffic to several cellular processes such as cell cycle progression and cell polarization. It will be important to study how these cellular processes are coordinated at the molecular level. The

realization that many proteins involved in the vesicle trafficking pathway are conserved from yeast to mammals has prompted the identification and isolation of the exocyst complex in higher eukaryotes such as the fruitfly *Drosophila melanogaster* and mammals. Although these two systems, especially the mammalian system, do not have the advanced genetic screening methodology developed in yeast, they allow the characterization of exocyst function in a wide variety of biological processes ranging from tight junction formation to neurite outgrowth. Elucidating the role of the exocyst in these processes should provide valuable insights into the molecular mechanisms of exocyst function as well as the molecular events that coordinate many complex biological processes.

While there are many reasons to believe that the basic mechanisms of exocyst function are conserved, it is also clear that different protein–protein interactions and regulatory strategies have been gained or lost during evolution. This specialization may also occur within the same organism, in which the exocyst participates in distinct biological processes in different cell types. It is important to appreciate that the specialization/variation may also be generated by some common molecular basis. For example, the exocyst subunit Sec8 can interact with different type 1 PDZ domain proteins in different cells. There are about 300 PDZ domain proteins in mammals. Thus the PDZ domain proteins can function as adaptors to allow the exocyst to bind different proteins and target different protein cargoes to the plasma membrane in different cells and/or at different developmental stages. Second, exocyst function has been shown to be regulated by different Ras family members in different organisms and cell types. Because these small GTPases have been shown to function as secondary messengers downstream of many signaling pathways, the regulation of exocyst function by various Ras family members may be dependent on the signaling cascades and the different Ras members present in each cell type. These two mechanisms may explain, in part, how exocyst can bind to different proteins and participate in a multitude of biological processes.

In conclusion, the exocyst is an essential component in the exocytosis pathway in all cell types and organisms studied so far. Although different experimental approaches in various systems have led to the proposal of distinct models on the molecular basis of exocyst function, it is clear that mechanisms regulating exocyst subcellular localization and molecular associations play a major role in modulating exocyst function. In addition, these studies also show that the function of this multisubunit complex is required for a multitude of biological processes and is both spatially and temporally regulated. Elucidation of the biological functions of the exocyst will not only contribute to our understanding of vesicle traffic, but will also provide insights into the mechanisms of many complex biological processes requiring polarized secretion.

References

Aalto, M. K., Ronne, H., and Keranen, S. (1993). Yeast syntaxins Sso1p and Sso2p belong to a family of related membrane proteins that function in vesicular transport. *EMBO J.* **12,** 4095–4104.

Adamo, J. E., Rossi, G., and Brennwald, P. (1999). The Rho GTPase Rho3 has a direct role in exocytosis that is distinct from its role in actin polarity. *Mol. Biol. Cell* **12,** 4121–4133.

Adamo, J. E., Moskow, J. J., Gladfelter, A. S., Viterbo, D., Lew, D. J., and Brennwald, P. J. (2001). Yeast Cdc42 functions at a late step in exocytosis, specifically during polarized growth of the emerging bud. *J. Cell Biol.* **155,** 581–592.

Andrews, H. K., Zhang, Y. Q., Trotta, N., and Broadie, K. (2002). Drosophila Sec10 is required for hormone secretion but not general exocytosis or neurotransmission. *Traffic* **12,** 906–921.

Barral, Y., Mermall, V., Mooseker, M. S., and Snyder, M. (2000). Compartmentalization of the cell cortex by septins is required for maintenance of cell polarity in yeast. *Mol. Cell* **5,** 841–851.

Bennett, M. K., and Scheller, R. H. (1993). The molecular machinery for secretion is conserved from yeast to neurons. *Proc. Natl. Acad. Sci. USA* **7,** 2559–2563.

Bennett, M. K., Garcia-Arraras, J. E., Elferink, L. A., Peterson, K., Fleming, A. M., Hazuka, C. D., and Scheller, R. H. (1993). The syntaxin family of vesicular transport receptors. *Cell* **5,** 863–873.

Bowser, R., and Novick, P. (1991). Sec15 protein, an essential component of the exocytotic apparatus, is associated with the plasma membrane and with a soluble 19.5S particle. *J. Cell Biol.* **6,** 1117–1131.

Bowser, R., Muller, H., Govindan, B., and Novick, P. (1992). Sec8p and Sec15p are components of a plasma membrane-associated 19.5S particle that may function downstream of Sec4p to control exocytosis. *J. Cell Biol.* **5,** 1041–1056.

Brennwald, P., Kearns, B., Champion, K., Keranen, S., Bankaitis, V., and Novick, P. (1994). Sec9 is a SNAP-25-like component of a yeast SNARE complex that may be the effector of Sec4 function in exocytosis. *Cell* **2,** 245–258.

Brymora, A., Valova, V. A., Larsen, M. R., Roufogalis, B. D., and Robinson, P. J. (2001). The brain exocyst complex interacts with Ra1A in a GTP-dependent manner: Identification of a novel mammalian Sec3 gene and a second Sec15 gene. *J. Biol. Chem.* **32,** 29792–29797.

Charron, A. J., Bacallao, R. L., and Wandinger-Ness, A. (2000a). ADPKD: A human disease altering Golgi function and basolateral exocytosis in renal epithelia. *Traffic* **8,** 675–686.

Charron, A. J., Nakamura, S., Bacallao, R., and Wandinger-Ness, A. (2000b). Compromised cytoarchitecture and polarized trafficking in autosomal dominant polycystic kidney disease cells. *J. Cell Biol.* **1,** 111–124.

Dingledine, R., Borges, K., Bowie, D., and Traynelis, S. F. (1999). The glutamate receptor ion channels. *Pharmacol. Rev.* **1,** 7–61.

EauClaire, S., and Guo, W. (2003). Conservation and specialization: The role of the exocyst in neuronal exocytosis. *Neuron* **3,** 369–370.

Fan, J. S., and Zhang, M. (2002). Signaling complex organization by PDZ domain proteins. *Neurosignals* **6,** 315–321.

Field, C. M., and Kellogg, D. (1999). Septins: Cytoskeletal polymers or signalling GTPases? *Trends Cell Biol.* **9,** 387–394.

Finger, F. P., Hughes, T. E., and Novick, P. (1998). Sec3p is a spatial landmark for polarized secretion in budding yeast. *Cell* **4,** 559–571.

Friedrich, G., and Soriano, P. (1991). Promoter traps in embryonic stem cells: A genetic screen to identify and mutate developmental genes in mice. *Genes Dev.* **9,** 1513–1523.

Friedrich, G. A., Hildebrand, J. D., and Soriano, P. (1997). The secretory protein Sec8 is required for paraxial mesoderm formation in the mouse. *Dev. Biol.* **2,** 364–374.

Fukai, S., Matern, H. T., Jagath, J. R., Scheller, R. H., and Brunger, A. T. (2003). Structural basis of the interaction between Ra1A and Sec5, a subunit of the sec6/8 complex. *EMBO J.* **13,** 3267–3278.

Garcia, E. P., Gatti, E., Butler, M., Burton, J., and De Camilli, P. (1994). A rat brain Sec1 homologue related to Rop and UNC18 interacts with syntaxin. *Proc. Natl. Acad. Sci. USA* **6,** 2003–2007.

Gengyo-Ando, K., Kamiya, Y., Yamakawa, A., Kodaira, K., Nishiwaki, K., Miwa, J., Hori, I., and Hosono, R. (1993). The *C. elegans unc-18* gene encodes a protein expressed in motor neurons. *Neuron* **4,** 703–711.

Goode, B. L., Drubin, D. G., and Barnes, G. (2000). Functional cooperation between the microtubule and actin cytoskeletons. *Curr. Opin. Cell Biol.* **1,** 63–71.

Grindstaff, K. K., Yeaman, C., Anandasabapathy, N., Hsu, S. C., Rodriguez-Boulan, E., Scheller, R. H., and Nelson, W. J. (1998). Sec6/8 complex is recruited to cell–cell contacts and specifies transport vesicle delivery to the basal–lateral membrane in epithelial cells. *Cell* **5,** 731–740.

Guo, W., Roth, D., Gatti, E., De Camilli, P., and Novick, P. (1997). Identification and characterization of homologues of the exocyst component Sec10p. *FEBS Lett.* **2–3,** 35–39.

Guo, W., Roth, D., Walch-Solimena, C., and Novick, P. (1999a). The exocyst is an effector for Sec4p, targeting secretory vesicles to sites of exocytosis. *EMBO J.* **4,** 71–80.

Guo, W., Grant, A., and Novick, P. (1999b). Exo84p is an exocyst protein essential for secretion. *J. Biol. Chem.* **33,** 23558–23564.

Guo, W., Sacher, M., Barrowman, J., Ferro-Novick, S., and Novick, P. (2000). Protein complexes in transport vesicle targeting. *Trends Cell Biol.* **10,** 251–255.

Guo, W., Tamanoi, F., and Novick, P. (2001). Spatial regulation of the exocyst complex by Rho1 GTPase. *Nat. Cell Biol.* **3,** 353–360.

Hazuka, C. D., Hsu, S. C., and Scheller, R. H. (1997). Characterization of a cDNA encoding a subunit of the rat brain rsec6/8 complex. *Gene* **1,** 67–73.

Hazuka, C. D., Foletti, D. L., Hsu, S. C., Kee, Y., Hopf, F. W., and Scheller, R. H. (1999). The sec6/8 complex is located at neurite outgrowth and axonal synapse-assembly domains. *J. Neurosci.* **4,** 324–334.

Hoogenraad, C. C., and Sheng, M. (2003). The return of the exocyst. *Cell Biol.* **6,** 493–495.

Hsu, S. C., Ting, A. E., Hazuka, C. D., Davanger, S., Kenny, J. W., Kee, Y., and Scheller, R. H. (1996). The mammalian brain rsec6/8 complex. *Neuron* **6,** 209–219.

Hsu, S. C., Hazuka, C. D., Foletti, D. L., Heuser, J., and Scheller, R. H. (1998). Subunit composition, protein interactions and structures of the mammalian brain sec6/8 complex and septin filaments. *Neuron* **20,** 111–122.

Hsu, S. C., Hazuka, C. D., Foletti, D. L., and Scheller, R. H. (1999). Targeting vesicles to specific sites on the plasma membrane: The role of the sec6/8 complex. *Trends Cell Biol.* **4,** 150–153.

Hung, A. Y., and Sheng, M. (2002). PDZ domains: Structural modules for protein complex assembly. *J. Biol. Chem.* **8,** 5699–5702.

Inoue, M., Chang, L., Hwang, J., Chiang, S. H., and Saltiel, A. R. (2003). The exocyst complex is required for targeting of Glut4 to the plasma membrane by insulin. *Nature* **6932,** 629–633.

Jahn, R. (2002). Sec1/Munc18 proteins: Mediators of membrane fusion moving to center stage. *Neuron* **27,** 201–204.

Kartmann, B., and Roth, D. (2001). Novel roles for mammalian septins: From vesicle trafficking to oncogenesis. *J. Cell Sci.* **114,** 839–844.

Kee, Y., Yoo, J. S., Hazuka, C. D., Peterson, K. E., Hsu, S. C., and Scheller, R. H. (1997). Subunit structure of the mammalian exocyst complex. *Proc. Natl. Acad. Sci. USA* **26,** 14438–14443.

Kinoshita, M., Kumar, S., Mizoguchi, A., Ide, C., Kinoshita, A., Haraguchi, T., Hiraoka, Y., and Noda, M (1997). Nedd5, a mammalian septin, is a novel cytoskeletal component interacting with actin-based structures. *Gene Dev.* **11,** 1535–1547.

Kinoshita, M., Field, C. M., Coughlin, M. N. L., Straight, A. F., and Mitchison, T. J. (2002). Self- and actin-templated assembly of mammalian septins. *Dev. Cell* **3,** 791–802.

Kreitzer, G., Schmoranzer, J., Low, S. H., Li, X., Gan, Y., Weimbs, T., Simon, S. M., and Rodriguez-Boulan, E. (2003). Three-dimensional analysis of post-Golgi carrier exocytosis in epithelial cells. *Nat. Cell Biol.* **2,** 126–136.

Kroschewski, R., Hall, A., and Mellman, I. (1999). Cdc42 controls secretory and endocytic transport to the basolateral plasma membrane of MDCK cells. *Nat. Cell Biol.* **1,** 8–13.

Lazar, T., Gotte, M., and Gallwitz, D. (1997). Vesicular transport: How many Ypt/Rab-GTPases make a eukaryotic cell? *Trends Biochem. Sci.* **12,** 468–472.

Lipschutz, J. H., and Mostov, K. E. (2002). Exocytosis: The many masters of the exocyst. *Curr. Biol.* **6,** R212–R214.

Lipschutz, J. H., Guo, W., O'Brien, L. E., Nguyen, Y. H., Novick, P., and Mostov, K. E. (2000). Exocyst is involved in cystogenesis and tubulogenesis and acts by modulating synthesis and delivery of basolateral plasma membrane and secretory proteins. *Mol. Biol. Cell* **12,** 4259–4275.

Lipschutz, J. H., Lingappa, V. R., and Mostov, K. E. (2003). The exocyst affects protein synthesis by acting on the translocation machinery of the endoplasmic reticulum. *J. Biol. Chem.* **23,** 20954–20960.

Longtine, M. S., DeMarini, D. J., Valencik, M. L., Al-Awar, O. S., Fares, H., De Virgilio, C., and Pringle, J. R. (1996). The septins: Roles in cytokinesis and other processes. *Curr. Opin. Cell Biol.* **8,** 106–119.

Mark, B. L., Jilkina, O., and Bhullar, R. P. (1996). Association of Ral GTP-binding protein with human platelet dense granules. *Biochem. Biophys. Res. Commun.* **1,** 40–46.

Matern, H. T., Yeaman, C., Nelson, W. J., and Scheller, R. H. (2001). The Sec6/8 complex in mammalian cells: Characterization of mammalian Sec3, subunit interactions, and expression of subunits in polarized cells. *Proc. Natl. Acad. Sci. USA* **17,** 9648–9653.

Mitchison, T. J., and Field, C. M. (2002). Cytoskeleton: What does GTP do for septins? *Curr. Biol.* **12,** R788–R790.

Mondesert, G., Clarke, D. J., and Reed, S. I. (1997). Identification of genes controlling growth polarity in the budding yeast *Saccharomyces cerevisiae*: A possible role of N-glycosylation and involvement of the exocyst complex. *Genetics* **2,** 421–434.

Moskalenko, S., Henry, D. O., Rosse, C., Mirey, G., Camonis, J. H., and White, M. A. (2002). The exocyst is a Ral effector complex. *Nat. Cell Biol.* **1,** 66–72.

Mott, H. R., Nietlispach, D., Hopkins, L. J., Mirey, G., Camonis, J. H., and Owen, D. (2003). Structure of the GTPase-binding domain of Sec5 and elucidation of its Ral binding site. *J. Biol. Chem.* **19,** 17053–17059.

Murthy, M., Garza, D., Scheller, R. H., and Schwarz, T. L. (2003). Mutations in the exocyst component sec5 disrupt neuronal membrane traffic, but neurotransmitter release persists. *Neuron* **3,** 433–474.

Musch, A., Cohen, D., Kreitzer, G., and Rodriguez-Boulan, E. (2001). cdc42 regulates the exit of apical and basolateral proteins from the trans-Golgi network. *EMBO J.* **9,** 2171–2179.

Nagata, K., Kawajiri, A., Matsui, S., Takagishi, M., Shiromizu, T., Saitoh, N., Izawa, I., Kiyono, T., Itoh, T. J., Hotani, H., and Inagaki, M. (2003). Filament formation of MSF-A, a mammalian septin, in human mammary epithelial cells depends on interactions with microtubules. *J. Biol. Chem.* **20,** 18538–18543.

Ngsee, J. K., Elferink, L. A., and Scheller, R. H. (1991). A family of ras-like GTP-binding proteins expressed in electromotor neurons. *J. Biol. Chem.* **4,** 2675–2680.

Novick, P., and Zerial, M. (1997). The diversity of Rab proteins in vesicle transport. *Curr. Opin. Cell Biol.* **4,** 496–504.

Novick, P., and Guo, W. (2002). Ras family therapy: Rab, Rho and Ral talk to the exocyst. *Trends Cell Biol.* **6,** 247–249.

Novick, P., and Schekman, R. (1979). Secretion and cell-surface growth are blocked in a temperature-sensitive mutant of *Saccharomyces cerevisiae*. *Proc. Natl. Acad. Sci. USA* **4,** 1858–1862.

Novick, P., Field, C., and Schekman, R. (1980). Identification of 23 complementation groups required for post-translational events in the yeast secretory pathway. *Cell* **1,** 205–215.

Novick, P., Ferro, S., and Schekman, R. (1981). Order of events in the yeast secretory pathway. *Cell* **2,** 461–469.

Pevsner, J., Hsu, S. C., and Scheller, R. H. (1994). n-Sec1: A neural-specific syntaxin-binding protein. *Proc. Natl. Acad. Sci. USA* **4,** 445–449.

Pfeffer, S. R. (1999). Transport-vesicle targeting: Tethers before SNAREs. *Nat. Cell Biol.* **1,** E17–E22.

Polzin, A., Shipitsin, M., Goi, T., Feig, L. A., and Turner, T. J. (2002). Ral-GTPase influences the regulation of the readily releasable pool of synaptic vesicles. *Mol. Cell. Biol.* **6,** 714–722.

Riefler, G. M., Balasingam, G., Lucas, K. G., Wang, S., Hsu, S. C., and Firestein, B. L. (2003). Exocyst complex subunit sec8 binds to postsynaptic density protein-95 (PSD-95): A novel interaction regulated by cypin (cytosolic PSD-95 interactor). *Biochem. J.* **373,** 49–55.

Robinson, N. G., Guo, L., Imai, J., Toh-E, A., Matsui, Y., and Tamanoi, F. (1999). Rho3 of *Saccharomyces cerevisiae*, which regulates the actin cytoskeleton and exocytosis, is a GTPase which interacts with Myo2 and Exo70. *Mol. Cell. Biol.* **5,** 3580–3587.

Rogers, K. K., Jou, T.-S., Guo, W., and Lipschutz, J. H. (2003). The Rho family of GTPases is involved in epithelial cystogenesis and tubulogenesis. *Kidney Int.* **5,** 1632–1644.

Roth, D., Guo, W., and Novick, P. (1998). Dominant negative alleles of *SEC10* reveal distinct domains involved in secretion and morphogenesis in yeast. *Mol. Biol. Cell* **7,** 725–739.

Salminen, A., and Novick, P. J. (1987). A ras-like protein is required for a post-Golgi event in yeast secretion. *Cell* **4,** 527–538.

Salminen, A., and Novick, P. J. (1989). The Sec15 protein responds to the function of the GTP binding protein, Sec4, to control vesicular traffic in yeast. *J. Cell Biol.* **3,** 1023–1023.

Saltiel, A. R., and Pessin, J. E. (2002). Insulin signaling pathways in time and space. *Trends Cell Biol.* **2,** 65–71.

Salzberg, A., Cohen, N., Halachmi, N., Kimchie, Z., and Lev, Z. (1993). The *Drosophila* Ras2 and Rop gene pair: A dual homology with a yeast Ras-like gene and a suppressor of its loss-of-function phenotype. *Development* **4,** 309–319.

Sans, N., Prybylowski, K., Petralia, R. S., Chang, K., Wang, Y. X., Racca, C., Vicini, S., and Wenthold, R. J. (2003). NMDA receptor trafficking through an interaction between PDZ proteins and the exocyst complex. *Nat. Cell Biol.* **6,** 520–530.

Shin, D. M., Zhao, X. S., Zeng, W., Mozhayeva, M., and Muallem, S. (2000). The mammalian Sec6/8 complex interacts with Ca^{2+} signaling complexes and regulates their activity. *J. Cell Biol.* **5,** 101–112.

Short, B., and Barr, F. A. (2002). Membrane traffic: Exocyst III makes a family. *Curr. Biol.* **1,** R18–R20.

Simons, M., Saffrich, R., Reiser, J., and Mundel, P. (1999). Directed membrane transport is involved in process formation in cultured podocytes. *J. Am. Soc. Nephrol.* **8,** 1633–1639.

Sjolinder, M., Uhlmann, J., and Ponstingl, H. (2002). DelGEF, a homologue of the Ran guanine nucleotide exchange factor RanGEF, binds to the exocyst component Sec5 and modulates secretion. *FEBS Lett.* **12,** 211–215.

Sugihara, K., Asano, S., Tanaka, K., Iwamatsu, A., Okawa, K., and Ohta, Y. (2002). The exocyst complex binds the small GTPase RalA to mediate filopodia formation. *Nat. Cell Biol.* **1,** 73–78.

Surka, M. C., Tsang, C. W., and Trimble, W. S. (2002). The mammalian septin MSF localizes with microtubules and is required for completion of cytokinesis. *Mol. Biol. Cell* **10,** 3532–3545.

TerBush, D. R., and Novick, P. (1995). Sec6, Sec8, and Sec15 are components of a multisubunit complex which localizes to small bud tips in *Saccharomyces cerevisiae*. *J. Cell Biol.* **130,** 299–312.

TerBush, D. R., Maurice, T., Roth, D., and Novick, P. (1996). The exocyst is a multiprotein complex required for exocytosis in *Saccharomyces cerevisiae*. *EMBO J.* **23,** 6483–6494.

TerBush, D. R., Guo, W., Dunkelbarger, S., and Novick, P. (2001). Purification and characterization of yeast exocyst complex. *Methods Enzymol.* **329,** 100–110.

Ting, A. E., Hazuka, C. D., Hsu, S. C., Kirk, M. D., Bean, A. J., and Scheller, R. H. (1995). rSec6 and rSec8, mammalian homologs of yeast proteins essential for secretion. *Proc. Natl. Acad. Sci. USA* **21,** 9613–9617.

Toikkanen, J. H., Miller, K. J., Soderlund, H., Jantti, J., and Keranen, S. (2003). The β subunit of the Sec61p endoplasmic reticulum translocon interacts with the exocyst complex in *Saccharomyces cerevisiae*. *J. Biol. Chem.* **23,** 20946–20953.

Vega, I. E., and Hsu, S. C. (2001). The exocyst complex associates with microtubules to mediate vesicle targeting and neurite outgrowth. *J. Neurosci.* **11,** 3839–3848.

Vega, I. E., and Hsu, S. C. (2003). The septin protein Nedd5 associates with both the exocyst complex and microtubules and disruption of its GTPase activity promotes aberrant neurite sprouting in PC12 cells. *Neuroreport* **1,** 31–37.

Walch-Solimena, C., Collins, R. N., and Novick, P. J. (1997). Sec2p mediates nucleotide exchange on Sec4p and is involved in polarized delivery of post-Golgi vesicles. *J. Cell Biol.* **7,** 1495–1509.

Wang, S., and Hsu, S. C. (2003). Immunological characterization of exocyst complex subunits in cell differentiation. *Hybrid Hybridomics.* **22,** 159–164.

Waters, M. G., and Hughson, F. M. (2000). Membrane tethering and fusion in the secretory and endocytic pathways. *Traffic* **8,** 588–597.

Whyte, J. R., and Munro, S. (2002). Vesicle tethering complexes in membrane traffic. *J. Cell Sci.* **1,** 2627–2637.

Yamochi, W., Tanaka, K., Nonaka, H., Maeda, A., Musha, T., and Takai, Y. (1994). Growth site localization of Rho1 small GTP-binding protein and its involvement in bud formation in *Saccharomyces cerevisiae*. *J. Cell Biol.* **5,** 77–93.

Yeaman, C., Grindstaff, K. K., Wright, J. R., and Nelson, W. J. (2001). Sec6/8 complexes on trans-Golgi network and plasma membrane regulate late stages of exocytosis in mammalian cells. *J. Cell Biol.* **4,** 593–604.

Zhang, X., Bi, E., Novick, P., Du, L., Kozminski, K. G., Lipschutz, J. H., and Guo, W. (2001). Cdc42 interacts with the exocyst and regulates polarized secretion. *J. Biol. Chem.* **50,** 46745–46750.

This Page Intentionally Left Blank

INDEX

A

B

C

D

E

F

G

H

I

K

L

M

N

O

P

R

S

T

V